INFORMATION TO USERS

This manuscript has been reproduced from the microfilm master. UMI films the text directly from the original or copy submitted. Thus, some thesis and dissertation copies are in typewriter face, while others may be from any type of computer printer.

The quality of this reproduction is dependent upon the quality of the copy submitted. Broken or indistinct print, colored or poor quality illustrations and photographs, print bleedthrough, substandard margins, and improper alignment can adversely affect reproduction.

In the unlikely event that the author did not send UMI a complete manuscript and there are missing pages, these will be noted. Also, if unauthorized copyright material had to be removed, a note will indicate the deletion.

Oversize materials (e.g., maps, drawings, charts) are reproduced by sectioning the original, beginning at the upper left-hand corner and continuing from left to right in equal sections with small overlaps.

Photographs included in the original manuscript have been reproduced xerographically in this copy. Higher quality 6" x 9" black and white photographic prints are available for any photographs or illustrations appearing in this copy for an additional charge. Contact UMI directly to order.

ProQuest Information and Learning
300 North Zeeb Road, Ann Arbor, MI 48106-1346 USA
800-521-0600

Université d'Ottawa · University of Ottawa

ELECTROCHEMICAL REACTIVATION OF GRANULAR ACTIVATED CARBON

by

Ayoub Karimi-Jashni

Ph.D. Thesis

Submitted to the School of Graduate Studies and Research

Under the Supervision of Dr. R. M. Narbaitz

In partial Fulfillment of the Requirements for the Degree of Ph.D. in Civil Engineering (Environmental)

Department of Civil Engineering
University of Ottawa
Ottawa, Ontario
Canada, K1S 6N5

***The Ph.D. in Civil Engineering is a joint program with Carleton University, administrated by the Ottawa-Carleton Institute for Civil Engineering.**

ABSTRACT

The main objectives of this dissertation were to refine electrochemical GAC reactivation technology, a promising alternative technology, and to investigate its technical feasibility. The specific objectives of the study were: 1) to evaluate alternative reactor designs; 2) to assess the effect of contaminant and GAC types on the regeneration efficiency; 3) to study the electrolyte post-treatment; and 4) to investigate reactivation mechanisms and model them. To achieve these objectives many interrelated topics were investigated using phenol, 2-nitrophenol (2NP) and naturally occurring background organic matter (NOM) as adsorbates and Filtrasorb 400 (F-400), Westvaco Carbon (WV-B), Darco Norit, and Filtrasorb 300 (F-300) as adsorbents.

Different reactor configurations (divided-cell, undivided-cell, stainless steel column type, and a simple batch reactor) were studied. The divided-cell reactor had slightly higher efficiencies than the undivided reactor, however it had a number of disadvantages that counterbalanced the slightly better performance. The stainless steel column reactor performed poorly under the conditions tested. Experiments on the reactivation of different numbers of layers of GAC particles showed a significant decrease in the reactivation efficiency with increasing number of layers. It was demonstrated that the decrease in reactivation efficiency was due to the need for direct contact between GAC particles and the electrode. Electrolyte mixing resulted in a decrease in the cathodic reactivation efficiencies, while there was no significant change in the anodic reactivation. Higher degrees of electrolyte mixing decreased the local pH at the cathode and reduced the reactivation efficiency. Thus mixing is not recommended.

The impact of reactor operation conditions (reactivation time, current density, pH) on the reactivation efficiency showed that the reactivation efficiency (RE%) could be increased to

a maximum by increasing the current and/or time. The RE% increases rapidly with increasing reactivation time in the first few hours followed by a more gradual increase for longer times. Also the effect of current was very marked from 10 to 50 mA and gradual from 50 to 250 mA.

It was concluded that electrochemical reactivation of GAC is contaminant-type dependent. The reactivation efficiencies of F-400 loaded with 2NP and phenol at different reactivation currents and times showed similar patterns. However, 2NP-loaded F-400 showed higher reactivation efficiencies (maximum 108%) than phenol-loaded F-400 (maximum 92%). This is consistent with the full reversibility of 2NP from F-400 and partial reversibility of phenol from F-400. Reactivation of GAC loaded with NOM showed that there was a linear relation between the reactivation efficiency and reactivation time; the reactivation efficiency increased to 80% as the reactivation time increased to 25 hours at 50 mA.

A comparison of the percent reactivation of GACs showed that F-400 and WV-B performed essentially the same for the tested conditions. Darco GAC showed lower performance at higher reactivation times and/or currents. These results were in agreement with GACs conductivities. Darco GAC, which had lower conductivity comparing to F-400 and WV-B, had lower performance at higher reactivation times and/or currents. It is possible that the surface chemistry of Darco deteriorated over longer reactivation times and/or higher currents due to its lower conductivity (higher electrical resistance).

Total destruction of desorbed contaminants and their by-products were possible. Desorbed phenol and 2NP from loaded GAC react to form a number of reaction by-products that are eventually oxidized to CO_2 and H_2O. The phenol and 2NP conversion reactions were relatively rapid and followed first-order kinetics. However, the destruction

of the phenol and 2NP by-products was very slow. The rate of by-products destruction could be increased by increasing the applied current.

The main mechanism responsible for electrochemical reactivation is high-pH induced desorption at the cathode. It accounts for approximately 50-60% of the total reactivation of a single layer of GAC. The changes in pH that occur within the electrochemical reactivation reactors are fundamental to this type of reactivation. The hydrolysis reactions at the electrodes produce H^+ ions at the anode and OH^- at the cathode that cause pH near the anode to decrease to approximately 2 and near the cathode to increase to about 12. Because the adsorption and desorption of phenolics are pH dependent, the high local pH at/near the cathode enhances the phenolics desorption and results in higher cathodic than anodic reactivation. The presence of charge on the GAC particles results in additional desorption. that for the single layer of GAC particles increases the reactivation by approximately 25-30%. For reactivation of a single layer of GAC at 50 mA, the reactions involving the oxidation/reduction of phenolics accomplished about 10-20% of the total reactivation. Overall it was concluded that electrochemical reactivation is feasible as reactivation efficiencies of up to 108% were reached and electrochemical reactivation had lower energy and GAC replacement cost than thermal reactivation.

It is recommended that the GAC electrochemical reactivation should be a three step process. First, the GAC is reactivated with a relatively low current to minimize potential alterations of the GAC surface. Second, the GAC is drained and rinsed with a buffered solution. Finally, the electrolyte is treated electrochemically for an extended time at a much higher current (and possibly a different electrode) to reduce the electrolyte's TOC so that it may be reused or discharged.

ACKNOWLEDGEMENTS

I would like to express my appreciation to all who contributed to my work. I am particularly indebted:

to my supervisor, Dr. R. M. Narbaitz, for his guidance, encouragement, financial assistance, and friendship;

to the Department of Civil Engineering, for their financial support and for the use of their facilities;

to the professors of the Environmental Group, Dr. R. Droste, Dr. K. Kennedy, and Dr. L. Fernandes for their help;

to the support staff of the Department of Civil Engineering, particularly Fransisco Aposaga, Noella Simard, Yollande Hogan, and A. Boisvenue for their cooperation;

to Dr. M. Gattrell for helpful discussions;

to the proposal committee, Dr. B.E. Conway, Dr. W. Parker, Dr. Tezel, and Dr. Droste for their helpful suggestions.

to the graduate students of the Environmental Group, and in particular, Dr. Yassine Djebar, Dr. Hassan Mahmud, John Minnery, Jianqi Cen, and Fraser Kent for their helpful discussions;

to my friends, Dr. Kazem Fakharian, Dr. Mehdi Azhdary Moghaddam, Dr. Said Alerezaei, Dr. Hassan Mirnejad, Dr. Dariush Motezedian, Dr. Majid Sartaj, Dr. Majid Sarraf, and Dr. Syed Abdoulhossein Mokhtabad for their encouragement.

Finally and most of all, to all my family particularly my: wife Sanaz, daughter Syna, parents, brothers and sisters, and in-laws for the constant encouragement, help and sacrifice which permitted me to complete this study. There is no way I can thank them enough. But, I hope I can do better in the future. I also would like to dedicate this thesis to my parents (Hossein and Sanam), my wife (Sanaz), and my daughter (Syna).

TABLE OF CONTENTS

NOMENCLATURE

a	coefficient
a_c	coefficient
Å	Angstrom
AC	activated carbon
b	coefficient
b_c	coefficient
b_r	coefficient
BET	Brunauer, Emmett, and Teller adsorption isotherm model
°C	Celsius degree
$C_{control}$	final contaminant concentration of the control samples (mg/L)
C_d	liquid phase concentration after the desorption step (mg/L)
C_{di}	equilibrium liquid phase concentration at the end of desorption cycle (mg/L)
C_e	equilibrium contaminant liquid phase concentration (mg/L)
C_{e1}	liquid phase contaminant concentration for the first cycle (mg/L)
C_{e2}	liquid phase contaminant concentration for the reloading cycle (mg/L)
C_o	initial contaminant liquid phase concentration (mg/L)
C_{o1}	initial liquid phase contaminant concentration for the loading cycle (mg/L)
C_{o2}	initial liquid phase contaminant concentration for the reloading cycle (mg/L)
C_{od}	initial liquid phase concentration of the desorption solution (mg/L)
C_{odi}	liquid phase concentration at the start of desorption step i (mg/L)
Darco	Norit Darco GAC
DBPs	disinfection by-products
$Des._t$	desorption (with current) at time t
2,4-DCP	2,4-dichlorophenol
2,4-DNP	2.4-dinitrophenol
EBCT	empty bed contact time (min)
EPA	Environmental Protection Agency
2-EP	2-ethylphenol
F	Faraday
F-300	Filtrasorb 300 GAC
F-400	Filtrasorb 400 GAC
GAC	granular activated carbon
GC	gas chromatography
HPLC	high pressure liquid chromatograph
HSSD	homogeneous solid surface diffusion model
4-IPP	4-isopropyl phenol
k	Freundlich constant
K_{reg}	Freundlich coefficients of the isotherm with the reactivated GAC
M	mass of GAC (g);
M_1	mass of GAC used in the loading cycle (g)
M_2	mass of GAC used in the reloading cycle (g)
MB	methylene blue
1/n	Freundlich constant

$1/n_{reg}$	Freundlich coefficients of the isotherm with the reactivated GAC
2NP	2-nitrophenol
4NP	4-nitrophenol
NOM	natural organic material
NPOC	non purgeable organic carbon
O-C	O-cresol
O-M	O-methoxy phenol
PAC	powdered activated carbon
Ph	phenol
pK_a	acidic dissociation constant
PNP	paranitrophenol
q_{ad}	solid phase concentration after adsorption equilibrium (mg/g of GAC)
q_e	equilibrium contaminant solid phase concentration (mg of contaminant/g of GAC)
q_{e1}	solid phase concentration of virgin GAC after the first adsorption cycle
q_{e2}	adsorptive capacity of GAC after the readsorption cycle
q_d	solid phase concentration after the desorption step (mg/g of GAC)
$(q_d)_i$	equilibrium solid phase loading at the end of desorption step i (mg/g of GAC)
q_r	adsorption capacity of regenerated carbon
q_v	adsorption capacity of virgin carbon
Q_{total}	total solid-phase concentration
$Q_{contaminant}$	solid-phase concentration due to contaminant
$Q_{by\text{-}products}$	solid-phase concentration due to by-products
RE	reactivation efficiency
RE1	RE calculated via method 1
RE2	RE calculated via method 2
RE3	RE calculated via method 3
RE4	RE calculated via method 4
RE_{max}	maximum reactivation efficiency
RMOC	Regional Municipality of Ottawa-Carleton
SBS	sodium benzenesulfonate
SDBS	sodium dodecyl benzene sulfonate
SOCs	synthetic organic compounds
t	time (hour)
T	temperature (°C)
TCD	thermal conductivity detector
TOC	total organic carbon
USEPA	United States Environmental Protection Agency
V	volume of the desorption solution (L)
V_i	volume of the desorption solution of step i (L)
V_1	volume of contaminated water in the equilibrium vessel during loading cycle (L)
V_2	volume of contaminated water in the equilibrium vessel during reloading cycle (L)
VOCs	volatile organic compounds

WV-B Westvaco Carbon

LIST OF FIGURES

LIST OF TABLES

CHAPTER 1

INTRODUCTION

1.1 Introduction

In response to more stringent water quality regulations, many treatment systems use granular activated carbon (GAC) column adsorbers. GAC column adsorbers are being used in upgrading water treatment plants (for taste, odour and toxic organics removal), in groundwater remediation (toxic organics removals), in upgrading wastewater treatment plants (for toxics removal and for polishing to permit reuse) and in home water treatment units. The United States Environmental Protection Agency (USEPA) has designated GAC adsorption as the "best available technology" for treating drinking water contaminated with a variety of hazardous synthetic organic chemicals (Oxenford and Lykins, 1991).

GAC removes contaminants from water by the process of adsorption, a surface phenomenon in which matter migrates from one phase and is concentrated at the surface of another. Due to its extremely large internal surface area (500-1500 m^2/g), GAC can adsorb large quantities of a very wide variety of organic compounds, as well as some inorganic compounds. However, this internal surface area is finite and eventually becomes covered with adsorbate (contaminant) and adsorption ceases. When GAC becomes exhausted or when the effluent from a GAC bed or column reaches the maximum allowable discharge level, the GAC must be replaced by fresh or reactivated GAC.

1.2 Statement of the Problem

The high cost of GAC and its reactivation are the main disadvantages of GAC adsorbers and have prevented it from being applied more widely. Carbon reactivation or replacement costs may represent up to 50% of the total expenditure of GAC treatment systems (Adams and Clark, 1989). The cost can be significantly reduced by reactivating spent GAC rather than replacing it with virgin carbon (Adams *et al.*, 1988; Adams and Clark, 1989; Clark and Lykins, 1989).

Although, thermal, chemical, biological, and electrochemical methods of reactivation have been researched, in practice, thermal reactivation is used almost exclusively. It involves the gradual heating of the GAC to 800°C in furnaces with an oxygen deficient atmosphere. This causes the adsorbed impurities to volatilize and desorb without burning the GAC. The high temperature also oxidizes some of the desorbed contaminants. This process has resulted in reactivation efficiencies greater than 90%. However, the process characteristics include: a) the loss of carbon (5-15% during each cycle) due to oxidation and attrition; b) the transfer of the contaminants to air; and c) the high energy cost of heating the GAC to 800-850°C (Clark and Lykins, 1989). Usually a minimum activated carbon usage of 680 kg/d is needed before the capital cost of an on-site thermal reactivation facility can be justified.

The electrochemical reactivation technique possesses several potential advantages over thermal reactivation. They include possible in-situ reactivation, minimal GAC losses, high reactivation efficiencies, destruction of the contaminants desorbed from GAC, and its suitability for use in small and medium size treatment facilities. The main potential benefit of this technology is that it will make GAC treatment a less costly and more common

process. This technology will hopefully lead to the development of adsorbers that can reactivate GAC in-situ, this being particularly useful for home filters that are currently discarded with residential solid waste.

The literature reports several electrochemical reactivation studies using different reactor configurations, different GACs loaded with contaminants, different operating conditions, etc. (Sveshnikova *et al.*, 1987; Lazareva *et al.*, 1991; Narbaitz and Cen, 1994). Due to the reactor configuration and the single adsorbent/adsorbate combinations used in these studies many questions about the process remain unanswered. For further development of this technology there is an obvious need for a systematic evaluation of many design and operational variables of electrochemical GAC reactivation systems, so that the impact of each variable can be ascertained. These variables include the impact of reactor configuration, electrolyte flow, current density, reactivation time, GAC type, contaminant type, multi-layer reactivation, and cathodic versus anodic reactivation.

1.3 Objectives

The main objectives of this thesis were to refine electrochemical reactivation of GAC and to investigate its technical feasibility. The specific objectives of the study were: 1) to evaluate a more optimal reactor design; 2) to assess the regeneration efficiency for different contaminants and different types of GAC; 3) to investigate electrolyte post-treatment (i.e., oxidation of desorbed organics); and 4) to investigate the reactivation mechanisms and model them.

CHAPTER 2

LITERATURE REVIEW

2.1 Introduction

The length of the operational cycle of GAC columns/filters used in water treatment plants varies with the application. For taste and odour removal it normally lasts from 1 to 5 years (Schuliger *et al.*, 1987). However, for other applications such as for the removal of disinfection by-products (DBPs), the on-stream life of activated carbon beds could be reduced to 3 to 6 months (Schuliger *et al.*, 1987). In this situation, the economics could be very favourable for on-site reactivation. Thermal reactivation is used almost exclusively in practice. However, chemical, biological and electrochemical reactivation processes have also been investigated primarily at the laboratory scale. This chapter provides general information about activated carbon, adsorption, desorption, factors affecting adsorption and desorption, and a review of previous studies on activated carbon reactivation.

2.2 Granular Activated Carbon

GAC is used to remove volatile organic compounds (VOCs), synthetic organic compounds (SOCs), and DBPs and their precursors, as well as color-causing and taste-and-odor-causing compounds. GAC typically has a total (internal + external) surface area of 500-1,500 m^2/g. Most of the surface area available for adsorption within GAC particles is found in the internal pores of molecular dimensions created during the activation process. Activated carbons are classified according to their form: powdered or granular. GAC are those whose particles are larger than approximately U.S. sieve series #50, while powdered activated

carbons (PAC) are those that are smaller. GAC and PAC are the same materials with virtually the same total surface area per unit mass.

GACs can be made from a number of raw materials having a high carbonaceous content including wood, coal, peat, lignin, nut- shells, sawdust, lignite, bone, and petroleum residues (Faust and Aly, 1987). The quality of the resulting activated carbon is influenced by the starting material as well as the activation process (Sontheimer *et al.*, 1988).

GAC is manufactured by a process consisting of material dehydration and carbonization followed by activation. The starting material is dehydrated and carbonized by slowly heating it in the absence of air, sometimes using a dehydrating agent, such as zinc chloride or phosphoric acid (Sontheimer *et al.*, 1988). Excess water, including structural water, must be driven from the organic material. Carbonization converts this organic material to primary carbon, which is a mixture of ash (inert inorganics), tars, amorphous carbon, and crystalline carbon. Non-carbon elements (such as H and O) are removed as gases and the freed elementary carbon atoms are grouped into oxidized crystallographic formations (Weber, 1972). During carbonization, some decomposition products or tars will be deposited in the pores, but they will be removed in the activation step. Activation is essentially a two-phase process requiring burn-off of amorphous decomposition products (tars), plus enlargement of pores within the carbonized material. Burn-off frees the pore openings, increasing the number of pores, and activation enlarges these pore openings.

2.3 Adsorption

Adsorption plays an important role in the modification of water quality. GAC has excellent adsorption capacity for many undesirable substances. Adsorption from aqueous solutions onto GAC occurs as the result of either a low solubility of a particular solute in the solution or/and a high affinity of a particular solute in the aqueous solution for the activated carbon. The most common adsorption mechanisms are: Van der Waals attraction, electrical attraction of the solute to the carbon, or a chemical type of bond (chemisorption).

If the reaction is reversible, as it is for many compounds adsorbed by GAC, contaminants continue to accumulate on the surface of the GAC until the rate of the adsorption and desorption become the same, i.e., adsorption equilibrium is reached and no further accumulation will occur. Adsorption equilibrium experiments are generally conducted at a constant temperature so they are called isotherms. The most common experimental isotherm technique is the bottle-point method, so called because each bottle in the test generates a point in the equilibrium curve. These experiments are conducted by contacting the solution of interest in a set of bottles with different doses of activated carbon until equilibrium is reached. Then the solutions are separated from the GAC and are analyzed for the solute concentration. The experiments yield the equilibrium liquid phase concentration as a function of GAC dosage. The equilibrium solid phase concentration, which is also called the equilibrium capacity, equilibrium loading or loading, can be calculated by using a mass balance.

$$q_e = \frac{V\,(C_o - C_e)}{M} \qquad (2\text{-}1)$$

where q_e is the equilibrium contaminant solid phase concentration (mg of contaminant/g of GAC); C_e is the equilibrium contaminant liquid phase concentration (mg of contaminant/L); C_0 is the initial contaminant liquid phase concentration (mg of contaminant/L); M is the mass of GAC (g); and V is the liquid volume (L). The adsorption equilibria are generally presented as a graph of the amount of solute adsorbed per unit mass of adsorbent, q_e, as a function of equilibrium concentration in the bulk solution, C_e. This graph is also called the adsorption isotherm.

2.4 Single Component Isotherm Models

Different isotherm equations have been proposed either based on empirical data or on physico-chemical or thermodynamic models. The models that have been most suitable for describing aqueous solutions are discussed by Sontheimer *et al.* (1988). Adsorption equilibria for most aqueous systems can be modelled by the Langmuir model and/or the Freundlich model. The Langmuir model, which is also called the ideal localized monolayer model, is based on the following basic assumptions: first, the molecules are adsorbed on definite sites on the surface of the adsorbent. Second, each site can accommodate only one molecule (monolayer). Third, the area of each site is a fixed quantity determined solely by the geometry of the surface. Fourth, adsorption energy is the same at all sites. Finally, the adsorbed molecules cannot migrate across the surface or interact with neighbouring molecules.

The Langmuir isotherm originally was derived from kinetic analysis and later on by thermodynamic considerations (Adamson, 1982). For adsorption from solution by solid adsorbents, the Langmuir adsorption isotherm is expressed as:

$$q = \frac{q_m bCe}{(1 + bCe)} \qquad (2\text{-}2)$$

where q_m is the amount of solute adsorbed per unit weight of adsorbent required for monolayer coverage of the surface (mg/g of AC); and b is a constant related to the heat of adsorption. The Langmuir isotherm model has been shown to fit some aqueous systems over limited concentration ranges (Razzaghi, 1976).

The Freundlich adsorption equation is the most widely used mathematical expression for the adsorption from dilute aqueous solutions. The Freundlich equation is an empirical expression that was later found to correspond to adsorption on a heterogenous surface with adsorption sites whose adsorption energies follow an exponential distribution (Young and Crowell, 1962). The heterogeneous surface of activated carbon probably makes it the most compatible isotherm model. The equation has the form

$$q_e = K C_e^{1/n} \tag{2-3}$$

where K and 1/n are constant characteristics of the system. Equation 2-3 can be linearized as:

$$\log(q_e) = \log(K) + \frac{1}{n}\log(C_e) \tag{2-4}$$

If the data fit this model, plotting log (q_e) versus log (C_e) yields a straight line with a slope of 1/n and log (K) is the value of log (q_e) at C_e = 1 (log [C_e] = 0). The constant K in the Freundlich equation is related primarily to the capacity of the adsorbent for the adsorbate, and 1/n is a function of the strength of adsorption (Snoeyink, 1990). For fixed values of C_e and 1/n, the larger the value of K the larger the capacity, q_e. For fixed values of K and C_e the smaller the value of 1/n, the stronger the adsorption bond. The value of 1/n for the adsorption of most organic compounds by activated carbon is < 1. When 1/n is close to 1 (i.e., steep slopes), it indicates a high adsorptive capacity at high equilibrium liquid phase

concentrations and rapidly diminishing capacities at lower equilibrium concentrations. When $1/n << 1$ (flat slopes) the capacity tends to be independent of C_e, and the isotherm plot approaches the horizontal. In this case the value of q_e is essentially constant. If the value of 1/n is large, the adsorption bond is weak, and the value of q_e changes markedly with small changes in C_e. The Freundlich equation may not apply to all values of C_e. As C_e increases, q_e increases only until the adsorbent approaches saturation. At saturation, q_e is a constant, independent of further increases in C_e, and the Freundlich equation no longer applies. As can be deduced from equation 2-3, higher capacities are obtained at higher equilibrium concentrations. The amount of activated carbon required to reduce any initial concentration to a predetermined final concentration can be calculated from the Freundlich equation by substituting $V(C_0 - C_e)/M$ for q_e in eq. (2-3) and rearranging to obtain an expression for M.

2.5 Factors Affecting Adsorption Equilibria

Different factors such as the nature of the GAC and the nature of the solution can influence adsorption equilibria. The adsorptive characteristics of an activated carbon (AC) surface depend upon the source material of carbon as well as on the activation technique (Sontheimer *et al.*, 1988). Adsorbent characteristics that affect isotherms include activated carbon surface area, pore size distribution, and surface chemistry. Temperature, salt concentration, presence of molecular oxygen, and hydronium ion concentration (pH) are the most important experimental system factors affecting adsorption.

2.5.1 Activated Carbon Surface Area and Pore Size Distribution

Adsorption of a contaminant by GAC could be of a physical or chemical nature. Physical adsorption involves only relatively weak intermolecular forces, and chemisorption involves

essentially the formation of a chemical bond between the sorbate molecule and the surface of the adsorbent. If adsorption results from physical attraction forces (i.e., van der Waals) between adsorbate and adsorbent, the maximum amount of adsorption is proportional to the amount of surface area accessible to the adsorbate. For example, Oda *et al.* (1981) found that the adsorption capacity of benzoic acid was surface area limited. However, in general there is no direct way of predicting adsorption capacity based on surface area measurements because other factors also affect the extent of adsorption. An activated carbon with higher surface area than another, which is made of a different raw material or via a different manufacturing process, may or may not yield a higher adsorption capacity. When adsorption occurs via specific chemical interactions between the adsorbate and certain functional groups on the carbon surface, the adsorption depends on the number of suitable functional groups present on the carbon surface and not on the surface area.

The pores in GAC have been divided into macropores, transitional pores and micropores (Dubinin, 1966). Macropores are pores greater than 1,000-2,000 Å radii with specific volumes from 0.2 to 0.8 cm^3/g and specific surface areas from 0.5 to 2 m^2/g (Peel, 1980). The macropores play a negligible role in physically adsorbing material because of their low area, but they provide rapid access to the interior of the carbon particle. Transitional pores are 15 to 1,500 Å in size. Their specific surface area ranges from 20-70 m^2/g and the specific volume varies from 0.02 to 0.1 cm^3/g (Peel, 1980). However, these numbers differ from adsorbent to adsorbent. Micropores are pores with radii less than 15 Å and are of a comparable size to many adsorbing molecules. Micropores often contribute 90 to 97% of the total surface area within the carbon (Ying, 1978, Yenkie and Natarajan, 1993) and they have

specific volumes of 0.2 to 0.6 cm^3/g. Adsorbate molecules have to be several times smaller than the pores in order to penetrate them (Peel, 1980).

Both the rate of adsorption and the adsorptive capacity can be influenced by the pore structure. If the size of the adsorbate is greater than the largest pore opening, adsorption is limited to the external surface of the carbon particles. Usually the adsorbate is smaller than the macropore openings. In this case the amount of adsorption will greatly depend upon the fraction of the total measured surface area which is accessible to the adsorbate. Graham (1955) found that cationic dye adsorption was pore-size limited. Similar results are reported for different humic substances (Summers, 1986; Summers and Roberts 1988a,b). Kuhl *et al.* (1986) examined over 30 carbons and reported linear correlations between the adsorption capacity for p-chlorophenol and the micropore volume of pores with radii less than 3 Å.

2.5.2 Surface Chemistry

The surface chemistry of activated carbon can affect adsorption. Activated carbon is usually composed of 5 to 20 percent oxygen by weight and 80-95% carbon (Sontheimer *et al.*, 1988; Zogorski, 1975). The characteristics and amount of the oxygen chemically sorbed onto the surface of the activated carbon depend on the raw material and the activation technique (Sontheimer *et al.*, 1988). Based on the temperature at which activation was performed, the activated carbon can exhibit acidic or basic characteristics. Under most manufacturing and treatment conditions, the oxygen chemisorbed on the carbon surface is in the form of acidic surface oxides.

Coughlin and Ezra (1968) demonstrated that extensive oxidation of activated carbon with ammonium persulfate in aqueous solutions led to large decreases in the amount of phenol,

nitrobenzene, and benzenesulfonate that could be adsorbed. Oxidation of activated carbon surfaces with aqueous chlorine was also found to increase the number of oxygen surface functional groups and, correspondingly, to decrease the adsorption capacity for phenol (Snoeyink *et al.*, 1974). Graham (1955) observed that acidic oxygen groups on the carbon surface reduce the adsorption capacity of metanil yellow from water, while there was no effect on the adsorption of methylene blue. Graham attributed this to a repulsive interaction between the anionic form of metanil yellow and the oxygen sites. Graham noted that this kind of interaction might be expected for all anionic adsorbates. Similar results have been documented in numerous studies (i.e. Oda *et al.*, 1981; Youssef *et al.*, 1982; Matsumura *et al.*, 1985; Sontheimer *et al.*, 1988). Thus, oxygenated surfaces do not adsorb simple aromatic compounds strongly. The rates of adsorption were also reduced by the presence of oxygen surface functional groups (Coughlin *et al.*, 1970).

2.5.3 Temperature

Many researchers have studied the dependence of the rate of adsorption and adsorption capacity on the temperature. As mentioned earlier the adsorption mechanisms could be chemisorption (that is most frequently irreversible adsorption) or physical adsorption (that is most probably reversible adsorption) or a combination of both. Physical adsorption normally predominates because of the lower energy requirement. Physical adsorption capacity decreases with increasing temperature of the system due to breaking of weak bonds. However, increasing the temperature will result in a higher rate of diffusion and consequently will increase the rate of adsorption of organic compounds from solution (Weber and Morris, 1963).

Snoeyink (1968) studied the temperature dependence of phenol and 4-nitrophenol adsorption onto a coconut-shell-based GAC. These studies indicated that the rate of adsorption increases as the temperature of the system increases, however, the adsorption capacity decreases. Zogorski and Faust (1978) developed isotherms for phenol and 2,4-dichlorophenol (2,4-DCP) at temperatures of 8, 20, and 29°C using Columbia LCK carbon (Fig 2.1). The quantity adsorbed decreased with increasing temperature. However, when the phenol concentration was greater than 200 μmol/L (18.8 mg/L), temperature had a lesser influence on the adsorption process. They also observed an increase of removal rate as the temperature of the system was increased. Raising the temperature from 10 to 30°C increased the removal rate of phenol by 21% and of 2,4-DCP by 28%. According to Weber (1972), normal temperature variations have only minor effects on activated carbon adsorption processes at water treatment plants.

2.5.4 Salt Concentration

The effect of salt concentration on adsorption has been investigated by a number of researchers. Couglin and Tan (1968) studied the effect of adding 0.002 M and 0.004 M $CaCl_2$ to solutions of sodium benzenesulfonate (SBS) prior to adsorption onto activated carbon. The adsorption of SBS, which was strongly ionized in the solutions, increased by a factor of 1.15 to 3 by the addition of $CaCl_2$. Cooney and Wijaya (1987) reported similar results for benzoic acid. They proposed that adjacently adsorbed benzoate ions strongly repel each other, as both have the same charge. The only way to counteract the repulsion of adjacently adsorbed SBS ions is to add positive ions to the solution. As more and more positive ions are placed in the solution (by the addition of a salt), there will be more intrusion of these positive ions between the negative benzoate ions, nullifying to some

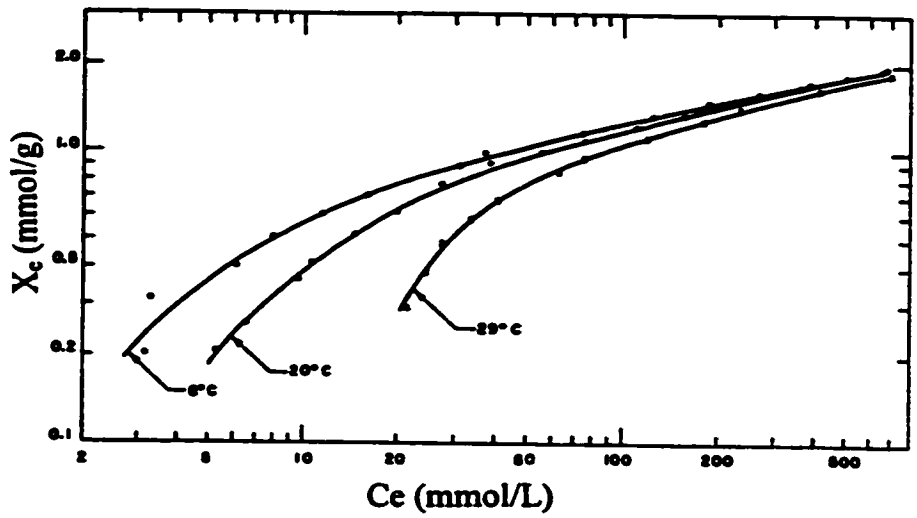

Fig. 2.1 Influence of temperature on the adsorption of phenol at pH 6.3 using LCK carbon. (Source: Zogorski and Faust, 1978)

degree the repulsive forces between adjacent benzoate ions. The net result will be that the benzoate ions can adsorb much more densely on the carbon surface.

A 0.05 M phosphate buffer exhibited no discernable effect on the rate of adsorption and adsorption capacity of undissociated 2,4-dichlorophenol (2,4-DCP) and 2,4-dinitrophenol (2,4-DNP) (Zogorski and Faust, 1976-a). However, the amount of adsorption of the dissociated compounds was increased around 10% for 2,4-DCP and around 25% for 2,4-DNP in the presence of the phosphate buffer. Snoeyink *et al.* (1969) added 1 M NaCl (58,000 mg/L) to a solution of 4-nitrophenol (4NP) ($pK_a = 7.1$) and found that the presence of NaCl had no effect on activated carbon adsorption at pH 2. However, at pH 10, where the PNP is highly ionized, the NaCl markedly increased PNP adsorption.

Jawaid and Weber (1979) investigated the effect of several salts on SBS adsorption on activated carbon. These salts were zinc chloride, calcium chloride, or potassium carbonate in the amount of 1 part salt per 100 parts charcoal. They found increases in adsorption of 19, 24, and 11% respectively, for these three salts. Randtke and Jepsen (1982) found that the presence of salts increased the activated carbon's adsorption capacity of different humic and fulvic acids. The anions had no detectable effect, Na had a slight gradual increase in capacity, while Ca and Mg produced very sharp increases in loading at concentrations of less than 1 mmole/L. In conclusion, salt addition significantly increases the adsorption capacity of GAC in adsorbing the ionized form of organic compounds. Karimi-Jashni (1994) showed that the 2NP adsorption is reversible in Milli-Q water and in 1% NaCl (0.17 M) solution at pH 4.6. He also demonstrated that the NaCl solution did not have a significant effect on reversibility of 2NP at pH 4.6.

2.5.5 Molecular Oxygen

Based on different applications of GAC, the adsorption process can occur in the presence or the absence of molecular oxygen. Prober *et al.* (1975) showed that dissolved oxygen adsorbs on GAC in the range of 10 to 40 mg/g. This adsorption of oxygen increases the concentration of acidic oxide groups on the carbon surface, which increases the base sorption capacity. Magne and Walker (1986) showed changes in the GAC adsorptive capacity for nitrobenzene and phenol as a result of chemisorption of oxygen.

Vidic *et al.* (1990) indicated that the presence of molecular oxygen has a major effect on the adsorption capacity of GAC for several phenolic compounds: phenol, o-cresol and 3-ethylphenol. In some instances, the adsorption capacity in the presence of molecular oxygen was up to three times the capacity that was measured in the absence of molecular oxygen. They hypothesized that the presence of molecular oxygen promotes polymerization of the compound on the surface of the activated carbon, which lead to the increased removals. However, Vidic *et al.* (1993) observed that the presence of molecular oxygen had very little influence on the adsorptive capacity of F-400 GAC in adsorbing nitrophenols (2-nitrophenol, 3-nitrophenol, and 4-nitrophenol). They explained that the first step in this polymerization reaction involves formation of a phenoxy radical which, as a highly reactive species, participates in polymer formation through either carbon-carbon or carbon-oxygen bonding. However, the presence of a nitro group, which is an electron-attracting substituent that causes an increase in the redox potential, inhibited this first step and consequently, no polymers were formed.

Van der Loop *et al.* (1997) concluded that the adsorption of some compounds such as o-cresol and 2,4-dinitrotoluene onto GAC is often not governed by physical adsorption and undergo surface catalyzed polymerization in the presence of molecular oxygen . Uranowski *et al.* (1998) found that the adsorptive capacity of GAC for many phenolic compounds increases in the presence of molecular oxygen (oxic condition). This enhanced adsorption is due to oxidative coupling of the adsorbed molecules and is accompanied by significant oxygen consumption and decreased adsorbate recovery by solvent extraction.

2.5.6 pH

2.5.6.1 Effect of pH on Adsorption Equilibria

Many researchers have studied the changes in measured adsorption of various types of organic compounds caused by lowering or raising the hydrogen ion concentration. The extent of the changes depends on the physicochemical properties of individual organic solutes. Several types of organic compounds have been studied. These include: organic acids in general (Ward and Getzen, 1970; Muller *et al.*, 1980; Semmens *et al.*, 1986; Cooney and Wijaya, 1987), phenolic compounds (Snoeyink *et al.*, 1969; Zogorski and Faust, 1978; Muller *et al.*, 1980; Suzuki and Takeuchi, 1986; Seidel and Radeke, 1990; Gomez Serrano *et al.*, 1992; Karimi-Jashni, 1994; Karimi-Jashni and Narbaitz, 1997), humic substances (Brauch, 1984), organic bases (Cooney and Wijaya, 1987; Seidel and Radeke, 1990), ampholytes (Andersen, 1947; Cooney and Wijaya 1987) and anionic surface-active agents (Weber and Morris, 1963; Leyva-Ramos, 1989). Only the effect of pH on adsorption of phenolic compounds is discussed below because they are the focus of the present research. It is of note that as the pH increases above the pK_a the ionized species become increasingly predominant.

Snoeyink *et al.* (1969) showed that the isotherms of phenol and 4NP on a coconut-shell AC were pH dependent and the adsorption capacity of anionic forms is less than that for the corresponding neutral species (Figs. 2.2 and 2.3). Fig. 2.2 shows that there is no marked effect of pH on the sorption of the neutral form of 4NP (pH << pK_a = 7.1) in the pH range from 2 to 6.5. However, the capacity for the neutral phenol (pH << pK_a = 9.9) molecules decreases significantly with decreasing pH in the same range (Fig. 2.3). Snoeyink *et al.* (1969) suggested that the hydrated proton competes effectively with phenol for active sites. Similar results for adsorption of phenol on Hydraffin 71 AC and phenol on F-400 AC were reported by Seidel and Radeke (1990), and Karmi-Jashni (1994), respectively.

The experimental isotherm of 4NP (pK_a = 7.1) on B10(II) activated carbon illustrated the important influence of pH on adsorption capacity (Muller *et al.*, 1980). For high solute concentrations; changing the equilibrium pH from approximately 7 to 11 reduced the adsorption of 4NP by 70% (Muller *et al.*, 1980). Below pH 6.8 no further increase in adsorption capacity was noted. Similar results for adsorption of 2,4-dinitrophenol on Columbia LCK carbon and 4NP on GAC (Cal. 24/32 mesh) are reported by Zogorski and Faust (1978), and Suzuki and Takeuchi (1986), respectively. These studies also indicated that solutes of unionized form are more easily adsorbed onto activated carbon than those of ionic form. The repulsive forces between the anionic sorbate and the adsorbent were considered as the cause for the significant decreases in adsorption capacity at high pH.

Gomez Serrano *et al.* (1992) studied the adsorption of 4NP from a $NaOH/H_3PO_4$ buffered aqueous solution on 1.5 mm particle size AC (supplied by Merk) at pH 2, 7, and 8.5. At acidic pHs, the 4NP adsorption was found to be markedly higher than at neutral and weakly

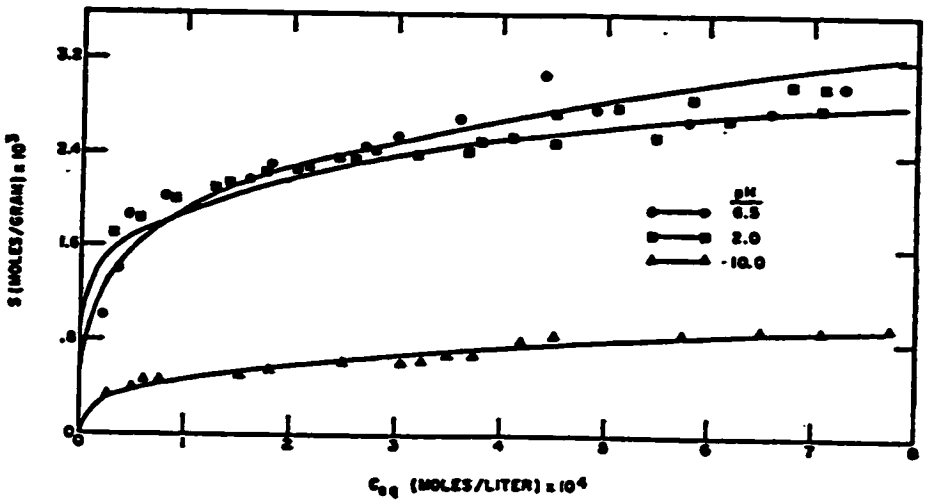

Fig 2.2 Isotherms for p-nitrophenol(4NP) at different pH on coconut-shell based GAC (Columbia, LC Grade). (Source: Snoeyink *et al.*, 1969)

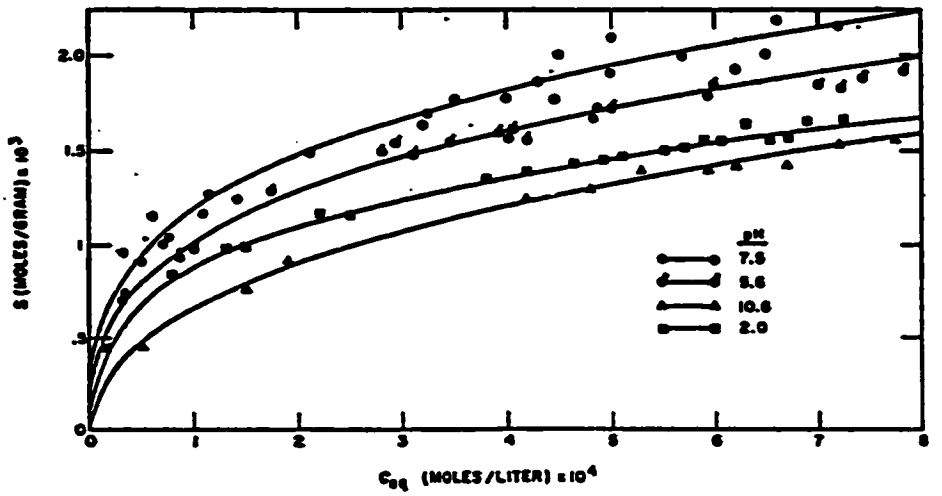

Fig. 2.3 Isotherms for phenol at different pH on coconut-shell based GAC (Columbia, LC Grade). (Source: Snoeyink *et al.*, 1969)

basic pHs. They hypothesized that the greater 4NP adsorption at pH 2 is consistent with a lesser competition for active sites between 4NP and anion species from H_3PO_4 dissociation. At neutral and basic pHs, OH^- competes more successfully with 4NP for active centers on the adsorbent surface.

Karimi-Jashni (1994) and Karimi-Jashni and Narbaitz (1997) investigated the effect of pH on adsorption equilibrium and adsorption kinetics. Phenol and 2-nitrophenol (2NP) were used as organic pollutants and F-400 and WV-B activated carbons as adsorbents. Isotherm studies showed that 2NP adsorption by GAC was markedly enhanced at the acidic pH, with no appreciable difference between pH 1 to 7 (Fig. 2.4). However at pH 13 the adsorption capacities were markedly lower. Similar results were achieved for WV-B. The effect of pH on adsorption was also investigated using the bottle-point method with a single fixed mass of GAC. Both GACs were similarly impacted by pH variation (Fig.2.5). Adsorption of 2NP was almost constant over the pH range 1 to 7 and dropped off rapidly at pHs greater than its pK_a (pH = 7.23). Experimental data for phenol and the two GACs showed that they have similar adsorption capacities and were similarly impacted by pH (Fig. 2.6). Maximum adsorption of phenol on F-400 occurred over the pH range 4.6 to 7 and it dropped off at pH values greater than 7. Note that the pK_a of phenol was 9.99. In general, adsorption of 2NP and phenol was much higher at low pH (i.e., the compounds are present in the undissociated form) than at high pH (i.e., the compounds are present in the dissociated form).

Summarizing, for all phenolic compounds, decreased adsorption has been observed as pH increases. Research indicates that maximum adsorption is generally attained at pHs slightly

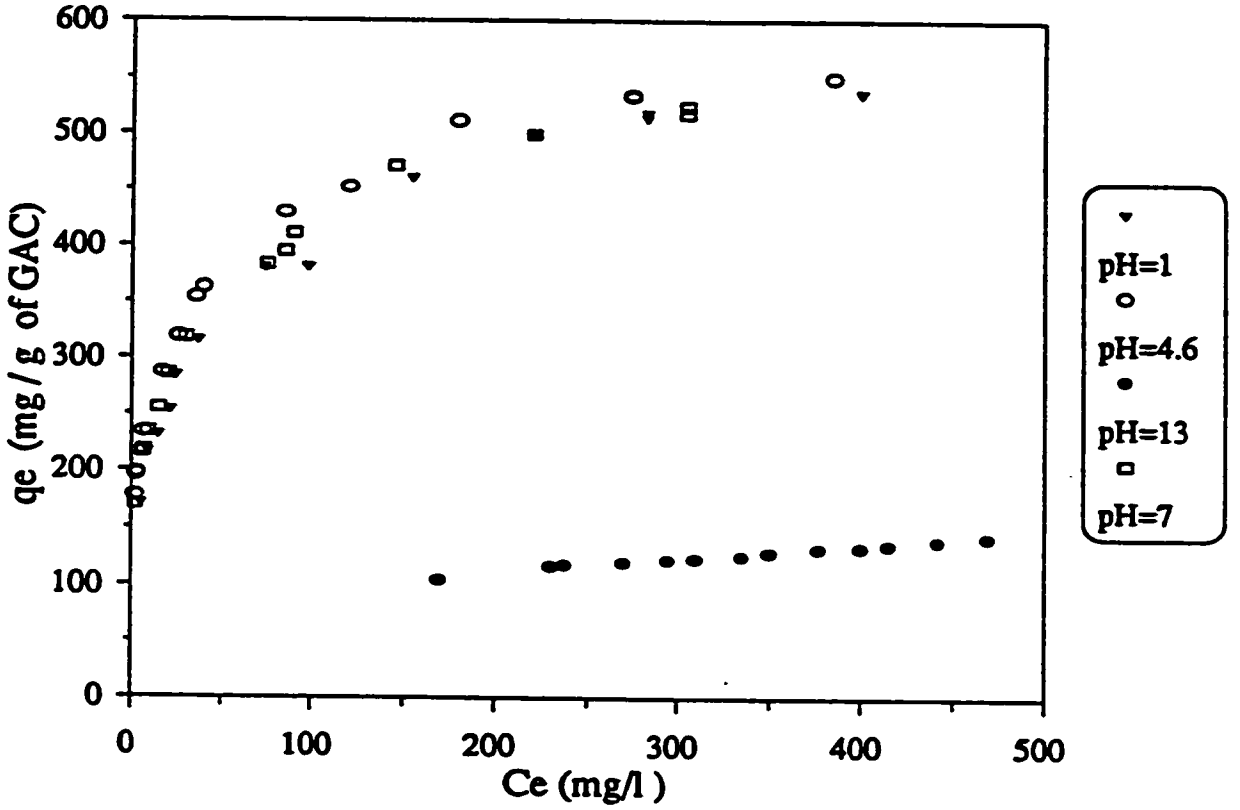

Fig. 2.4 Effect of pH on adsorption isotherms of 2NP on F-400.
(Source: Karimi-Jashni, 1994)

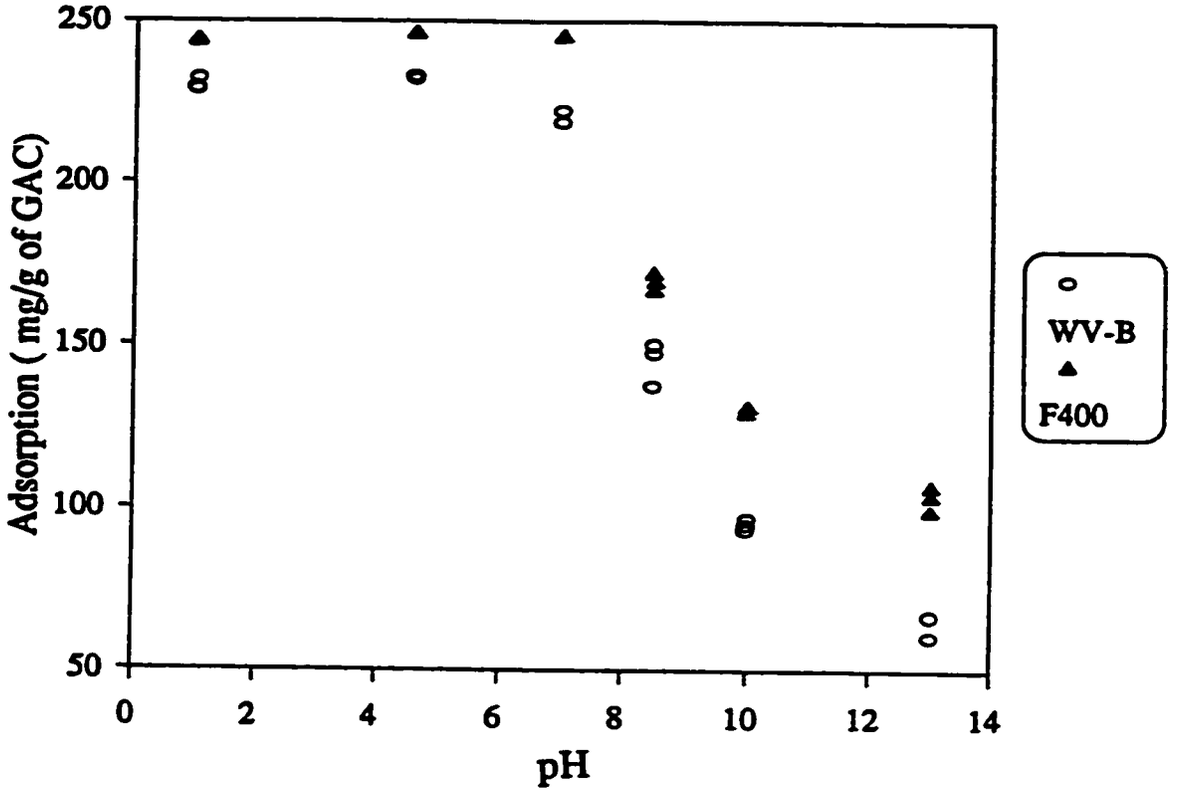

Fig. 2.5 Effect of pH on adsorption of 2NP on F-400 and WV-B (C_i=500 mg/L, GAC, 2g/L). (Source: Karimi-Jashni, 1994)

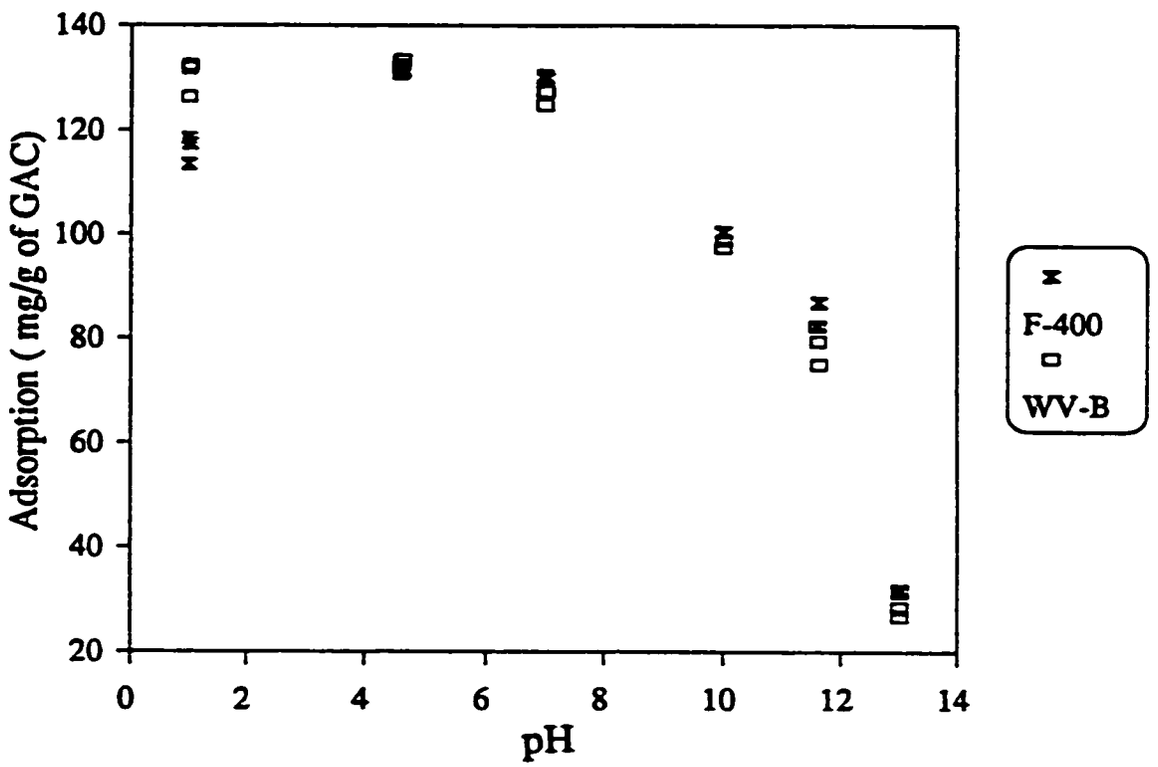

Fig. 2.6 Effect of pH on adsorption of phenol on F-400 and WV-B (C_i=300 mg/L, GAC, 2g/L). (Source: Karimi-Jashni, 1994)

lower than the pK_as and the following mechanisms may be responsible for a large decrease in the amount adsorbed at pH values greater than the pK_a of the adsorbate.

1- The dissociated form is more soluble in solution (Mattson and Mark, 1971) thus, is less adsorbable.

2- The nature of the carbon surface is apparently altered in some manner by the acid or base used for pH adjustment (Ward and Getzen, 1970). The surface of activated carbon is negatively charged in the neutral pH ranges as a result of the dissociation of surface carboxylic groups. A reduction in pH can be expected to improve adsorption since the protonation of the carboxylic functional group on both the organic acids in solution and the carbon surface reduces electrostatic repulsion forces (Semmens *et al.*, 1986), therefore promoting a greater degree of adsorption.

3- The anionic form of compounds may have different mechanisms of adsorption (Karimi-Jashni, 1994).

4- Repulsive forces between the anionic adsorbate species and adsorbate on the adsorbent can also be significant at high pH. Increased negative surface charges at high pH values may be caused by physical adsorption of OH^- or by dissociation of very weakly acidic surface functional groups (Cooney and Wijaya, 1987 and Snoeyink *et al.*, 1969).

5- The lighter and hence more mobile OH^- anion may compete more successfully with adsorbates for active sites on the adsorbent surface at high pH (Gomez Serrano *et al.*, 1992).

2.5.6.2 Effect of pH on Adsorption Kinetics

Fig. 2.7 shows the effect of solution pH on the observed rate of uptake of 3-dodecylbenzenesulfonate (pK_a 1.5), an anionic surface active agent, by 0.126 mm Columbia carbon (Weber and Morris, 1963). The authors mentioned several possible explanations for the observed pH effects. Because most carbons bear net negative charges, the uncharged molecular species of the alkylbenzenesulfonates would be expected to be taken up by the carbon more rapidly than the negatively charged ionic species. The effect of hydrogen ion concentration is observed even in pH ranges for which the relative changes in absolute concentration of the two species of solutes are negligible. Weber and Morris (1963) suggested the increase in rate observed for decreasing pH may be due to alteration in the carbon surface, particularly its electrokinetic character, with changing hydrogen ion concentration. Therefore, a decrease in pH probably results in a reduction of the negative charges at the surface of the carbon subsequently enhancing the adsorption of the negatively charged alkylbenzenesulfonates.

The dependence of the initial removal rate of Columbia LCK carbon adsorption with hydrogen ion concentration for 2,4-dinitrophenol ($pK_a = 4.1$) and 4-chlorophenol ($pK_a = 9.4$) are shown in Figs. 2.8 and 2.9 (Zogorski and Faust, 1976-b). The rates of adsorption of these two compounds are most rapid at hydrogen ion concentrations greater than 10^{-5} (for 2,4-dinitrophenol) and $10^{-7.5}$ (for 4-chlorophenol). Also, it is evident that the presence of high concentration of hydrogen ions does not influence the initial removal rate of adsorption of these phenolics. Moreover, increasing the pH value from 5 to 6.3 decreased the removal rate of 2,4-dinitrophenol by 20% and further increasing the pH beyond 6.3 appears to have no subsequent influence. While, a very rapid and almost linear decrease in the removal rate of 4-chlorophenol occurs at pH values greater than 9. The repulsive forces between

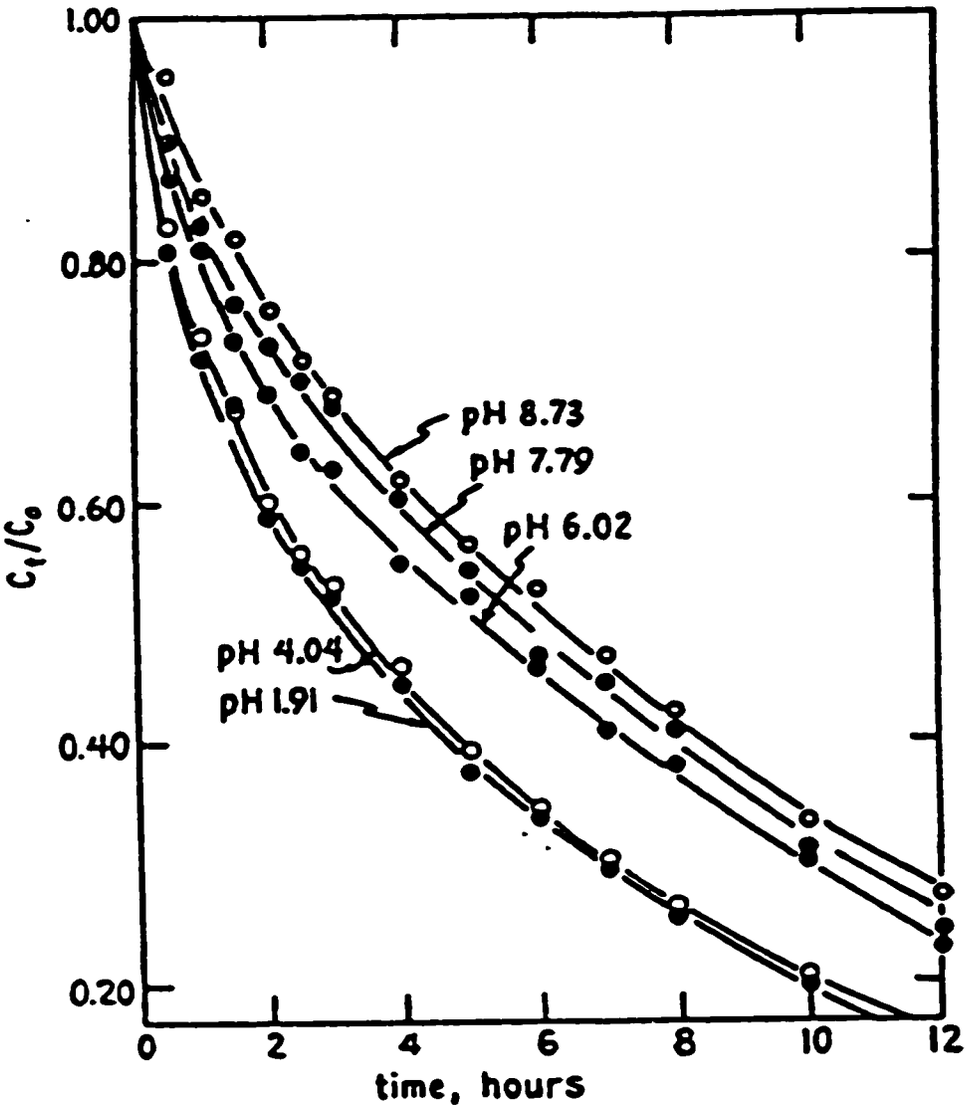

Fig. 2.7 Effect of pH on rate of 3-dodecylbenzensulfonate adsorption onto Columbia carbon. (Source: Weber and Moris, 1963)

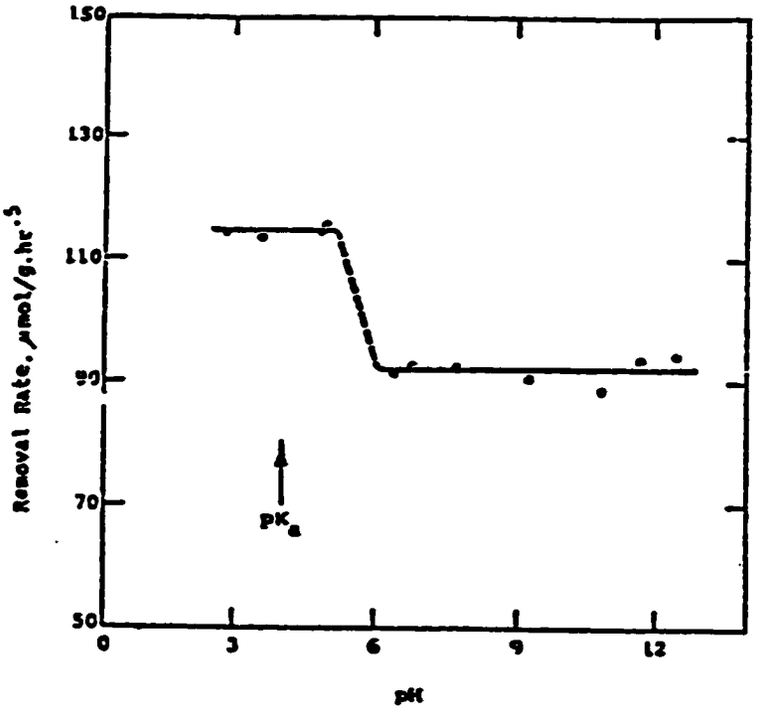

Fig.2.8 Effect of pH on the rate of adsorption of 2,4-dinitrophenol on GAC (Columbia, LCK). (Source: Zogorski and Faust, 1976-b)

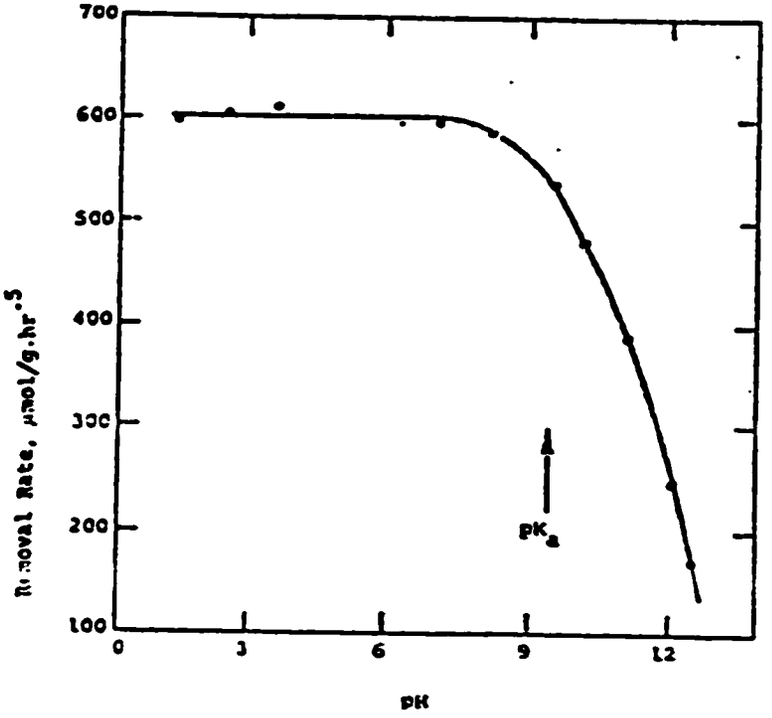

Fig. 2.9 Effect of pH on the rate of adsorption of 2,4-dichlorophenol on GAC (Columbia, LCK). (Source: Zogorski and Faust, 1976-b)

adsorbate/adsorbent and adsorbate/adsorbate were hypothesized for decrease in initial removal rate at high pHs.

Gomez Serrano *et al.* (1992) studied the kinetic adsorption of 4NP on 1.5 mm activated carbon (supplied by Merck) at pH 2 and 8.5. They concluded that the initial removal rate was faster at acidic pH than at basic pH. Karimi-Jashni (1994) also investigated the effect of pH on the adsorption kinetics of 2NP of F-400 and WV-B activated carbons. He observed that at low pH, where molecules were in undissociated form, the rate of adsorption was faster than at high pH (dissociated form of molecules). He observed that the maximum rate of adsorption occurred at pH 4.6 and there was a sharp decrease in the removal rate above a pH greater than pK_a of 2NP (pH 7.23).

2.6 Desorption and Reversibility

2.6.1 Desorption

Desorption isotherms are used to determine the extent of reversibility. The extent of reversibility is a function of the strength of the sorbent-sorbate bond. Most research relating to desorption has been conducted on single-solute systems by using batch desorption procedures (Yonge *et al.*, 1985; Narbaitz and Cen, 1994). Single cycle or multiple cycles of the bottle-point type technique can be used for desorption experiments. In some cases, a single GAC dose is tested; in others the tests are conducted for many doses (Narbaitz and Cen, 1994); yet in others large batch reactors are used (Snoeyink *et al.* 1969). The first step is always loading the GAC with adsorbate using a batch loading procedure, such as the bottle-point technique. Following equilibration, the liquid and the AC are separated by filtration or by sedimentation. In the case of filtration, the GAC retained on the filters is rinsed back into a clean glass bottle with sorbate-free solution (Narbaitz, 1985). In the case

of GAC separation by sedimentation a large fraction of the solution is decanted and replaced with sorbate-free solution (Snoeyink *et. al*, 1969). The bottles are then agitated until a new equilibrium is reached. The liquid phase concentration is then measured and the solid phase loading on the GAC is calculated via a mass balance using

$$q_d = q_{ad} - \frac{V(C_d - C_{od})}{M} \tag{2-5}$$

where q_d is the solid phase concentration after the desorption step (mg/g of GAC); q_{ad} is the solid phase concentration after adsorption equilibrium (mg/g of GAC); C_d is the liquid phase concentration after the desorption step (mg/L); V is the volume of the desorption solution (L); M is the mass of activated carbon in each bottle (g); and C_{od} is the initial liquid phase concentration of the desorption solution (mg/L). In the case of multiple desorption cycles this process is repeated until the resultant liquid phase sorbate concentration is less than the analytical detection limit. The solid phase loading on the GAC is calculated after each desorption step by using

$$(q_d)_i = q_{ad} - \sum \frac{(C_{d_i} - C_{od_i})V_i}{M} \tag{2-6}$$

where $(q_d)_i$ is the equilibrium solid phase loading at the end of desorption step i (mg/g of GAC); M is the mass of GAC in the desorption bottle (g); q_{ad} is the equilibrium solid phase concentration after the initial adsorption loading step (mg/g of GAC); C_{odi} is the liquid phase concentration at the start of desorption step i (mg/L); and C_{di} is the equilibrium liquid phase concentration at the end of desorption cycle i and V_i is the volume of the desorption solution of step i.

2. 6.2 Effect of pH on Desorption Equilibria

Summers and Roberts (1988a) conducted desorption experiments with four humic substances under a variety of experimental conditions. Desorption was found to occur at pH above 10.5 and the mass desorbed ranged from 0 to 25% (at pH 10.5) of the original mass adsorbed. Desorption at elevated pHs was explained in terms of surface electrostatics. Increasing pH to 11 during desorption tests results in repulsion between negatively charged humic macromolecules and the adsorbent surface. Davis (1980) observed that lacustrine organic matter adsorbed on aluminum oxide at pH 5, partially desorbed at pH 9 and completely desorbed at pH 11.

NaOH has been used as a reactive chemical in the regeneration of GAC used for treatment of phenolic compounds (Fox *et al.*, 1970; Himmelstein *et al.*, 1973; Goto *et al.*, 1986; and Newcombe and Drikas, 1993). Adsorbed phenol reacts with the caustic soda to form sodium phenate which is readily desorbed and carried out of the carbon bed in the regenerant stream. Goto *et al.* (1986) found that the total amount of sodium phenate desorbed from GAC was only 70% of the adsorbed phenol and the adsorptive capacity of GAC gradually decreased with multiple regeneration cycles.

Karimi-Jashni (1994) and Karimi-Jashni and Narbaitz (1997) investigated the effect of pH on desorption equilibria and desorption kinetics. The study was conducted using 2NP and phenol as organic pollutants and F-400 and WV-B activated carbons as adsorbates. For both compounds the extent of desorption was much higher at pHs greater than the pK_a, i.e., when the adsorbate is in its dissociated form. Maximum desorption of 2NP occurred at pH greater

than pK_a (pH = 7.23) and decreased dramatically at pHs less than pK_a (Fig. 2.10). Also minimum desorption of phenol occurred at pHs smaller than the pK_a (pH = 9.99) and increased sharply at pHs greater than pK_a (Fig. 2.11). Both GACs were similarly impacted by the pH.

2.6.3 Effect of pH on Desorption Kinetics

There is limited information available related to the effect of pH on desorption kinetics. Karimi-Jashni (1994) studied the kinetic desorption of 2NP from preloaded F-400 and WV-B at pHs 1, 4.6, and 13. He concluded that the maximum rate of desorption occurred for pH 13 and a sharp decrease in the desorption rate was observed for acidic pHs. He also observed that the magnitude and nature of the pH effect varied from adsorbent to adsorbent.

2.6.4 Reversibility

Generally, the type of adsorption can be divided into three groups: completely reversible, completely irreversible, and partially irreversible.

Identical adsorption and desorption isotherms represent completely reversible adsorption. The desorption isotherm overlaps the adsorption isotherm and C_d and q_d from the desorption isotherms can also be described by the adsorption isotherm. Karimi-Jashni (1994) showed that the adsorption of 2NP on F-400 and WV-B is completely reversible at different pHs and the presence of 1% NaCl had no significant influence on the reversibility (Fig. 2.12).

Irreversible adsorption is caused by chemisorptions or hysteresis effects. For completely irreversible adsorption, C_d equals C_{od} and the contaminant liquid phase and solid phase

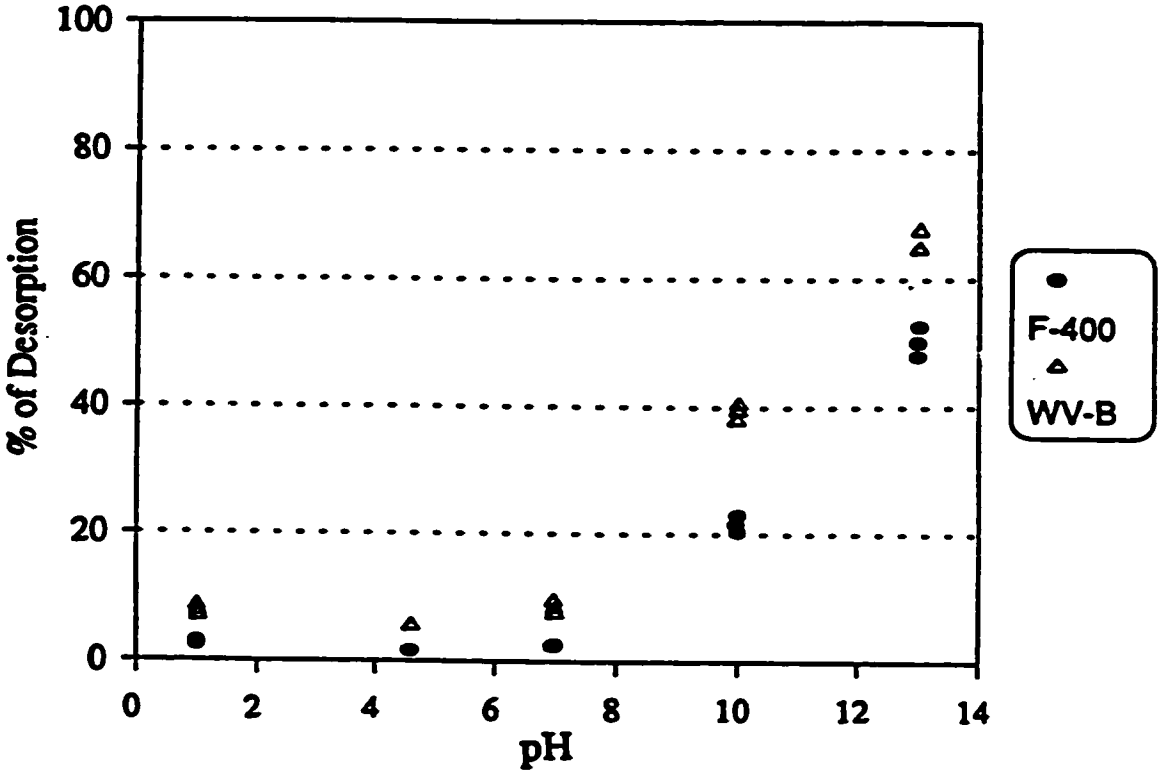

Fig. 2.10 Effect of pH on desorption of 2NP from F-400 and WV-B.
(Source: Karimi-Jashni, 1994)

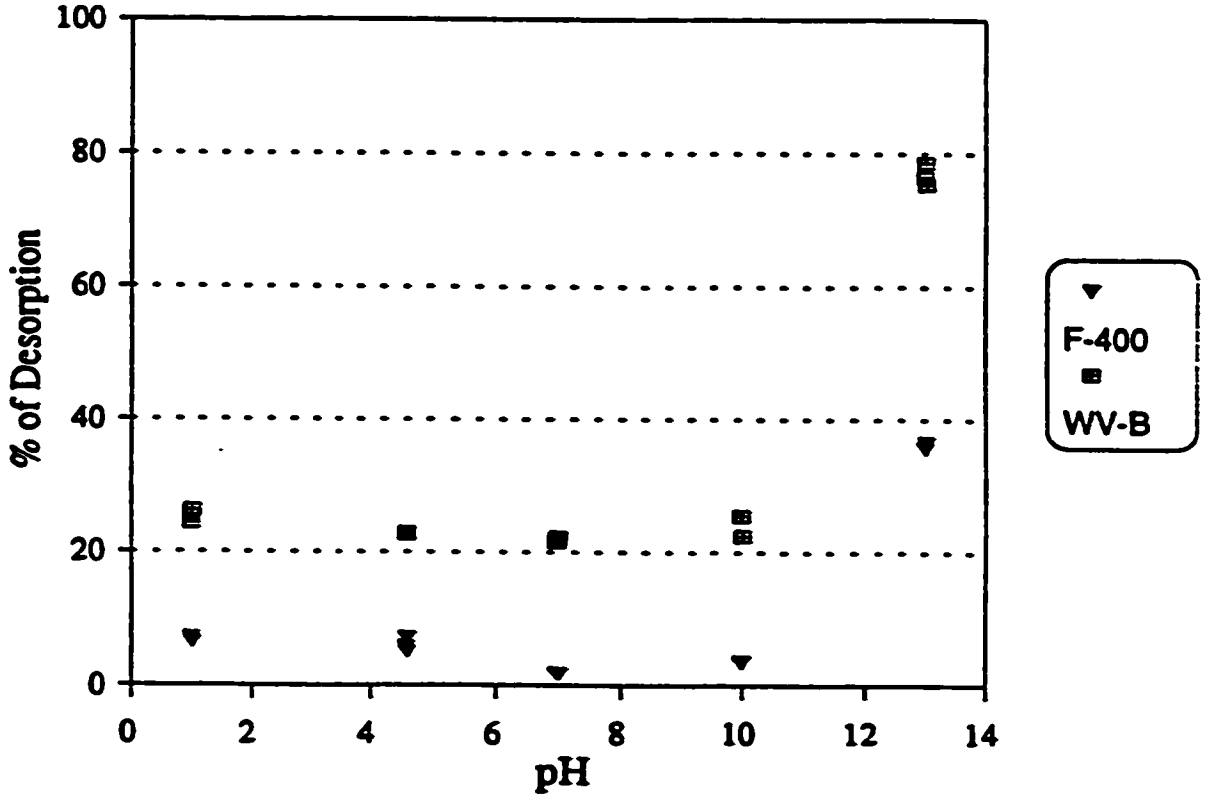

Fig. 2.11 Effect of pH on desorption of phenol from F-400 and WV-B.
(Source: Karimi-Jashni, 1994)

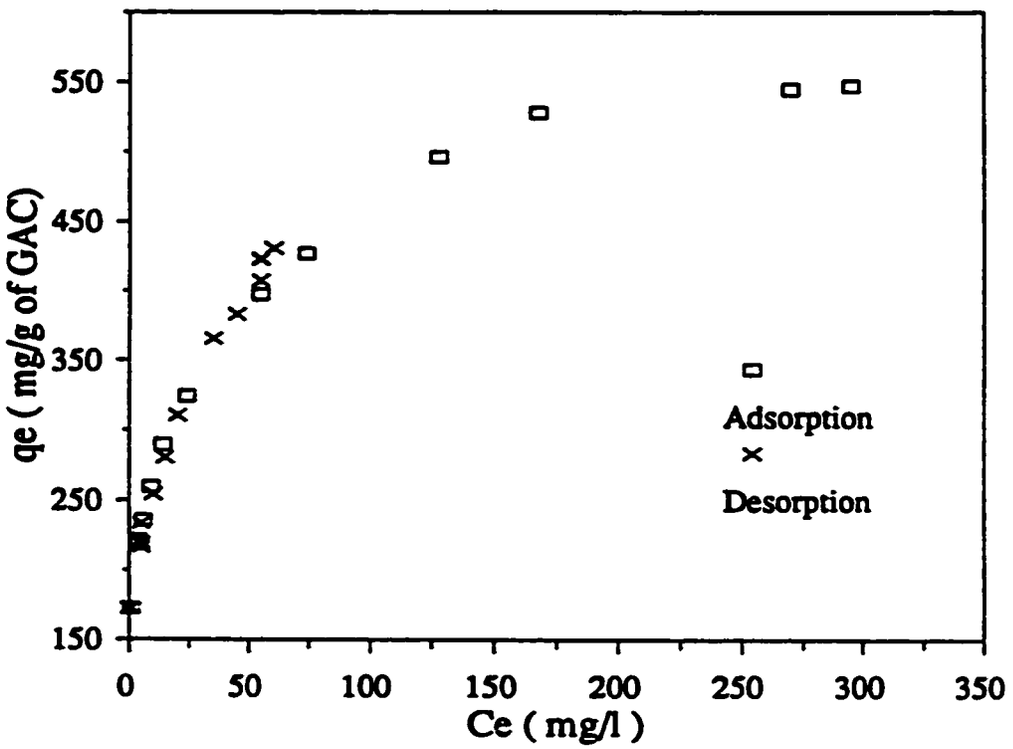

Fig. 2.12 2NP adsorption and desorption isotherms at pH 4.6 (F-400, desorption solution: 1% NaCl solution). (Source: Karimi-Jashni, 1994)

concentration remains unchanged regardless of the initial liquid phase concentration of the desorption solution. So, the solid phase concentration is only a function of the loading attained during the adsorption cycle, and the desorption isotherms are horizontal, constant loading lines connecting the adsorption loading with the ordinate.

Partially irreversible adsorption is similar to that of the fully irreversible case. These isotherms have higher loadings than the adsorption isotherm and they are slightly sloped. Fig. 2.13 represents the phenol desorption isotherms for two masses of Columbia LC carbon, which is an example of partially irreversible adsorption (Snoeyink *et al.* 1969). These desorption isotherms were obtained from multiple desorption cycles and the solid triangles and circles represent the conditions at the end of a cycle. Narbaitz and Cen (1994) used a single desorption cycle of different doses of F-400 GAC to obtain phenol desorption isotherms (Fig. 2.14). This figure shows that phenol adsorption on F-400 is also partially irreversible.

Chemisorption is the most logical explanation for irreversible adsorption (Yonge *et. al*, 1985). Depending on the type of surface functional group and the type of adsorbent, a relatively strong bond that resists desorption can be formed. Therefore, the number of strong bonds will determine the degree of irreversibility. Physical adsorption is primarily caused by Van der Waals forces, which creates weaker bonds, and should be reversible. Snoeyink (1968) has shown that only 50% of the adsorbed phenol was desorbed from a Columbia LC GAC. In contrast, Schultz (1982) obtained 100% adsorption reversibility for phenol adsorbed on a powdered coconut-shell-based activated carbon. Pirbazari and Weber (1981-a and 1981-b) indicated that benzene exhibits complete reversibility, while polychlorinated

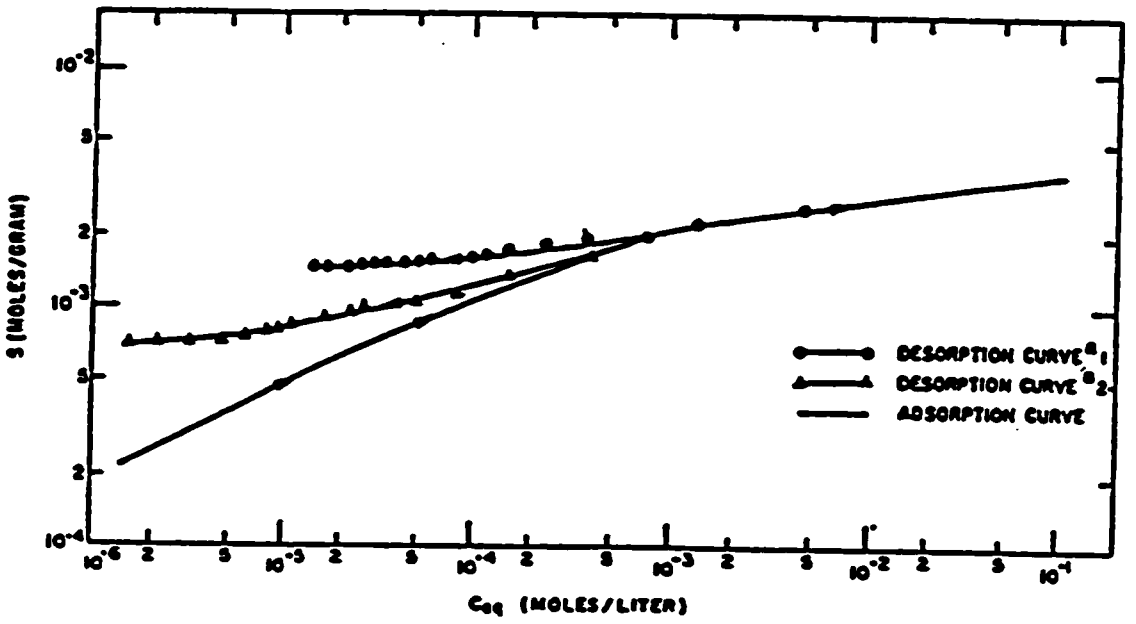

Fig. 2.13 Adsorption and desorption isotherms of phenol.
(Source: Snoeyink *et al.*, 1969)

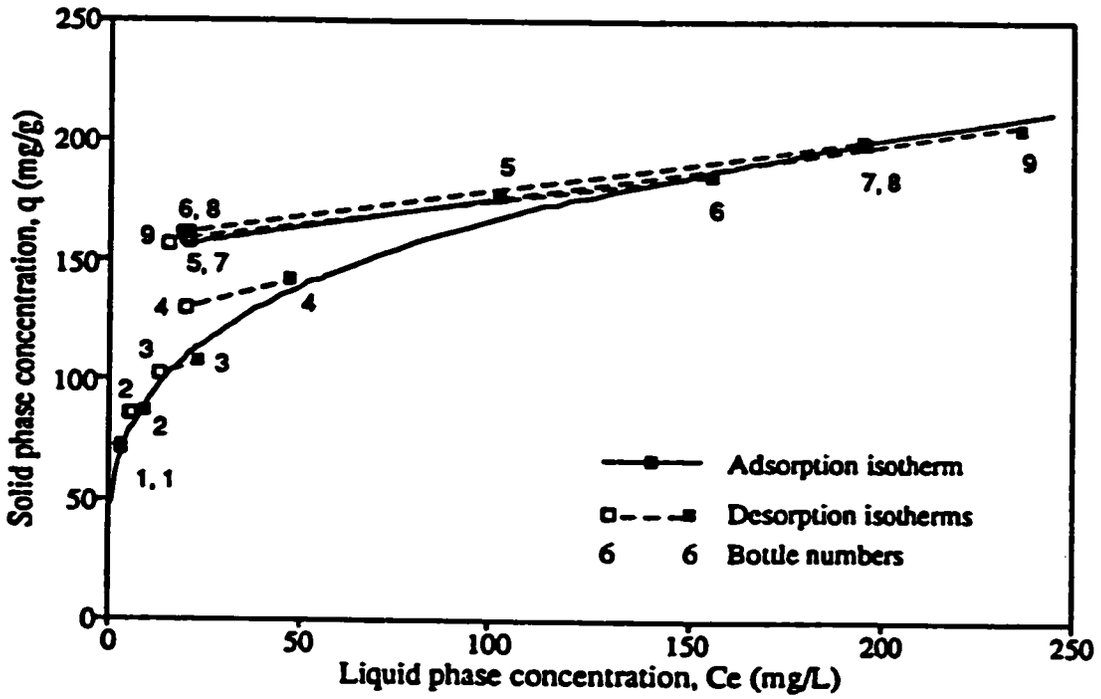

Fig. 2.14 Phenol adsorption and desorption isotherms (desorption solution: 1% NaCl solution). (Source: Narbaitz and Cen, 1994)

biphenyls behaved completely irreversibly in batch and continuous-flow column studies on GAC. Leyva-Ramos (1989) observed that the adsorption of the anionic detergent sodium dodecyl benzene sulfonate (SDBS) onto a wood-based activated carbon from aqueous solutions was irreversible and the order of magnitude of the heat of adsorption indicates that SDBS is chemisorbed on activated carbon. Thus, these results prove that the occurrence of irreversible adsorption is a function of both adsorbate and adsorbent type.

Yonge *et al.* (1985) tested the desorption of 2-ethylphenol (2-EP), O-cresol (O-C), O-methoxy phenol (O-M), 4-isopropyl phenol (4-IPP), and phenol from F-400 carbon. These experiments showed a high degree of irreversibility associated with the adsorption of each of the sorbates. They hypothesized that the dominant adsorption mechanism is high-energy bonding to specific functional groups on the activated carbon surfaces. They also found that phenol and 4-IPP had the lowest degree of irreversible adsorption while 2-EP, O-C and O-M were the most irreversible. They suggested that the addition of the methyl, ethyl and methoxy groups in the ortho position of the phenol molecule intensifies the binding energy to the activated carbon surface functional group. This can result in an inductive effect that is stronger than that exhibited by the same group in the para position. They hypothesised that this more intense inductive effect could result in a stronger sorbate-sorbent bond and therefore, a higher degree of irreversibility as observed for the ortho-substituted phenols.

Vidic *et al.* (1990, 1993) observed that the adsorption of phenol, o-cresol, and 3-ethylphenol on F-400 carbon was more irreversible in the presence of oxygen due to their reaction with the AC to form polymeric species on the carbon surface. However, Vidic *et al.* (1993), reported that experiments with three nitrophenols (2-nitrophenol, 3-nitrophenol, 4-

nitrophenol) showed almost 100% reversibility in the presence and absence of oxygen from loaded F-400 carbon. The lack of polymerization in the case of adsorption of nitrophenols was the reason for their reversibility. This shows that not all phenolics adsorb irreversibly even on the same carbon. They also showed that some adsorbates adsorb reversibly on some carbons and partially irreversibly on others.

2.7 Electrochemical Oxidation of Phenol

During the reactivation of phenol-loaded GAC the adsorbed phenol may desorb to bulk electrolyte and eventually can become oxidize on the surface of electrodes. Thus it is of interest to investigate the oxidation of phenol. The anodic oxidation of phenol has been studied by various researchers (Sharifian and Kirk, 1986; Kotz *et al.*, 1991; Gattrell and Kirk, 1993; Iotov and Kalcheva, 1998; Taher and Savall, 1999). The general oxidation pathways of phenol decomposition are given in Fig. 2.15. Further oxidation leads to intermediates that are usually less stable than the quinone and quickly decompose forming a variety of products including maleic and oxalic acids and eventually CO_2. Catechol solutions are grey in colour, p-benzoquinone solutions are yellow and hydroquinone solutions are light brown.

Sharifian and Kirk (1986) have monitored the concentrations of phenol, benzoquinone, malic acid, and carbon dioxide in an electrochemical reactor as a function of time (Fig. 2.16). In their study the CO_2 concentration was not a true concentration but was the number of moles of CO_2 purged from the electrolyte and was reported as mmol/L of anolyte. As expected from the reaction sequence, benzoquinone concentration increased initially as phenol started to be oxidized; its concentration began to decrease after 1.5

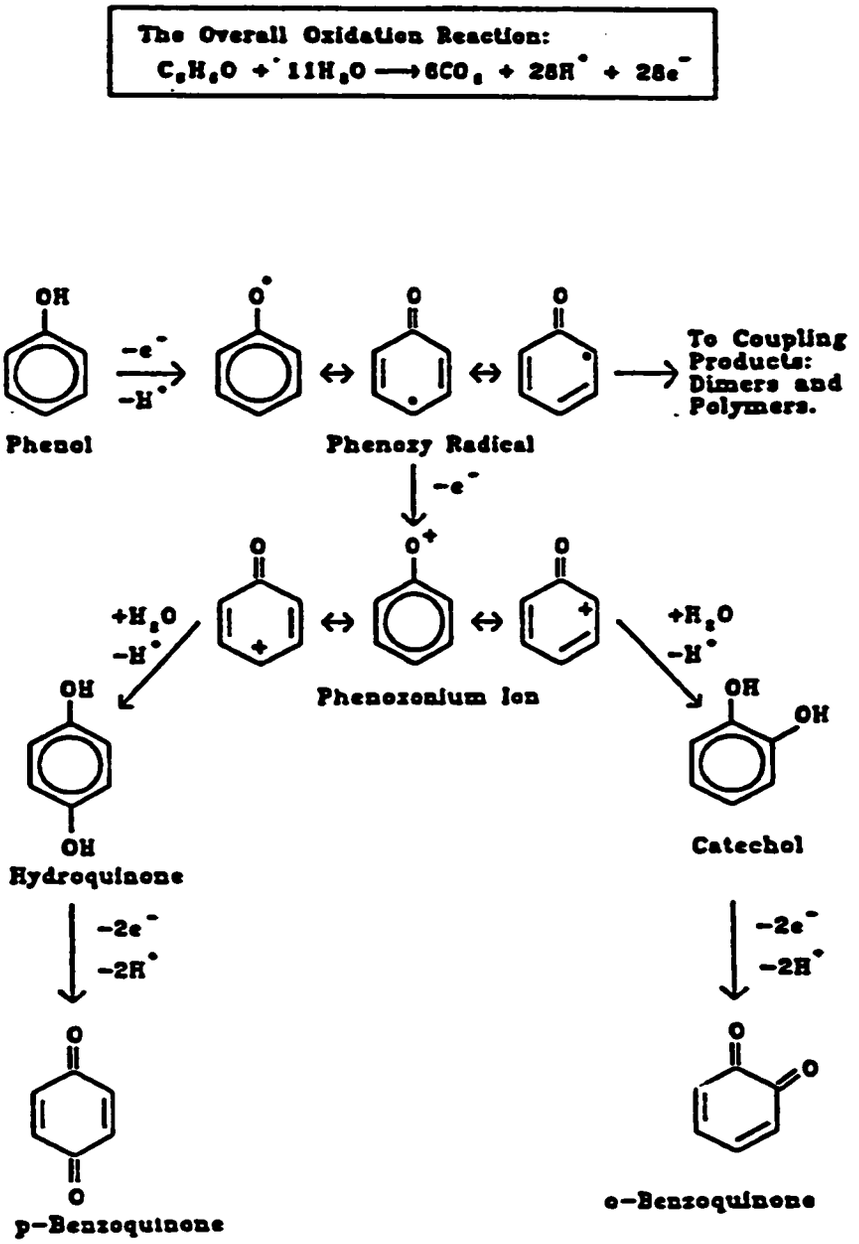

Fig. 2.15 The oxidation pathways of phenol (source: Gattrell and Kirk. 1990).

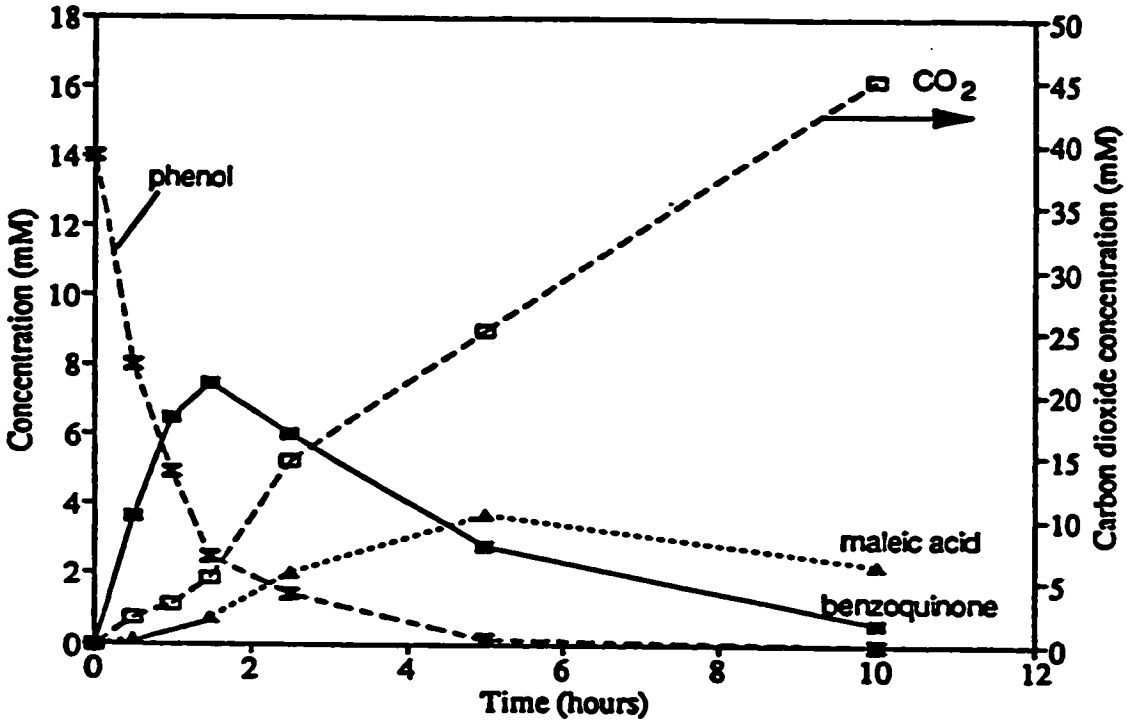

Fig. 2.16 Concentration of phenol, benzoquinone, maleic acid, and carbon dioxide as a function of electrolysis time for 0.014 M phenol in 1.0 M sulfuric acid solution at a cell current of 2A. (source: Sharifian and Kirk, 1986).

hours due to oxidation. Malic acid concentration built up more slowly and began to decay after 5 hours. At longer times, the rate of CO_2 production remained relatively constant over 10 hours and this indicated possibly complete oxidation. Sharifian and Kirk (1986) concluded that the CO_2 formation depended on the degree of oxidation and was favoured by high currents, acid concentration (electrolyte), temperature, and dissolved oxygen. Low concentrations of phenol (≤0.0035 M = 329 mg/L) displayed greater conversion to carbon dioxide than high concentrations. Hence the experimental conditions affected the degree of oxidation and consequently the CO_2 production.

A comparison of typical electrode materials such as platinized titanium and lead dioxide with the performance of the SnO_2 electrode for TOC removal during phenol oxidation was conducted by Kotz *et al.* (1991) and is shown in Fig. 2.17. The SnO_2 electrode exhibited a higher efficiency for TOC elimination than Pt or even PbO_2. For the total elimination of TOC on SnO_2, 8 ampere-hours (Ah) were needed, while Pt as well as PbO_2 removed TOC rather ineffectively. The low efficiency of Pt and PbO_2 was due to the relatively large leakage current for oxygen evolution (Kotz *et al.*, 1991). In addition, it has been demonstrated for platinum anodes, that the oxidation reaction stops with products such as malic acid or oxalic acid (Comninellis and Plattner, 1988). For example Kotz *et al.* (1991) showed that by using the SnO_2 electrode with a cell voltage of 4V, elimination of 1 kg of phenol ($1m^3$ at a concentration of 1000 ppm) consumed 20 kWh, while for the elimination of 1 kg of TOC 110 kWh were needed. Hence, total elimination of TOC was possible by using a proper anode material and higher charges.

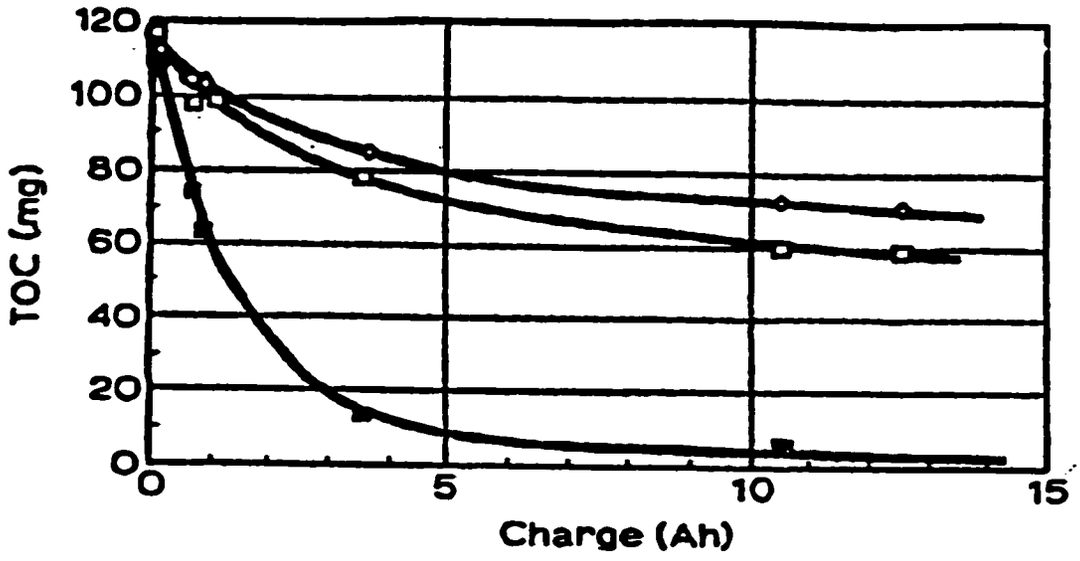

Fig. 2.17 Removal of TOC originating from 1000 ppm phenol in the electrolyte as a function of consumed charge for different electrode materials for ( ) SnO_2, ( ) PbO_2 and ( ) Pt. Current density: 30 mA Cm^{-2}. (source: Kotz *et al.*, 1991).

2.8 Previous Studies on Activated Carbon Reactivation

The adsorption capacity of spent GAC can be reactivated by thermal, chemical, biological, or electrochemical techniques. The following provides a brief review of previous studies on the reactivation of GAC with an emphasis when possible on phenolics-loaded GAC.

2.8.1 Thermal Reactivation

Since the early 1950s thermal reactivation has been a standard GAC reactivation process in the United States. The process has also been used extensively worldwide for reactivating GAC from potable water treatment plants. The thermal reactivation process involves three steps: drying, baking (pyrolysis of adsorbates) and activating (oxidation of the residue from the adsorbate). During the first step wet spent GAC enters a furnace, it is heated to almost 100°C and dried. During baking, the temperature increases from 100 to 815°C. which causes the adsorbed organics to be thoroughly carbonized. This is accompanied by the evolution of gases and the formation of a carbon residue in the micropores of the AC. The objective of the reactivating step is to oxidize the carbon residue with minimum damage to the basic pore structure, thereby maximizing the restoration of the GAC's original properties. The activating gas temperature during this step is about 930°C, while the AC temperature range is from 815 to 900°C. A flue gas supplemented by varying amounts of additional steam and limited oxygen produces the desired oxidizing atmosphere (US EPA, 1973).

The most important phase of the reactivation process is the activation, with the critical parameters being carbon temperature, duration of the activation, and the steam or carbon dioxide concentration in the activating gas mixture. If the temperature increase (controlled by the heat input) is too fast for a given time of reactivation, the process will cause an attack

on the base GAC, which can result in enlarged pores and reduced adsorptive capacity because of the reduction in surface area. On the other hand, too slow a temperature increase for a given reactivation time will result in reactivation furnaces that are larger than necessary and possibly in failure to remove all of the adsorbate. This can also cause reduced adsorptive capacity because of the inaccessibility of partially filled pores. Studies of thermal reactivation have focused on the optimum conditions to restore the maximum GAC capacity and to retain, as much as possible, the original pore structure (Knappe *et al.*, 1992; Waer *et al.*, 1992; Cannon *et al.*, 1994; Sebastiani *et al.*, 1994; Waer and Snoeyink, 1994).

Kuo *et al.* (1998) reported the results of the thermal reactivation of saturated GAC, which was used to treat wastewater for reuse, at the County Sanitation Districts of Los Angeles County's Pomona Water Reclamation plant. They observed that after 10 reactivation cycles with an average of 10% makeup of virgin GAC per reactivation cycle, the Iodine Number dropped from 1,000 mg/g to a plateau value of 600 mg/g; apparent density decreased slightly; ash content increased steadily from 6.5% to more than 15% after 15 reactivation cycles. After 20 reactivation cycles the GAC filters exerted a TOC removal of 20% while its initial removal was more than 80%. The removal of true color by the reactivated GAC decreased from 90% initially to 30%. van Vliet and Venter (1984) studied the thermal reactivation of spent GAC from a GAC contactor treating secondary effluent. The optimum reactivation conditions were 8 minutes oxidation at 800°C in an infrared furnace. They were able to restore only 70% of the virgin micropore volume (on a unit bed volume basis) after the fourth reactivation cycle.

Chiang *et al.* (1997) investigated thermal reactivation of nine compounds, i.e., phenol, 2-aminophenol, aniline, 2-chlorophenol, chlorobenzene, β-naphthol, naphthalene, and α-chloronaphthalene. The exhausted GAC from column tests served as the spent adsorbents for the reactivation experiments. It was observed that the reactivation efficiency of the GAC was not dependent on the adsorbate characteristics and was highly related to the weight loss of the GAC during the thermal oxidation process. The maximum reactivation efficiency of GAC saturated with phenol was 88% at 900°C and a steam pressure of 0.12 atm.

Waer *et al.* (1992) investigated fluidized-bed reactivation to determine the effects of reactivation temperature and time on volume losses and recovery of adsorptive capacity. For coal-based GAC loaded with naturally occurring organic material (NOM) and methylene blue (MB), GAC capacity was returned to that of virgin GAC at a temperature of 850°C in 15 minutes. Shorter times and lower temperatures resulted in a loss of adsorptive capacity. Longer times resulted in increased capacity for large molecules but the same or reduced capacity for small adsorbates. Surface area and micropore volume analysis for MB-loaded GAC at 850°C showed that both BET surface area and micropore volume increased with increasing time of reactivation. The 15 min reactivation time sample had a BET surface area and micropore volume very close to the virgin GAC. The 5 min reactivation time sample had a lower BET surface area and micropore volume than virgin GAC. The 30 min reactivation showed slightly higher BET surface area and about the same micropore volume as the virgin GAC. Waer *et al.* (1992) concluded that reactivation for times longer than 15 min at 850°C produced a carbon with lower density caused primarily by the increase in mesopore volume.

Although thermal reactivation is the most common reactivation method in water applications, it has some disadvantages. The main disadvantages of thermal reactivation are: 1) the loss of carbon (5-15% per cycle) due to oxidation and attrition (Schuliger and MacCrum, 1974); 2) the high energy cost of heating the GAC to approximately 800°C (Clark and Lykins, 1989); 3) the transfer of contaminants to the air phase; and 4) the extremely high cost for small facilities (Adams and Clark, 1989).

The loss of carbon could be due to transport and in-furnace losses. Transport losses are fairly constant at 2-3%. In-furnace losses vary widely and depend on the type of carbon used. Because lignite-based GAC is softer than bituminous coal-based GAC, GAC abrasion losses are suspected to be greater with this material. Lost GAC needs to be replaced with virgin GAC. Clark and Lykins (1989) have shown that the cost of purchasing replacement GAC can be up to four times greater than the energy costs for thermal reactivation systems.

Thermal reactivation has very high unit costs associated with small facilities and their operations. When spent carbon requirements are less than 680 kg/d, the on-site reactivation alternative is not cost effective (Adams and Clark, 1989). Thus, replacement of spent carbon with virgin carbon is recommended.

2.8.2 Chemical Reactivation

In some cases, chemical reactivation is a potentially feasible alternative to thermal reactivation. It has been used primarily in industrial systems designed to recover adsorbates. The basis of chemical reactivation is that organic adsorbates can be partially desorbed from GAC by conventional liquid solvents (Cooney *et al.* 1983; Martin and Ng, 1984 and 1985; Goto *et al.*, 1986; Tan and Liou, 1989; Mundale *et al.*, 1991; Ferro-Garcia *et al.*, 1993;

Newcombe and Drikas, 1993). The chemical reactivation of spent GAC can be achieved by two main categories of substances: inorganic chemical regenerants with oxidizing powers and chemical regenerants with solubilizing powers.

Rinkus *et al.* (1997) studied NaOH (regenerant with solubilising power) reactivation of GAC saturated with Pb and phenol via batch tests. Four variables were investigated: regenerant concentration (0, 0.1, and 1.0 N), regenerant to GAC mass ratio (5:1 and 10:1), regenerant temperature (22 and 80°C), and reactivation time (0.33, 1, 3, 7, and 21 days). Maximum reactivations of 47% for Pb and 48% for phenol were observed. The 1.0 N NaOH reactivated a higher percentage of both Pb and phenol when compared to the other regenerants. The 10:1 regenerant to GAC ratio resulted in increased reactivation over the 5:1 reactivation. Pb reactivation was slightly higher at 80°C than at 22°C whereas phenol reactivation was slightly lower at 80°C than at 22°C. Maximum reactivation for both Pb and phenol were observed within the first day of reactivation.

Chiang *et al.* (1997) used different solvents and a GAC saturated with nine different compounds (i.e., phenol, 2-aminophenol, aniline, 2-chlorophenol, chlorobenzene, β-naphthol, naphthalene, and α-chloronaphthalene) to investigate chemical reactivation. The chemical reactivation efficiency associated with the GAC saturated by the above compounds varied from 15.2 to 96.8%. The maximum reactivation efficiency of GAC saturated with phenol was 81.1%. It was observed that reactivation efficiency of the GAC by chemical treatment depends strictly on the properties of the adsorbates and the choice of chemical regenerant. For instance, the reactivation efficiency of GAC exhausted with the phenolic compounds, i.e. phenol, aniline, 2-chlorophenol, or β-naphthol reactivated by the

alcohol, amine, chloroamine, or organic solvents had relatively higher reactivation efficiency than the other chemical regenerants. It was concluded that satisfactory reactivation efficiency could be maintained if a suitable organic solvent was selected.

Chemical reactivation of GAC loaded with phenol using nineteen solvents has been studied by Cooney *et al.* (1983). They showed that methanol could restore 88% of the fixed-bed adsorptive capacity for phenol after one regeneration cycle, and 81% of the capacity after five cycles. They also found that 18% of the adsorbed phenol was desorbed in distilled water. Mundale *et al.* (1991) and Ding *et al.* (1987) investigated the reactivation of GAC loaded with phenol using wet air oxidation. At a temperature of 150°C and oxygen partial pressure of 0.5 MPa up to 95% of fresh GAC adsorptive capacity was achieved. A further increase in temperature reduced the reactivation efficiency. They concluded that such a loss could be due to the formation of groups with an oxygenated chemical structure on the adsorbing surfaces.

Modell *et al.* (1980) applied supercritical carbon dioxide (a reagent with oxidizing power) to recover about 80% of capacity of a very small amount of GAC exhausted with phenol. Repeated cycles of exhaustion and reactivation indicated that this level of recovery could be maintained.

Chemical reactivation's advantages over thermal regeneration include: 1) it can be done in situ and is relatively fast, thus minimizing down time for the adsorbers and eliminating unloading, transporting and repacking of the carbon; and 2) no carbon attrition losses occur, thus the cost of replacing the lost carbon is avoided. However, the main disadvantages associated with chemical reactivation are: 1) the low reactivation efficiency (usually below

70%), and 2) the reactivation capacity is highly dependent on the GAC, the contaminant, the regenerant, and the reactivation conditions. To avoid potential leaching of residual regenerant from the GAC, this technique has not been used in potable water treatment systems. However, this technique is most likely suitable for reactivating GAC used in industrial wastewater treatment. Steam reactivation of GAC loaded with VOCs works quite well. However, the chemical reactivation of phenol-loaded GAC has not been very effective.

2.8.3 Biological Reactivation

Biological reactivation is usually discussed with respect to the addition of PAC to a biological wastewater treatment process, or with respect to increased apparent adsorptive capacities as a result of microbial growth on the GAC during treatment (Lowry and Burkhead, 1980; Suidan *et al.*, 1981; Khan *et al.*, 1981; Kim *et al.*, 1986; Ha *et al.*, 2000). Only a few studies related to separate biological reactivation processes have been conducted (Sigurdson and Robinson, 1978; Wallis and Bolton, 1982; Hutchinson and Robinson, 1990 a and b). These studies showed that biological reactivation is limited by the low desorption rate of the contaminant, possibly due to bacterial fouling of the pore openings and/or by the adsorption of microbially produced compounds.

Ha *et al.* (2000) investigated the role of mixed microorganisms on the bioregeneration of GAC loaded with a mixture of phenol and 2,4-DCP. In a biological activated carbon-sequencing batch reactor (BAC-SBR), bioregeneration efficiency for phenol-loaded lignite-based-GAC was enhanced from 39 to 48% and for 2,4-dichlorophenol-loaded lignite-based-GAC from 38 to 43% by increasing solids retention time from 3 to 8 days. Prolonging the sludge retention time induced both progressive desorption of adsorbates due to

biodegradation in the bulk solution and direct assimilation of adsorbates on GAC by attached microorganisms.

Hutchinson and Robinson (1990 a and b) studied the microbial reactivation of F-300 GAC with phenol and a bisolute feed containing phenol and p-cresol. Bacterial fouling of the column occurred when fermentation broth was contacted directly with the GAC during the reactivation. The reactivated GAC showed an immediate breakthrough of phenol on subsequent reloading. They concluded that the bacterial fouling produced an additional mass transfer resistance that greatly reduced adsorption rates during reloading. Reactivation of GAC using cell-free permeate filtered from the fermentation broth exhibited only a gradual deterioration in the breakthrough performance with successive reactivation. Reactivation efficiencies up to 56% of the virgin GAC adsorptive capacity were achieved in the first reactivation cycle and decreased further with subsequent reactivation cycles.

Speitel and DiGiano (1987) observed that microbial activity in GAC has the potential to extend the service life of GAC beds through in-situ biological reactivation of sorption sites. Bioregeneration with phenol and para-nitrophenol (PNP) was examined over the concentration range of 20-100 μg/L. Bioregeneration ranged from 5 to 22% over a 10 day period and typically showed a lag phase, followed by rapid bioregeneration rate and finally a fairly constant, much lower rate. The experimental results, in combination with mathematical modelling, suggested that bioregeneration could significantly affect the removal of low concentrations of synthetic organic chemicals.

Sigurdson and Robinson (1978) studied the in-situ biological reactivation of GAC loaded with phenol by a pure culture. Only 47% of the fresh carbon adsorptive capacity was

achieved after one reactivation cycle and no further loss of adsorptive capacity was observed in the subsequent reactivation cycles. They hypothesized that extracellular metabolities competing for adsorption sites on the GAC were responsible for the observed decline in the adsorptive capacity. Thus biological reactivation performs poorly for the reactivation of phenol-loaded GAC.

2.8.4 Electrochemical Reactivation

Although the use of electrochemical techniques for the destruction of organic contaminants in water has received some attention (Dabrowski *et al.*, 1975; Chettiar and Watkinson, 1983; Sharifian and Kirk, 1986; Smith de Sucre and Watkinson, 1981; Murphy *et al.*, 1992), they have not been used commercially because of their low efficiencies and low reaction rates. One reason for the low reaction rates is that the oxidation products block the electrode surface and reduce the rate of further reactions. To overcome this problem and simultaneously adsorb organics, a reticulate glassy carbon and carbon felt were employed as electrodes with a large surface area (Gattrell and Kirk, 1990; Kudo and Wayner, 1990). This inspired the Narbaitz and Cen (1994) study on the electrochemical reactivation of spent GAC. A literature review showed that a few other researchers had also studied the electrochemical reactivation of activated carbon (Table 2.1). As Table 2.1 shows, tests on electrochemical reactivation of GAC have achieved from moderate (Owen and Barry, 1972) to high restoration of GAC adsorptive capacity (Wills, 1971; Narbaitz and Cen, 1994; and Slavinskii *et al.*, 1984). However, the various researchers used different methods to test the regeneration process and several researchers did not specify how they evaluated the reactivation efficiency. Comparisons between the reactivation efficiencies they achieved are

Table 2.1 Summary of previous studies on electrochemical reactivation of GAC

Researcher	GAC Type	Contaminant Type	Electrolyte Type	Time (h)	Electrode Type	Anodic/ Cathodic	Voltage (v)	Current (mA/cm^2)	Mixing	Reactor configuration	Max. %RE	Flow velocity	Initial Concentration (mg/L)	Other measurements
Narbaitz and Cen (1994)	F-400	phenol	0.17 N NaCl	up to 24	platinum plate	cathodic& anodic	-	10 - 100 mA	no	batch reactor	95	-	300	
Lazareva *et al.* (1991)	carbon mesoporous	dye (RBR,ABB, DR)	0.1 N Na_2So_4	up to 3	gold mesh	anodic	0.3-0.9	0.00001	?	?	75	?	?	
Khabalov *et al.* (1989)	? 0.16-0.25 mm	benzoic acid	0.1 N K_2SO_4	?	?	?	0.7	?	?	column	?	0.03 cm/s	244	
Sveshnikova et al. (1987)	BAU DAK	phenol	0.25-1.15 N NaCl	1-5	graphite rods	?	hydrogen electrode	1-2	?	?	70	?	40,000	
Slavinskii *et al.* (1984)	AG-3	p-nitrophenol	0.2-0.6 N NaCl	10-30 min	graphite steel	anodic	-	1.8	no	batch reactor	97	-	?	pH
Owen and Barry (1972)	F-400	wastewater	0.25-1.15 N NaCl 0.05-0.23 Na_2SO_4	4-36	lead dioxide - stainless steel	carbon out of regeneration cell	3-4	2-13	yes	batch recirculated but GAC was not in regeneration cell	61	24 gpm/ft^2		gas pH conductivity color
Wills G. B. (1971)	Union carbide graphitar	Dieldrin	%20 HCl	5 min	?	anodic	_	0-125	?	batch	110	?	0.2	

difficult since they employed different calculation methods and these methods can influence the results greatly (Narbaitz and Cen, 1997).

Wills (1971) investigated the electrochemical carbon reactivation process by anodically electrolyzing the carbon surface in 20% hydrochloric acid. Carbon slabs (Graphite 39, 18 and 2690, Union Carbide Carbon, Catalogue N. 52306) were loaded with dieldrin. In his tests, current densities ranged from 0 to 125 mA/cm^2, and were held constant in the given test for 5 minutes. After 5 minutes of treatment, the sample was cathodically electrolyzed at a current density of 38 mA/cm^2 for one minute to free the surface of adsorbed chlorine. Results showed that the activated carbon adsorption capacity using electrochemical reactivation was 10% greater than that of the original carbon.

Owen and Barry (1972) investigated the electrochemical reactivation of F-400 GAC spent in the treatment of municipal secondary effluent. Their reactivation system circulated a brine solution through an electrolytic reactivation cell and the exhausted carbon column (Fig. 2.18). Electrochemical reactivation was able to restore working capacity up to 61% of the corresponding virgin capacity over the range of experimental conditions investigated. Cost analysis showed that electrochemical reactivation is much less costly than thermal regeneration, particularly when labour cost is considered. This may be due to the in-situ nature of the electrochemical reactivation technology. Although variables such as electrolyte type and its conductivity, current and voltage were studied, there did not appear to be any obvious relationship between reactivation efficiency and the variables studied. This is due to the fact that in these reactivation experiments several parameters were changed simultaneously. Another problem encountered in interpretation of the data was variation in

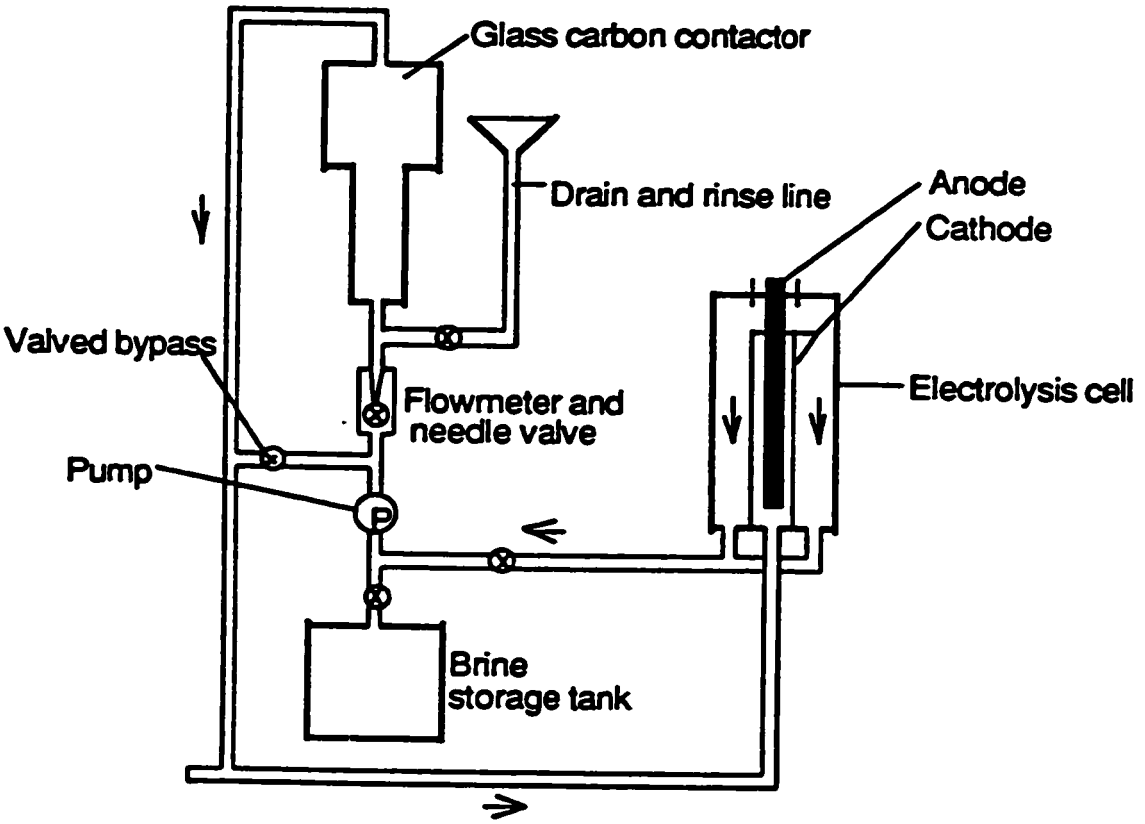

Fig. 2.18 Diagram of brine recirculating in regeneration apparatus.
(Source: Owen and Barry, 1972)

loadings achieved by the virgin GAC in the columns. Also there has been a number of Russian studies into electrochemical reactivation, however the publications arising from these studies are rather short and lack some critical information about their experiments (Slavinskii *et al.*, 1984; Sveshinikova *et al.*, 1987; Lazareva *et al.*, 1991).

Slavinskii *et al.* (1984) studied the electrochemical reactivation of AG-3 GAC loaded with wastewater contaminated by organic substances. The anode was a bed of GAC loaded with p-nitrotoluene, the cathode was the column shell, and the electrolyte was a sodium chloride solution. In order to prevent the bulk anode (the activated carbon) from contacting the column shell (the cathode), the column was lined with a special perforated cylinder of polycaprolactum. The size of the openings in the lining was chosen to prevent direct contact of the activated carbon with the column shell. Under optimum reactivation conditions (current of 30 A/m^2, electrolyte concentration of 0.2 M NaCl, and a treatment time of 30 minutes), the adsorptive capacity of the carbon after the first regeneration cycle was 97.4% of the initial capacity, then remained almost constant for four cycles. Very good results were obtained in this study, but limited GAC and contaminant types were investigated and further research is needed to make firm and more general conclusions.

Sveshinikova *et al.* (1987) conducted experiments on electrochemical reactivation of activated carbon loaded with phenol in a plexiglass laboratory cell. Graphite rods were used as the current conductors. Under optimum conditions (electrolysis for 1 to 1.5 hours, 1 ampere current and a 20 g/L NaCl solution), the reactivated capacity of BAU type GAC was about 70% of the initial adsorptive capacity and it was almost constant in the subsequent cycles. For DAK type GAC, the adsorptive capacity was 40% of the virgin capacity and

remained unchanged for subsequent cycles. The cause of the different behaviour by different GACs was related to the oxidation of the DAK carbon matrix at the tested potentials. Further research with commercial GACs manufactured from different raw materials is needed to evaluate the impact of the GAC type on electrochemical reactivation.

Lazareva *et al.* (1991) also evaluated the possibility of repeated adsorption and electrochemical reactivation of carbon adsorbent loaded with dyes. Reactivation efficiencies up to 75% of the virgin capacity were achieved. It was established that restoration of the adsorption capacity is determined by the cell voltage and depends, to a significant extent, on the nature of the dye. Experiments were conducted with only 1 g of carbon adsorbent; however for practical purposes the impact of larger masses of carbon needs to be examined.

Narbaitz and Cen (1994) investigated the feasibility of electrochemical reactivation of the F-400 GAC. F-400 was loaded with phenol, via batch adsorption tests, then electrochemically reactivated and finally loaded with phenol. Reactivation was conducted in a batch reactor filled with a 1% NaCl solution as the electrolyte. A reactivation efficiency up to 95% was achieved, multiple reactivations only reduced the reactivation efficiency by 2% per cycle, and the electrochemical process yielded no apparent GAC losses. Narbaitz and Cen (1994) concluded that electrochemical reactivation of GAC at a laboratory-scale is a feasible alternative to thermal reactivation. They studied a single layer of GAC particles placed on a platinum electrode. The only mixing within their reactor was natural (free) convection. Natural convection occurred when local variations in fluid density (often caused by local variation in temperature) or/and the movement of electrogenerated gas bubbles produced velocity gradients. Due to the reactor configuration, evaluation of the impact of electrolyte

mixing on the reactivation efficiency was not possible. These authors speculated that forced mixing might improve the reactor's performance. Therefore, further evaluation is necessary.

2.9 Evaluation of Reactivation Efficiency

2.9.1 General Methods

As discussed earlier, GAC regeneration technologies are frequently compared in terms of regeneration efficiencies, however several different methods for evaluating the reactivation process have been used. The Iodine Number has been used in thermal reactivation. The Iodine Number is an index to quantify the general adsorption capacity of the GAC which is based on a standardized adsorption test using an iodine solution. In thermal reactivation the quality control of regenerated carbon is performed by measuring the apparent density of the regenerated carbon and by conducting laboratory tests to measure the capacity of the regenerated carbon to adsorb a standard iodine solution (U.S. Environmental Protection Agency, 1973). Because dry-regenerated carbon can be sampled from the outlet of a furnace, the apparent density can be easily determined by weighing the regenerated GAC of a particular volume.

A second method, which has been used in chemical regeneration evaluation, is by determining the percentage of desorbed contaminant (Cooney *et al.*, 1983; Tan and Liou, 1989). In this kind of solvent regeneration experiment, it is assumed that all the desorbed contaminant is in the solvent. Evaluation of regeneration efficiency (effectiveness of solvent) is based on measuring the equilibrium concentrations of the adsorbates. From the measurements, it is possible to determine the quantity of both adsorbate originally adsorbed onto the carbon and adsorbate subsequently desorbed from the carbon by the solvent. Then,

the percentage of desorption (i.e., adsorbed contaminant desorbed in the solution) can be calculated (Cooney *et al.*, 1983).

A third method which has been used mostly in chemical regeneration evaluation and sometimes with other regeneration methods (Martin and Ng, 1984 and 1985; Narbaitz and Cen, 1994), is calculated as:

$$RE = \frac{q_r}{q_v} * 100 \tag{2.7}$$

where RE is regeneration efficiency, q_v is the adsorption capacity of virgin carbon, and q_r is the adsorption capacity of regenerated carbon. The adsorption capacities are determined via either batch loading tests or via column experiments using the virgin and the regenerated GAC. For batch loading tests, the virgin GAC is contacted with the aqueous solution in question until equilibrium is achieved. The adsorption capacity or equilibrium solid phase concentration of virgin GAC after the first adsorption cycle, q_{e1}, is given by:

$$q_{e1} = \frac{V_1 (C_{o1} - C_{e1})}{M_1} \tag{2.8}$$

where C_{o1} is the initial liquid phase contaminant concentration for the loading cycle, C_{e1} is the equilibrium liquid phase contaminant concentration for the first cycle, V_1 is the volume of contaminated water in the equilibrium vessel during the loading cycle. M_1 is the mass of GAC used in the loading cycle. In the reloading cycle, the reactivated GAC is reloaded via a batch equilibrium-reloading test. The total adsorptive capacity, q_{e2}, of the GAC after the readsorption cycle is:

$$q_{e2} = \frac{V_2 (C_{02} - C_{e2})}{M_2} \tag{2.9}$$

where Co_2 is the initial liquid phase contaminant concentration for the reloading cycle, C_{e2} is the equilibrium liquid phase contaminant concentration for the reloading cycle, V_2 is the volume of contaminated water in the equilibrium vessel during the reloading cycle, M_2 is the mass of GAC used in the reloading cycle. Knowing the adsorption capacity of the virgin GAC and of the regenerated GAC, the reactivation efficiencies can be calculated.

Many researchers have employed carbon columns in adsorption and regeneration tests (Picht *et al.*, 1982; Cooney *et al.*, 1983; Goto *et al.*, 1986). The carbon capacities are calculated through integration of the area between the feed and breakthrough curves, multiplying it by flow and dividing it by the carbon mass. However the column experiment involves more equipment (i.e., columns and pumps) and requires chemical analysis of more samples to monitor the effluent breakthrough curve.

2.9.2 Alternative Methods for Determining the Reactivation Efficiencies in Batch Loading Tests

Narbaitz and Cen (1997) discussed alternative methods for determining the reactivation efficiencies of GAC. The first method is that the readsorption experiments should be designed such that q_r in eq. 2.7 should equal q_{ee}, the regenerated GAC solid phase concentration that is in equilibrium with the same liquid phase concentration as was produced by the initial loading cycle, C_{e1} (i.e., point 3 in Fig. 2.19). This is the correct way of evaluating the reactivation efficiency because both the q_r and q_{e1} are compared on the same basis. The difficulty with this method is the additional experiments required to determine q_{ee}. To obtain the loading of the regenerated GAC at the same equilibrium

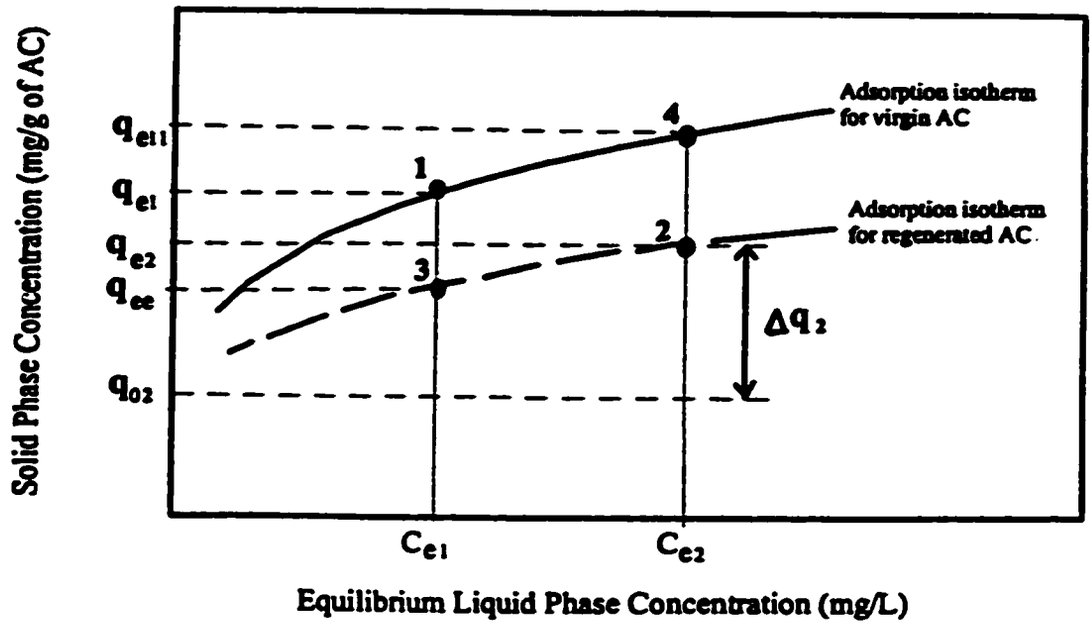

Fig. 2.19 Schematic of the loadings achieved by a batch of virgin activated carbon and the same batch after it is regenerated. (Source: Narbaitz and Cen, 1997)

liquid phase concentration as for the virgin GAC requires a number of trial experiments and interpolation. The reactivation efficiency as calculated for this method will be:

$$RE1 = \frac{q_{ee}}{q_{e1}} * 100 \tag{2.10}$$

where RE1 is the reactivation efficiency calculated using method 1. The most logical approach to determine q_{ee} is to conduct an adsorption isotherm with the reactivated GAC and establish q_{ee} via interpolation.

$$q_{e1} = KC_{e1}^{1/n} \tag{2.11}$$

$$q_{ee} = K_{reg}C_{e1}^{1/n_{reg}} \tag{2.12}$$

$$RE1 = \frac{K_{reg}C_{e1}^{1/n_{reg}}}{KC_{e1}^{1/n}} \tag{2.13}$$

where K and 1/n are Freundlich coefficients for the isotherm with virgin GAC and K_{reg} and $1/n_{reg}$ are Freundlich coefficients of the isotherm with the reactivated GAC. This approach requires the reactivation of a larger mass of GAC to be able to conduct the isotherm test. Considering that six points is about the lowest number of points that can be used to generate a reasonable isotherm, method 1 increases the number of loading tests required by a factor of six. This will limit the scope of an exploratory research study.

In the second method discussed by Narbaitz and Cen (1997), the most important criterion for assessing the effectiveness of reactivation is to use the identical initial conditions for the reloading (i.e., $C_{02} = C_{01}$, $M_2 = M_1$, and $V_2 = V_1$). As the reactivation process frequently alters the GAC, the reloading equilibrium liquid phase concentration C_{e2}, (i.e., point 2 in Fig. 2.13) will usually be different from C_{e1} (generally C_{e2} is greater than C_{e1}).

This method has been used by many researchers (Narbaitz and Cen 1994, Srivastava and Tyagi 1995). In this method RE is calculated as:

$$RE2 = \frac{q_{e2}}{q_{e1}} * 100 \qquad (2.14)$$

$$RE2 = \frac{(C_{o2} - C_{e2})V_2 / M_2}{q_{e1}} * 100 \qquad (2.15)$$

where RE2 is the RE calculated via method 2. As C_{e2} is generally greater than C_{e1}, then q_{e2} will be greater than q_{ee}, as they are both on the dashed line isotherm in Fig. 2.19. Thus, RE2 will be greater than RE1. Method 1 is more logical than method 2, as it compares solid phase concentrations for the reactivated and virgin GAC at the same liquid phase concentration. Hence method 1 is correct and should be used instead of method 2, and the findings of those researchers which used method 2 needs to be re-evaluated.

Given the experimental effort required to use method 1, Narbaitz and Cen (1997) suggested an alternative consistent method of calculating the reactivation efficiencies. They proposed that the RE should be the ratio of the solid phase concentration (q_{e2}) of the reloaded GAC to that of the virgin GAC at the liquid phase concentration achieved during the reloading (C_{e2}) instead of that achieved during the initial loading cycle (C_{e1}). While this is not the classical definition of reactivation efficiency, it does compare the virgin and reactivated loading on a common basis (i.e. the same liquid phase concentration), it yields similar values to the classical definition (Narbaitz and Cen, 1997), and it requires less experimental effort to obtain results. To use this method, one has to conduct the adsorption isotherm experiment for the virgin GAC once and the reloading process can be conducted at the same initial conditions as for the initial

loading. That is: a) the initial liquid phase contaminant concentration for reloading cycle (Co_2) equals that for loading cycle (C_{o1}); b) the mass of GAC used in reloading cycle (M_2) equals that for loading cycle (M_1); and c) the volume of contaminated water in the equilibrium vessel during reloading cycle (V_2) equals that for loading cycle (V_1). The RE is:

$$RE3 = \frac{q_{e2}}{q_{e1}} * 100 \tag{2.16}$$

$$= \frac{(C_{o2} - C_{e2})V_2 / M_2}{q_1} * 100 \tag{2.17}$$

$$= \frac{(C_{o2} - C_{e2})V_2 / M_2}{kC_{e2}^{1/n}} * 100 \tag{2.18}$$

where RE3 is the reactivation efficiency using method 3, q_{e2} is the adsorption capacity of the reactivated carbon, q_1 is the adsorption capacity of the virgin carbon at the equilibrium liquid phase concentration reached during the reloading (C_{e2}), and k and n are the Freundlich constants for the adsorption isotherm of the virgin GAC. Narbaitz and Cen (1997) also developed an alternative method (RE4) for extreme cases such as control samples with low reactivation efficiencies.

$$RE4 = \frac{q_{e1} + (C_o - C_{e2})\dfrac{V}{M} - KC_{e2}^{1/n}}{q_{e1}} \tag{2.19}$$

where C_o is the initial concentration for both loading and reloading and M is the mass of GAC used for loading and reloading.

For the above-mentioned reasons Method 3 (RE3) of calculating reactivation efficiencies will be used in this study.

2.10 Conclusions

This chapter has reviewed many aspects of liquid-phase adsorption onto activated carbon as well as the characteristics of several types of GAC reactivation technologies. Although thermal reactivation can achieve high reactivation efficiency and is used almost universally for the reactivation of GAC from water and wastewater applications, it has some disadvantages. The main disadvantages of thermal reactivation are: loss of GAC mass (5-10% per cycle); high energy cost of heating the GAC; transfer of contaminants to the air phase; and extremely high cost for small facilities. Chemical reactivation techniques are most likely suitable for reactivating GAC used in industrial wastewater treatment. There are disadvantages associated with these techniques. First, the reactivation efficiency is low (usually below 70%). Second, the reactivation capacity is highly dependent on the GAC type, the contaminant type, the regenerant type, and the reactivation conditions. Biological reactivation studies indicate that it yields low reactivation efficiencies and is a time consuming process.

Electrochemical reactivation techniques possess several potential advantages over thermal reactivation. They include possible in-situ reactivation, minimal GAC loss, high reactivation efficiency, oxidation and destruction of the desorbed contaminants from GAC, and its suitability for use in small and medium size treatment facilities.

The literature reports several electrochemical reactivation studies, which used different reactor configurations, different GACs loaded with contaminants, different operating conditions, etc. For the further development of the GAC electrochemical reactivation technology there is an obvious need for a more systematic evaluation of many design and

operational variables, so that the impact of each variable can be ascertained and the mechanisms of reactivation can be understood. Specifically the following questions need to be answered:

1- Does the electrolyte mixing improve the reactivation efficiency?

2- Does a flow through batch reactor perform better than a simple batch reactor?

3- Does a column type reactor perform better than a batch type reactor?

4- Is there a need for direct contact between GAC particles and the electrode?

5- Does the GAC type influence the reactivation efficiency?

6- Does the contaminant type influence the reactivation efficiency?

7- What is the influence of constant current density?

8- How important is the reactivation time?

9- Are there different reactivation mechanisms prevalent at the anode and the cathode?

10- Are accelerated desorption at the cathode, and anodic contaminant destruction, responsible for the reactivation, as speculated by Narbaitz and Cen (1994)?

11- Does polarization of the GAC surface enhance desorption?

12- Is electrochemical reactivation efficiency higher than chemical reactivation efficiency?

In general, this research was planned to answer the above questions.

CHAPTER 3

EXPERIMENTAL MATERIALS AND METHODS

3.1 Introduction

The overall objectives of this study were to investigate the technical feasibility and the mechanisms of electrochemical reactivation of GAC. To reach these aims new reactors were designed and the reactivation efficiencies of a number of adsorbents loaded with different adsorbates under different conditions were determined. The following sections will describe the materials, the analytical techniques, the tests utilized to assess the reactivation efficiency, the electrochemical reactivation apparatus, and the experimental plan.

3.2 Materials

3.2.1 Adsorbates

Three organic chemicals: 2-nitrophenol (2NP), phenol and naturally occurring background organic matter (NOM) were used as adsorbates in this research. Phenol (pK_a = 9.99) is a common industrial chemical and thus is found in many industrial effluents. Phenol was also used in previous electrochemical regeneration research by Narbaitz and Cen (1994) and using it in this study will help to compare the results particularly with respect to the reactor configuration. 2NP (pK_a = 7.23) was selected because it was used in a previous study on the impact of pH on desorption (Karimi-Jashni and Narbaitz, 1995) which will potentially help identify the mechanisms of electrochemical reactivation. 2NP adsorption on the two commercial GACs (F-400 and WV-B) that were used in this study is completely reversible and its adsorption is pH dependent (Karimi-Jashni and Narbaitz, 1995) while phenol adsorbs

partially irreversibly onto F-400 and its adsorption is also pH dependent (Narbaitz and Cen, 1994).

NOM, which is present in all water sources, is the most prevalent organic chemical group in surface waters entering treatment plants. NOM is the result of the microbial breakdown of vegetation and often gives water a yellowish or brownish tint. In fact, the adsorption of NOM tends to reduce the adsorption of other compounds by up to 70 percent (Narbaitz and Benedek, 1994). Herzing *et al.* (1977) showed that the presence of 10 mg/L of a humic substance caused about 90 percent reduction in capacity for the musty-odor compound geosmin. Displacement of previously adsorbed toxic compounds via competitive adsorption with NOM can result in a column effluent concentration of the toxic compound that is greater than the influent concentration. A reasonable strategy to prevent the occurrence of an undesirable situation is to regenerate or replace the activated carbon before complete saturation occurs. Because humic substances (i.e., NOM) are the predominant organic fraction in most surface waters and they readily adsorb, the need to remove adsorbed humic substances will probably control the regeneration step even though the primary purpose in applying the activated carbon may be to remove trace organic compounds (Snoeyink, 1990). In another words, regardless of the target adsorbate, due to the strong competitive adsorption interaction with NOM, the NOM adsorption often controls the regeneration frequency. Thus, it is of great practical interest to study the reactivation of GAC loaded with NOM.

The experiments used laboratory reagent grade (min. assay 99% by HPLC) 2-nitrophenol (Fluka Cheemie AG, Switzerland) and ACS grade (>99% purity) phenol (Aldrich Chemical Co, Milwaukee, WI). The characteristics of phenol and 2NP are given in Table 3.1.

Table 3.1 Adsorbates Characteristics

	Phenol	2-nitrophenol
Structural formula	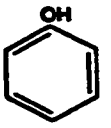	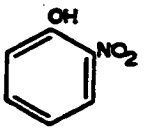
Empirical formula	C_6H_6O	$C_6H_5O_3$
Formula weight	94.11	139.11
Boiling point	182 °C	215 °C
Melting point	40-42 °C	45-46 °C
Solubility in water	93,000 mg/L	2,000 mg/L
Flash point	79 °C	73.5 °C
Henry's law constant ($atm.m^3/mol$)@ 25 °C	2.7E-7	3.5E-6
Dissociation constant	9.99	7.23
Odor	sweet tarry odor	aromatic odor
Appearance	white crystals which slowly turns brown on exposure to air	pale yellow crystals

(Source: Montgomery and Welkom, 1990)

Filtrasorb F-300 GAC loaded at the pilot-scale facilities of the Regional Municipality of Ottawa-Carleton (RMOC) was used to investigate the reactivation of GAC loaded with NOM.

The phenol and 2NP solutions were prepared by adding them to distilled water in a glass carboy and mixing them overnight to obtain a uniform concentration. The initial phenol and 2NP concentrations were set at 300 and 500 mg/L, respectively. These concentrations were selected for two reasons. First, to compare the results with those of Narbaitz and Cen (1994). Second, they yielded readily measurable equilibrium concentrations when using 1.2 g of GAC and 500 mL solution. The 1.2 g of GAC was needed for one layer of GAC particles in the reactivation reactor. The initial pH of unbuffered solution was 6.5 and 5 for phenol and 2NP, respectively. Whenever buffered solution was required a 0.05 M phosphate buffer was utilized. Solutions were adjusted to a desired pH by using HCl (assay 36.5-38% ACS grade, BDH Chemicals, Toronto) and NaOH (assay 50%, Fisher Scientific, New Jersey). These solutions required different proportions of analytical grade KH_2PO_4 and Na_2HPO_4 (BDH Chemicals, Toronto) to obtain a specific pH. The pH was measured by a digital pH meter (Accumet 910, Fisher Scientific, New Jersey).

3.2.2 Adsorbents

Since the properties of GAC depend on the raw material and the method of activation, this study tested three adsorbents: Filtrasorb 400 (Calgon Corp., Pittsburg, PA), Westvaco Carbon (Westvaco Chemical Division, Covington, WV) and Darco (American Norit Company Inc., Atlanta, GA). Filtrasorb 400 (F-400) is manufactured from bituminous coal, Westvaco Carbon (WV-B) is made from wood and Darco Norit (DA-N) is a lignite-based

activated carbon. Filtrasorb F-300, which was used in the NOM-loaded tests, differs from Filtrasorb F-400 only in its particle size distribution. Moreover, F-400 was studied because its reactivation was investigated by Narbaitz and Cen (1994). They suspected that the less than perfect reactivation of phenol-loaded F-400 was related to the fact that this phenol adsorbs partially irreversibly on this GAC. Thus, it was of interest to study the reactivation of sorbate/sorbent systems involving fully reversible adsorption. The sorbate/sorbent combinations of phenol/WV-B, 2NP/WV-B, and 2NP/F-400 were chosen because Vidic *et al.* (1993) and Karimi-Jashni and Narbaitz (1995) showed that they exhibit fully reversible adsorption. As reactivation is likely to be aided by the conductivity of the GACs, the selected GACs have different conductivities (WV-B has the highest conductivity and Darco has the lowest conductivity). It was expected that higher GAC conductivity would increase the reactivation efficiency. The specifications of these carbons are presented in Table 3.2. Considerable care was taken to clean the adsorbents before using them in the experiments. The activated carbons were prepared by boiling in distilled water for 30 minutes, cooling and settling, then rinsing three times with distilled water to remove fines and impurities that may have desorbed from the GAC. All GAC samples were then placed in glass drying pans and dried in an oven at 105°C for 24 hours. Finally, the GACs were cooled and stored in desiccators until needed.

3.2.3 Electrolyte

The electrolyte, which is necessary for electron transfer, was a 0.1 M NaCl solution (5850 mg/L). The choice of NaCl arose from the facts that it is an inexpensive salt and it showed a better performance than other salts (Narbaitz and Cen, 1994).

Table 3.2 Adsorbents properties.

	F-400[1]	WV-B[2]	Darco[3]
Total surface area (m^2/g)	900-1100	1400-1600	600
Bulk density (g/cm^3)	0.401	0.2	0.384
Apparent particle density (g/cm^3)	0.75	0.3	0.7
Pore volume (cm^3/g)	0.85-0.95	1.31	1
Mesh size	12*16	12*16	12*16
Mean particle diameter (mm)	1.4	1.4	1.4
Original raw material	bituminous coal	wood	lignite-based
Resistance in air[4] (Ω/ 4 cm bed GAC)	13	2	124

Source:

[1] Calgon Carbon Corporation, Pittsburgh, PE.

[2] Westvaco Chemical Division, Covington, VA.

[3] American Norit Company, Inc., Jacksonville, FL.

[4] Lab measurements in this study.

3.3 Analytical Techniques

Phenol and 2NP concentrations in solution were measured using a High Pressure Liquid Chromatograph (model 1090 HPLC, Hewlett Packard, Palo Alto, CA) with a Hypersil-ODS column 10*0.21 cm. The diode array detector was set at wavelenghths of 271 and 276 nm for phenol and 2NP, respectively. The column was maintained at 40°C and the flowrate of the mobile phase was set at 0.3 mL/min. For the mobile phase, a mixture of HPLC grade methanol (40%) and 0.05 M sodium acetate (60%) at pH 4.7 was applied (Ning, 1997). Concentration versus area calibration curves were prepared for both compounds using standards prepared in Milli-Q water. The linear part of the calibration curve was used and samples beyond this range were diluted to bring them into the linear range. As a check on the HPLC measurements, standards were added to each set of analysis. The HPLC detection limit was 0.1 mg/L.

The total organic carbon (TOC) concentrations of the aqueous solutions in the mg/L range were determined by a high-temperature TOC analyzer (model DC-190, Dohrmann Division, Rosemount Analytical Inc., Santa Clara, CA). This TOC analyzer uses the high temperature catalytic combustion method with a non-dispersive infrared (NDIR) detector (STM 5310B). The furnace was maintained at 680°C and the flowrate of carrier gas (high purity O_2) was set at 200 cc/min. The TOC detection limit was 0.1 mg/L.

CO_2 gas-phase concentrations were measured by a gas chromatographic (GC) method using a Hewlett Packard 5710A gas chromatograph equipped with a porapak T column (0.635 cm * 304.8 cm), a thermal conductivity detector (TCD), and an integrator. The column was maintained at 70°C and helium was used as the carrier gas (40 mL/min).

3.4 Electrochemical Regeneration Apparatus

The electrochemical reactivation apparatus consists of a power supply and the reactivation reactor. Several types of reactors were evaluated.

3.4.1 Power Supply

There are three alternative arrangements generally used to provide a steady supply of electrical power to an electrochemical cell: constant electrode potential; constant current; and constant cell voltage. For constant electrode potential and constant cell voltage a potentiostat is required. A major cost in the installation of electrochemical processes is that of the power supply for cell operation. The supply of electrical energy to the cells using transformer-rectifier units (which provide constant current) is considerably cheaper than the use of potentiostats (which control the electrode potential or cell voltage). The cost differential can amount to a factor of 5-10. Thus, although potentiostatic control can, in principle, offer the advantage of higher yields and current efficiencies, in large-scale operations this is generally outweighed by the higher cost and by the lack of availability of higher-rating power units. An additional factor is the practical limitation of relying on the potential of an electrode (i.e., in an industrial electrolyte, electrode surface characteristics may change due to corrosion). For these reasons constant current was used in this study. The electrical power was supplied by a potentiostatic controller (model 410, Electrosynthesis, Buffalo, NY) and an accessory power supply (model 420A, Electrosynthesis, Buffalo, NY). This unit was used as a transformer-rectifier to provide constant current.

3.4.2 Electrochemical Reactors

The following four different reactor configurations were investigated: a glass batch reactor used by Narbaitz and Cen (1994) (i.e., old reactor), a stainless steel column type reactor, a new glass batch reactor with the capability of electrolyte re-circulation, and a divided-cells reactor with separation of the electrodes using an ion exchange membrane.

3.4.2.1 Old Batch Reactor

This reactor was used as a baseline to establish the improvements achieved by modifying the reactor configuration. This batch reactor consisted of a two-compartment reactivation cell that was submerged in a 1 L glass dish filled with an electrolyte (Fig. 3.1). This cell consists of three 7.6 cm diameter platinum sheets and two plexiglass rings that keep the GAC particles on the platinum electrodes and maintain the platinum electrodes 2 cm apart. The plexiglass rings are inclined and have several perforations to allow bubbles generated at the electrodes to escape. The perforations also allow the electrolyte to move in and out of the cell compartments.

3.4.2.2 Column Reactor

A stainless steel column of 3cm i.d. and 12 cm height was used as the cathode and a stainless steel bar was lowered into the cylinder as the anode (Fig. 3.2). The column was filled with GAC particles and in order to prevent contact of the bulk anode (the GAC contacted to the bar anode) with the column shell (the cathode), the column was lined with a perforated Teflon material. The size of the openings in the lining was chosen so as to prevent direct contact of the GAC particles with the column shell. The GAC bed was supported by a perforated Teflon plate, so there was no direct contact between the GAC and

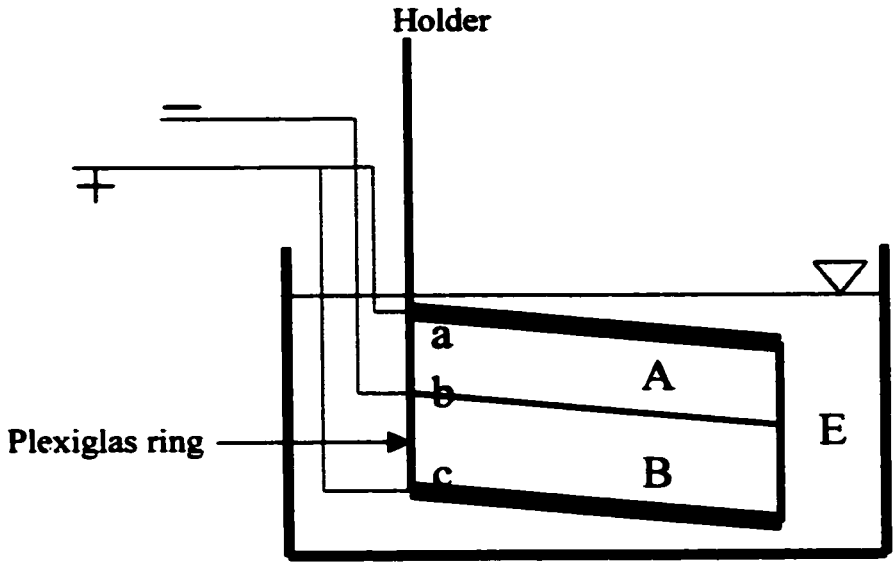

LEGEND:
a, b, and c platinum plates
A anode compartment
B cathode compartment
E electrolyte

Fi.g 3.1 The old electrochemical reactor

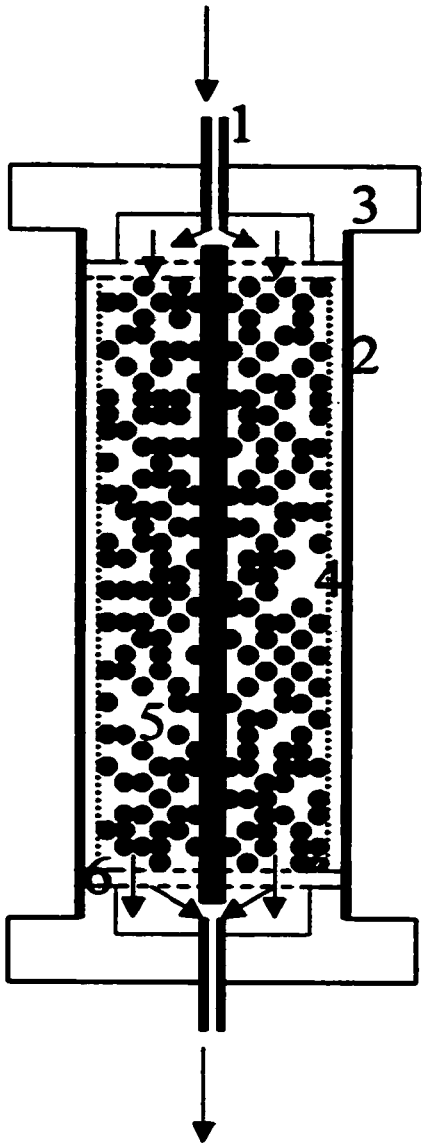

LEGEND:

1- Stainless steel bar
2- Stainless steel shell
3- Teflon holder
4- Perforated Teflon liner
5- Activated carbon
6- Perforated Teflon plates

Fig. 3.2 Column Reactor

the metal column. The electrochemical reactivation evaluation was conducted by the following method. First, the column was filled with the virgin GAC particles with a vertical stainless steel bar conductor within the GAC bed. Second, the phenol solutions passed through the column (flow rate of 6.6 mL/min) to load the GAC. Third, after saturation of the GAC, the phenol solution was drained from the column and the column with the GAC was filled with 0.1 M NaCl solution. Fourth, a constant electrical current was passed through the electrodes. After the reactivation, the GAC in the column was reloaded with the same phenol solution.

3.4.2.3 New Batch Reactor (Undivided-cell Reactor)

A 7.6 cm i.d. and 25 cm high glass column reactor was built with the capability of working as a simple batch reactor, re-circulating batch reactor, or as a flow through reactor (Fig. 3.3). This reactor holds the preloaded GAC on top of a platinum wire mesh electrode and the electrolyte can be continuously recirculated with a diaphragm Master Flex pump (Model 7553-70, Cole-Parmer, Chicago, IL, USA) to provide electrolyte mixing. The electrodes can be placed 2 cm or more apart. Sampling valves were used for collecting the liquid samples to monitor the adsorbate concentration in the electrolyte. The gas produced during reactivation was sampled via the gas vent and analysed for CO_2. A pH electrode was used to monitor the pH changes of the electrolyte 2.5 cm from the surface of the electrodes.

3.4.2.4 Divided-Cell Reactor

To study the mechanism of electrochemical reactivation and to compare reactor configurations, a series of experiments was conducted with a two-cell reactor (Fig. 3.4). This reactor was similar to the new batch reactor and was operable as two compartments or

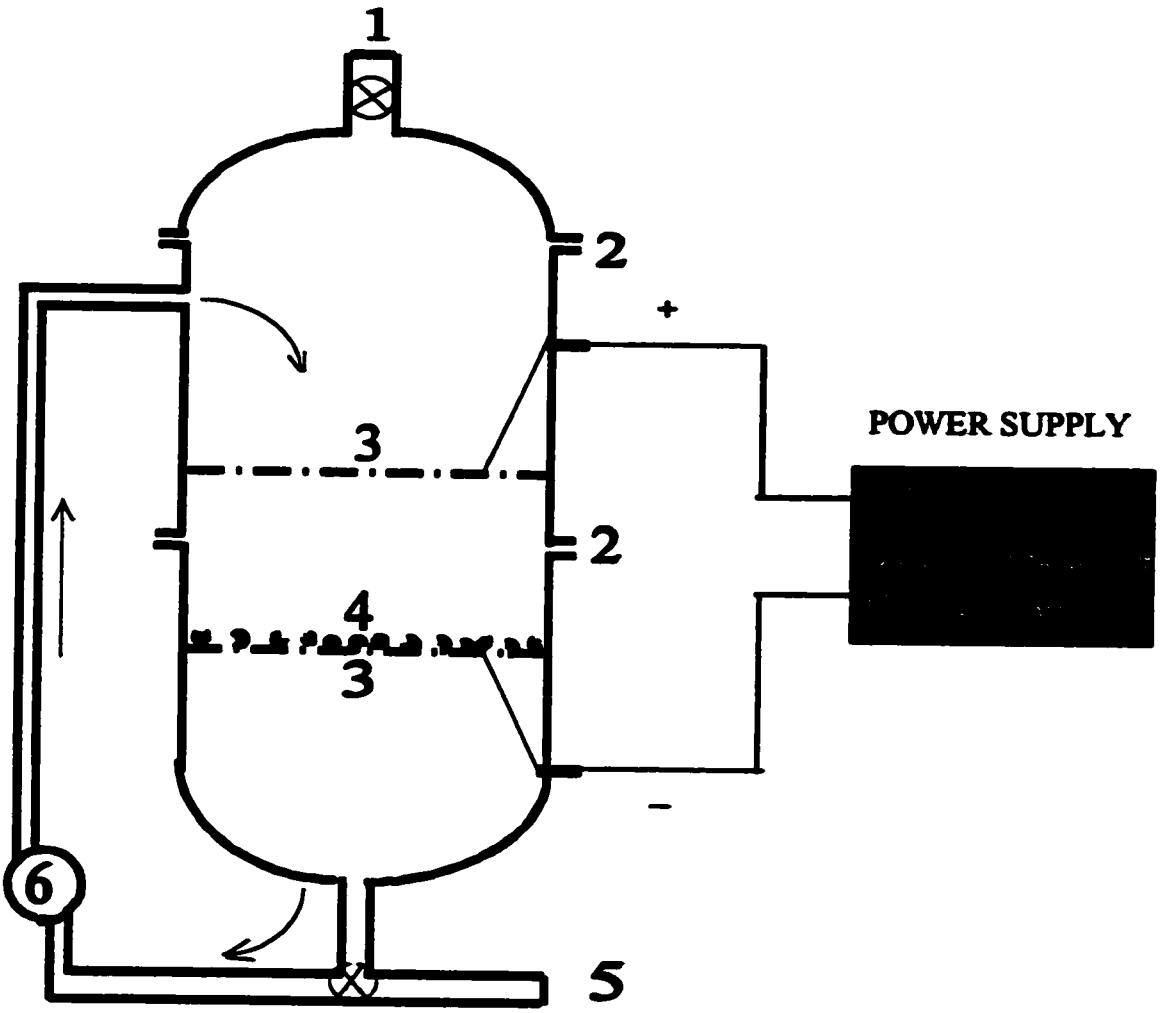

LEGEND:
1. Gas vent 2. Clamped joints 3. Wire mesh electrode 4. GAC on an electrode
5. Sampling points 6. Pump

Fig. 3.3 Undivided-cell electrochemical reactor.

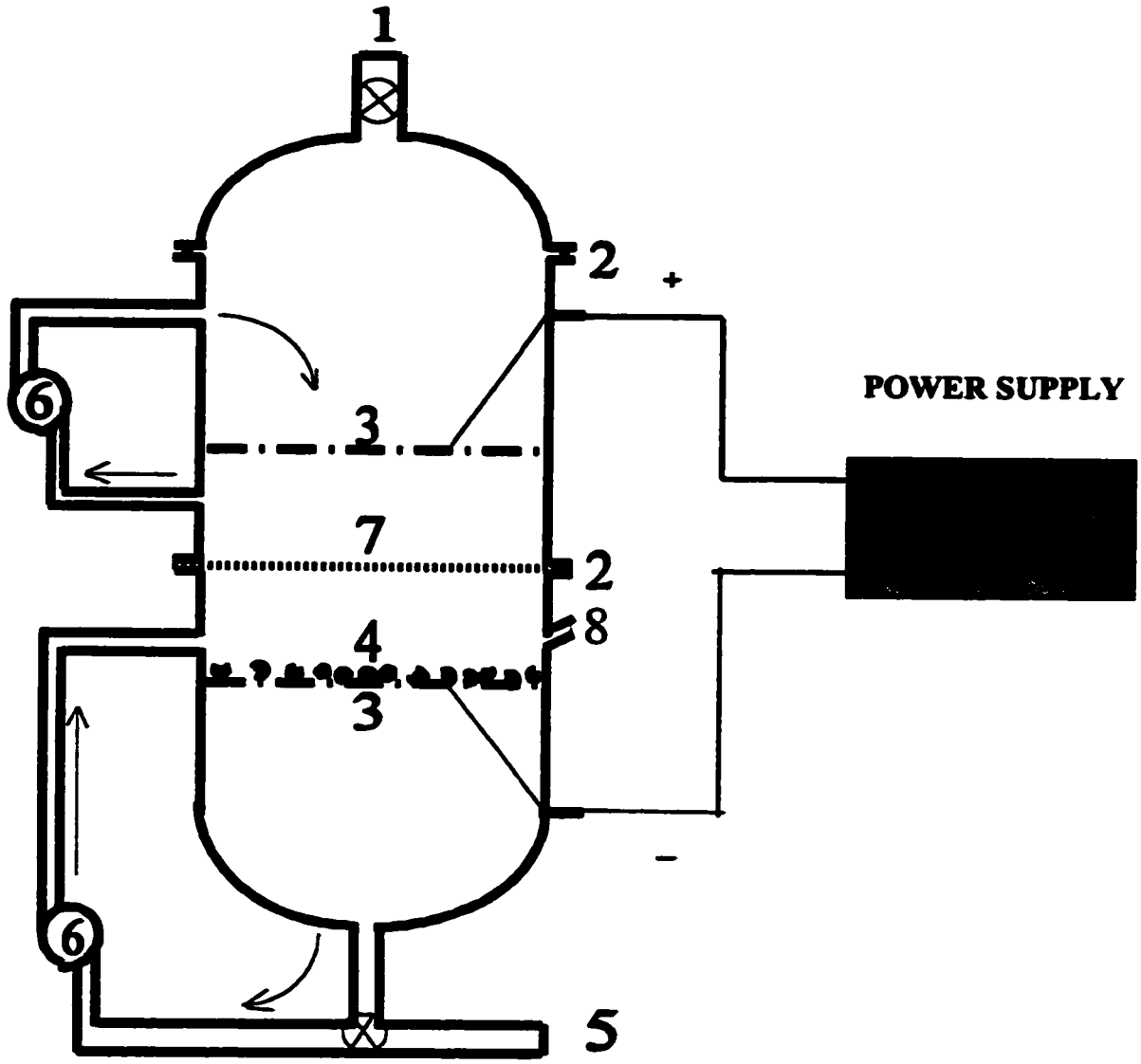

LEGEND: 1. Gas vent 2. Clamped joints 3.Wire mesh electrode 4.GAC on an electrode 5. Sampling points 6. Pump 7. Ion selective membrane 8.Opening for the pH probe

Fig. 3.4 Divided-cell electrochemical reactor.

cells (with an electrode in each cell) separated by an ion selective membrane (shown as 7 in Fig. 3.4). It is operable as a simple two-cell reactor with no forced mixing of the electrolyte or with forced mixing in either or both compartments.

To investigate the mechanism of electrochemical reactivation, experiments were conducted at the anode and at the cathode. The anode and cathode were separated using two ion selective membranes: Cationic Raipore PTFE R4010 iion exchange Membranes and Anionic PTFE Raipore ion exchange Membranes (Electrosynthesis, Lancaster, NY). Ion-exchange materials have the characteristic property of being able to distinguish between cations and anions. The interest in ion-exchange membranes arises from two characteristics. First, they can be used to stop, selectively, either anions or cations from transferring from one cell compartment to the other. Second, they allow electrolysis to be carried out under close control of compartment pH. For example, when the working electrode is the cathode, a cation-exchange membrane will prevent the transfer of OH^- ions (generated at the cathode during hydrogen evolution) into the anolyte chamber and thus allow a pH differential to be set up in the cell. The main properties required of ion-exchange membranes for them to be successful in technical processes are: low electrical resistance, high permselectivity, good mechanical stability, and good chemical stability. The selected membranes satisfied most of these required properties.

3.5 GAC Loading Procedure

For most of the phenol and 2NP related experiments, the GAC batch loading tests were conducted via the bottle-point method (Narbaitz, 1985). The batch loading approach was selected as opposed to the column loading approach as it is less expensive and much less

time consuming. Accordingly, this would permit the evaluation of many more reactivation conditions. However, to investigate the electrochemical reactivation efficiency of a column type reactor, the column approach loading was used. Also, to study the electrochemical reactivation of GAC loaded with NOM, GAC loaded in the pilot-scale columns of the Regional Municipality of Ottawa-Carleton (RMOC) was used.

3.5.1 Batch Loading Procedure

In the bottle-point method, an accurately weighed mass of GAC and the solution of known initial concentration were contacted in 500 mL glass bottles with Teflon lined caps (Fig. 3.5). Each bottle was prewashed with chromic acid, rinsed 3 times with hot tap water and 3 times with distilled water, then dried in an oven at 105°C prior to usage. Clean bottles were rinsed twice with the solution to be used in the experiment prior to filling them with GAC and the solution. In each set of experiments, GAC particles were accurately weighed and then were added to the bottles. Because dried activated carbon gains weight rapidly on exposure to air by absorbing moisture, care was taken to have desiccatory media in the analytical balance's chamber and to weigh the adsorbent as quickly as possible. To provide necessary mixing, the bottles were placed in an end-over-end tumbler that rotated the bottles at approximately 10 revolutions per minute. Using an end-over-end tumbler allow the GAC particles to move up and down the bottle which provides good mixing and results in less friction between GAC particles than in orbital shakers. The tumbler was operated in a constant temperature room at 22 ± 1°C.

Each set of experiments had three controls and two blanks, one blank containing only Milli-Q water and the other Milli-Q water plus one gram of GAC. Blanks were used to identify

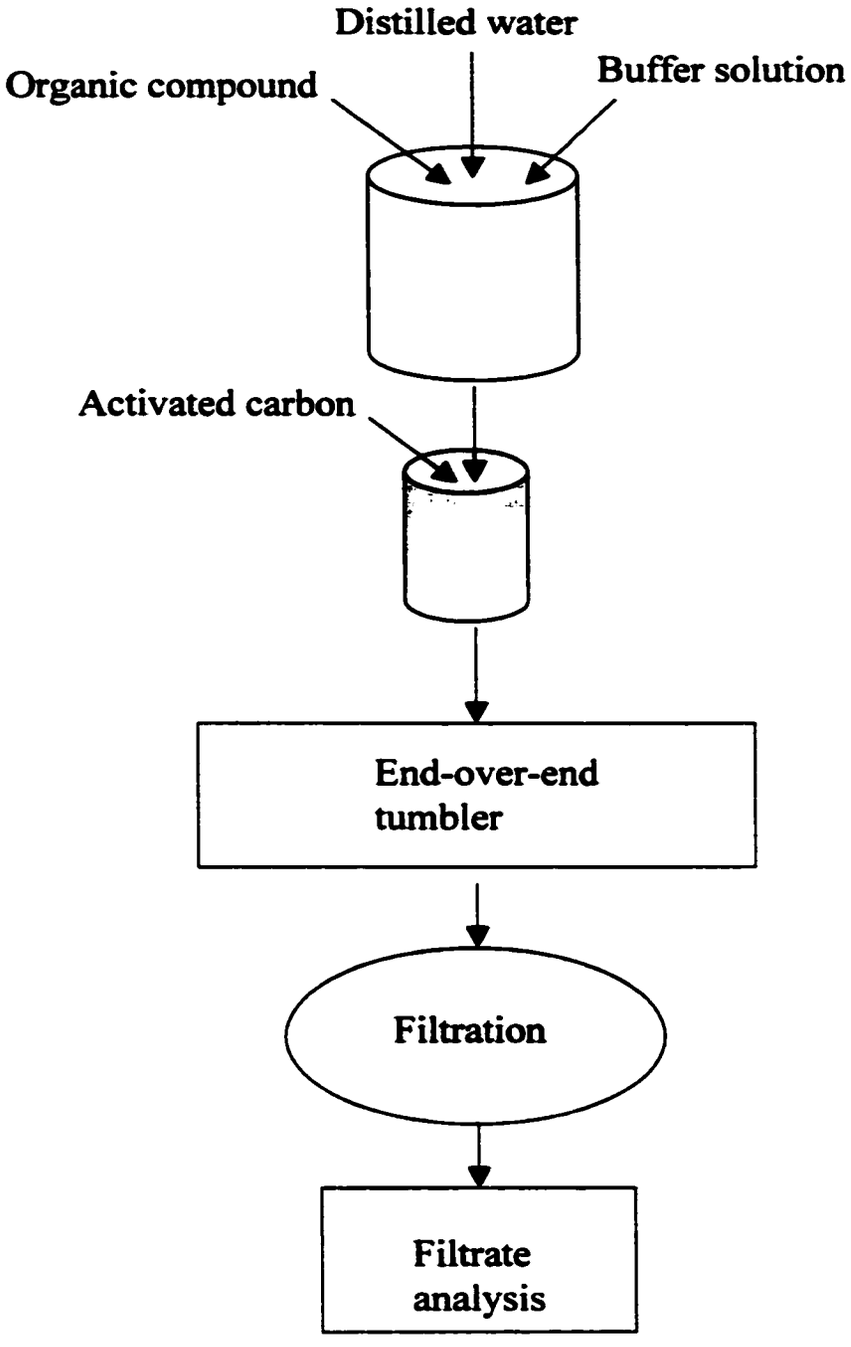

Fig. 3.5 Bottle-point adsorption tests loading.

possible leaching from the bottles or the GAC. The controls were used to determine the possible adsorbate losses. The bottles were filled as much as possible, without overspilling to avoid loss of GAC, as some of the GAC floats to the surface of the liquid. The bottles were filled with the solution in random order to minimize systematic errors. The controls were filled among the other bottles as well. After a two-week equilibrium period, the GAC was separated from the solution by vacuum filtration through a pre-washed 0.45 μm pore size MSF cellulose nitrate membrane filter (Micro Filtration System, Dublin, Ca., U.S.A). The filters were pre-soaked in Milli-Q water overnight to leach potential organic contaminants. Before each filtration, the glass filter holder apparatus was taken apart and washed with an Alconox detergent solution (Alconox Inc. N.Y., U.S.A.). It was then rinsed with hot tap water and Milli-Q water and then reassembled with a membrane filter in place. Around 150 mL of solution were filtered to saturate the surfaces (including the membrane filter, apparatus and collection bottles) prior to filtrate collection for analysis. A sample was taken from the second 150 mL volume of filtered solution and stored in a refrigerator at 4°C until analyzed.

3.5.2 Column Loading Procedure

This type of loading used 3 cm i.d. stainless steel columns packed with a known mass of GAC and operated in the downflow mode. A schematic of the system is presented in Fig. 3.6. The GAC was packed to a depth of 6.5 cm, providing an empty bed contact time of approximately 7 minutes and a hydraulic loading rate of 0.56 m^3/m^2-hr (flow rate of 6.6 mL/min). The feed solution was prepared in a glass carboy and mixed overnight to ensure that a uniform solution was attained. The effluent lines passed through a small reservoir that was used for sample collection.

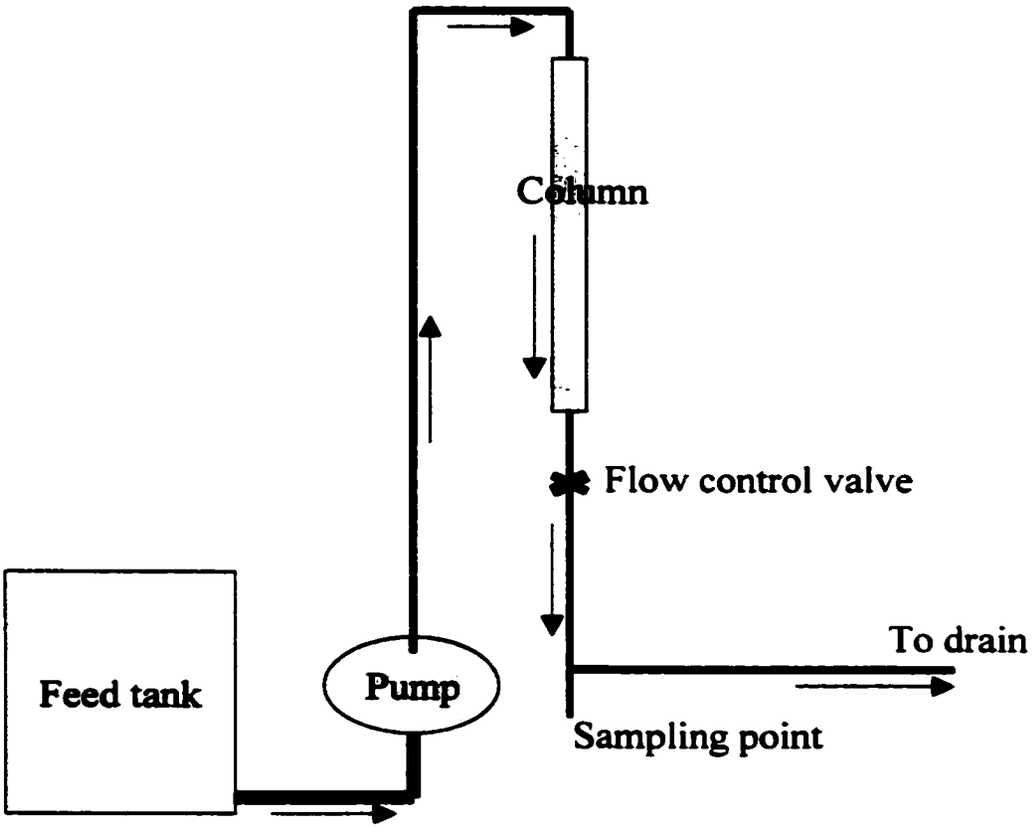

Fig. 3.6 Schematic of column apparatus.

3.6 Evaluation of Reactivation Efficiency (RE)

3.6.1 GACs Loaded with 2NP and phenol

For phenol and 2NP the reactivation efficiencies were evaluated via three sets of experiments in series: 1) loading of virgin GAC with a contaminant using the bottle-point method, 2) reactivation of the loaded GAC, and 3) repetition of the loading procedure with the reactivated GAC. In the second step of the tests, the loaded GAC was electrochemically reactivated in the electrochemical reactor. For safety reasons the experiments were conducted in a fume hood because phenol and 2NP are semi-volatile hazardous chemicals and H_2 is an explosive gas. Following the electrochemical reactivation, the GAC particles were separated from the electrolyte via vacuum filtration through a membrane filter. The total organic carbon (TOC) and the desorbed contaminant concentration of the filtrate were determined using TOC and HPLC analyzers, respectively. The reactivated GAC particles were then reloaded following the same loading procedure. Knowing the adsorption capacity of GAC in steps 1 and 3, the reactivation efficiencies were calculated by method RE3 discussed in section 2.9.2.

Because in this study the electrochemical regeneration was conducted via batch tests, equation 2.7 (and consequently the RE3 method) was selected to determine the RE over others for the following reasons. First, the GAC drying procedure, which is needed in the apparent density and Iodine Number measurements, may cause a certain amount of contaminant to be removed (volatilised) from the carbon. Second, the electrochemical process may oxidize the contaminant after desorbing it from the GAC into the electrolyte and/or may destroy the contaminant on the GAC surface. If the contaminant is oxidized or

transformed, it is impossible to determine the percentage of contaminant desorbed by measuring the contaminant concentration in the electrolyte solution.

3.6.2 GACs Loaded with NOM

Because the reloading of GAC with NOM takes a long time (few months), in the case of GAC loaded with NOM the iodine number of the virgin GAC and the iodine number of the reactivated GAC were used to calculate the reactivation efficiency. This method uses the capacity of the reactivated carbon to adsorb a standard iodine solution (ASTM D4607-94). The iodine number method is a questionable method when assessing GAC loaded with phenol and 2NP, because in this technique the reactivated GAC must first be dried and the GAC drying procedure may cause losses of residual phenol and 2NP (on the GAC surface) due to volatilization, as they are semi-volatile. Since NOM is not volatile, the drying procedure would not affect the residual NOM on the GAC surface. Thus, the iodine number method is a valid method to asses the GAC loaded with NOM. Following the electrochemical reactivation, GAC particles were separated from the electrolyte by membrane filtration. The total organic carbon (TOC) of desorbed residual in the electrolyte was determined using a TOC analyzer.

3.7 Experimental Plan

The general objectives of this research were: to optimize the performance of the electrochemical GAC reactivation technology and to obtain a better understanding of the electrochemical reactivation mechanism. To reach the goals of this research a variety of experiments was conducted. These experiments were intended to investigate the reactor design; process applicability; reactivation mechanisms and modelling. In order to calculate

the reactivation efficiency and the extent of desorption, adsorption and desorption studies were also conducted. The experimental plan is shown in Table 3.3.

3.7.1 Adsorption Kinetics Experiments

The objective of the adsorption kinetics test was to determine the required contact time for GAC adsorption to ensure that adsorption equilibrium has been attained. Kinetics tests measure the change in liquid phase concentration with time. These experiments were conducted via the bottle-point technique with two critical modifications: all bottles used the same GAC dosage, and each bottle had a different contact time. To maintain a constant carbon dosage the target GAC masses were adjusted based on the volume of the individual bottles. The GAC dose and initial solution's concentrations were chosen so that they were the same as those of the loaded GAC in the electrochemical reactivation experiments. The contact time of each bottle was calculated as the difference between the halfway point of the filling of the bottle and the halfway point of the filtration step.

3.7.2 Adsorption Equilibrium Studies

Adsorption isotherms were developed to describe the adsorptive properties of F-400, WV-B and DARCO activated carbons under loading conditions. The isotherms were conducted by the bottle point method, using a range of carbon masses and the same solution of known initial concentration. The initial phenol and 2NP concentration were set at 300 and 500 mg/L, respectively. The initial pH of the unbuffered solution was 6.5 and 5 for phenol and 2NP, respectively. The pH of the buffered solutions was set at 5.0. Each isotherm run consisted of a large number of bottle experiments, and duplicates were conducted for at least two points per run. The differences in the liquid phase concentrations between these

Table 3.3 Research plan.

Topic	Experiment #	Purpose of the Experiment	Reactor Type	Electrolyte Flow (L/min)	Time (h)	Current (mA)	GAC Type	Contaminant	GAC (g)	Working Electrode
adsorption studies	1	adsorption kinetics	---	---	---	---	F-400, WV-B	phenol	---	---
	2	adsorption kinetics	---	---	---	---	F-400, WV-B, Darco	2NP*	---	---
	3	isotherm	---	---	---	---	F-400, WV-B, Darco	phenol	---	---
	4	isotherm	---	---	---	---	F-400, WV-B, Darco	2NP	---	---
	5	isotherm	---	---	---	---	F-300	NPOC	---	---
	6	effect of buffering on isotherms	---	---	---	---	F-400	phenol	---	---
	7	effect of buffering on isotherms	---	---	---	---	F-400	2NP	---	---
	8	TOC isotherms	---	---	---	---	F-400	phenol-TOC 2NP-TOC	---	---
reactor design	9	comparison of reactors	undivided-cell reactor, old reactor	0	1,2.5,5,7.5,10	50	F-400	phenol	1.2	cathode
	10	comparison of reactors	undivided-cell reactor, old reactor	0	2.5	10,30,50, 100	F-400	phenol	1.2	cathode
	11	column reactor performance	column reactor	0, 0.2	5	50	F-400	phenol	19.2	cathode
	12	column reactor performance	column reactor	0	5	250	F-400	phenol	19.2	cathode
	13	column reactor performance	column reactor	0	0.5	750	F-400	phenol	19.2	anode
	14	comparison of reactors	undivided-cell reactor, divided-cell reactor	0	2.5	10,30,50, 100	F-400	phenol	1.2	cathode
	15	reactivation of multi-layer GAC	undivided reactor	0	5	50	F-400, WV-B, Darco	phenol	1.2 to 19.2	cathode
	16	reactivation of multi-layer GAC	old reactor	0	5	50	F-400, WV-B, Darco	phenol	1.2 to 19.2	cathode
	17	effect of electrolyte mixing on oxidation	undivided reactor	0.2, 1	0-40	50	---	phenol	----	---
	18	effect of electrolyte mixing on oxidation	undivided reactor	0.2, 1	0-40	50	---	2NP	----	---

Table 3.3 Research plan (continued).

Topic	Experiment #	Purpose of the Experiment	Reactor Type	Electrolyte Flow (L/min)	Time (h)	Current (mA)	GAC Type	Contaminant	GAC (g)	Working Electrode
reactor design	19	effect of electrolyte mixing on cell voltage	undivided reactor	0, 1	0-48	50	---	-----	----	---
	20	effect of electrolyte mixing on reactivation	undivided reactor	0, 0.2, 0.5	1.2.5,5,7.5,10	50	F-400	phenol	1.2	cathode
	21	effect of electrolyte mixing on reactivation	undivided reactor	0, 0.1,0.2, 0.5,1	2.5	50	F-400	phenol	1.2	cathode
	22	pH variation within the reactor	undivided reactor	0	0 to 5	50	F-400	phenol	1.2	cathode
	23	effect of pH on adsorption	--	--	--	--	F-400	phenol	---	---
	24	effect of pH on desorption	--	--	--	--	F-400	phenol	---	---
	25	effect of electrolyte mixing on reactivation	undivided reactor	0, 0.1,0.2, 0.5,1	2.5	50	F-400	phenol	1.2	cathode, anode
	26	effect of electrolyte mixing on reactivation	undivided reactor	0, 0.1,0.2, 0.5,1	2.5	50	F-400, WV-B	phenol	1.2	cathode
process applicability	27	voltage variation	undivided reactor	0	0 to 50	50, 100	F-400,	phenol	1.2	cathode
	28	effect of current and time on reactivation	undivided reactor	0	1, 2.5, 5, 7.5, 10, 18, 25	10, 30, 50, 100	F-400,	phenol	1.2	cathode
	29	effect of current and time on reactivation	undivided reactor	0	1, 2.5, 5, 7.5, 10, 18, 25	10, 30, 50, 100	WV-B	phenol	1.2	cathode
	30	Effect of pH on reactivation	undivided reactor	0	1 to 45	50	F-400	phenol	1.2	cathode
	31	effect of GAC type on reactivation	undivided reactor	0	1, 2.5, 5, 7.5, 10, 18, 25	50	F-400, WV-B, Darco	phenol	1.2	cathode
	32	effect of GAC type on reactivation	undivided reactor	0	1, 2.5, 5, 7.5, 10, 18, 25, 65	50	F-400, WV-B, Darco	2NP	1	cathode
	33	effect of GAC type on reactivation	undivided reactor	0	5	10, 30, 50, 100, 200	F-400, WV-B, Darco	phenol	1.2	cathode
	34	effect of GAC type on reactivation	undivided reactor	0	5	10, 30, 50, 100, 200	F-400, WV-B, Darco	2NP	1	cathode
	35	reactivation of NOM-loaded GAC	undivided reactor	0	5, 10, 18, 25	50	F-300	NOM**	5	cathode
	36	reactivation of NOM-loaded GAC	undivided reactor	0	5	10, 50, 100, 200	F-300	NOM	5	cathode
	37	effect of loading-time on reactivation	undivided reactor	0	2.5	50	F-400	phenol	1.2	cathode

Table 3.3 Research plan (continued).

Topic	Experiment #	Purpose of the Experiment	Reactor Type	Electrolyte Flow (L/min)	Time (h)	Current (mA)	GAC Type	Contaminant	GAC (g)	Working Electrode
process applicability	38	effect of loading on reactivation	Undivided reactor	0	2.5	50	F-400	phenol	0.2 to 1.2	cathode
	39	effect of loading-time on reactivation	Undivided reactor	0	2.5	50	F-400	2NP	1	cathode
	40	effect of loading on reactivation	undivided reactor	0	2.5	50	F-400	2NP	0.2 to 1	cathode
	41	reactivation of GAC for isotherm comparison	undivided reactor	0	5	50	F-400	phenol	0.2 to 1	cathode
	42	reactivation of GAC for isotherm comparison	undivided reactor	0	5	50	F-400	2NP	0.2 to 1	cathode
re-evaluation of the results	43	reactivation of 2NP-loaded GAC	undivided reactor	0	2.5, 5, 10, 15, 25	50	F-400	2NP	1	cathode, anode
	44	effect of electrolyte mixing on reactivation	undivided reactor	0, 0.2, 0.5, 1	2.5	50	F-400	2NP	1	cathode
	45	reactivation of GAC, using buffered reloading solution	undivided reactor	0	1 to 30	50	F-400	2NP	1	cathode, anode
	46	reactivation of GAC, using buffered reloading solution	undivided reactor	0	1 to 30	50	F-400	phenol	1.2	cathode, anode
	47	pH variation	divided-reactor	0	0 to 25	50	F-400	phenol	1.2	cathode, anode
	48	reactivation of GAC, using buffered reloading solution	divided with anions and cations exchange membranes	0.2	1 to 18	50	F-400	2NP	1	cathode, anodic
	49	reactivation of GAC, using buffered reloading solution	divided with anions and cations exchange membranes	0.2	1 to 18	50	F-400	phenol	1.2	cathode, anodic
	50	diffusion of 2NP through membranes	divided with anions and cations exchange membranes	0	0 to 50	---	---	2NP	---	---

Table 3.3 Research plan (continued).

Topic	Experiment #	Purpose of the Experiment	Reactor Type	Electrolyte Flow (L/min)	Time (h)	Current (mA)	GAC Type	Contaminant	GAC (g)	Working Electrode
re-evaluation of the results	51	effect of electrolyte mixing on reactivation using buffered reloading solution	undivided reactor	0, 0.5, 1	2.5	50	F-400	2NP	1	cathode
	52	reactivation of GAC, using buffered reloading solution	undivided reactor	0	1 to 30	10, 50, 100, 250	F-400	phenol	1.2	cathode
	53	effect of catholyte volume	undivided reactor	0	5	50	F-400	phenol	1.2	cathode
	54	effect of NaCl concentration	undivided reactor	0	5	50	F-400	phenol	1.2	cathode
	55	aternative methods to buffering the reloaded solution	undivided reactor	0	5	50	F-400	2NP	1	cathode
electrolyte post treatment	56	destruction of phenol	undivided reactor	0.2	0 to 50	50, 250, 500	----	phenol	---	cathode
	57	destruction of phenol	divided reactor	0.2	0 to 50	50	----	phenol	---	anode, cathode
	58	destruction of 2NP	undivided reactor	0.2	0 to 50	50, 1000	----	2NP	----	cathode
	59	destruction of phenol	divided reactor	0.2	0 to 50	50	----	2NP	---	anode, cathode
mechanisms	60	desorption kinetics at pHs 2 and 12	undivided reactor	0.2	0 to 50	0	F-400	2NP	1	-----
	61	desorption kinetics at pHs 2 and 12	undivided reactor	0.2	0 to 50	0	F-400	phenol	1.2	----
	62	effect of current on desorption kinetics at pHs 2 and 12	divided reactor	0.2	0 to 50	50	F-400	2NP	1	cathode
	63	effect of current on desorption kinetics at pHs 2 and 12	divided reactor	0.2	0 to 50	50	F-400	phenol	1.2	cathode

2NP* = 2-nitrophenol

NOM** = Natural Organic Matter

points were less than 2%. The adsorption isotherms were fitted by the Freundlich model and the results were used in calculating the reactivation efficiencies.

3.7.3 Desorption Kinetics Experiment

Desorption kinetics tests determined the change in liquid phase concentration with time, resulting from desorption. Desorption was studied in the same reactor as the electrochemical reactivations but in these tests both desorption with an applied current and without an applied current were investigated. As a part of the investigation into the reactivation mechanisms, desorption of 2NP and phenol from preloaded GACs at pHs 2 and 12 were studied. The GAC was loaded with 2-nitrophenol (initial pH of 5) or phenol (initial pH of 6.5) solutions using the bottle-point technique. The desorption solution (buffered Milli-Q water with 0.1 M NaCl) and the electrochemical reactor were prepared before the end of the loading experiment. The loaded activated carbon particles were separated from the solution by membrane filtration, then transferred into the reactor, and the reactor was filled with the desorption solution. The desorption solution was re-circulated at a flow rate of 0.2 L/min. The desorbed contaminant concentration was determined by analyzing the samples taken at different time periods.

3.7.4 Reactor Design

In the reactor design section the impact of mixing (impact of electrolyte flow through the reactor) and the impact of direct contact between GAC particles and the electrode were studied. The reactor held the preloaded GAC on top of a platinum wire mesh electrode and the electrolyte was continuously re-circulated with a pump to provide electrolyte mixing. To avoid contamination in the recycling line, the pump had a Teflon head and the

tubing was made of Teflon. The electrodes were placed 5 cm apart. Sampling point valves were used for collecting the liquid samples to monitor the adsorbate concentration in the electrolyte. The gas produced at various times during the reactivation was sampled via the gas vent (located at the top of the vessel) and analyzed for CO_2. A pH electrode was used to measure the pH near the surface of the electrode. Since different GAC/contaminant systems may perform differently (because of factors such as: differences in GAC conductivity, and the pH dependence and reversibility or irreversibility of contaminant adsorption on different types of GAC) the impact of each factor was investigated by testing different GACs and contaminants.

The reactor evaluation was conducted using GACs loaded with phenol and 2NP via the batch procedure described earlier. These tests cover both partially irreversible adsorption (phenol on F-400) and completely reversible adsorption (2NP on F-400). The reactivations were conducted (using a fixed time period and a constant current) with different re-circulation flowrates, which provided different levels of turbulence and mixing.

Runs were conducted with different depth (multi-layer) of GAC bed on the electrode, i.e., a bed consisting of loosely contacting GAC particles. The reactor held a minimum of single layer (each layer consisted of 1.2 g of 12*16 mesh GAC particles (1-2 mm diameter)). As reactivation was likely to be aided by the conductivity of the GAC, the multi-layer evaluation was conducted using three GACs with different conductivities. Reactivation of up to19.2 g (16 layers) of GACs loaded with phenol were studied.

3.7.5 Process Applicability and Operating Conditions

In the process applicability section the following were studied. First, the impact of different GAC types, based on the GAC raw material. Second, the impact of the adsorbate (contaminant) types based on the reversibility or irreversibility of the GAC adsorption plus the pH dependence of their adsorption on the GAC surface. Third, the impact of reactor operation conditions (reactivation time and current). The process applicability was assessed by reactivating different types of GACs loaded with different contaminants. In each case reactivation tests were conducted using different currents and reactivation times, to assess the influence of GAC type, pollutant type, current, and reactivation time on reactivation efficiency. As GAC performance depends on both the carbonaceous raw material and the manufacturing process, the electrochemical reaction's applicability was investigated for different types of commercial GACs (F-400, WV-B, Darco) loaded with different contaminants. Phenol and 2NP were used as contaminants. These tests will cover both partially irreversible adsorption (phenol on F-400) and completely reversible adsorption (2NP on F-400). Also they cover pH dependent adsorption (phenol/F-400 and 2NP/F-400). Finally, F-300 loaded with NOM was investigated to test the applicability of the electrochemical reactivation method to a drinking water application.

3.7.6 Reactivation Mechanisms and Modelling

To investigate the mechanisms involved in electrochemical reactivation, the impact of cathodic reactivation versus anodic reactivation, and the impact of an ionic selective membrane as a separator between the two electrodes were studied. To identify the mechanism of electrochemical reactivation, a series of experiments were conducted. First,

the extent and kinetics of contaminant desorption from preloaded GAC in the reactor with and without current at pHs 2 and 12 were studied to determine the impact of pH and current on the contaminant desorption. Second, the undivided and divided reactors were used with solutions of the same contaminants (without GAC) to determine the rates of contaminant destruction at the electrodes. The kinetics of the destruction at both electrodes was measured. The contaminant concentration and the total organic carbon (TOC) were measured in all of these experiments. The TOC measurements coupled with individual contaminant analysis provide an indication of the extent of oxidation beyond contaminant removal without the need for analyzing for the many possible partially oxidized species (by-products). Third, a series of reactivation tests were conducted with loaded GAC. These tests included reactivation at: 1) the anode; 2) the cathode; 3) the anode of the divided-cell reactor; 4) the cathode of the divided cell-reactor. Anodic versus cathodic reactivation was achieved by reversing the leads on the power supply while the GAC was placed on top of the lower mesh. Fourth, these data along with the destruction rate constant from the second step and the desorption rate constant from the first step were used to model the extent of reactivation. These evaluations were conducted under constant current and electrolyte velocity by using phenol and 2NP/F-400 combinations.

CHAPTER 4

ADSORPTION STUDIES

4.1 Introduction

The evaluation of reactivation efficiency was based on three tests: loading, electrochemical reactivation and reloading of the reactivated GAC. The experimental conditions could have a significant effect on the adsorption equilibria and kinetics. One of the most important considerations in determining an equilibrium isotherm is the selection of an equilibration contact time sufficiently long to ensure that the equilibrium is actually reached or closely approached. Also to use the RE3 method in calculating the reactivation efficiencies, it is necessary to establish the virgin GAC isotherm. For these reasons the adsorption equilibria and kinetics of 2NP and phenol on the various GACs, the effect of the buffering solution on the phenolic isotherms, and the TOC isotherms were studied and the results are presented in this chapter. All the tests were conducted under oxic conditions.

4.2 Adsorption Kinetics

Batch kinetics experiments were conducted to determine the necessary contact time for GAC adsorption to ensure that the adsorption equilibrium has been reached. These experiments were conducted via the bottle point technique. The GAC dose was chosen so that it equaled that of the loaded GAC in the electrochemical reactivation experiments. In each experiment set, phenol or 2NP solutions were contacted with a fixed dose of GAC in different bottles and the changes in concentration with time in the liquid phase were monitored. The results of phenol adsorption kinetics at pH 6.5 are plotted in

Fig. 4.1. This figure shows that more than 80% of the uptake occurred in the first few hours and 4 and 8 days were sufficient to ensure equilibrium for phenol adsorption on F-400 and WV-B, respectively.

Fig. 4.2 shows the results of the adsorption kinetics experiment for 2NP at pH 5. As this figure shows, the adsorption reached equilibrium quickly and around 80-90% of the uptake occurred in less than 5 hours. This figure shows that one day was sufficient to ensure equilibrium for 2NP adsorption on F-400, WV-B, and Darco. However, during electrochemical reactivation the surface of the GAC may alter in some manner and this may affect the adsorption process and a longer contact time may be needed to ensure that the equilibrium has been attained in the reloading cycle. To be conservative a two-week contact time between GAC particles and the 2NP or phenol solutions was used in this research.

4.3 Isotherm Studies.

The isotherm results are shown in Figs. 4.3 and 4.4. The equilibrium solid phase concentrations (q_e) were calculated (via a mass balance) as:

$$q_e = (V/M)(C_{control} - C_e) \qquad (4\text{-}1)$$

where V is the volume of the solutions (L), M is the GAC dose (g), $C_{control}$ is the final contaminant concentration of the control samples (mg/L), and C_e is the equilibrium liquid phase concentration (mg/L).

The experimental isotherm data were regressed with the Freundlich isotherm model:

$$q_e = kC_e^{1/n} \qquad (4\text{-}2)$$

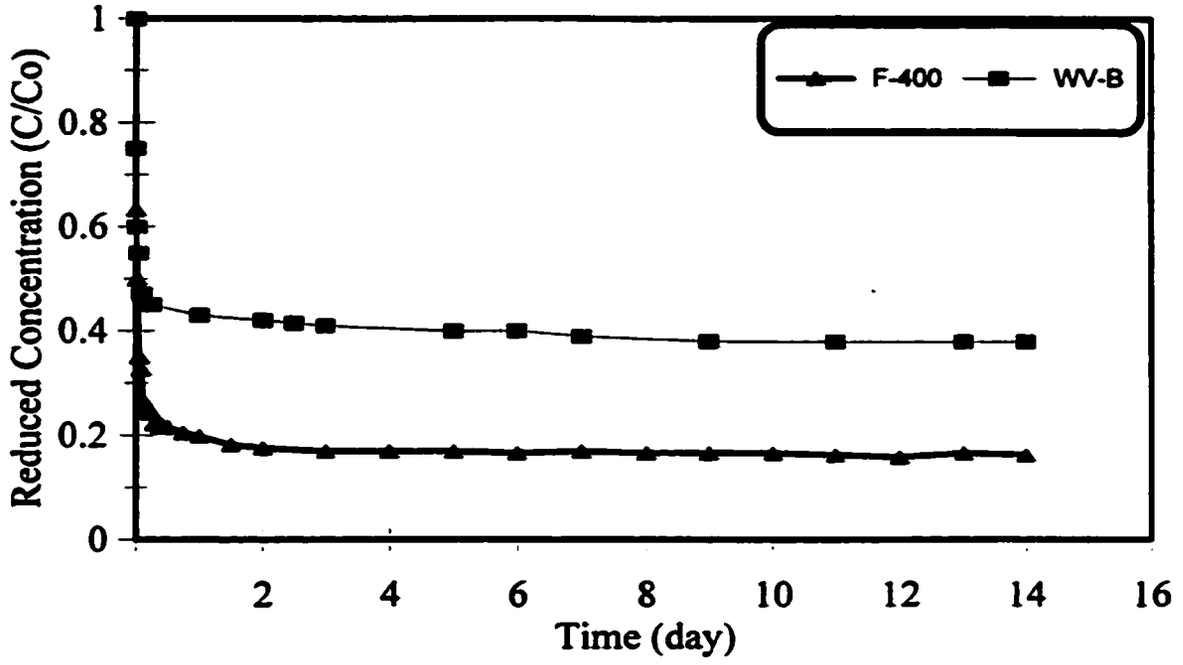

Fig. 4.1 Adsorption kinetics of phenol (GAC dose = 2g/L, C_o = 300 mg/L, temp. = 22°C, pH = 6.5).

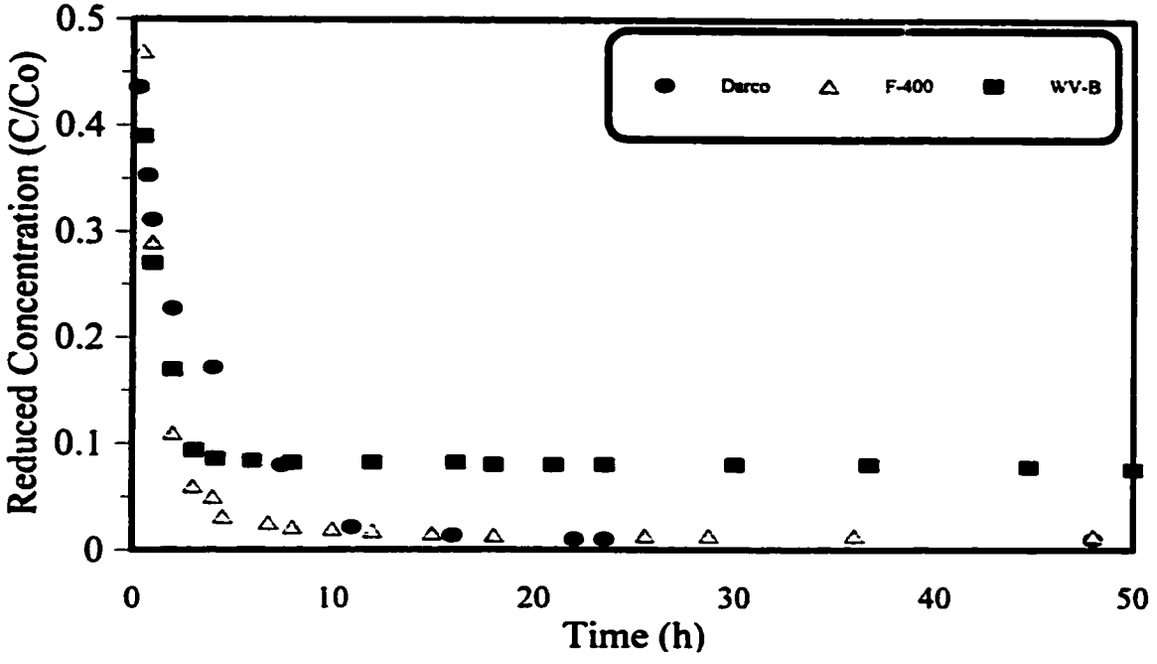

Fig. 4.2 Adsorption kinetics of 2NP (GAC dose = 2g/L, C_o = 500 mg/L, temp. = 22°C, pH = 5).

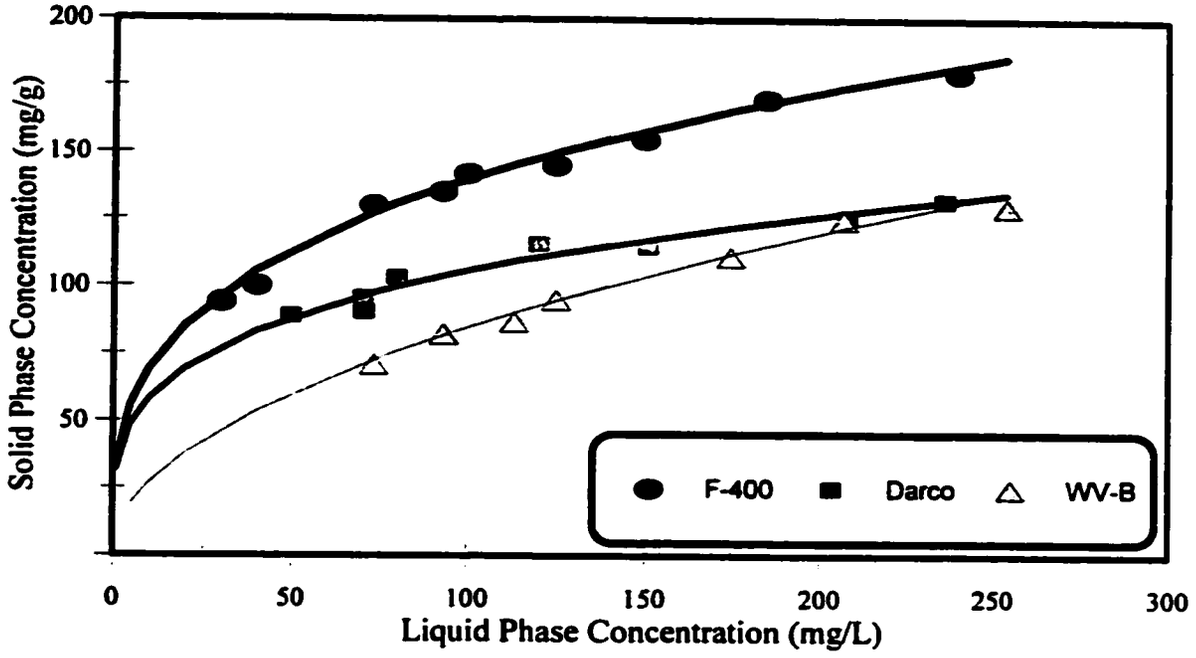

Fig. 4.3 Phenol isotherms (C_o = 300 mg/L, temp. = 22°C, pH = 6.5).

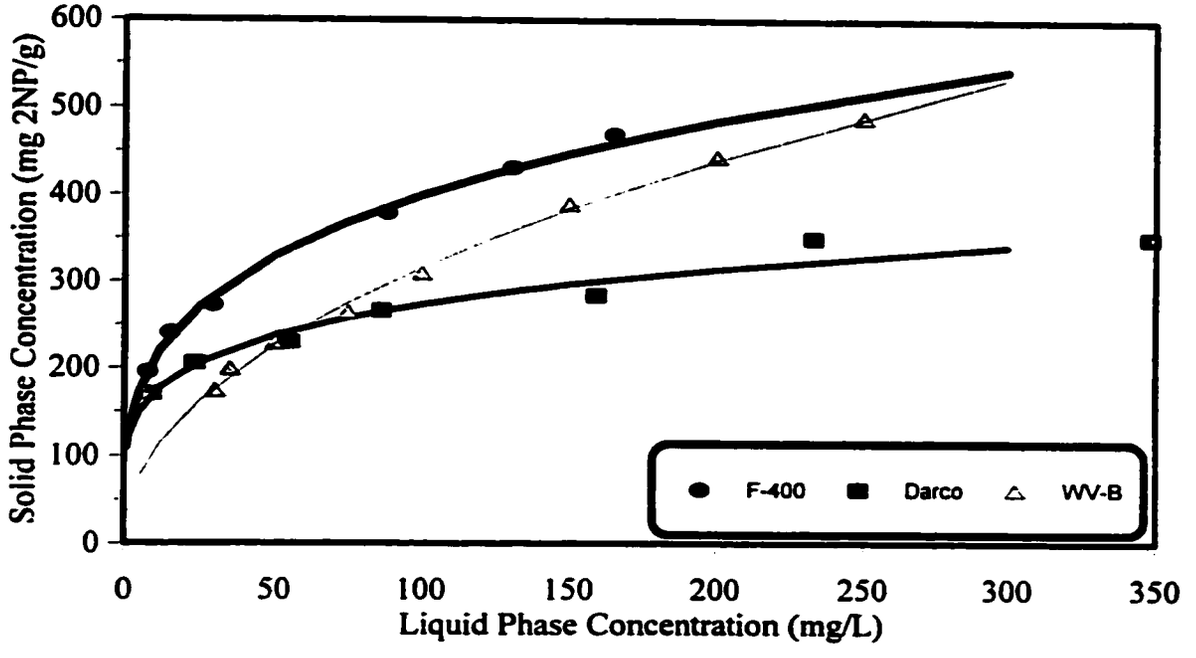

Fig. 4.4 2-nitrophenol isotherms (C_o = 500 mg/L, temp. = 22°C, pH = 5).

where q_e is the equilibrium solid phase concentration (mg of contaminant/g of GAC), and ***k*** and ***1/n*** are Freundlich model coefficients. The Freundlich model was chosen because it is the most widely used mathematical expression for the adsorption from aqueous solutions. The heterogeneous surface of activated carbon probably makes it the most compatible isotherm model. The values of the Freundlich coefficients, obtained by linearly regressing the logarithm-transformed data, are shown in Table 4.1. Visually, as well as based on the correlation coefficients (R^2), the fit was very good for the three GACs. For phenol the values of ***K*** and ***1/n*** are comparable with those of Vidic *et al.* (1993) and Narbaitz and Cen (1994). For 2NP the values of ***K*** and ***1/n*** are comparable with those of Karimi-Jashni (1994). These isotherms were used for calculation of the reactivation efficiencies in this study.

Because Filtrasorb F-300 loaded at the pilot-scale facilities of the Regional Municipality of Ottawa-Carleton (RMOC) was used to investigate the reactivation of GAC loaded with NOM, it was of interest to study the adsorption of Ottawa River NOM by F-300. The raw water sample was collected from the sedimentation tank effluent of the RMOC Britannia Water Treatment Plant. The initial concentration of non-purgeable organic carbon (NPOC) of the raw water sample was 2.95 mg/L. To accelerate the adsorption process the powdered form of virgin F-300 was used and the isotherm study was conducted by the batch bottle-point method. The adsorption isotherm of NOM by F-300 is shown in Fig. 4.5. The fitted Freundlich model coefficients are shown in Table 4.1.

Table 4.1 Isotherm parameters and their standard errors.

	pH	Temperature °C		F-400	WV-B	Darco	F-300
Phenol	6.5	22±1	K*	34.2±1.03	8.5±1.03	31.9±1.04	--
			1/n*	0.306±0.015	0.50±0.02	0.26±0.02	--
			R^2	0.990	0.990	0.950	--
2NP	5	22±1	K*	115±1.05	102±1.05	93±1.02	--
			1/n*	0.27±0.01	0.17±0.02	0.20±0.02	--
			R^2	0.996	0.920	0.920	--
TOC (phenol)	6.5	22±1	K*	31±1.03	--	--	--
			1/n*	0.288±0.011	--	--	--
			R^2	0.990	--	--	--
TOC(2NP)	5	22±1	K*	69±1.035	--	--	--
			1/n*	0.257±0.010	--	--	--
			R^2	0.991	--	--	--
NOM	6.2	22±1	K*	--	--	--	54±1.12
			1/n*	--	--	--	0.693±0.031
			R^2	--	--	--	0.976

* Where $q_e = KC_e^{1/n}$;
q_e is in (mg contaminant / g GAC);
C_e is in (mg contaminant / L);
K is in {(mg contaminant / g GAC)*[1/(mg contaminant / L)$^{1/n}$]};
1/n is unitless.

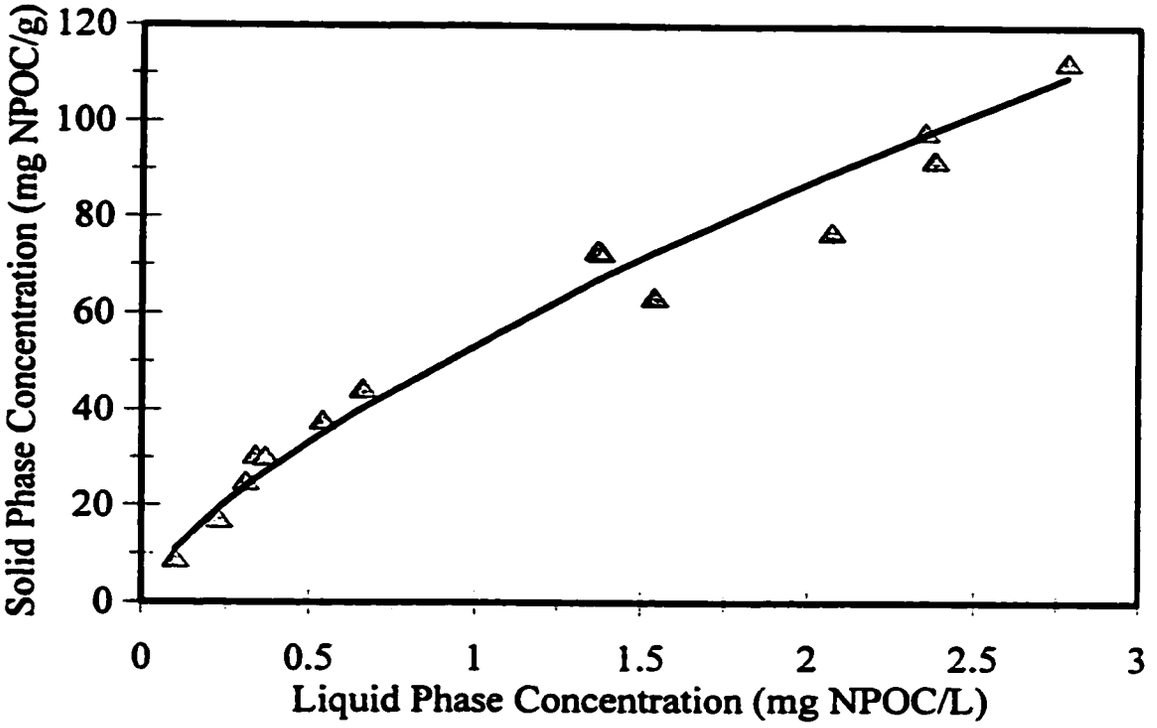

Fig. 4.5 NPOC isotherm on F-300 for coagulated/sedimented Ottawa River (temp. = 22°C, pH = 6.2, not buffered).

4.4 Comparison of Isotherms

During the electrochemical reactivation process the GAC was loaded and reloaded with both buffered and unbuffered solutions to investigate the effect of the pH of the reloaded solution on the reactivation efficiencies. Hence it was of interest to investigate the impact of buffering solution on the virgin GAC isotherms. Two phenol and 2NP solutions, one unbuffered (initial pH 6.5 for phenol and 5 for 2NP) and one buffered with phosphate salts at pH 4.5, were used for this purpose. As shown by Figs. 4.6 and 4.7 both isotherms were essentially identical. The similarities of the isotherms are also reflected in the isotherm parameters presented in Table 4.2. The parameter's intervals overlap each other which indicates that statistically the isotherms are the same. Hence, the buffering agent did not significantly affect the adsorption isotherms.

4.5 Total Organic Carbon Isotherms

Associated with electrochemical reactivation is the potential for producing by-products. These by-products may adsorb onto the GAC during the reactivation period and eventually desorb into the reloaded solution. There is a possibility that the method of evaluating the reactivation efficiency (i.e., measuring the concentration of the solution after the reloading step via HPLC and TOC) may affect the final results. To investigate the impact of these by-products on the reactivation efficiency, one needs to conduct the evaluation in terms of phenolics and TOC. Thus, there is a need for TOC isotherms. The TOC isotherms of phenol/F-400 and 2NP/F-400 were developed and are presented in Fig. 4.8. The experimental isotherm data were regressed on the Freundlich isotherm model. The values of the Freundlich coefficients, obtained by linearly regressing the logarithm-transformed data,

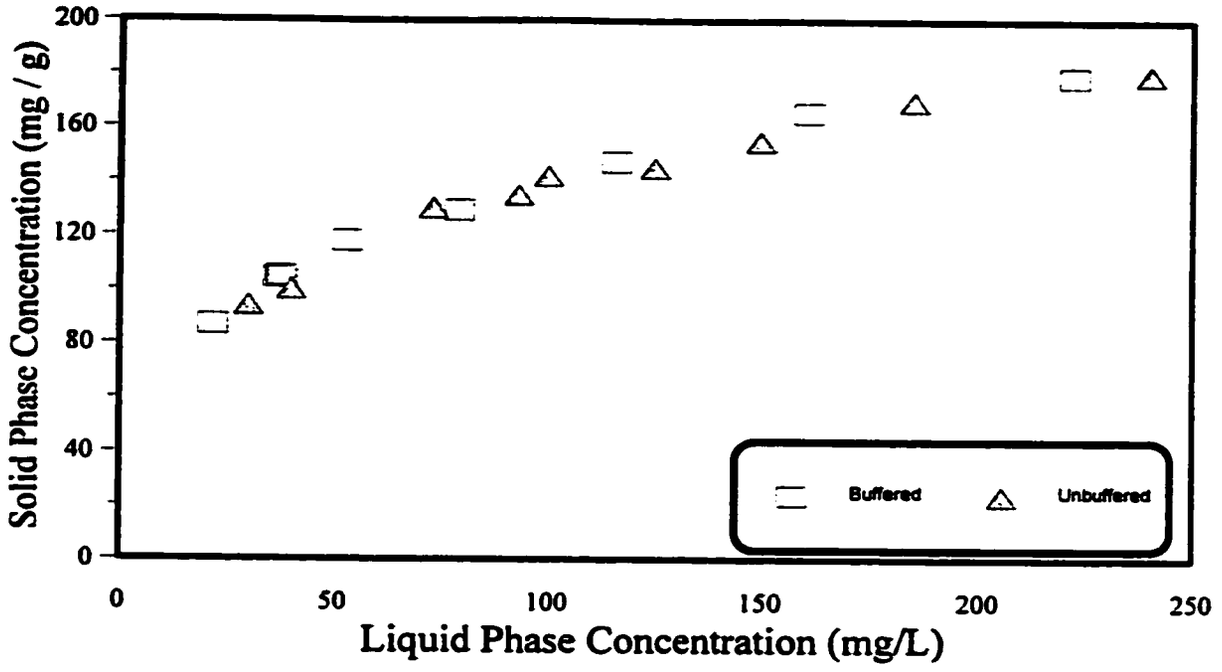

Fig. 4.6 Comparison of phenol isotherms on F-400 (C_o = 300 mg/L, temp. = 22°C, buffered pH = 4.5, unbuffered pH = 6.5).

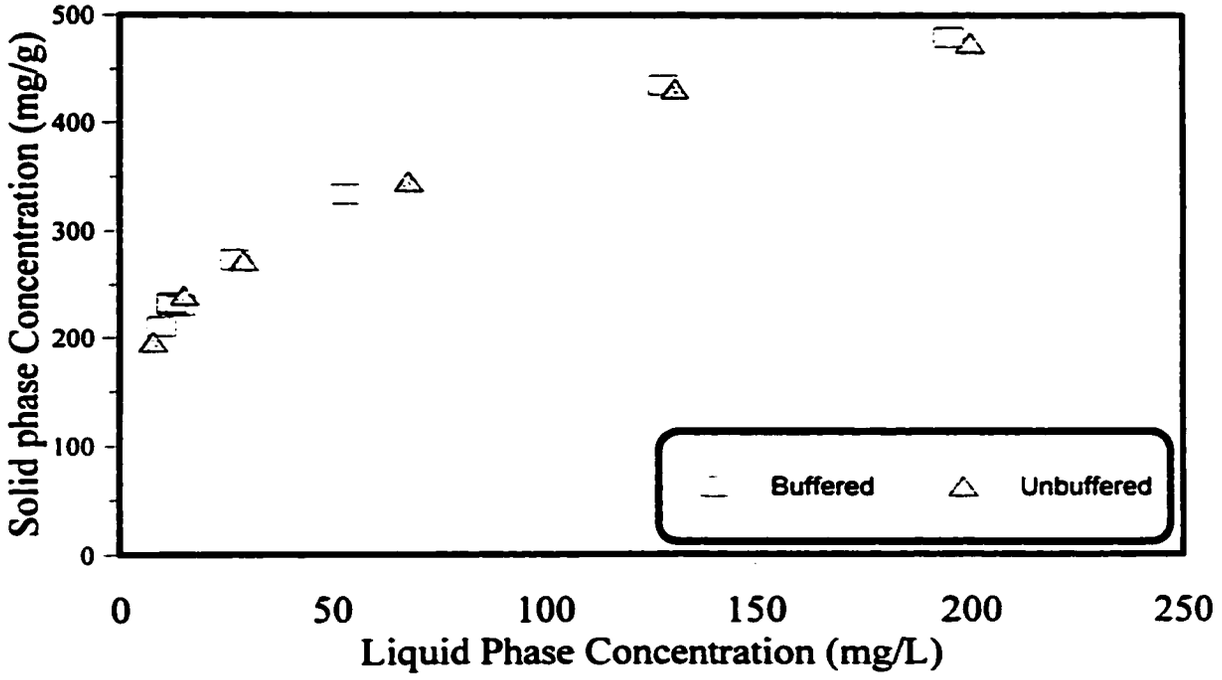

Fig. 4.7 Comparison of 2NP isotherms (C_o = 500 mg/L, temp. = 22°C, buffered pH = 4.5, unbuffered pH = 6.5).

Table 4.2 Comparison of buffered and unbuffered isotherm parameters and their standard errors on F- 400

	pH	Temperature °C		F-400
Buffered phenol	4.5	22±1	K*	34.1±1.02
			1/n*	0.308±0.015
			R^2	0.992
Unbuffered phenol	6.5	22±1	K*	34.2±1.03
			1/n*	0.306±0.015
			R^2	0.990
Buffered 2NP	4.5	22±1	K*	115±1.05
			1/n*	0.27±0.01
			R^2	0.996
Unbuffered 2NP	5	22±1	K*	113±1.03
			1/n*	0.27±0.01
			R^2	0.993

* Where $q_e = KC_e^{1/n}$;
q_e is in (mg contaminant / g GAC);
C_e is in (mg contaminant / L);
K is in {(mg contaminant / g GAC)*[1/(mg contaminant / L)$^{1/n}$]};
1/n is unitless.

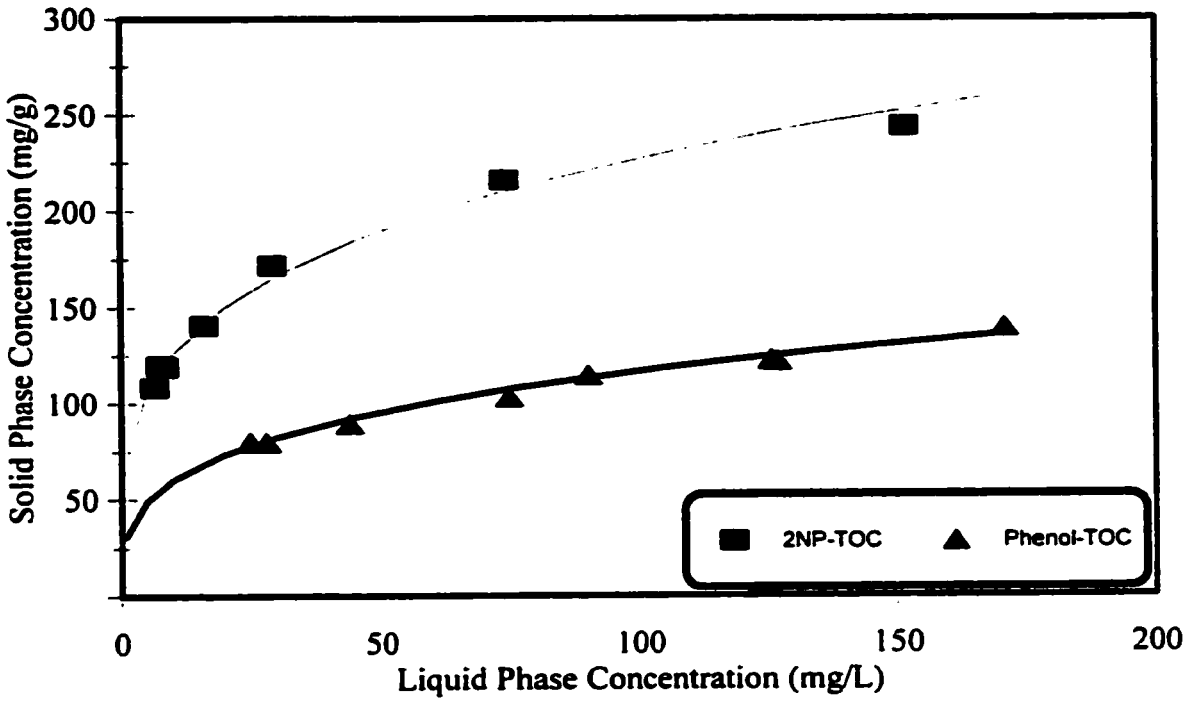

Fig. 4.8 TOC isotherms on F-400 (temp. = 22°C, buffered at pH = 4.5).

are shown in Table 4.1. These isotherms were used in section 6.6 to evaluate the possible impact of the desorbed by-products on the reactivation efficiencies.

4.6 Conclusions

- The adsorption kinetics experiments showed that for the large activated carbon dose, used in future adsorption experiments, 4 and 8 days were sufficient to reach equilibrium for phenol adsorption on F-400 and WV-B, respectively. Also it was observed that less than 1 day was sufficient to ensure equilibrium for 2NP adsorption on F-400, WV-B, and DARCO.
- The 2NP and phenol adsorption isotherms on F-400, WV-B, and DARCO were well described by the Freundlich isotherm model and the results were similar to those isotherms already reported by other researchers in the literature.
- The inclusion of a buffering agent in the phenol and 2NP solutions did not significantly affect the isotherms.

CHAPTER 5

REACTOR DESIGN

5.1 Introduction

The electrochemical reactor is a key unit in applying electrochemical technology to GAC reactivation. Consequently, it is important to optimise the reactor performance. A large number of interrelated factors must be considered during the development of a new reactor.

Narbaitz and Cen (1994) conducted a sensitivity analysis of the key process variables using a very simple bench-scale reactor and concluded that electrochemical reactivation of GAC at a laboratory-scale is a feasible alternative to thermal reactivation. Due to the reactor configuration and the single adsorbent/adsorbate combination used in their research many questions about the process remain unanswered. They studied a single layer of GAC particles placed on a platinum electrode and the only mixing within their reactor was natural (free) convection. Natural convection occurs by local variations in fluid density (often caused by local variation in temperature) and/or the movement of electro-generated gas bubbles. Due to the reactor configuration, evaluation of the effect of electrolyte mixing on the reactivation efficiency was not possible. These authors speculated that forced mixing of the electrolyte may improve the reactor's performance. The main objectives of this chapter were to evaluate the impact of the reactor configurations and to investigate the effect of forced mixing of the electrolyte on the performance of the electrochemical reactivation of GAC.

5.2 Reactor Configurations

The following four different reactor configurations were investigated: a glass batch reactor used by Narbaitz and Cen (1994), a new glass batch reactor with the capability of electrolyte re-circulation, a divided-cell reactor with electrode separation by an ion exchange membrane, and a stainless steel column type reactor.

5.2.1 Comparison of the New Batch Reactor with the Old Batch Reactor

The new batch reactor (Fig. 3.3) was compared with the reactor used by Narbaitz and Cen (1994) (Fig. 3.1). Cathodic reactivation of 1.2 g of F-400, which was loaded with phenol using the bottle-point loading method, was carried out at 50 mA constant current. In both reactors the electrodes were kept 2 cm apart and a single layer of GAC was tested. One liter of 0.1 M NaCl solution was used as the electrolyte. There was no forced mixing and the reactivation was carried out for different reactivation times. The RE3 method was used to calculate the reactivation efficiency and the results are shown in Fig. 5.1. It shows that both reactors behaved similarly and that the reactivation of F-400 increased almost linearly with reactivation time. Fig. 5.1 also shows that the new batch reactor demonstrated slightly higher reactivation efficiencies for this set of conditions. The REs for the old reactor were about 40% lower than those reported by Narbaitz and Cen (1994), however they calculated the reactivation efficiencies by the RE2 method which causes the calculated reactivation efficiencies to be higher than the actual efficiencies (Narbaitz and Cen, 1997).

The two reactors were also compared at different current densities using the same F-400 and reactivation time of 2.5 h. As Fig. 5.2 shows, the reactivation efficiencies increased as

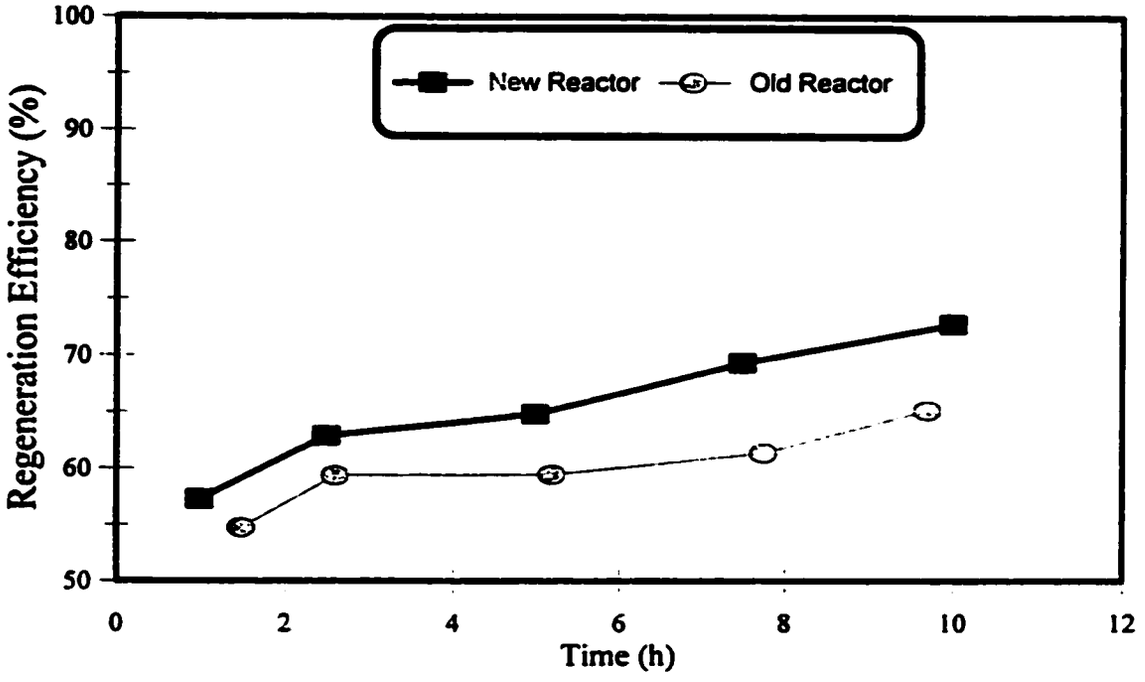

Fig. 5.1 Comparison of reactors (1.2 g of phenol-loaded F-400, I = 50 mA, no mixing).

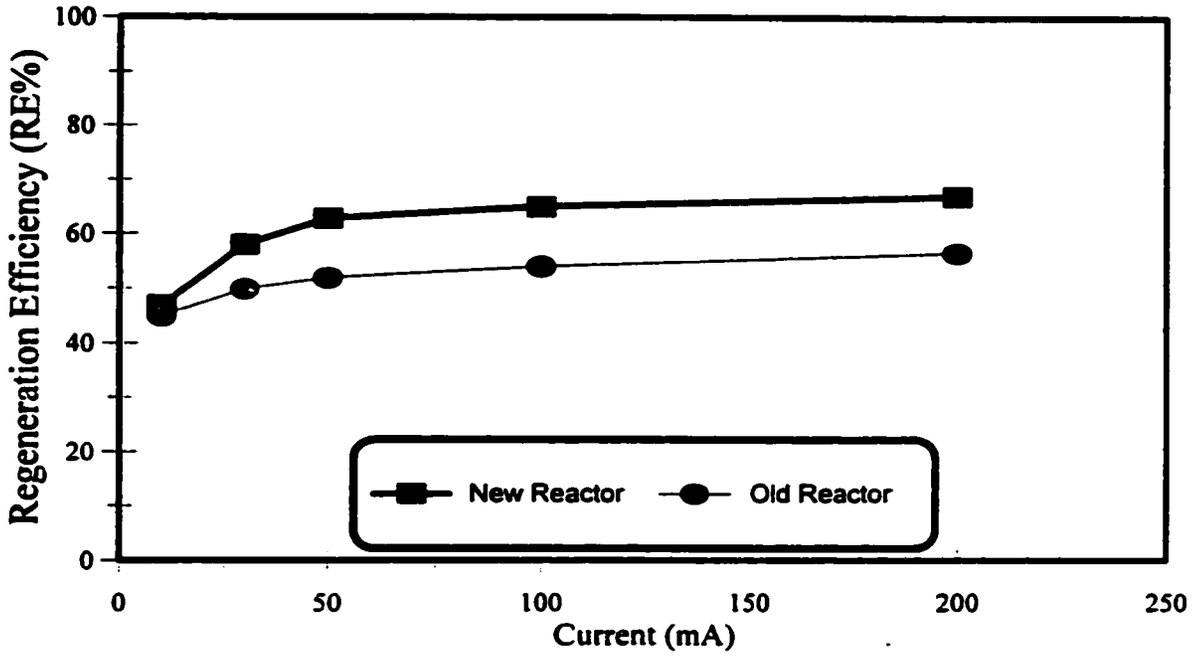

Fig. 5.2 Comparison of reactors (1.2 g of phenol-loaded F-400, reactivation time = 2.5 h, no mixing).

current increased up to 50 mA then levels off. Fig. 5.2 also shows that the new batch reactor demonstrated slightly higher reactivation efficiencies for all the currents tested.

The two reactors were different in a number of ways. The cell of the old reactor (Fig. 3.1) consisted of two 7.6 cm diameter platinum sheets and two plexiglas rings that kept the GAC particles on the platinum electrodes and maintained the platinum electrodes apart. The plexiglas rings had several perforations to allow bubbles generated at the electrodes to escape and allow the electrolyte to move in and out of the cell compartments. The new batch reactor was a glass column of 7.6 cm i.d. and 25 cm high with the capability of working as a simple batch reactor, a re-circulating batch reactor, or as a flow through reactor (Fig. 3.3). The cell of the new batch reactor consisted of two 7.6 cm diameter platinum wire meshes and two Teflon rings that kept the meshes and the GAC particles on the platinum mesh. The mesh structure of the electrodes allowed bubbles generated at the electrodes to escape and the electrolyte to move in and out of the mesh's openings. The improved performance of the new reactor could be due to a better movement of the desorbed phenol from the GAC to the whole bulk solution through the openings within the platinum mesh, while in the old reactor the movement of the desorbed phenol may have been limited by the few perforations of the plexiglas rings. Thus, desorption of phenol from GAC may have been somewhat hindered by the higher phenol concentration in the adjacent liquid.

5.2.2 Column Reactor

The 3 cm i.d. stainless steel column reactor (Fig. 3.2) was studied as another possible reactor configuration. Electrochemical reactivation was conducted by filling the stainless steel column with 19.2 g of the GAC particles. A vertical stainless steel bar conductor was

positioned in the GAC bed. The phenol solutions (TOC_o = 800 mg/L) entered the column at a flow rate of 6.6 mL/min (Empty Bed Contact Time = 7 min.) and the GAC sorbed the phenol during the filtration. For simplicity the phenol concentrations were measured by TOC rather than the more specific HPLC-based method. The results are presented in Fig. 5.3. After saturation of the GAC, the phenol solution was drained from the column and it (with the GAC) was filled with 100 mL of a 0.1 M NaCl solution. A constant electrical current was then passed through the electrodes. A few tests were conducted to evaluate the column reactor performance under different conditions. First, the column shell was used as the anode and the stainless steel bar as the cathode. Cathodic reactivation was carried out at a constant current of 50 mA. One test was conducted with no electrolyte flow and another test was performed with re-circulating electrolyte (1 L). After 5 hours of reactivation the electrolyte was drained and the reactivated GAC was reloaded with the same phenol solution and loading method. The reloading results are also presented in Fig. 5.3. As Fig. 5.3 shows, there was no appreciable difference between the two conditions tested. The reactivation efficiency was calculated by:

$$RE\% = \frac{\int_0^t Q(C_{in} - C_{out})dt|_{reloading}}{\int_0^t Q(C_{in} - C_{out})dt|_{loading}} * 100 \qquad (5\text{-}1)$$

where RE represents the reactivation efficiency, C_{in} is the influent concentration and C_{out} is the effluent concentration. Applying equation (5-1), the reactivation efficiency from Fig. 5.3 was about 30%.

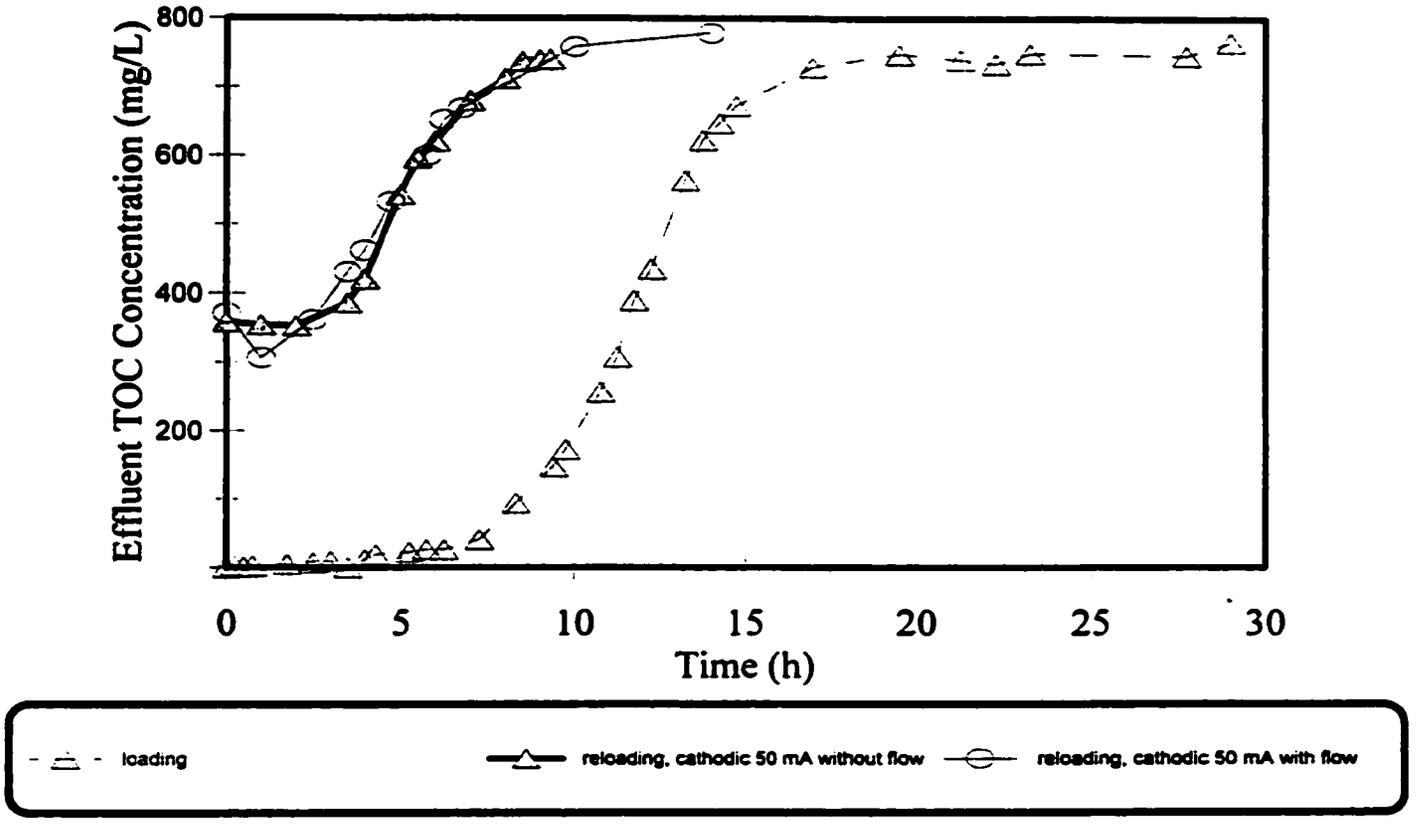

Fig. 5.3 Effluent concentrations during the column loading and reloading (phenol-loaded F-400, GAC = 19.2 g, I = 50 mA)

Two more sets of experiments were conducted. One set used the column shell as the anode and the stainless steel bar as the cathode. A constant current of 250 mA (cathode as working electrode) was applied for 5 hours. The reloading results are shown in Fig. 5.4. The second test was conducted using the column shell as the cathode and the stainless steel bar as the anode. In order to be able to compare the results with those of Slavinskii *et al.* (1984) a constant current of 750 mA (anode as working electrode) was applied for 35 minutes. The reloading results are also shown in Fig. 5.4. At the end of both experiments the column shell and the stainless steel bar were partially corroded and some reddish dissolved metal was observed in the electrolyte. The reactivation efficiencies were about 10 to 15%, far less than the 97% claimed by Slavinskii *et al.* (1984) for a similar set-up. Unfortunately the paper by Slavinskii *et al.* (1984) presents only a superficial description of their work so it is impossible to arrive at a solid conclusion regarding the cause of such a large difference in reactivation efficiencies.

5.2.3 Comparison of the Divided-Cell Reactor with the New Undivided Batch Reactor

The divided-cell reactor was different from the undivided batch reactor as it was operable as two compartments (with an electrode in each compartment) separated by an ion selective membrane (Fig. 3.4). It was operable as a divided-cell reactor with no forced mixing of the electrolyte or with forced mixing in either or both compartments. The results of reactivating 1.2 g of phenol-loaded F-400 (single layer) at 50 mA without any mixing are plotted in Fig. 5.5. The anode and cathode compartments were separated by a Raipore R4010 cation exchange membrane. As Fig. 5.5 shows, the divided-cell reactor had higher efficiencies that may have been due to the higher pH within the cathodic compartment (section 5.4.5) where

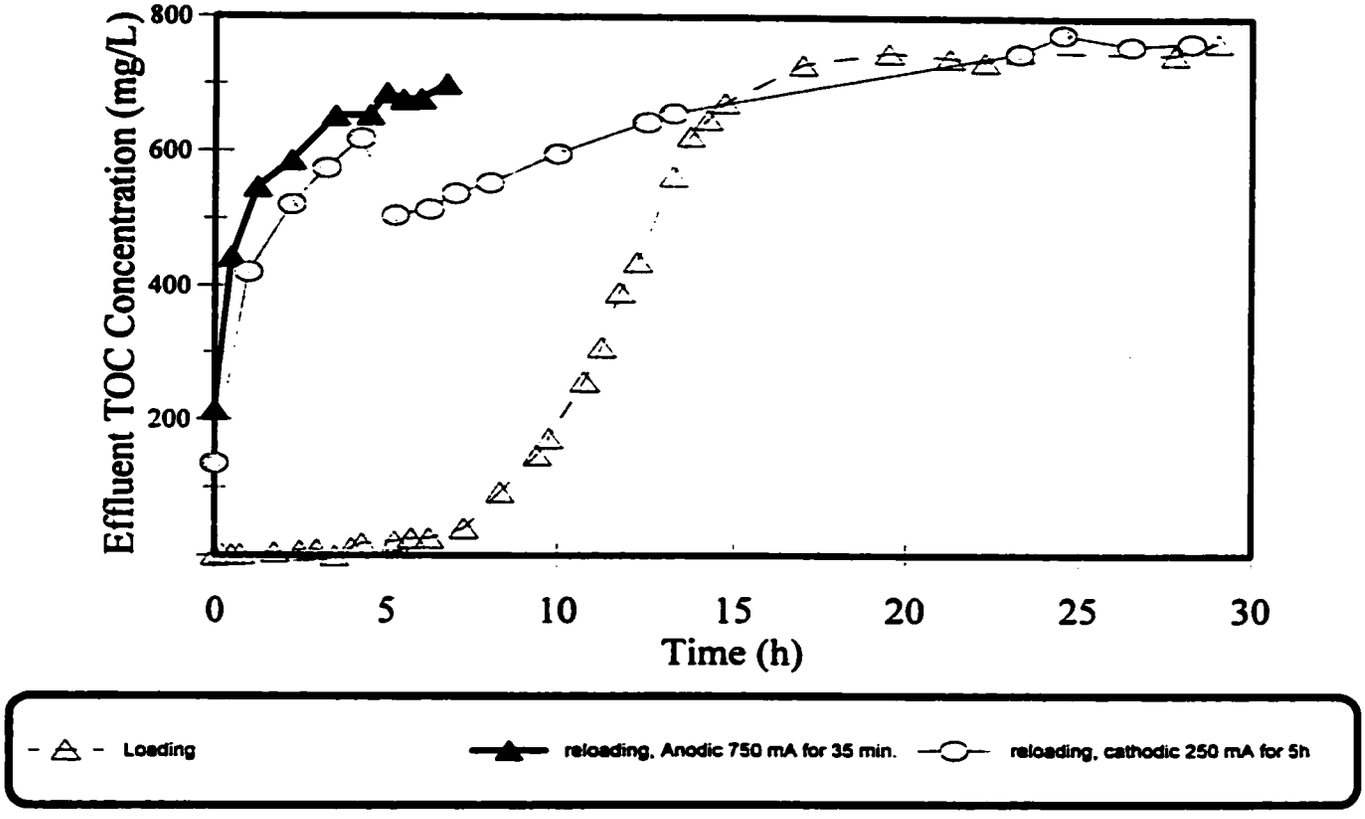

Fig. 5.4 Effluent concentrations during the column loading and reloading (phenol-loaded F-400, GAC = 19.2 g)

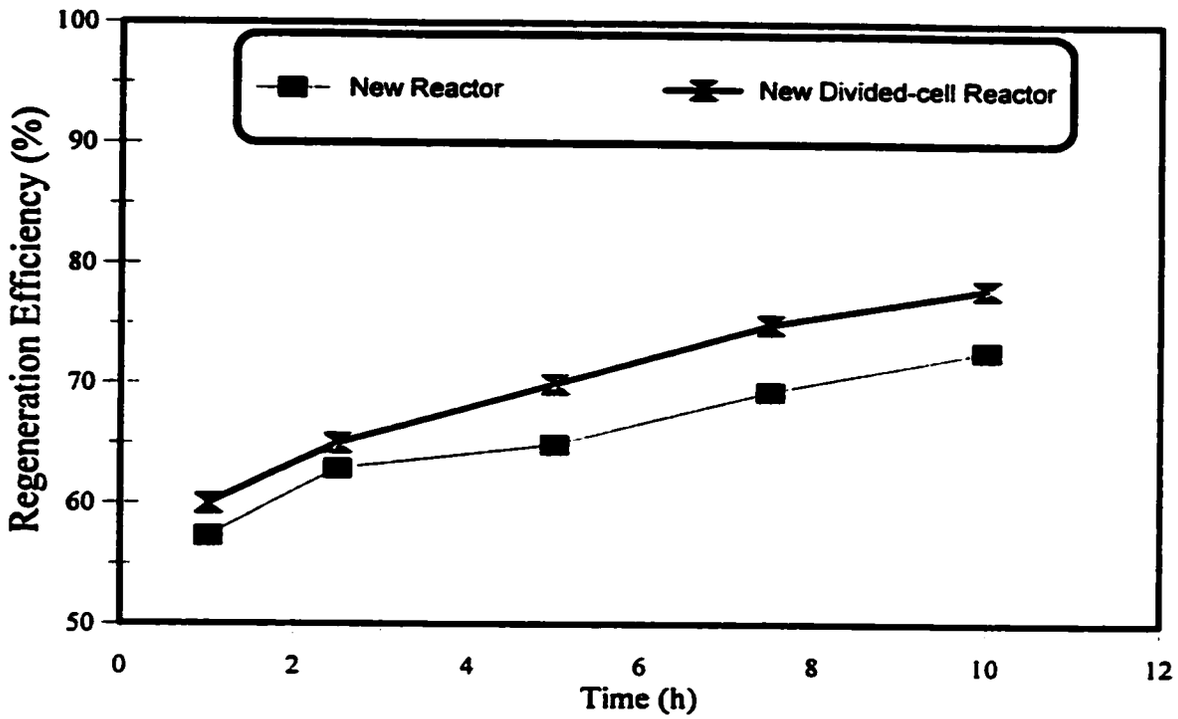

Fig. 5.5 Comparison of reactors (1.2 g of phenol-loaded F-400, I = 50 mA, no mixing).

the GAC was located. However, the high cost of the ion exchange membrane, the need for oxidation of the desorbed contaminants at the anode, the difficulty in setting up and operating the divided-cell reactor, and the difficulty in the release of electro-generated gases (i.e., the electro-generated gas bubbles from the lower mesh accumulated underneath of membrane sheet) are disadvantages of the divided-cell reactor which counterbalance its better performance. Ideally it would be better if one could improve the undivided reactor performance rather than using divided-cell reactors.

5.3 Multi-Layer Reactivation

In this set of experiments the need for direct contact between GAC particles and the electrode surface was investigated. If direct contact between the GAC particles and the electrode surface was unnecessary, then electrodes could be used to reactivate greater volumes of GAC which would reduce the capital cost of electrochemical reactivation. To investigate the need for direct contact between GAC particles and the electrode surface, experiments (using the new undivided-cell and the old reactors) were conducted using a different number of layers of GAC particles on the electrode, i.e., a bed of GAC on the electrode constructed from loosely contacting GAC particles. The reactors held a minimum of 1.2 g of commercial size GAC particles (1-2 mm diameter) for each layer. As reactivation was likely to be aided by the conductivity of the GAC, the multi-layer evaluation was conducted using three GACs with different conductivities. In order to load up to 19.2 g of F-400 with a phenol solid concentration of 105 mg phenol/g of GAC while using 500 and 1000 ml bottles, the concentration of the phenol loading solution had to be increased to 1000 mg/L.

Fig. 5.6a shows the multi-layer reactivation of three GACs (F-400, WV-B, and Darco) loaded with phenol, using the new undivided-cell electrochemical reactor. Reactivation of up to 19.2 g of GAC loaded with phenol was studied. Increasing the mass of GAC from 1.2 to 19.2 g caused a decrease in the reactivation efficiency of about 40%. Fig. 5.6a shows that all the GACs followed a similar pattern. Hence, the significant differences in the electrical resistance of the various types of GAC (Table 3.2) did not translate into significant differences in reactivation efficiency for this reactivation current and reactivation time. Fig 5.6b shows the same results plotted as reactivation efficiency versus number of the GAC layers. Since density of the three types of GACs are different, a given mass of GAC represents different number of layers for the different GACs. For example, 19.2 g of GAC creats 16 layers of F-400, 17 layers of Darco and 32 layers of WV-B. Fig. 5.6b shows that increasing the number of layers of GAC decreased the reactivation efficiency. Fig. 5.6b also shows that all the GACs followed a similar pattern and WV-B performance is higher than the F-400 and Darco. However, since design is based on the mass of GAC rather than the number of the GAC layers, Fig. 5.6a is a better representation of the results.

The multi-layer tests were repeated using the old reactor (Narbaitz and Cen, 1994) and the results are shown in Figs. 5.7a and 5.7b. They demonstrated similar results to those obtained by the new reactor (Figs. 5.6a and 5.6b) in that increasing the GAC mass, i.e. increasing the number of layers of GAC, decreased the reactivation efficiency. Such a decrease in reactivation efficiency could be due to either the need for direct contact between the GAC particles and the electrode surface or due to the high variation from high pH at the cathode to low pH at the anode (section 5.4.5). The top layers of GACs which are closer to the

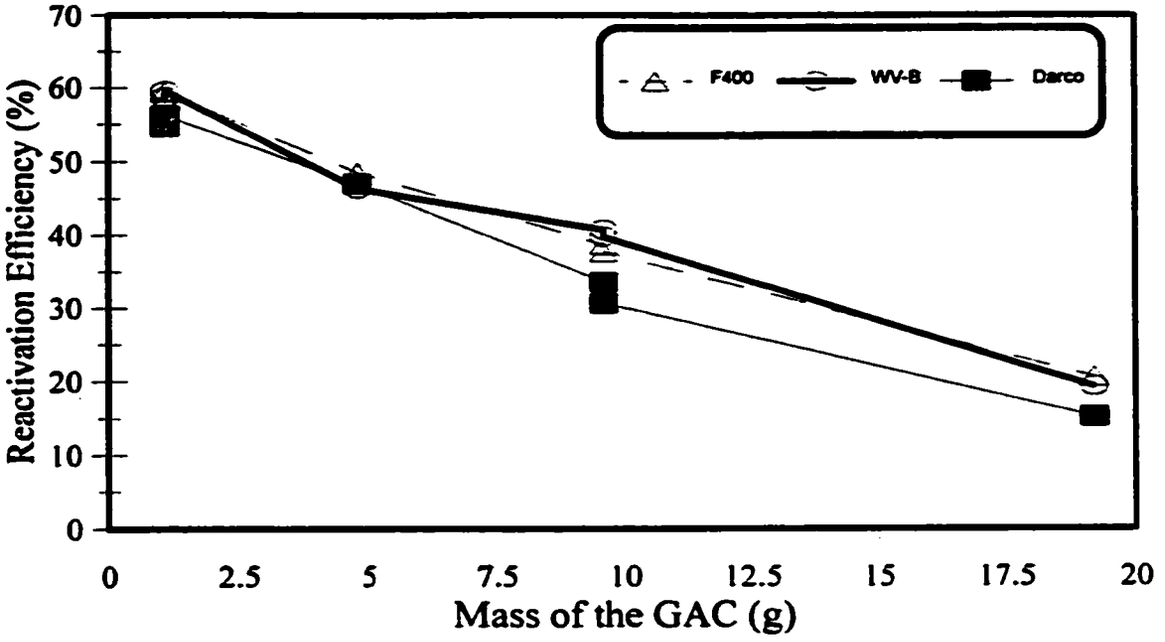

Fig. 5.6a Reactivation efficiency versus GAC mass for three types of GAC loaded with phenol at 50 mA and 5 hours reactivation using the new reactor.

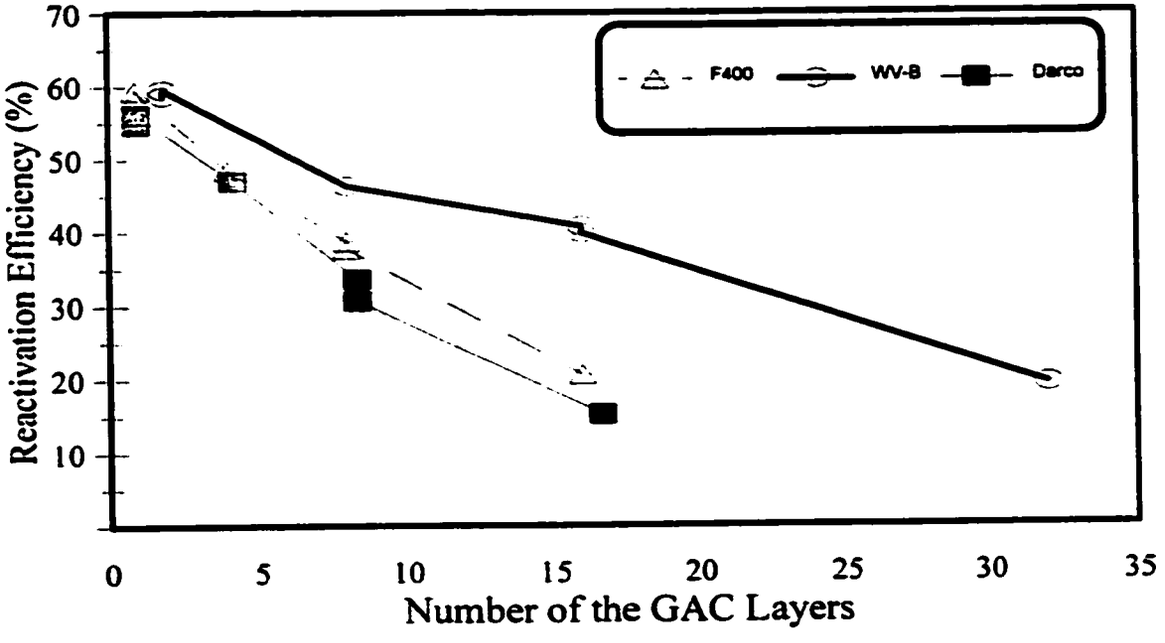

Fig. 5.6b Reactivation efficiency versus number of GAC layers for three types of GAC loaded with phenol at 50 mA and 5 hours reactivation using the new reactor.

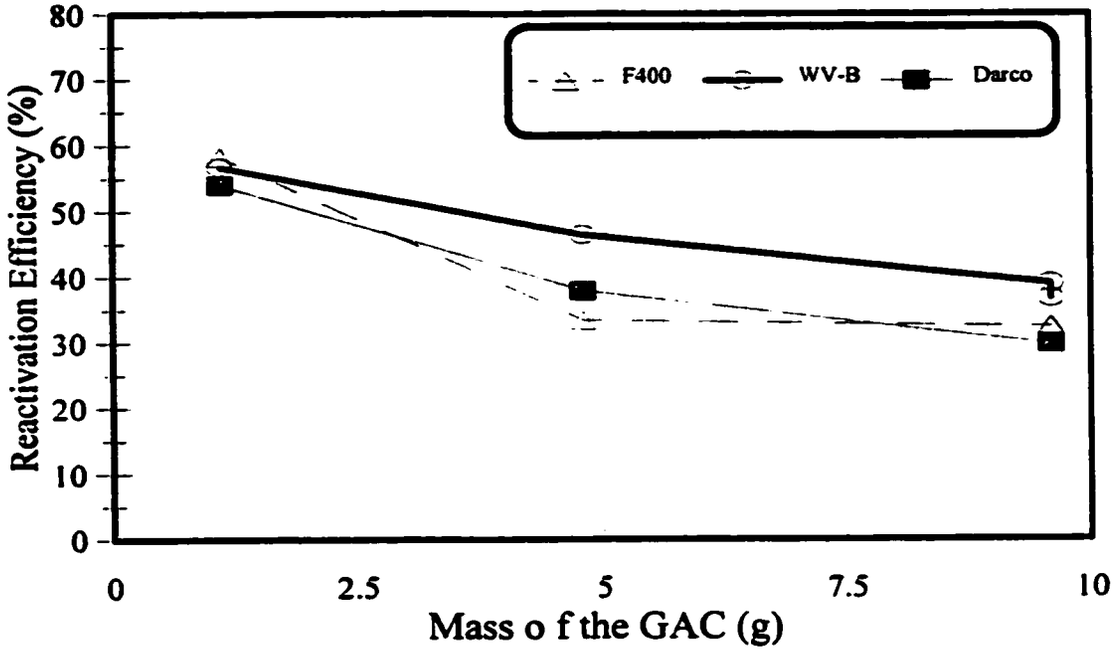

Fig. 5.7a Reactivation efficiency versus GAC mass for three types of GAC loaded with phenol at 50 mA and 5 hours reactivation using the old reactor.

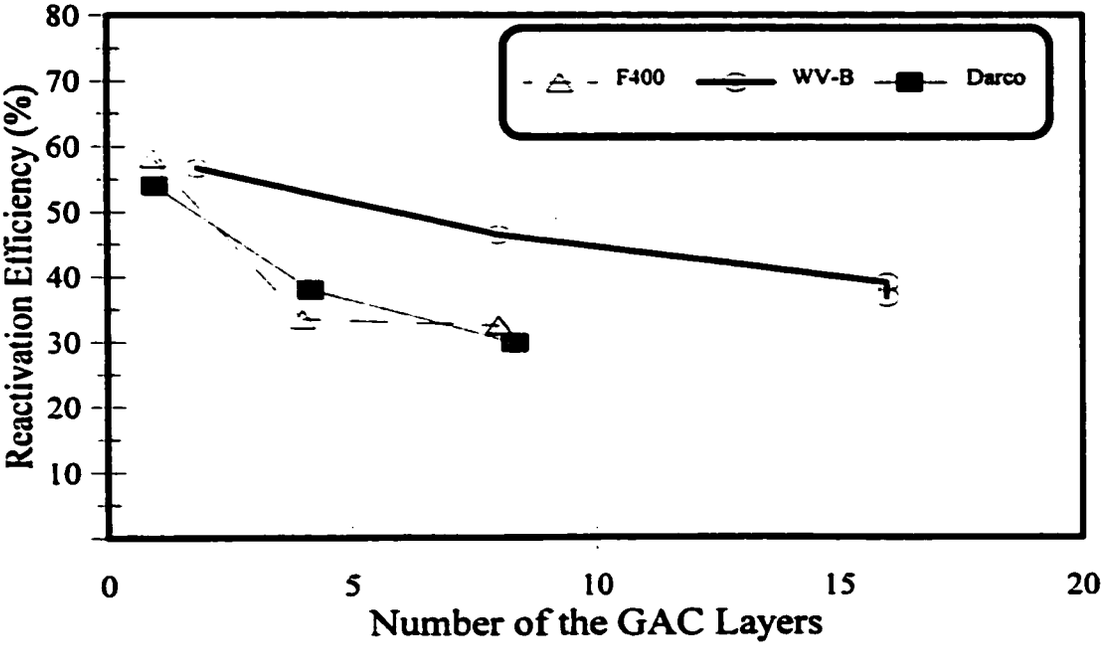

Fig. 5.7b Reactivation efficiency versus number of GAC layers for three types of GAC loaded with phenol at 50 mA and 5 hours reactivation using the old reactor.

anode may be subjected to a lower pH than the pK_a of the phenol (pH=9.9), consequently it caused a reduced phenol desorption and lower reactivation efficiency.

In order to eliminate possible pH variations through the GAC bed from cathode to anode, tests were conducted with the new divided-cell reactor which had the cathode separated from the anode by a cation-exchange membrane. A mass of 4.8 g of phenol-loaded WV-B was placed on the cathode and reactivated for 5 h. The calculated reactivation efficiency was 45%, which was almost the same as the one without membrane separation (i.e., GAC was subjected to possible pH variation) in Fig. 5.6. This suggests that the pH variation was not the main reason for lower reactivation efficiencies of the multi-layer reactivation. However, because of the limited number of experiments these results need to be verified.

5.4 Effect of Electrolyte Mixing on the Electrochemical Reactivation of GAC

5.4.1 Introduction

The following is a discussion of the importance of electrolyte mixing. The final goal of the GAC electrochemical reactivation process is the total destruction of the adsorbed contaminants (organics). Destruction of the organics may occur on the GAC surface, on the surface of the electrode, and in solution. If the destruction occurs in solution or on the GAC's outer surface then it is most likely that the desorption rate of the contaminants from the internal surface of the GAC to the liquid phase will control the reactivation process (assuming the electrochemical transformations are fast). If the destruction occurs only at the electrode surface, then a succession of four steps must take place: desorption of reactant (contaminant) from the GAC surface to the liquid phase; mass transfer of reactants to the electrode surface; electrochemical transformations; and mass transfer of products from the

electrode surface. Fig. 5.8 shows different steps involved in the overall anodic oxidation. In general both the kinetics of electron transfer and the mass transport of reacting species determine the rate of electrochemical reactions at the surface of electrodes. With increasing polarization (charging) of the electrode, as current density is increased, the electrode can become starved of reactant. The rate of mass transport then governs, and it limits the overall reaction rate (Scott, 1995). The mass transport of ionic species is determined by the desorption rate of the contaminant from the GAC, and the hydrodynamics of the electrolyte flow in the vicinity of the electrode. The rate of desorption depends on the concentration gradient as well as on the environmental conditions, such as pH and temperature. The hydrodynamics of electrolyte flow includes the convective movement of species associated with the bulk movement. Also the diffusion of the species to the electrode due to the existence of a concentration gradient, and the migration of species under the influence of a potential gradient, may influence the mass transport.

In general in the electrochemical reactivation of GAC, the electrolyte flow velocity may be important for several reasons. A high flow velocity may result in the following beneficial characteristics: (a) a high rate of mass transport of the desorbed contaminant from the surface of the GAC particles to the surface of the oxidizing electrode; and (b) assistance in the removal of electrogenerated gases, which would affect the electrolyte conductivity. However, a high value of electrolyte velocity may have the following disadvantages: (a) it will increase the energy consumption required in electrolyte pumping because of the increased pressure drop in the bed; and (b) it may reduce the desorption rate of the adsorbed contaminant from the GAC by lowering the pH near the cathode, where the GAC is located.

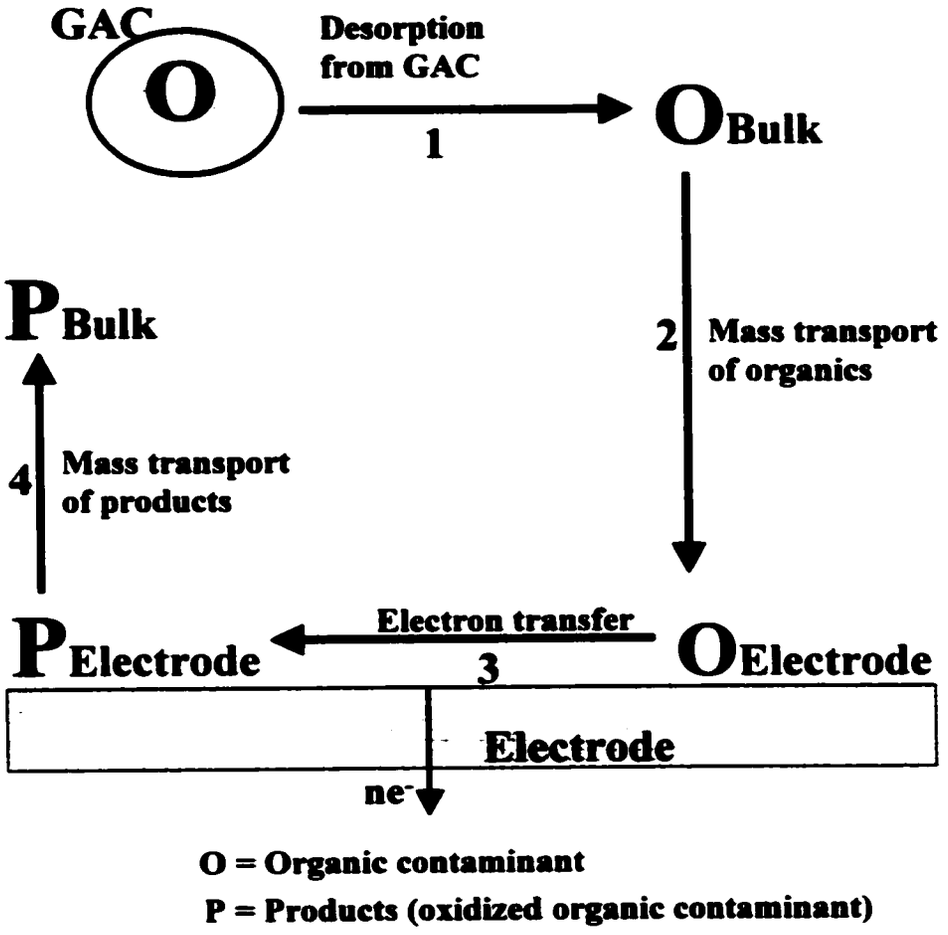

Fig. 5.8 Steps involved in the overall anodic process.

To investigate the effect of electrolyte mixing on reactivation efficiency, GAC reactivation was carried out in the new undivided batch reactor (Fig. 3.3). This reactor held one layer of the preloaded GAC (1.2 g) on top of a platinum wire mesh electrode and the electrolyte was continuously re-circulated with a pump to provide electrolyte mixing. Different electrolyte flow rates provided different degrees of mixing. The influence of forced mixing on the oxidation of phenol, cell voltage, and reactivation efficiencies are discussed in the next sections.

5.4.2 Effect of Electrolyte Flow on the Oxidation of Phenol and 2NP

One of the potential advantages of GAC electrochemical reactivation over other methods of reactivation is the oxidation of contaminants desorbed from the GAC during the reactivation process. Thus, not only is the GAC reactivated but also the organic contaminant(s) is potentially oxidized to H_2O, CO_2, and intermediates. As oxidation is expected to occur primarily at the anode and the contaminant-loaded GAC is normally at the cathode, it is important that the effect of electrolyte mixing on the oxidation of the contaminant be investigated.

The electrochemical reactor without GAC was used to study the phenol oxidation kinetics. One liter of 50 mg/L phenol solution was used in this study. A 50 mg/L concentration was chosen because it was the maximum phenol concentration measured during the GAC reactivation at 50 mA current. Flow rates of 1 L/min (with a theoretical retention time of 1 min) and 0.2 L/min (with a theoretical retention time of 5 min) were used in this study. Fig. 5.9 shows the kinetics of the oxidation of phenol at different flow rates and a current of 50 mA. It demonstrates that the oxidation rate of phenol was slow and about 20 to 30 hours

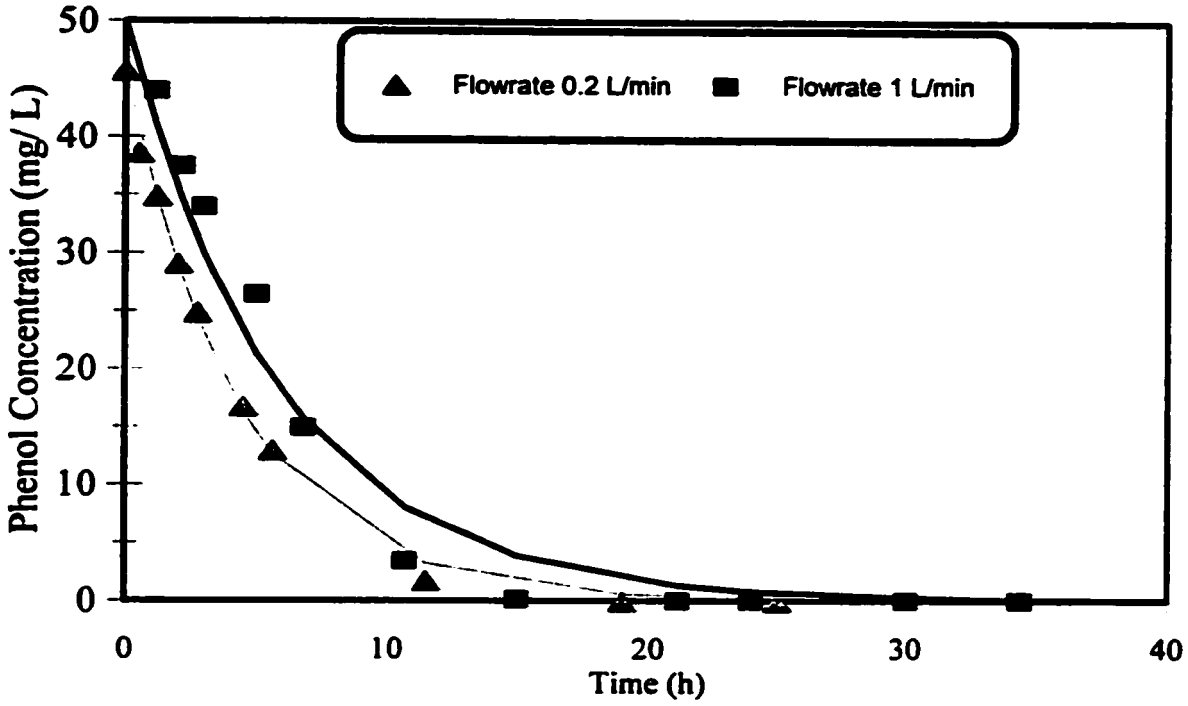

Fig. 5.9 Oxidation of phenol at different electrolyte flowrates (I = 50 mA, undivided reactor, no GAC).

were needed to reduce the phenol concentration to the detection limit. The phenol oxidation rate followed a first-order electrochemical reaction and this is in agreement with the results of Azzam *et al.* (1999), Murphy, *et al.* (1992), and Smith De Sucre and Watkinson (1981). The first-order coefficients were determined by a non-linear regression routine in STATGRAPHICS PLUS (Manugistics, Inc., Rockville, Maryland, USA) and are shown as lines in Fig. 5.9. The experimental data were defined by first-order expressions:

$$C = C_o(\exp(-0.18*t)) \qquad (5\text{-}2)$$

and

$$C = C_o(\exp(-0.23*t)) \qquad (5\text{-}3)$$

for flow rates of 1 L/min and 0.2 L/min, respectively, where C_o is the initial phenol concentration (mg/L) and t is the time (h). The oxidation rate at a flow rate of 0.2 L/min was slightly higher than the oxidation rate at 1 L/min. This shows that the oxidation of phenol was not mass transport controlled, so it must be electrochemical transformation limited. This is consistent with the findings of Smith De Sucre and Watkinson (1981). They studied the effect of electrolyte flow rate on the anodic oxidation of phenol in a single pass through an undivided-cell using lead dioxide anodes. They observed that single pass phenol conversion decreased with increasing flow rate.

Fig. 5.10 shows the kinetics of oxidation of 2NP at different flow rates and a current of 50 mA. A 70 mg/L concentration was chosen because it was the maximum 2NP concentration measured during the 2NP loaded GAC reactivation at 50 mA current. Fig. 5.10 demonstrates that the oxidation rate of 2NP is also slow and more than 10 hours are needed

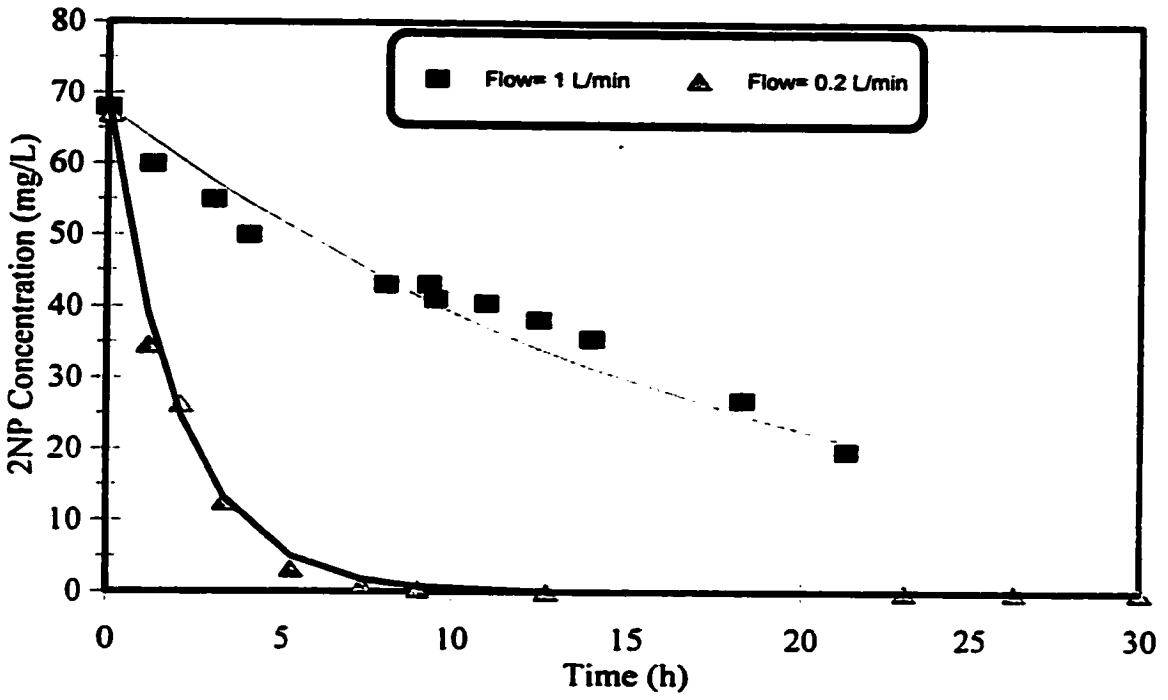

Fig. 5.10 Oxidation of 2NP at different electrolyte flowrates (I = 50 mA, undivided reactor, no GAC).

to reduce the 2NP concentration to the detection limit. The experimental data were defined by the first order expressions:

$$C = C_o(\exp(-0.055*t)) \qquad (5\text{-}4)$$

and

$$C = C_o(\exp(-0.5*t)) \qquad (5\text{-}5)$$

for flow rates of 1 L/min and 0.2 L/min, respectively. Fig. 5.10 shows that the oxidation rate of 2NP at a flow rate of 1 L/min was lower than that at a flow rate of 0.2 L/min. This also demonstrates that the oxidation of 2NP was not mass transport controlled, but was electrochemical transformation limited.

5.4.3 Effect of the Electrolyte Flow on the Cell Voltage

The reactivation of phenol-loaded F-400 was carried out with a 50 mA current and various electrolyte flow rates. The corresponding cell potential varied with the degree of mixing. The cell potential measurements for two different electrolyte (0.1 M NaCl) flow rates are presented in Fig. 5.11. It shows that there was an increase in the cell potential during the first 10 hours of operations after which it remained almost constant for longer periods of time. The concentration of ions derived from the solutes (desorbed organics and NaCl) decreased with the reactions at the electrodes. For example, the concentration of Cl^- ions decreased with time as chlorine gas was released at the anode. The decrease in concentration of ions lowers the electrolyte conductivity. Thus, the cell potential increased correspondingly to maintain a constant current. However, when certain aqueous solutions are electrolyzed, the principal electrode reactions involve the water-generated ions rather than the ions derived from the solutes (Mortimer, 1979) and this will keep the potential

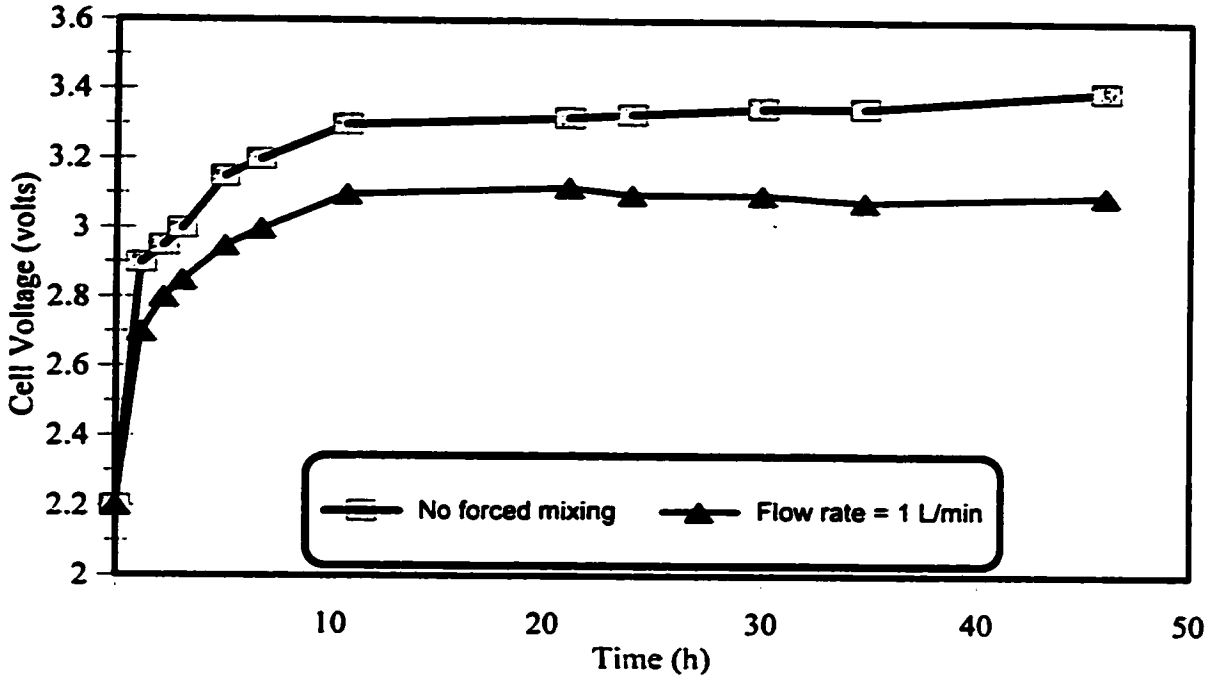

Fig. 5.11 Cell voltage versus time (I = 50 mA, 1.2 g of phenol-loaded F-400).

almost constant over an extended period of time. For the applied flow rate of 1 L/min, the cell potentials were about 10% lower than the potentials at 0 flow rate (no forced mixing). It is believed that the mixing assisted in the removal of electro-generated gases, which would affect the electrolyte conductivity, and lower the cell potential.

In the electrochemical reactivation process a major operational cost is the electricity consumption that is calculated by:

$$Electrical\ Energy = (voltage)*(current)*(time) \qquad (5\text{-}6)$$

A decrease in the cell potential due to mixing decreases the operational cost. However, one also has to consider the increase in the energy consumption required in electrolyte pumping and examine the reactivation efficiency of both systems. This has been studied in the following section.

5.4.4 Effect of Electrolyte Flow on the Reactivation Efficiency

Three electrolyte flow rates (and reactivation times up to 10 hours) were used to investigate the effect of mixing on cathodic reactivation efficiency of a monolayer (1.2 g) preloaded F-400 GAC (Fig. 5.12). This figure shows a decrease in reactivation efficiency with increasing electrolyte flow rates and this is evident for all reactivation times. Fig. 5.12 also shows that for the three flow rates the reactivation efficiency increased with increasing time.

To determine if the GAC location (upper mesh, or lower mesh) and/or the electrolyte flow mode (up-flow or down-flow) affected the results, a series of experiments was conducted. Fig. 5.13 presents the results of applying two electrolyte flow modes of up-flow and down-flow, and phenol-loaded F-400 particles located on the upper mesh or lower mesh for the

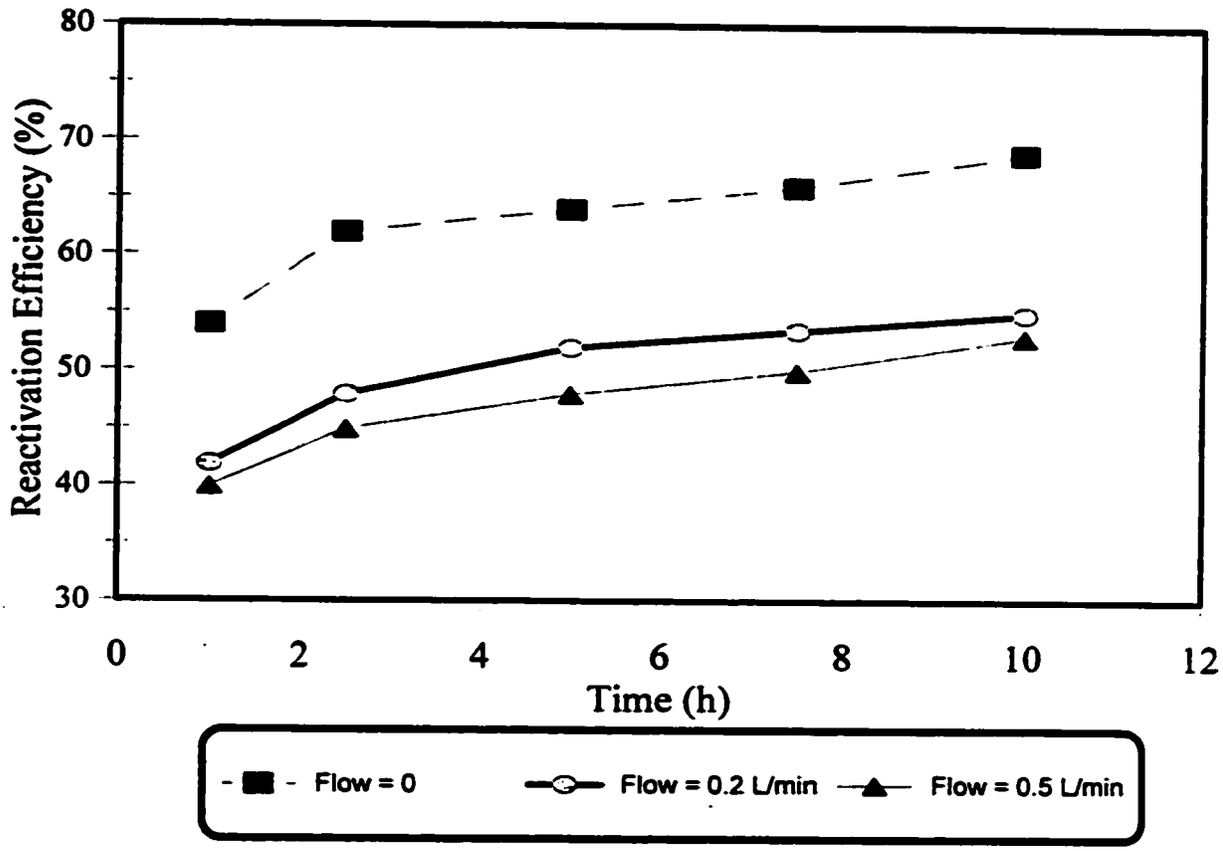

Fig. 5.12 Effect of electrolyte flow and time on cathodic reactivation (phenol/F-400, I = 50 mA, undivided reactor, 1.2 g of GAC).

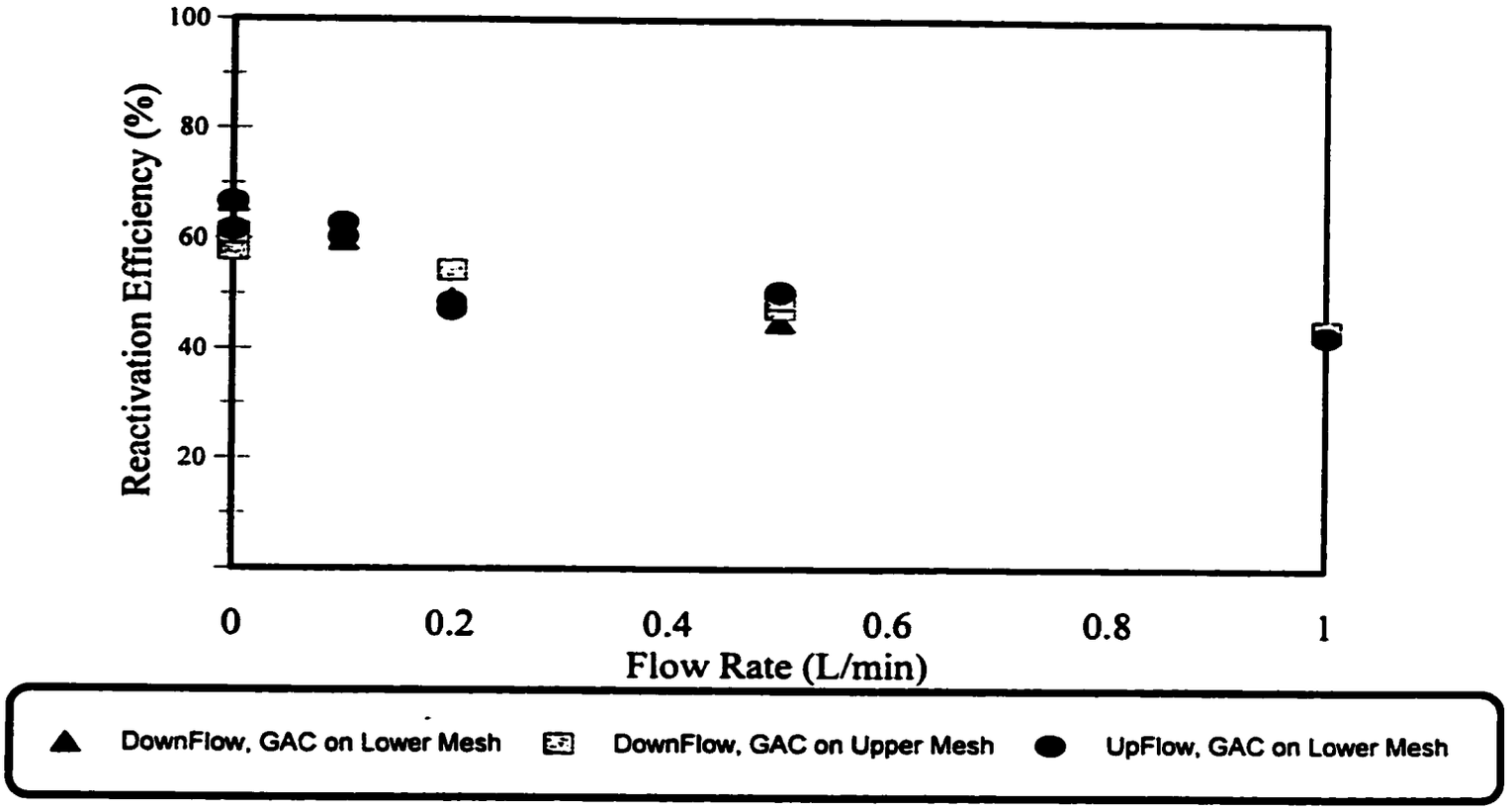

Fig. 5.13 Effect of GAC location and flow mode on cathodic reactivation (phenol-loaded F-400, I = 50 mA, reactivation time = 2.5 h, 1.2 g of GAC).

cathodic reactivation at a current of 50 mA. It shows lower reactivation efficiency at the higher electrolyte flow rates for all flow modes and GAC locations. This demonstrates that GAC location and the electrolyte flow mode did not affect the reactor performance. Thus it is unlikely that the differences in reactivation efficiency observed at different flow rates were caused by differences in flow patterns. Accordingly it was hypothesized that this phenomenon was caused by the variation of the local pH at the electrodes. To prove this hypothesis, the experiments in the following sections were conducted.

5.4.5 pH Variation Within the Reactor Compartments:

The pH variations within the reactor compartments during electrochemical reactivation with both modes of operations (with and without electrolyte mixing) were studied. The pH variation in the catholyte and anolyte when there was no electrolyte mixing (and no electrode separation) versus reactivation time are shown in Fig. 5.14. The pH of the catholyte was measured 2.5 cm below the cathode (lower mesh) and that of the anolyte was measured 2.5 cm above the anode (upper mesh). The pH of the solution between the two electrodes could not be measured due to the effect of the electrical field on the pH meter. In the case of electrolyte mixing, the pH of the re-circulated line was measured as the pH of the mixed solution.

As was expected, the catholyte yielded high pHs and the anolyte showed low pHs. This can be explained by the reactions at the cathode and anode, respectively.

$$2H_2O + 2e^- \text{ ----------> } H_2 + 2OH^- \quad (5\text{-}7)$$

$$2H_2O \text{ ----------> } O_2 + 4H^+ + 2e^- \quad (5\text{-}8)$$

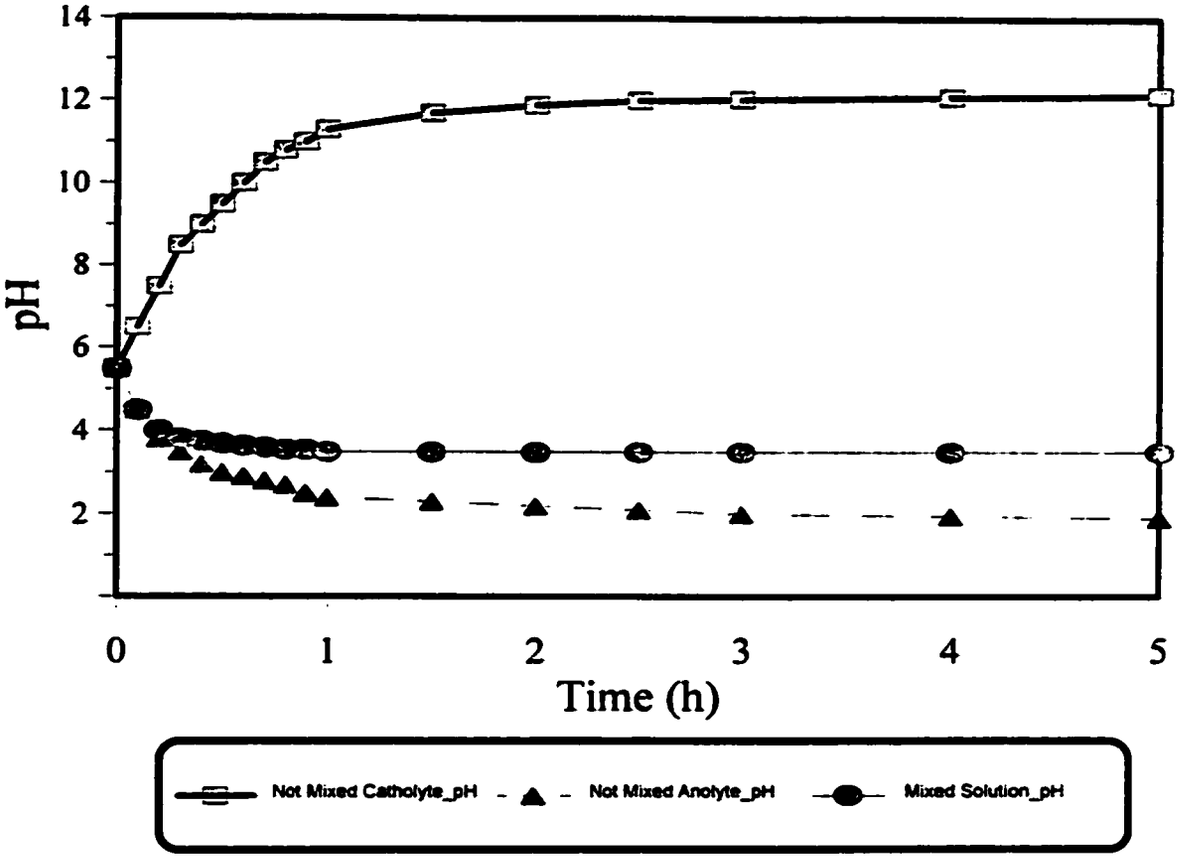

Fig. 5.14 pH variation within the reactivation reactor (I = 50 mA, undivided reactor).

The cathode is the reducing electrode and it generates OH^- ions (eq. 5-7) which increase the local pH at the cathode and its surrounding electrolyte (catholyte). The anode is the oxidizing electrode and it generates H^+ ions (eq. 5-8) which decrease the local pH at the anode and its surrounding anolyte.

Fig. 5.14 also shows that the pH of the mixed electrolyte at a flow rate of 1 L/min (HRT = 1 min) decreased to 3.5. As equations 5-7 and 5-8 show for each OH^- ion generated there are $2H^+$ ions generated and the pH of the mixed solution was expected to decrease. The forced electrolyte flow minimizes the variation of the electrolyte pH throughout the reactor. Thus with mixing, the pH at the electrodes where the GAC particles reside will be close to the mixed electrolyte pH rather than the extreme values associated with the electrodes. Fig. 5.14 also shows that the change in pH was greatest for the catholyte, and that the mixing reduced the catholyte pH from about 12 to 3.5 while it increased the anolyte pH from 2 to 3.5. This suggests that the effect of mixing on the anodic reactivation efficiency of GAC should be less than the effect of mixing on the cathodic reactivation.

Since the pH measurements showed that the pH of the electrolyte solution was 2 and 12 under anodic and cathodic conditions, respectively, it was necessary to establish the relationship between pH and reactivation efficiency. The following sections examine the effect of pH on adsorption and desorption of phenol on/from GAC at pHs 2, 3.5, and 12 which will help to establish a relation between pH and reactivation efficiency.

5.4.6 Effect of pH on Adsorption and Desorption:

All of these tests were conducted in triplicate using a single mass of 1.2 g F-400 GAC. Buffered phenol (300 mg/L) or 2NP (500 mg/L) solutions were used to load the GAC (via the bottle point method) at pH 2, 3.5, and 12. Fig. 5.15 demonstrates that the adsorption capacity of both 2NP and phenol on F-400 were similarly affected by pH. Adsorption of phenol and 2NP was higher at pHs 2 and 3.5 and was far less at pH 12. Note that the pK_as of phenol and 2NP are 9.99 and 7.23, respectively. The dissociation of compounds at pH higher than the pK_a results in lower adsorption. Similar results were reported by Snoeyink (1968), Seidel and Radeke (1990) and Karimi-Jashni (1994).

To study the effect of pH on desorption at pHs 2, 3.5, and 12, batch desorption experiments were conducted with preloaded F-400 GAC (at a single solid phase concentration) and buffered distilled water. To have the same phenolic loading on the GAC within all bottles prior to desorption, the GACs were loaded with solutions of undissociated phenol and 2NP at pH 5.5. The results of phenol and 2NP desorption from GACs at pHs 2, 3.5, and 12 are plotted in Fig. 5.16. The percentage of desorption was calculated by dividing the mass of contaminant desorbed into the desorption solution by the initial mass of adsorbed contaminant on the virgin GAC. Fig. 5.16 shows that higher desorption of both phenol and 2NP occurred at pH 12 and desorption decreased dramatically at pHs 2 and 3.5. This pattern was expected, given the impact of pH on adsorption shown in Fig. 5.15. Knowing that the pK_as of 2NP and phenol are 7.23 and 9.99, respectively, it is evident from Fig. 5.16 that the dissociated form of phenol and 2NP desorb much more than the undissociated form.

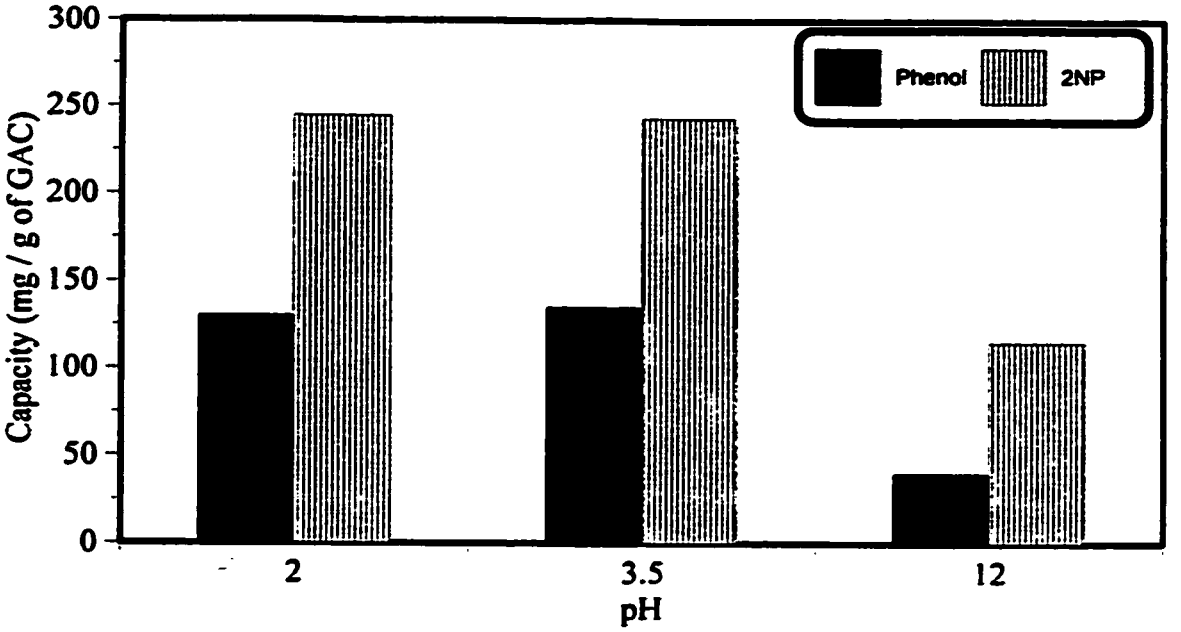

Fig. 5.15 Adsorption of phenol and 2NP into F-400 at different pHs.

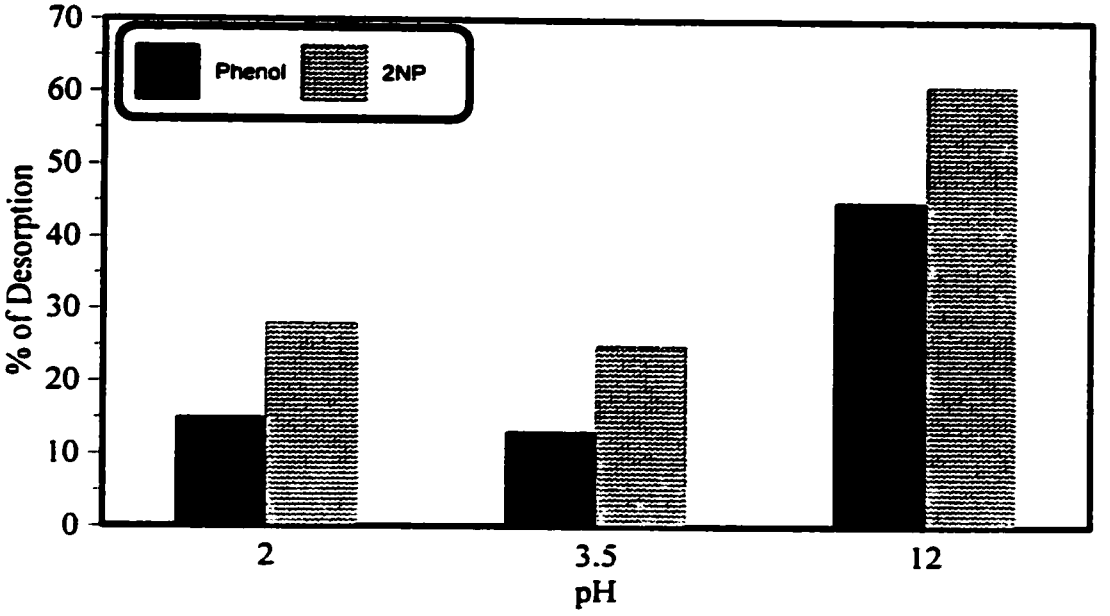

Fig. 5.16 Desorption of phenol and 2NP from F-400 at different pHs.

Fig. 5.16 also shows that the extent of desorption of 2NP (60% at pH 12 and 28% at pH 2) was higher than the extent of desorption of the phenol (45% at pH 12 and 15% at pH 2) from F-400. This is consistent with the full reversibility of the 2NP from F-400 (Karimi-Jashni, 1994; Vidic *et al.*, 1993) and the partial reversibility of phenol from F-400 (Narbaitz and Cen, 1994; Yonge *et al.*, 1985).

The higher desorption of contaminants at high pH and the high pH of the catholyte (Fig. 5.14) during cathodic reactivation suggests that the reactivation efficiencies will be higher when the GAC is placed on the cathode (cathodic reactivation) than when the GAC is placed on the anode (anodic reactivation). This has been investigated in the next section.

5.4.7 Cathodic Versus Anodic Reactivation:

Reactivation tests were conducted in the undivided reactor with a monolayer (1.2 g) of preloaded F-400 GAC placed on the cathode (cathodic reactivation) or on the anode (anodic reactivation). Anodic versus cathodic reactivation was achieved by reversing the leads on the power supply while the GAC was placed on top of the lower mesh. Fig. 5.17 shows the cathodic and anodic reactivation results of applying five electrolyte flow rates for a reactivation time of 2.5 hours and a fixed electrical current of 50 mA. For cathodic reactivation, the higher the electrolyte flow rate, the lower the reactivation efficiency. Increasing the electrolyte flow rate from 0 to 1 L/min caused a decrease in the reactivation efficiency from 62 to 45%. This decrease in the reactivation efficiency is consistent with the decrease of pH from 12 to 3.5 (Fig. 5.14) and the corresponding decrease in desorption from 45 to 15% (Fig. 5.16). The anodic reactivation efficiency was independent of the electrolyte flow rate. This is consistent with the small changes in the pH of the anolyte from 2 to 3.5 at

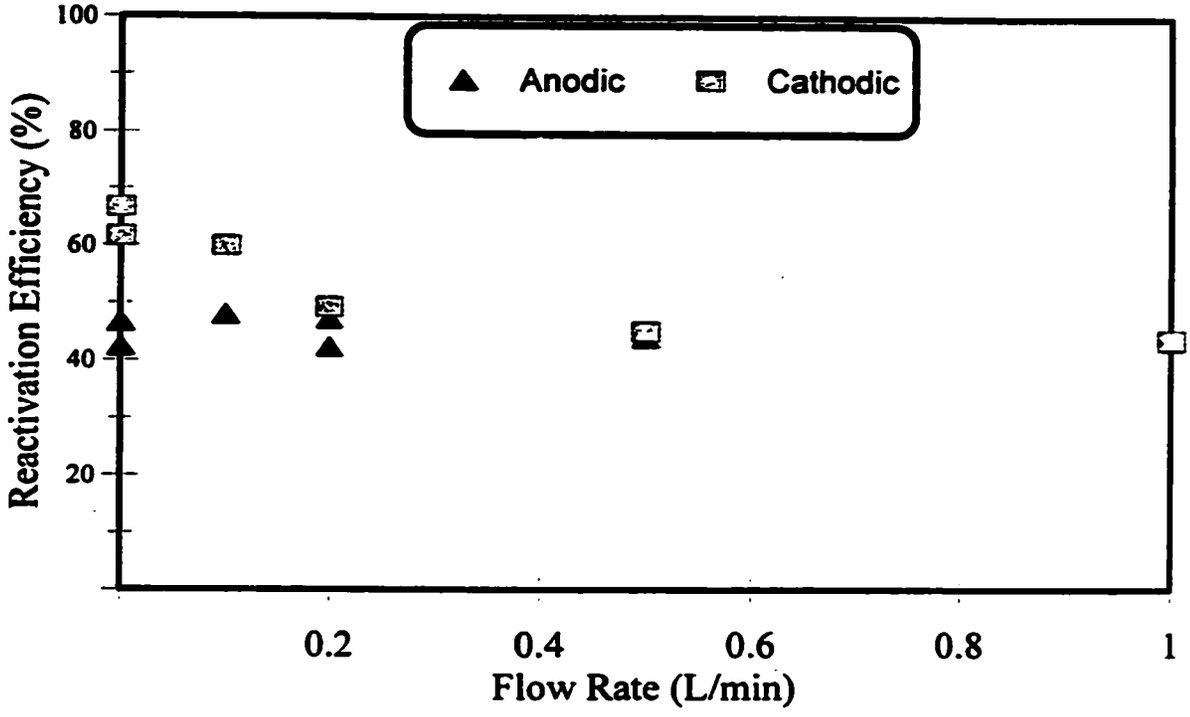

Fig. 5.17 Cathodic versus anodic reactivation (phenol-loaded F-400, I = 50 mA, reactivation time = 2.5 h, 1.2 g of GAC).

the different flow rates (Fig. 5.14). A comparison of the results shows that cathodic reactivation was more efficient than anodic reactivation. The superiority of cathodic over anodic reactivation was 20% when there was no forced flow, and decreased with increasing flow rate to the point that the difference was negligible at the flow rate of 1 L/min. The decrease in superiority of cathodic over anodic reactivation is consistent with the change in pH in the catholyte from 12 at no mixing to 3.5 with mixing (Fig. 5.14). Thus, this pH variation affects the adsorption capacity of the GAC (Fig. 5.14) and the amount of the contaminant desorbing from it (Fig. 5.16) and thus, the reactivation efficiency (Figs. 5.12 and 5.17).

5.4.8 Cathodic Reactivation of Two GACs:

As GAC performance depends on both the carbonaceous raw material and the manufacturing process, the influence of electrolyte mixing was investigated using both F-400 and WV-B GACs. The results of cathodic reactivation of phenol loaded F-400 and WV-B are shown on Fig. 5.18. It shows that both GACs were similarly impacted by the electrolyte flow rates. This is consistent with the effect of pH on the desorption of phenol (Fig 5.16).

Fig. 5.18 also shows that the reactivation efficiencies for both GACs at all the conditions tested were approximately the same. Because the adsorption of phenol on F-400 is partially irreversible (Narbaitz and Cen, 1994) and adsorption of phenol on WV-B is fully reversible (Vidic *et al.*, 1993), higher reactivation efficiencies were expected for WV-B. The irreversibility of phenol adsorption occurs because under oxic conditions the phenolics polymerize on the surface of certain activated carbons, forming more strongly adsorbed

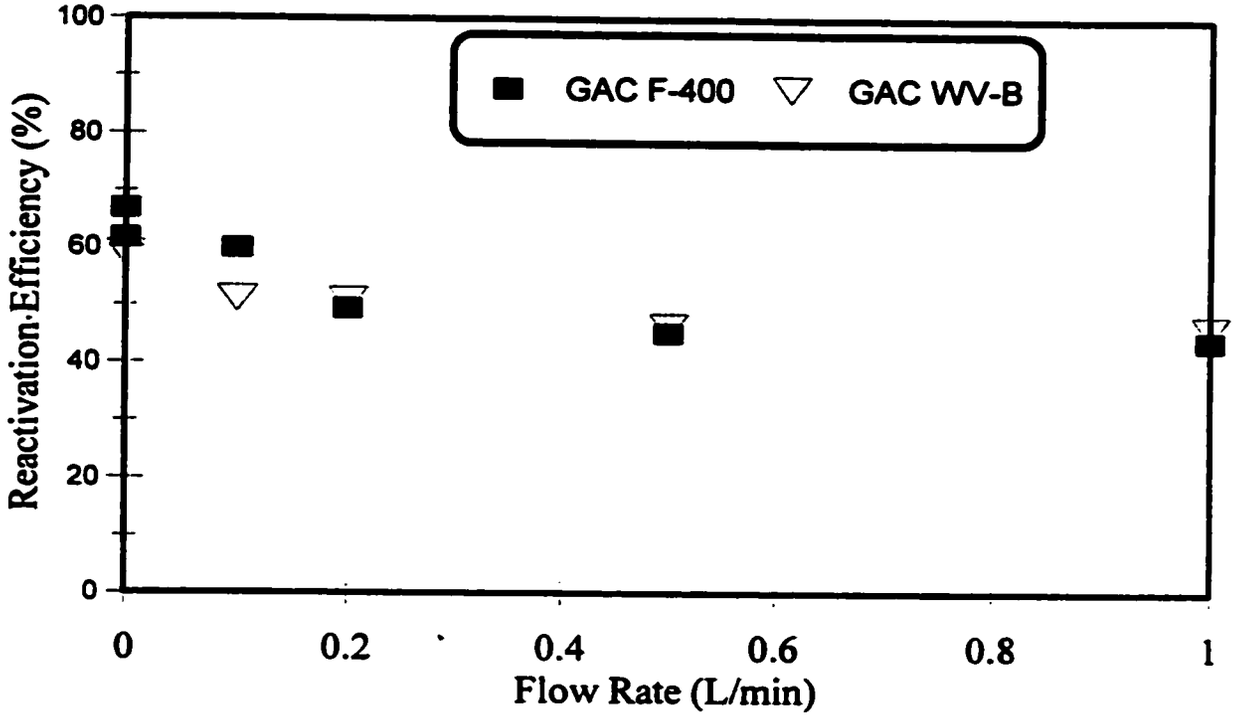

Fig. 5.18 Effect of GAC type on cathodic reactivation of phenol-loaded GAC (I = 50 mA, reactivation time = 2.5 h, 1.2 g of GAC).

species (Vidic *et al.*, 1993). Thus, the fact that the reactivation was equally effective for both GACs may indicate that electrochemical reactivation can also remove these species from the surface of the GAC.

5.5 Discussion

In general, for similarly loaded GACs there was much greater desorption at pH 12 (where phenol is in its dissociated form) than at pH 2 (where phenol is in its undissociated form) (Fig. 5.14). This suggests that the extent of dissociation of adsorbate influences the extent of its desorption. At pH 12 the dissociation of adsorbed phenol (i.e., the phenate ions) and activated carbon surface functional groups will increase negative repulsive forces between individual anionic adsorbed species and between the adsorbed species and the GAC surface functional groups (Summers and Roberts 1988, Cooney and Wijaya, 1987). These repulsive forces and/or the competition with OH^-, generated at the cathode, for active sites on the GAC will result in higher desorption of phenol/2NP from GAC (Fig. 5.14).

During cathodic reactivation, the pH of the catholyte increases (Fig. 5.12) above the pK_a of the phenol (pH 9.99) and stabilizes to pH 12, which results in higher desorption of phenol/2NP from GAC and higher cathodic reactivation efficiencies (Fig. 5.15).

Adsorption of phenol and 2NP was much higher at pH 2 than at pH 12 (Fig. 5.13). The surface of GAC is negatively charged in the neutral pH ranges as a result of the dissociation of surface carboxylic groups. A reduction in pH can be expected to improve adsorption since the protonation of carboxylic functional groups on both the organic acids in solution and the GAC surface reduces electrostatic repulsion forces (Semmens *et al.*, 1986), thereby

promoting a greater degree of adsorption. A reduction in pH, which is caused by forced mixing (Fig. 5.12), can be expected to improve the adsorption and lower the reactivation efficiency at the higher flow rates.

5.6 Conclusions

- A comparison of the different reactors proved that the new reactor is more efficient than the column reactor and the reactor used by Narbaitz and Cen (1994).
- Reactivation of multilayer phenol-loaded GACs showed that the reactivation efficiency decreased by about 40% as the mass of GAC increased from 1.2 to 19.2 g (1 to 16 layers). It was concluded that such a decrease in reactivation efficiency can be due to a need for direct contact between GAC particles and the electrode surface.
- The reactivation efficiency increased with increasing reactivation time.
- Electrochemical reactivation experiments showed that cathodic reactivation is more efficient than anodic reactivation and increasing the degree of electrolyte mixing resulted in a decrease in the cathodic reactivation efficiencies, while there were no significant changes in the anodic reactivation efficiencies.
- Both GACs (F-400 & WV-B) were similarly impacted by electrolyte mixing. Higher degrees of electrolyte mixing decreased the local pH at the cathode and consequently reduced the desorption driving force, thereby reducing the reactivation efficiency.
- Mixing lowered the cell voltage, however this advantage could not overcome the increase in energy consumption (required in electrolyte pumping), the reduction in the reactivation efficiencies of approximately 20%, and the decrease in the phenol/2NP oxidation rates. Thus, mixing is not recommended.

CHAPTER 6

PROCESS APPLICABILITY AND OPERATING CONDITIONS

6.1 Introduction

One of the most important questions that needs to be addressed is how applicable is electrochemical reactivation of GAC? To answer this question, experiments were conducted with different types of GACs loaded with different contaminants using the new undivided reactor. In each case reactivation was conducted using different currents and reactivation times, to assess the influence of GAC type and pollutant type on these key process variables. In this chapter the impact of the following variables was studied: GAC type; the adsorbate (contaminant) type; reactor operating conditions (reactivation time, current, pH); and the effect of loading and loading time on the reactivation. Also the virgin and reactivated GAC isotherm; different methods for evaluation of reactivation efficiencies, reactivation efficiency calculation based on TOC and phenol/2NP, and electro-gas generation were investigated.

6.2 Operating Conditions

6.2.1 Effect of Current and Time

As designed, the power source supplied a constant current to the electrochemical reactor. The current is used instead of current density because of its simplicity. The reactivation of GACs was carried out at various currents, and the corresponding cell potential varied with current and time. The cell potential measurements for two different currents (50 mA and 100 mA) in 0.1 M NaCl electrolyte are given in Fig. 6.1. There was an increase in the cell

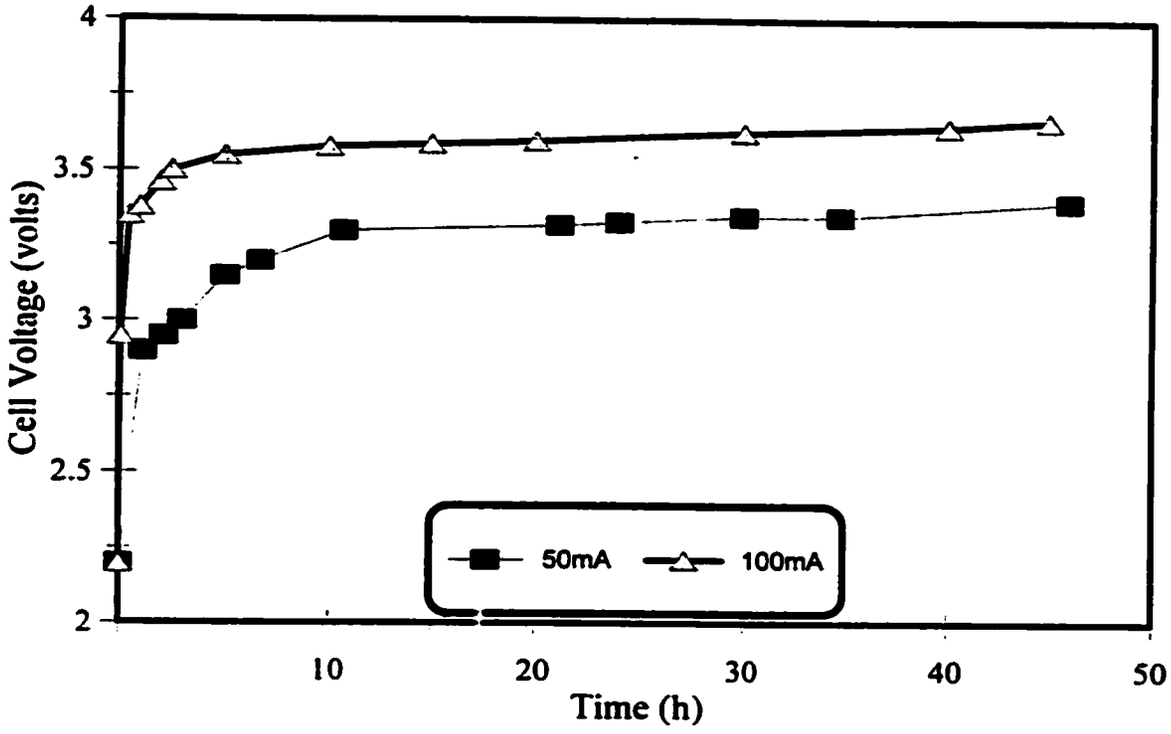

Fig. 6.1 Voltage versus reactivation time (0.1 M NaCl, 1.2 g of phenol-loaded F-400, no mixing).

potential during the first few hours of operation, and it then remained almost constant over longer periods of time. As discussed in section 5.4.3, the concentration of ions derived from the solutes (desorbed organics and NaCl) decreased with the reactions at the electrodes for the first few hours. The decrease in concentration of ions lowered the electrolyte conductivity. Thus, the cell potential increased correspondingly to maintain a constant current. However, over an extended period of time, the principal electrode reactions involve water-generated ions rather ions derived from the solutes (Mortimer, 1979) and this will keep the potential almost constant. For applied currents of 50 and 100 mA, the cell potentials were slightly different.

Figs. 6.2 and 6.3 show the reactivation efficiencies of single layer GACs (F-400 and WV-B) loaded with phenol at various currents and durations. Both figures show relatively high efficiencies at time = 0. This was due to the RE3 method used to calculate the efficiencies for all the conditions tested. As discussed by Narbaitz and Cen (1997) the RE3 method overestimates the efficiencies of control samples (i.e., time = 0 or current = 0) and the RE4 method is the method of choice for the evaluation of control samples. In the cases of control samples, the RE4 method would result in efficiencies of less than 10%. However, for consistency the RE3 method was used for all the conditions.

The reactivation efficiency (RE%) could be increased to about 80% by increasing the current and/or time. The effect of current was very marked from 10 to 50 mA and more gradual from 50 to 100 mA. A higher current might have rapidly accelerated the contaminant desorption due to rapid pH changes and/or polarization of the GAC surface. Also, a higher current might have rapidly oxidized the desorbed contaminant and increased the desorption driving force. However, applying a very high current may alter or deteriorate

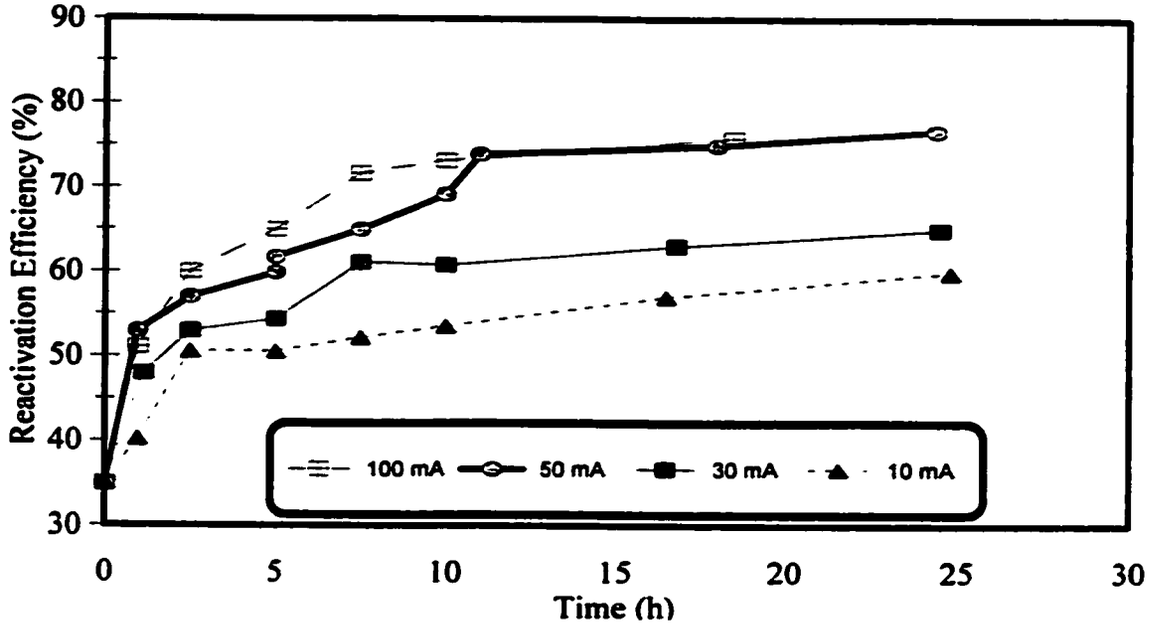

Fig. 6.2 Effect of current and time on the cathodic reactivation of phenol-loaded F-400 (1.2 g of phenol-loaded F-400, no mixing).

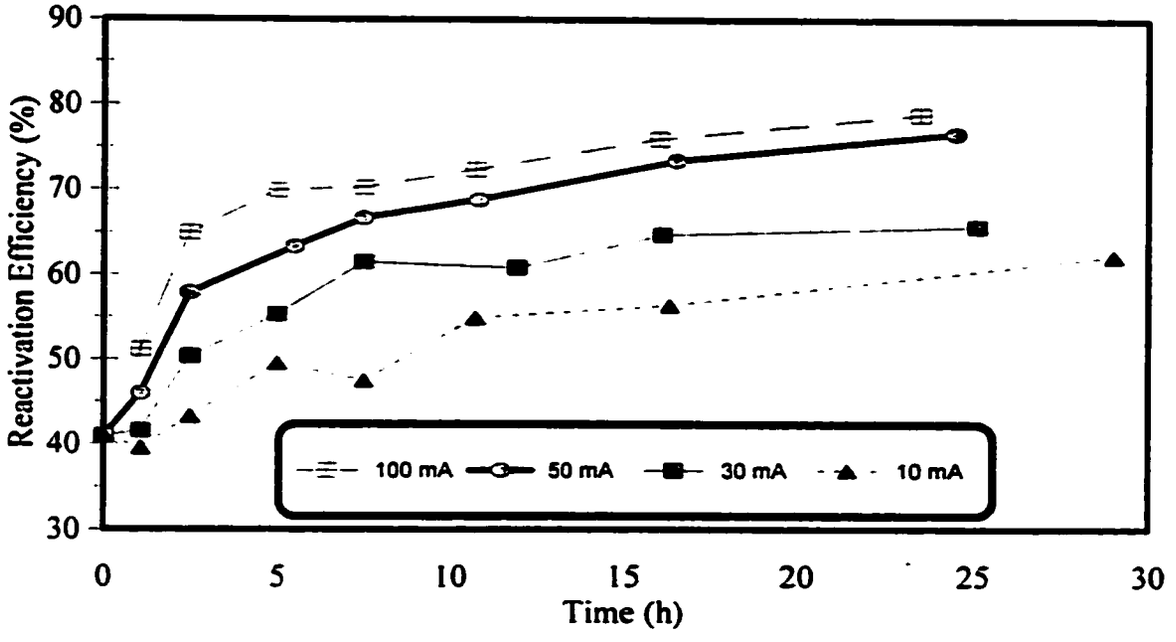

Fig. 6.3 Effect of current and time on the reactivation of phenol-loaded WV-B (1.2 g of phenol-loaded WV-B, no mixing).

GAC adsorption sites. Therefore, applying a lower current and long reactivation time may achieve higher coulombic efficiency.

The effect of time showed a similar pattern to that of the current in Figs. 6.2 and 6.3. The RE% increased rapidly with increasing reactivation time in the first few hours, followed by a more gradual increase for longer times. The longer reactivation time might have increased the GAC reactivation efficiency in two ways. First, one key step in GAC reactivation is the desorption of contaminant from the surface of the GAC. Since desorption is a time dependent phenomenon, longer reactivation times increased the extent of desorption. Second, with increased time more of the desorbed contaminant is oxidized resulting in lower contaminant concentrations in the electrolyte and an increased desorption driving force. This leads to greater desorption and a higher reactivation efficiency.

However, the longer reactivation time will also have some disadvantages. It will increase the energy consumption required in GAC electrochemical reactivation. The surface of the GAC may be altered by exposure to high currents for long periods. Another problem with longer reactivation time is that as the time passes there will be depletion in reactants and a potential accumulation of reaction products on the electrode surface. This may cause electrode fouling and as a result there will be changes in the level of electrode polarization, due to kinetic and mass transfer effects, consequently a decrease in the current efficiency. Therefore, it is important to use the optimum reactivation time.

Since high current and long reactivation time may contribute to the destruction of all the desorbed contaminant as well as oxidation of by-products, one could possibly drain the reactivated GAC and use another reactor (and possibly different electrode) for an extended

time at a much higher current to electrochemically oxidize the desorbed contaminants in the electrolyte before discharge or reuse.

Figs 6.4 and 6.5 represent the same reactivation current and time data in terms of RE% versus the charge (in coulombs) passed instead of the reactivation time. The charge was calculated by multiplying the current (in A) by time (in sec.). Figs 6.4 and 6.5 show that all currents produced almost the same RE% per charge passed. Therefore, the coulombic efficiency for GAC reactivation is independent of the current/time applied. However, a higher current can rapidly oxidize the phenol, but it may also alter or deteriorate the adsorption sites. Thus in general, a lower current may be more appealing. A similar conclusion was reached by Cen (1994).

6.2.2 Effect of pH

Cathodic reactivation tests at 50 mA were conducted at two extreme pHs (2 and 12) by using buffered electrolytes and reactivation times up to 45 hours. Fig. 6.6 shows the %RE versus time for F-400 loaded with phenol. This figure shows that reactivation was far higher at pH 12 than at pH 2. Similar results were obtained for 2NP-loaded F- 400. This is consistent with the higher desorption of phenol at pH 12 (Fig. 5.14). Although cathodic reactivation at 50 mA was used for both pH 2 and 12, the electrolyte pH controlled the contaminant desorption and consequently resulted in the different reactivation efficiencies. Therefore pH is critical to cathodic reactivation.

6.3 Process Applicability

The nature of the adsorbate and the surface chemistry of the activated carbon determine the adsorption capacity and consequently the ability to reactivate. Thus, the process

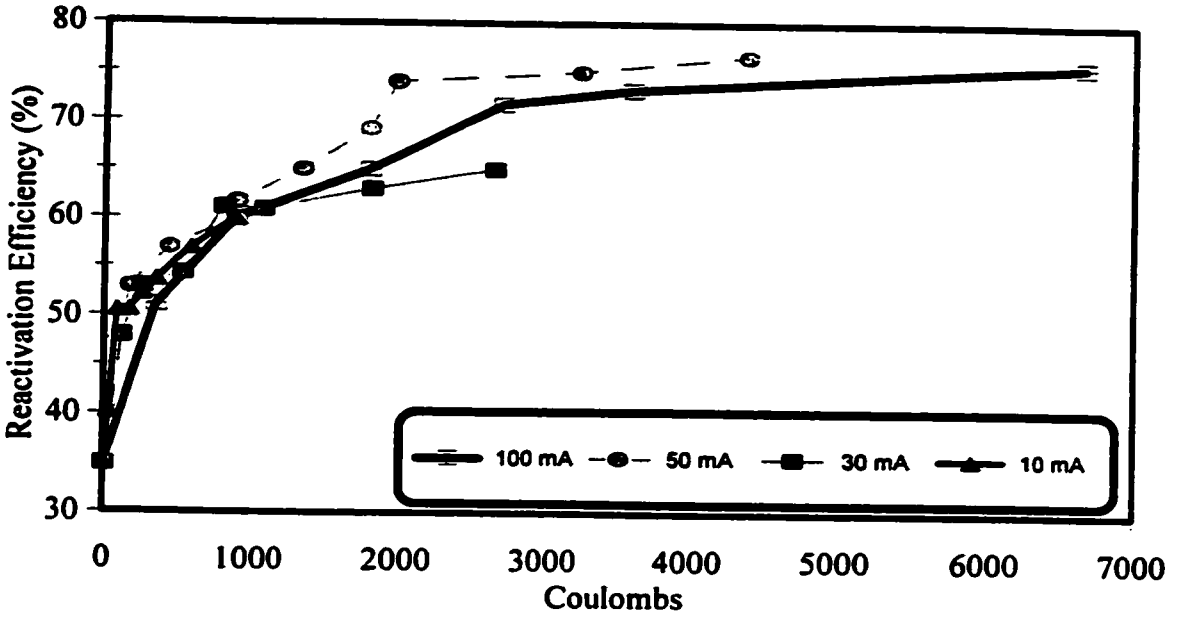

Fig. 6.4 Cathodic reactivation efficiency of phenol-loaded F-400 versus charge passed.

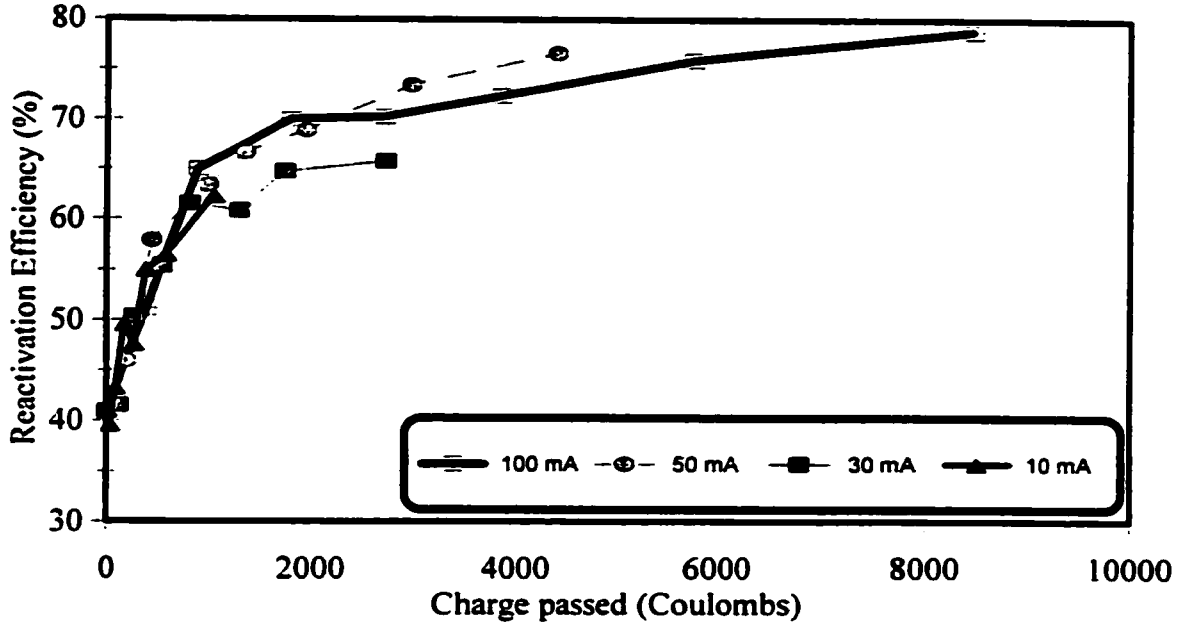

Fig. 6.5 Cathodic reactivation efficiency of phenol-loaded WV-B versus charge passed.

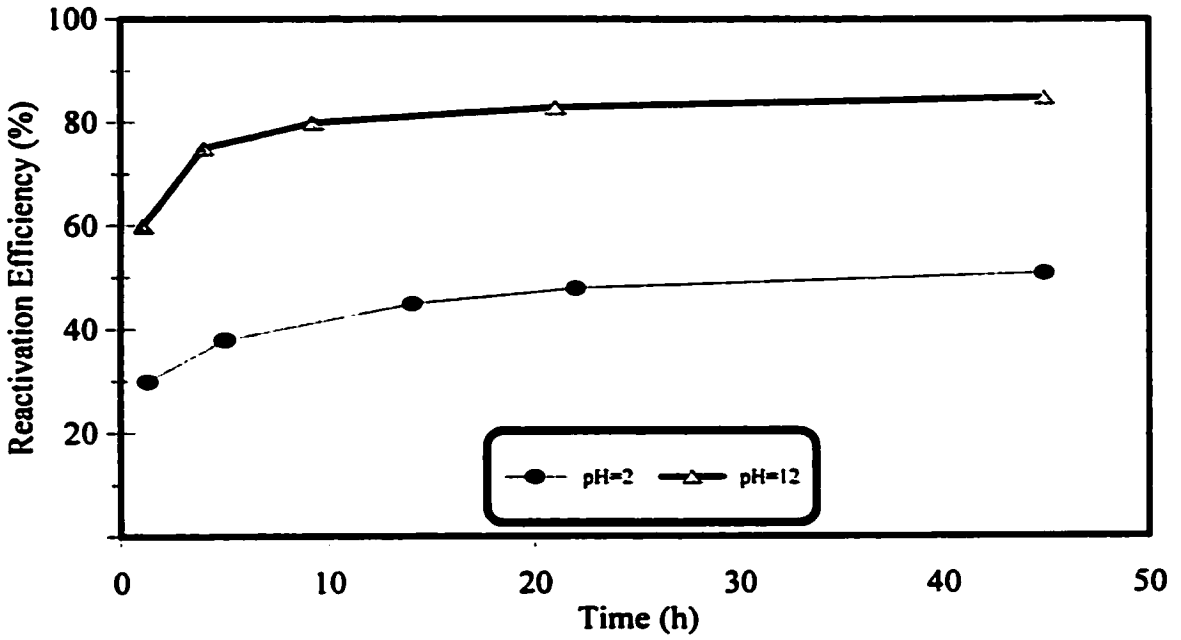

Fig. 6.6 Impact of pH on the cathodic reactivation of phenol-loaded F-400 at 50 mA.

applicability was investigated by reactivating different types of commercial GACs (F-400, WV-B, Darco) loaded with phenol and 2-nitrophenol, and F-300 loaded with NOM.

6.3.1 Comparison of the GACs

Three commercial GACs (F-400, WV-B, and Norit Darco) were studied. As mentioned previously, GACs were loaded at the same initial conditions and reactivated similarly. The ideal approach for determining the effects of GAC type on reactivation is to determine the GAC performance after reactivation compared to the corresponding virgin GAC. Figs. 6.7 and 6.8 evaluate the GACs reactivation efficiency at different reactivation periods of time and constant current (50 mA). Considering the experimental error, a comparison of the percent reactivation in these figures shows that F-400 and WV-B performed essentially the same for the conditions tested. In Fig. 6.7 phenol-loaded-Darco showed almost the same performance at lower reactivation times and lower performance at higher reactivation times. The similarity of the F-400 and WV-B performance was also reflected in the reactivation of GACs under different current densities (10, 30, and 100 mA) shown in Fig. 6.9.

Because adsorption of phenol on F-400 is partially irreversible and adsorption of phenol on WV-B is fully reversible, higher reactivation efficiencies were expected for WV-B. However, the reactivation efficiencies for all the conditions in Figs. 6.7, 6.8, and 6.9 were essentially the same for both F-400 and WV-B. There are two possible explanations. First, it may indicate that electrochemical reactivation could remove both the reversible and irreversible (polymerized) adsorbed species from the surface of the GAC. Second, because the maximum achieved reactivation efficiency was about 75%, it may be that the

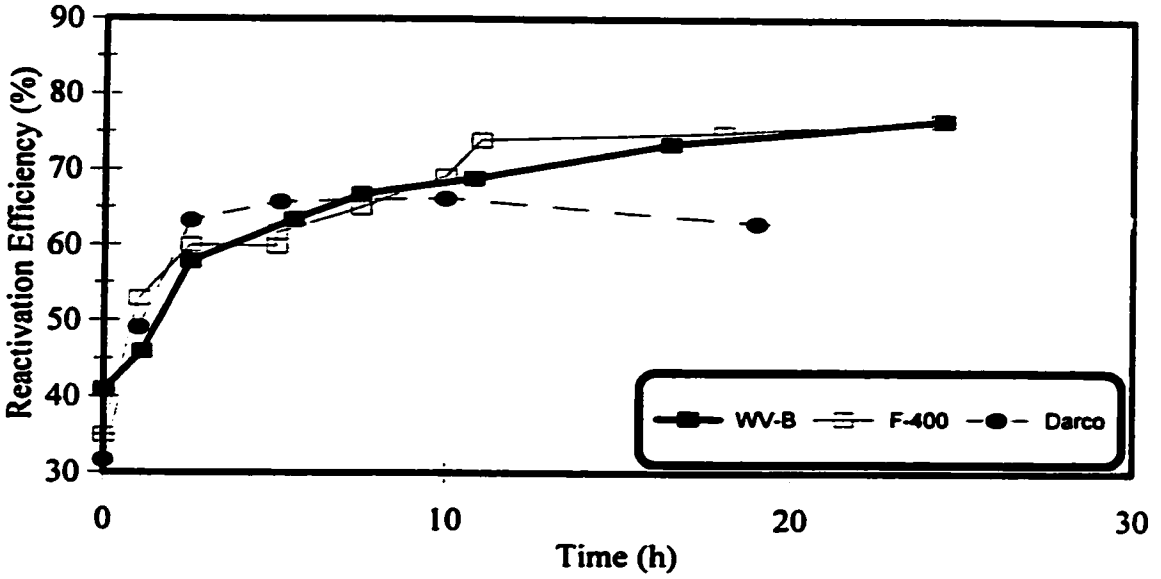

Fig. 6.7 Comparison of the cathodic reactivation of phenol-loaded GACs at 50 mA.

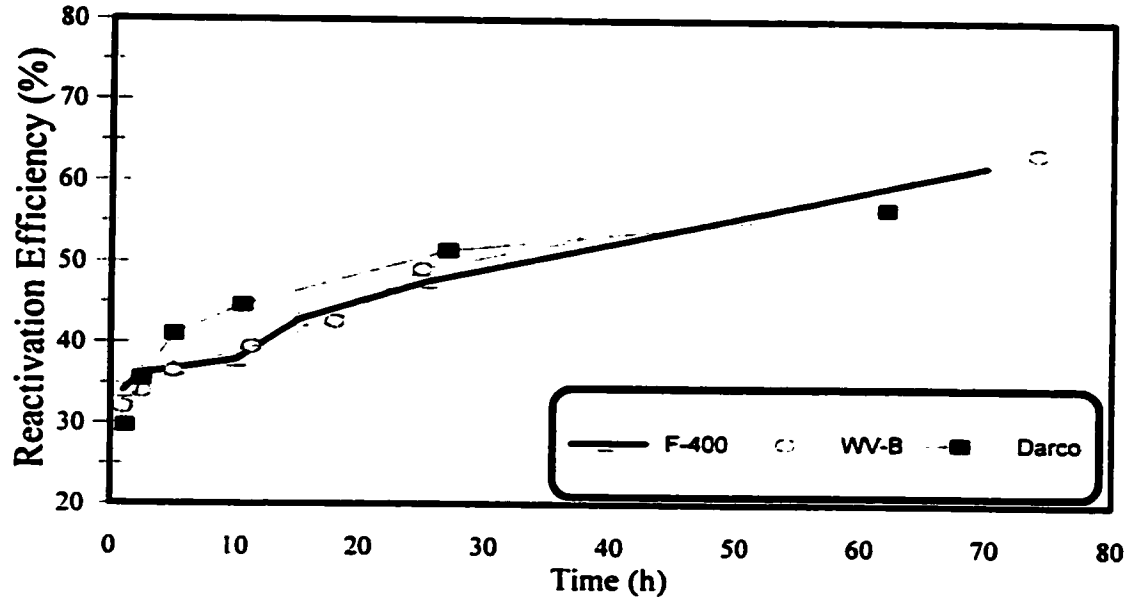

Fig. 6.8 Comparison of the cathodic reactivation of 2NP-loaded GACs at 50 mA.

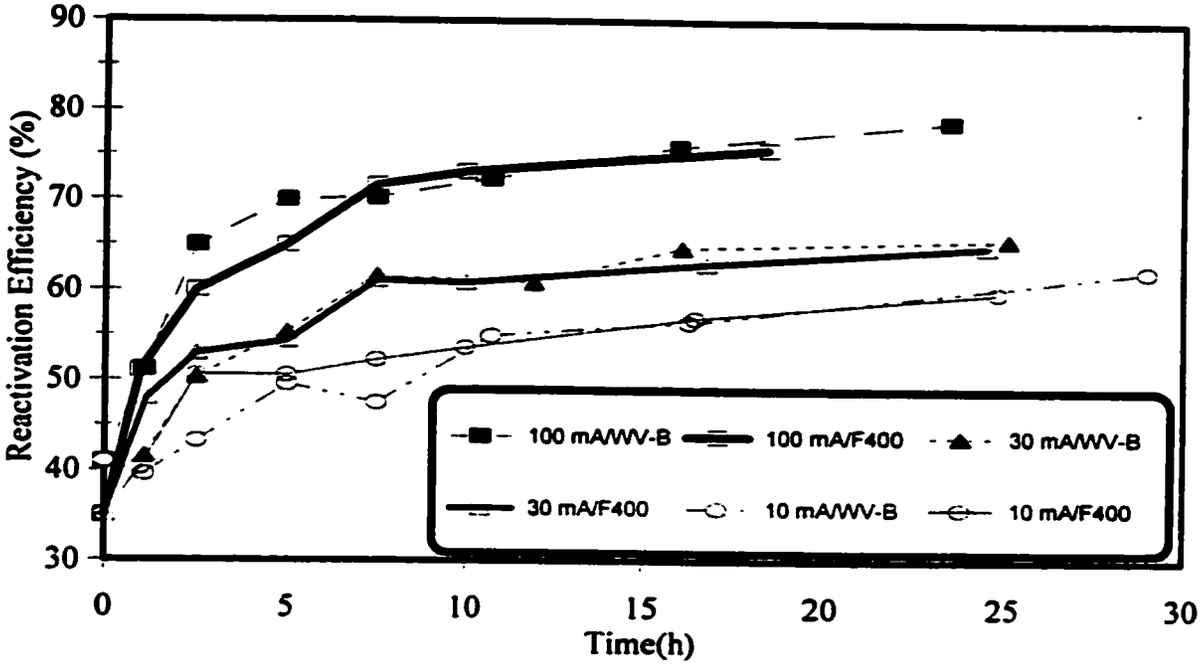

Fig. 6.9 Comparison of the cathodic reactivation of phenol-loaded GACs at different currents (single layer GAC, no mixing).

electrochemical reactivation affected only the reversible portion of the adsorbed contaminant and further reactivation (either longer reactivation time and/or higher current) would prove if electrochemical reactivation could remove the irreversible species from the surface of F-400. To deal with the second hypothesis further experiments were conducted.

The GAC's performance was compared after 5 hours of reactivation by applying different currents. The results are shown in Figs. 6.10 and 6.11. These figures show that a trend developed for the reactivation efficiency of Darco, showing lower performance at higher currents. This indicates that the surface of Darco may have been altered at high currents due to its lower conductivity. Fig. 6.10 shows that at higher currents the F-400 had slightly lower reactivation efficiencies than WV-B. This is consistent with partial reversibility of phenol sorbed on F-400 and full reversibility of phenol sorbed on WV-B. This seems to prove that the second hypothesis in the previous paragraph was correct. However Fig. 6.9 contradicts the difference observed in 6.10 for most conditions and does not support the second hypothesis. Fig. 6.11 indicates that the reactivation of 2NP preloaded F-400 and WV-B was comparable and this was consistent with the fully reversible adsorption of 2NP on both F-400 and WV-B.

6.3.2 Impact of the adsorbed contaminant

6.3.2.1 Phenol and 2NP

The nature of phenol and 2NP adsorption on GAC may have a significant impact on the reactivation efficiencies. To determine whether 2NP and phenol behave similarly, the reactivation efficiencies of F-400 (loaded with these contaminants) versus time is plotted in

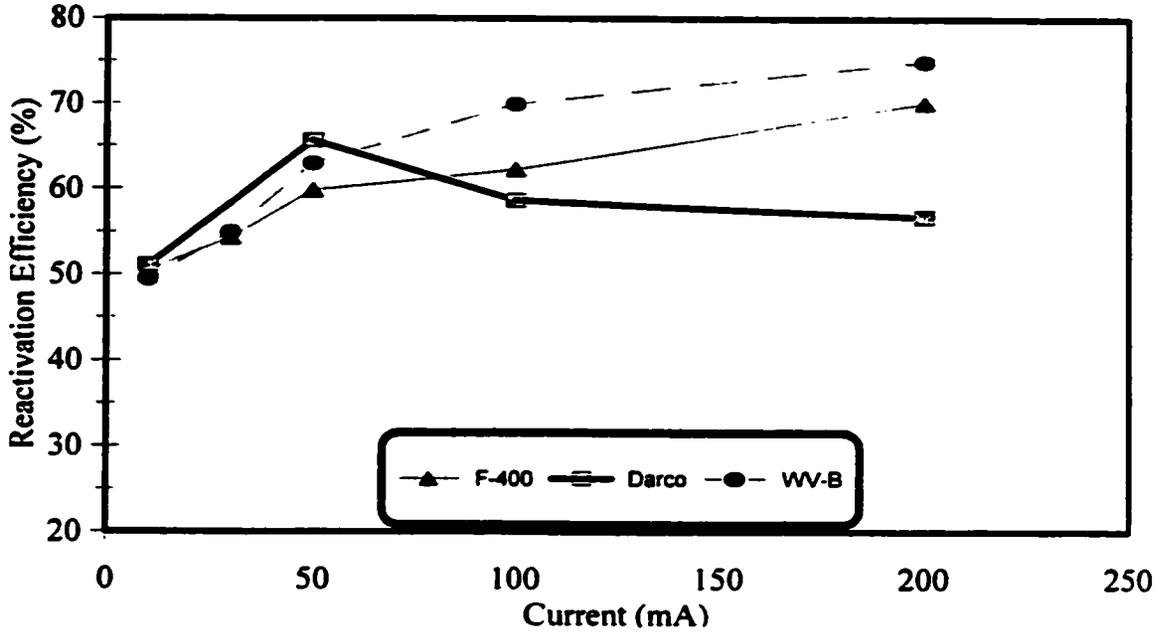

Fig. 6.10 Comparison of the cathodic reactivation of phenol-loaded GACs at different currents after 5 hours reactivation.

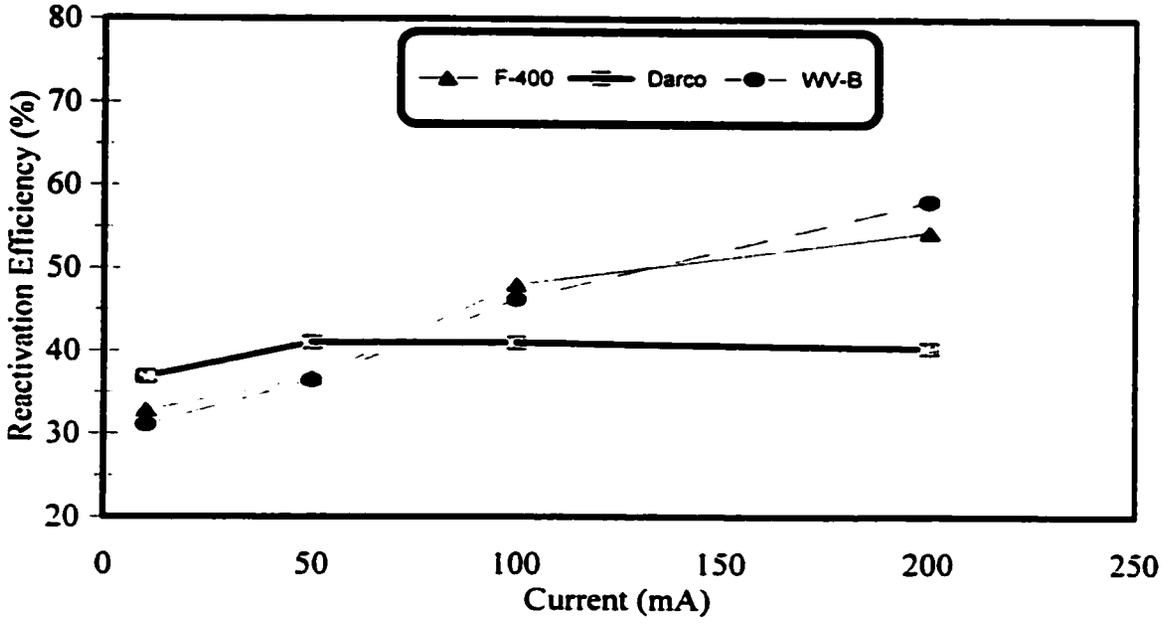

Fig. 6.11 Comparison of the cathodic reactivation of 2NP-loaded GACs at different currents after 5 hours reactivation.

Fig. 6.12. It shows that 2NP and phenol behaved similarly in that reactivation efficiencies increased with increasing reactivation time. The reactivation efficiencies of 2NP-loaded F-400 were 20 to 30% lower than the reactivation efficiencies of phenol-loaded F-400. However, higher reactivation efficiencies were expected for F-400 loaded with 2NP given that the adsorption of 2NP on F-400 is fully reversible while phenol adsorption on F-400 is partially reversible. Similar results were obtained for the reactivation of WV-B and Darco loaded with 2NP and phenol.

Comparison of the reactivation efficiencies of F-400 loaded with 2NP and phenol at different reactivation currents (after 5 hours of reactivation) is shown in Fig. 6.13. It shows a similar pattern, but phenol-loaded F-400 showed higher reactivation efficiencies than 2NP-loaded F-400. Both Figs. 6.12 and 6.13 are not consistent with the full reversibility of 2NP from F-400 and the partial reversibility of phenol from F-400. Similar results were obtained for the reactivation of WV-B and Darco loaded with 2NP and phenol at different reactivation currents after 5 hours of reactivation (Appendix A1 to A4). A full investigation and discussion of this matter is presented in Chapter 7, which explains the reasons for the lack of consistency.

6.3.2.2 Natural Organic Matter (NOM)

To evaluate the applicability of the electrochemical reactivation of GAC technology to the drinking water industry, the reactivation of F-300 loaded with NOM at the pilot-scale facilities of the Regional Municipality of Ottawa-Carleton was investigated.

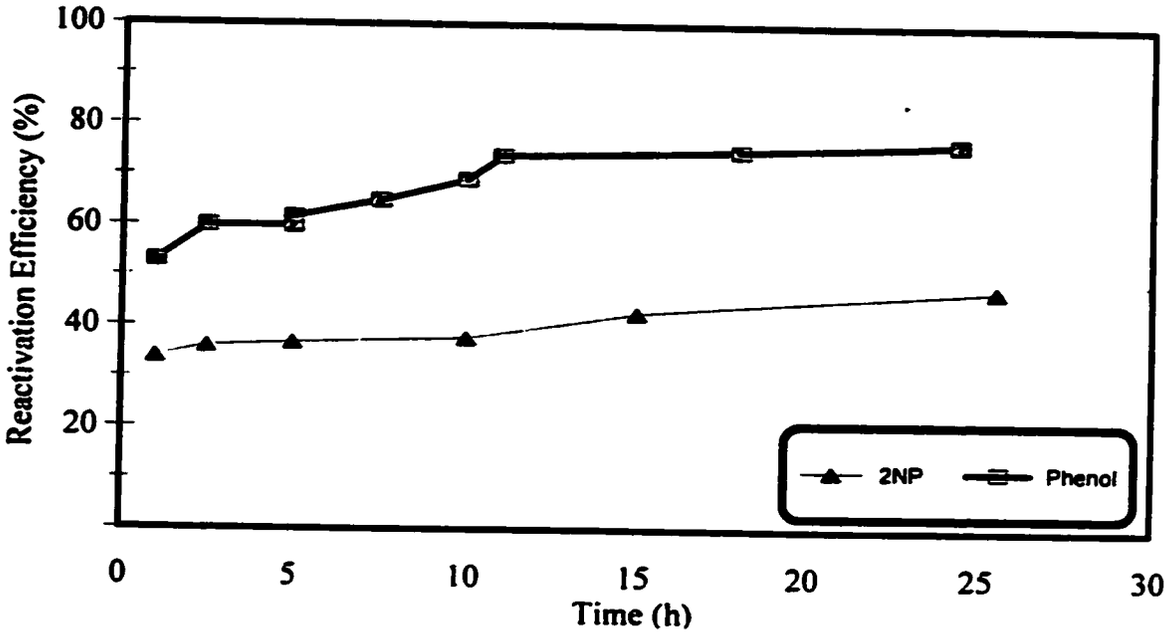

Fig. 6.12 Comparison of cathodic reactivation of 2NP and phenol-loaded F-400 at 50 mA.

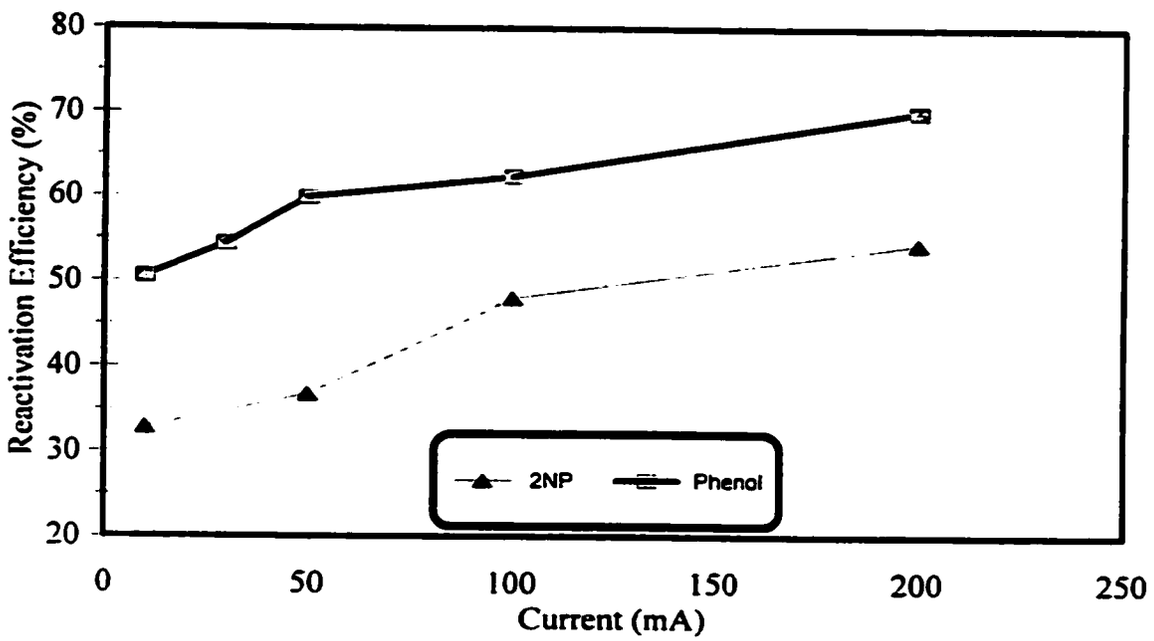

Fig. 6.13 Comparison of cathodic reactivation of 2NP and phenol-loaded F-400 at different currents after 5 hours reactivation.

Fig. 6.14 shows the impact of time on the reactivation of F-300 loaded with NOM at 50 mA current. Reactivation efficiencies were calculated by the iodine number method. As Fig. 6.14 shows, there was a linear relation between the reactivation efficiency and reactivation time; reactivation increased to 80% as the reactivation time increased to 25 hours. Fig. 6.14 also shows that the capacity of virgin F-300 subjected to 50 mA current for 25 hours was reduced by 2%. This decrease in performance may be caused by changes in GAC surface chemistry (Mehta and Flora, 1997) or may be an experimental error.

Fig. 6.15 also shows the impact of current on the reactivation of F-300 loaded with NOM after 5 hours of reactivation. Fig. 6.15 shows that the higher the reactivation current, the slightly higher the reactivation efficiency. Both Figs. 6.14 and 6.15 show that the F-300 loaded with NOM followed a similar pattern as the other GACs loaded with phenol and 2NP. A direct comparison between the reactivation efficiencies of phenol-loaded GACs and NOM-loaded GAC was not possible, as two different methods for the calculation of reactivation efficiencies were employed, but an indirect comparison was possible. The reactivation of 5 g of phenol-loaded F-400 showed a 47% RE3 after 5 hours reactivation at 50 mA (Fig. 5.6) while NOM-loaded F-300 showed 75% reactivation for the same conditions (Fig. 6.15). The higher reactivation of NOM-loaded GAC over phenol-loaded GAC is of interest because NOM adsorption is less reversible (about 10%) than phenol adsorption (Narbaitz, 1985) and lower reactivation efficiencies for NOM-loaded GAC are expected. Although the higher efficiency of NOM-loaded GAC reactivation may be partially a matter of the different way of measuring the reactivation efficiency, it may also indicate that electrochemical reactivation can also remove irreversible adsorbed species

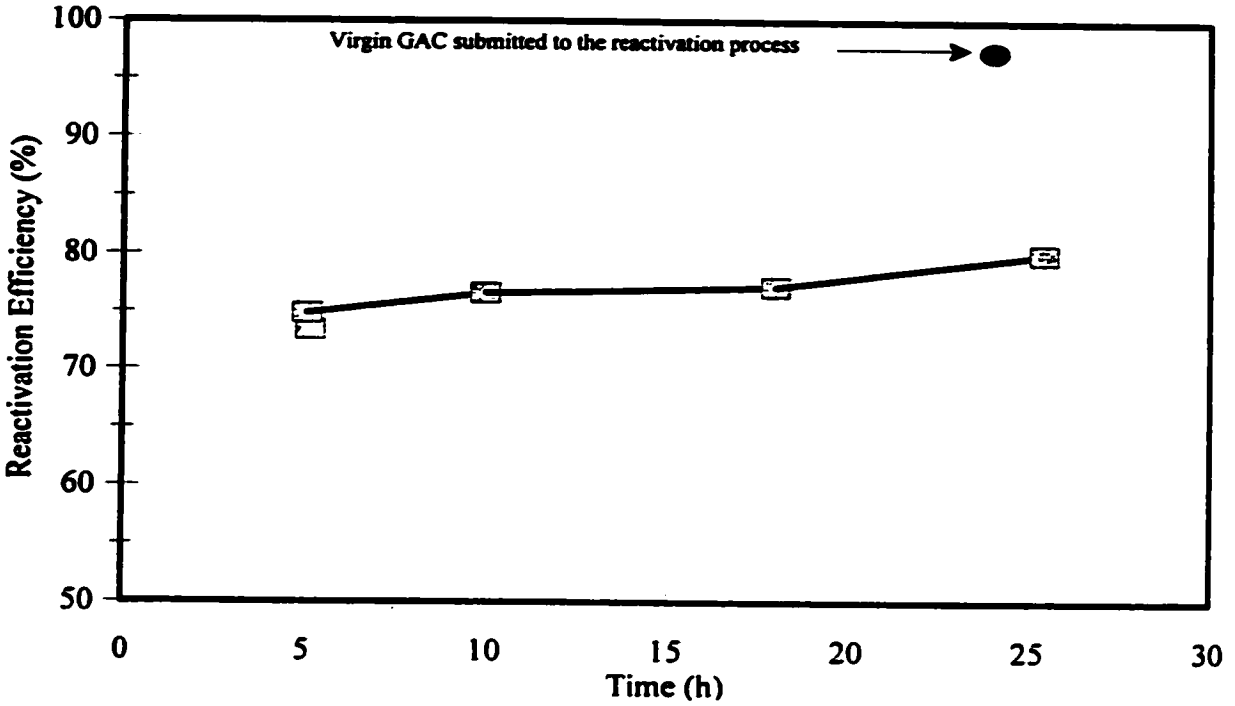

Fig. 6.14 Cathodic reactivation of 5g NOM-loaded F-300 versus time at 50 mA.

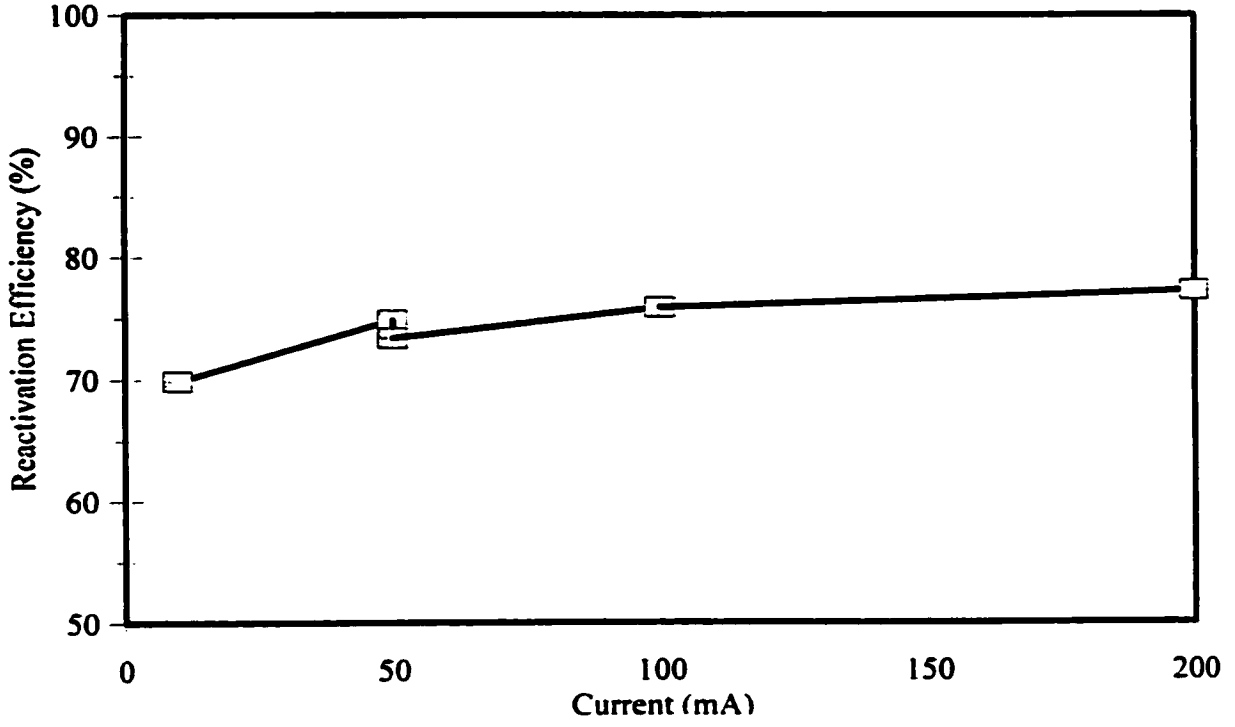

Fig. 6.15 Cathodic reactivation of 5g NOM-loaded F-300 at different currents after 5 hours reactivation.

from the surface of the GAC. This suggests that the electrochemical reactivation technology may be applicable in the drinking water industry, because the GAC are mostly loaded with partially irreversible NOM.

6.4 Effect of Loading and Loading time

Kinetic studies (Fig. 4.1 and 4.2) showed that adsorption apparently occurs at two different rates. The initial part of the adsorption was fairly fast, while the later adsorption was much slower. The slow rate of adsorption, which has been called a slow adsorption phenomenon, has been hypothesized to be caused by chemical or pore size limitations (Peel and Benedek, 1980a, b) and polymerization reactions (Vidic *et al.*, 1993).

The fraction of the slow adsorption in the adsorption processes has been found to be proportional to the molecular size of the adsorbate (Peel and Benedek,1980b). Peel and Benedek (1980b) used the following explanations for such behaviour. They assumed that a GAC particle can be divided into two regions loosly defined as: macropore and micropore. Macropores are those pores in which the pore radii are several times greater than the radii of the diffusing species. In these pores it can be assumed that transport occurs by either pore or surface diffusion. These larger pores can be assumed to be homogeneously distributed through the particle and provide access channels to the interior part of the GAC particles. It can be assumed that the rapid initial uptake of substrate takes place within this region. Similarly it can be speculated that an initial rapid desorption and consequently an initial rapid reactivation will be due to this region.

Micropores (or slow adsorbing and desorbing pores) are those pores that have radii of comparable size to the diffusing species and include all the remaining pores available for adsorption. It can be assumed that within these pores transport rates are strongly hindered, either by stearic constraints of the walls or by the restraining effect of the sorbate-sorbent interactive forces. It is in these small pores that the slow adsorption that follows the initial rapid uptake occurs. It can be speculated that a slow desorption and consequently a slow reactivation will be due to this region. Vidic *et al.* (1993) attributed the slow adsorption to polymerization reactions.

Adsorption studies show that longer-term kinetic tests are needed to observe both slow and rapid adsorption. It was hypothesised that if the adsorption is limited to macropore adsorption (by lowering the loading time and/or the amount of loading), then there may be higher desorption (and consequently higher reactivation efficiencies) in a lower reactivation time. To test this hypothesis the reactivation of samples with the same dose of GAC and different loading timse was conducted using F-400.

Fig. 6.16 shows the effect of loading and reloading time on reactivation of F-400 loaded with phenol at 50 mA cathodic reactivation after 2.5 hours. Since the RE3 method used the virgin isotherm equation (which represents equilibrium conditions), the RE3 method could not be used for the evaluation of reactivation efficiency because the loading and reloading batch samples were not in equilibrium. The RE2 method was therefore used to evaluate the reactivation efficiencies. Fig. 6.16 indicates that there appears to be no significant difference among the various loadings and reloading times. Also the GAC reactivation efficiency is

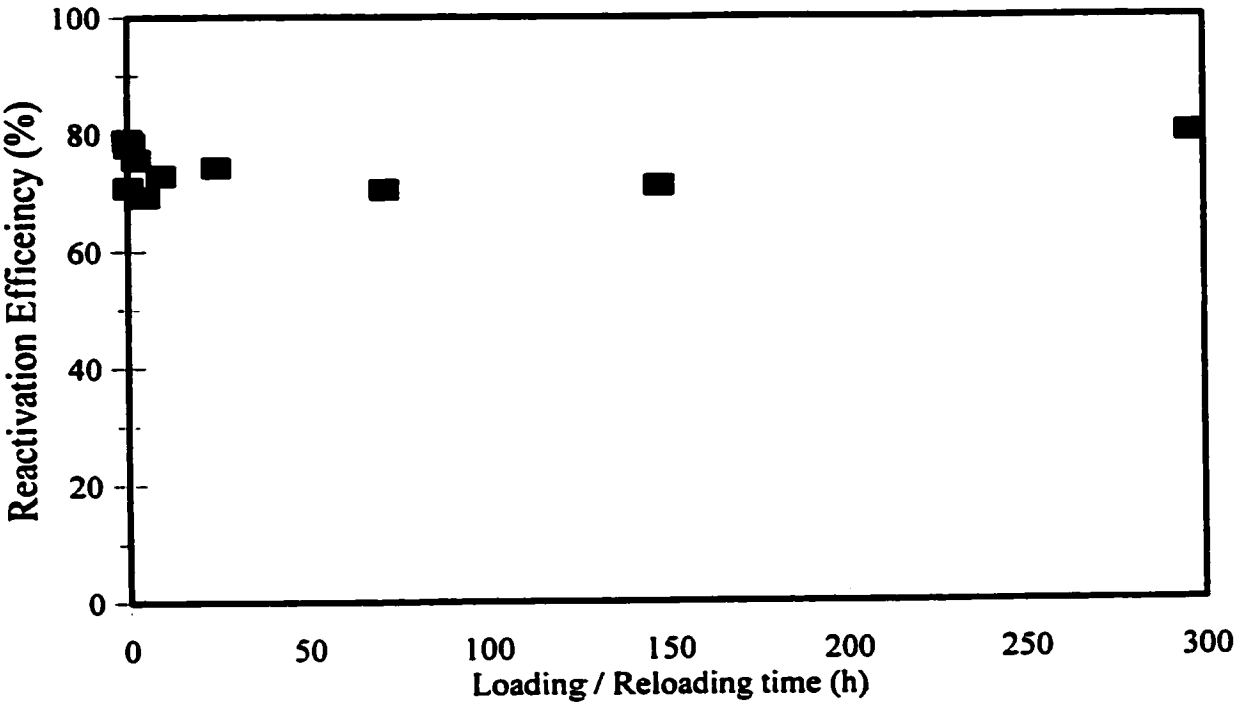

Fig. 6.16 Cathodic reactivation efficiency versus loading time for phenol-loaded F-400 at 50 mA after 2.5 hours reactivation (efficiencies are evaluated via RE2 method).

plotted against the solid phase concentration of phenol in Fig. 6.17. Different solid phase concentrations were achieved by loading the same doses of the GAC with the same phenol solution (300 mg/L), using different loading times. Fig. 6.17 shows that while the solid phase concentrations of phenol on the GAC ranged between 20 to 120 mg/g, the reactivation efficiencies were not significantly different. Narbaitz and Cen (1994) reported a slightly decreasing trend for the reactivation efficiencies with increasing GAC loading.

The 2NP-loaded GAC was also used to investigate the effect of loading time and loading on the reactivation efficiencies. The reactivation efficiencies are plotted versus the loading time in Fig. 6.18. Similarly to the phenol-loaded GAC there was no significant difference between the reactivation efficiencies. The reactivation efficiency increased slightly from 56 to 63% by increasing the loading and reloading time to 11 hours. Further increase in loading and reloading time did not significantly affect the reactivation efficiencies. Reactivation efficiency versus 2NP loading is plotted in Fig. 6.19. Different loadings were achieved by loading different doses of the GAC with the same 2NP solution (500 mg/L) using different loading times. Fig. 6.19 also shows that the reactivation efficiencies were essentially the same for the solid phase concentration from 30 to 480 mg of 2NP/g of GAC. This refutes the hypothesis that if one limits the adsorption to macropores adsorption (by lowering the loading time or perhaps the amount of loading) one may get a higher reactivation efficiency. Therefore the reactivation of GAC does not follow the Peel and Benedek (1980b) interpretation of dual rate adsorption.

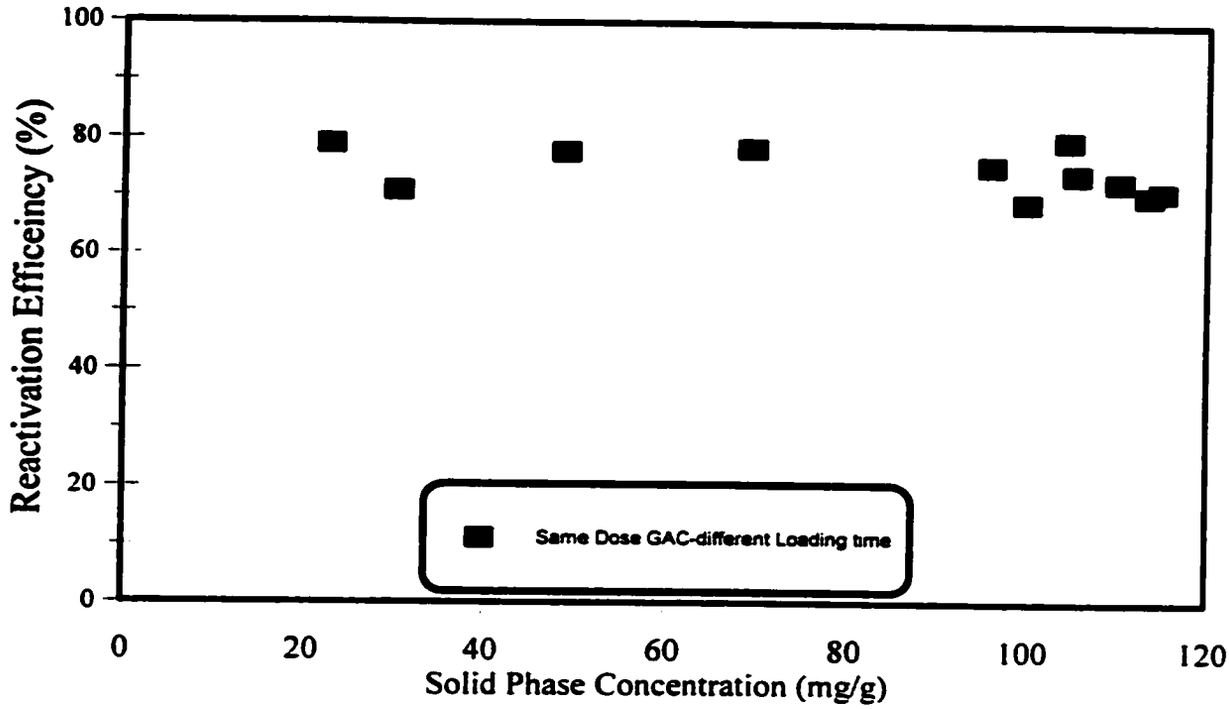

Fig. 6.17 Cathodic reactivation efficiency versus loading for phenol-loaded F-400 at 50 mA after 2.5 hours reactivation (efficiencies are evaluated via RE2 method).

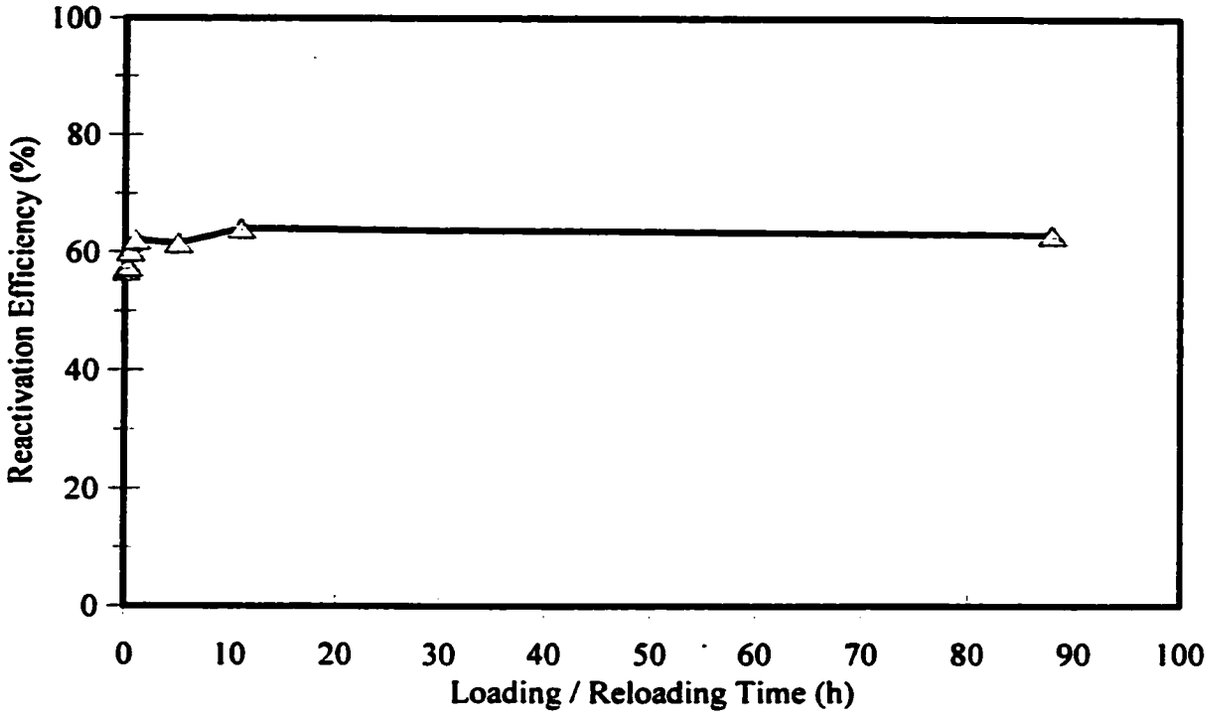

Fig. 6.18 Cathodic reactivation efficiency versus loading time for 2NP-loaded F-400 at 50 mA after 2.5 hours reactivation (efficiencies are evaluated via RE2 method).

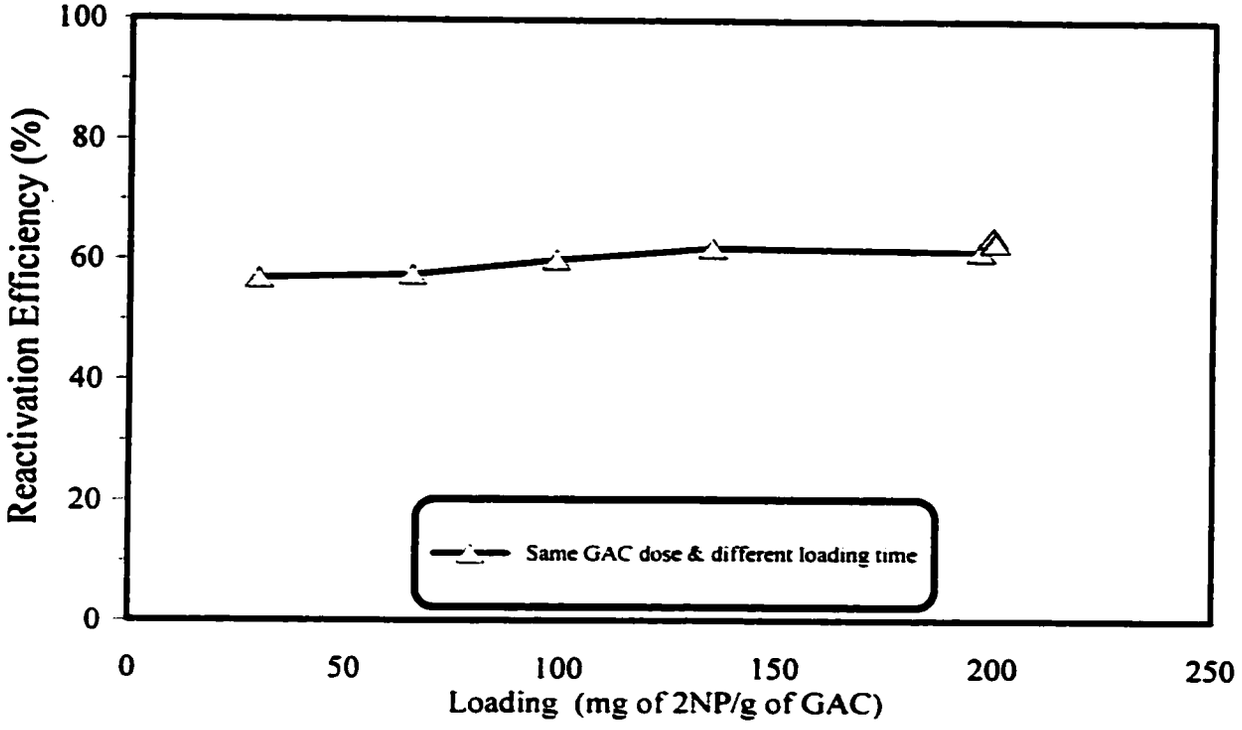

Fig. 6.19 Cathodic reactivation efficiency versus loading for 2NP-loaded F-400 at 50 mA after 2.5 hours reactivation (efficiencies are evaluated via RE2 method).

6.5 Comparison of the Virgin and Reactivated Isotherms

The adsorptive capacity of activated carbon is usually measured utilizing adsorption equilibrium tests conducted at a constant temperature (i.e., isotherm tests). In order to investigate the feasibility of the electrochemical reactivation process, differences between the virgin and reactivated GAC isotherms were evaluated. Experiments were performed by contacting phenol or 2NP solutions in a series of bottles with different masses of GAC. After equilibrium was reached, the GAC and solution were separated, the GAC samples were reactivated and then reloaded with the same solutions until equilibrium was again established. The virgin and reactivated GAC adsorption isotherms were obtained and are shown in Figs. 6.20 and 6.21. Note that the solid phase concentrations for the reactivated GAC assume that there was no residual contaminant on the reactivated GAC. This assumption was made because determining the residual contaminant concentration on the reactivated GAC is an inexact and very complicated process. As expected, based on reactivation efficiencies of less than 100%, for the same liquid phase concentrations the solid phase concentrations (loading capacity) for the reactivated GAC isotherm were less than those for the virgin GAC isotherm (Figs. 6.20 and 6.21). This demonstrates the need for improvements to the electrochemical reactivation process.

6.6 Comparison of the Reactivation Efficiencies

As mentioned earlier, associated with reactivation is the potential of producing by-products from the materials or organics adsorbed on the GAC (i.e., oxidation of organics to by-products). These by-products may adsorb onto the GAC during the reactivation process. The adsorbed by-products may desorb, due to competitive adsorption between

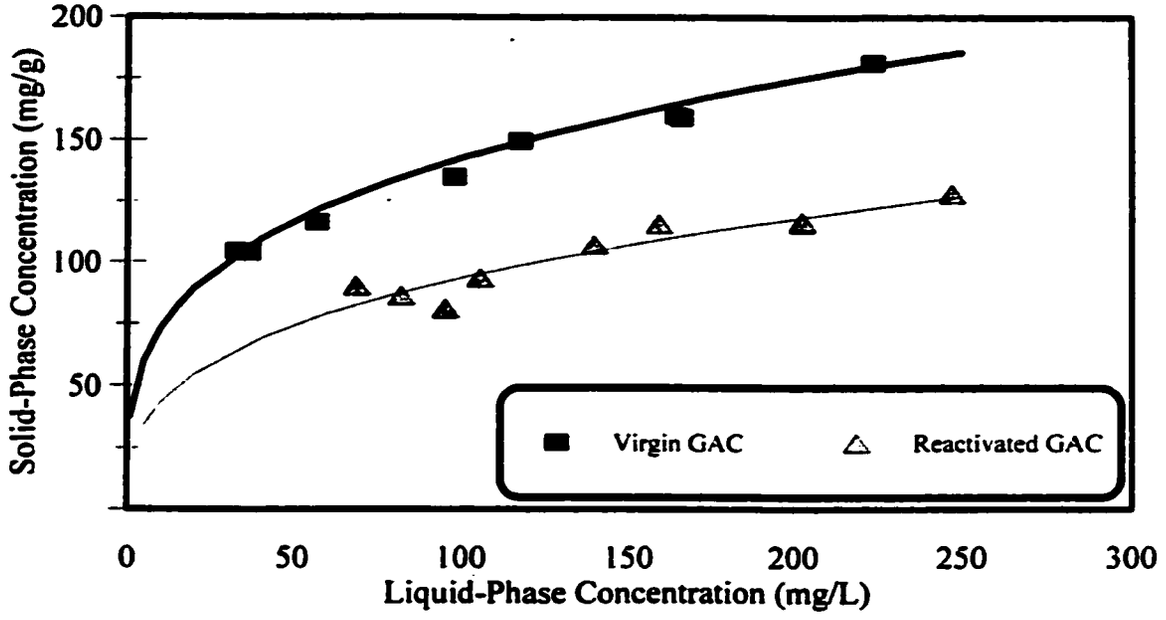

Fig. 6.20 Isotherms of virgin and reactivated phenol-loaded F-400 (reactivation conducted at 50 mA for 5 hours).

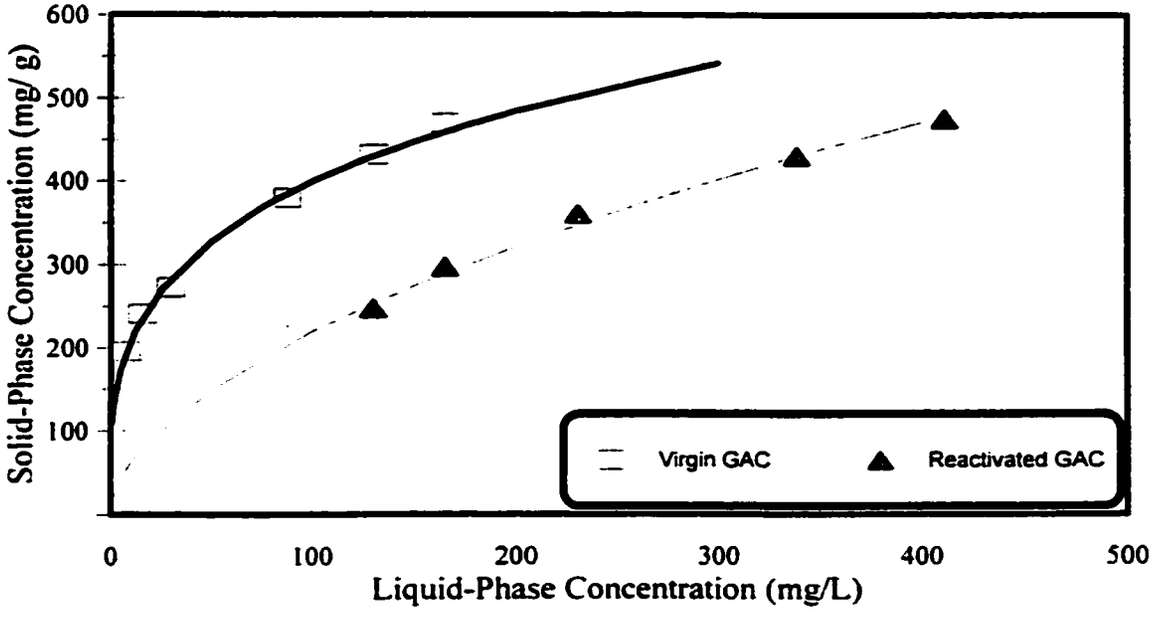

Fig. 6.21 Isotherms of virgin and reactivated 2NP-loaded F-400 (reactivation conducted at 50 mA for 5 hours).

the reloaded contaminant and the by-products, into the reloading solution. Since the reactivation efficiencies are evaluated based on the liquid-phase equilibrium concentration of the reloaded solutions (i.e., phenol or 2NP solutions), there is a possibility that the method of measuring the concentration of reloaded solution (i.e. using the HPLC or TOC analyzer) may influence the final results. The HPLC will only monitor the concentration of phenol or 2NP while the TOC will monitor the total TOC (TOC due to phenol/2NP plus the TOC of the potential desorbed by-products). If there is no desorption of the by-products materials, the reactivation efficiencies calculated by both HPLC and TOC results will be the same. If there is a desorption of by-products, the total TOC will be higher than the TOC due to phenol or 2NP and consequently the reactivation efficiency will be lower.

Fig. 6.22 compares the reactivation efficiencies of WV-B loaded with phenol using both TOC and HPLC results. Fig. 6.22 shows that there was no significant difference between the two plotted results. Similar results were obtained for the 2NP experiments as well. However, in practical applications (for example drinking water applications) there is a need to monitor desorption of possible regenerated by-products.

6.7 Comparison of the Different Methods for Evaluation of Reactivation Efficiency

The alternative methods for evaluation of reactivation efficiencies were compared using HPLC-based data from reactivation of phenol loaded F-400 at 50 mA after 5 hours of reactivation. Fig. 6. 23 presents the reactivation efficiencies of the four alternative methods: RE1. RE2, RE3. and RE4 described by Narbaitz and Cen (1997). The method RE2, which

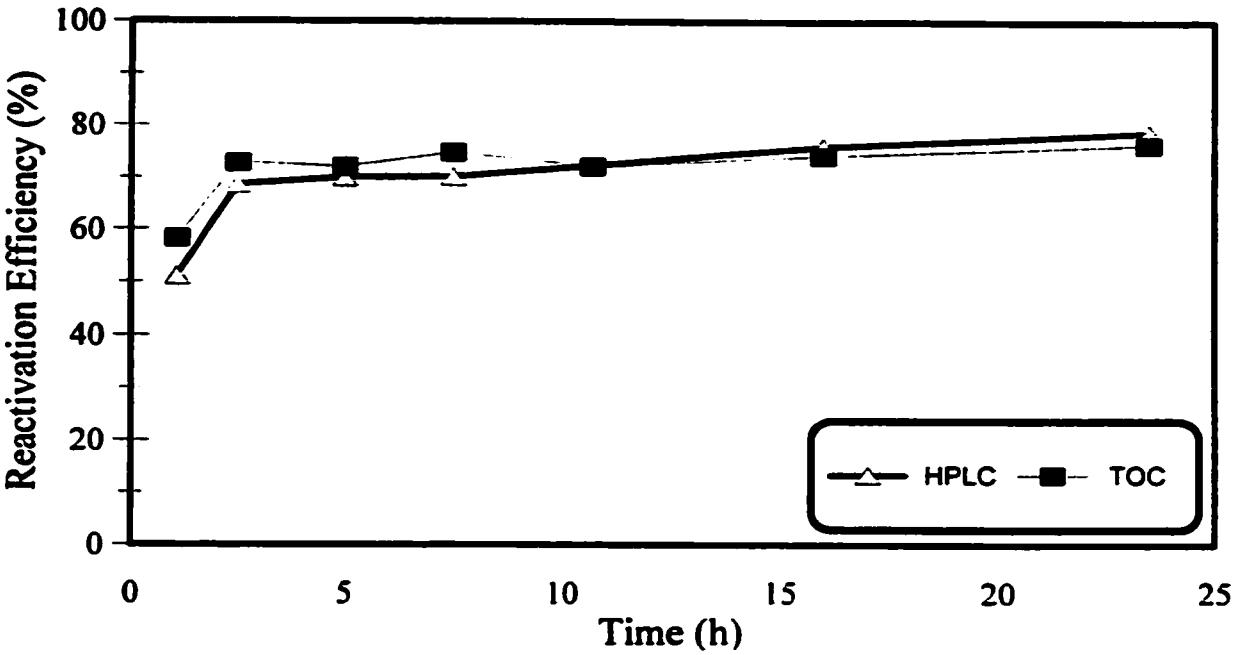

Fig. 6.22 Comparison of cathodic reactivation of phenol-loaded WV-B at 100 mA using HPLC and TOC results.

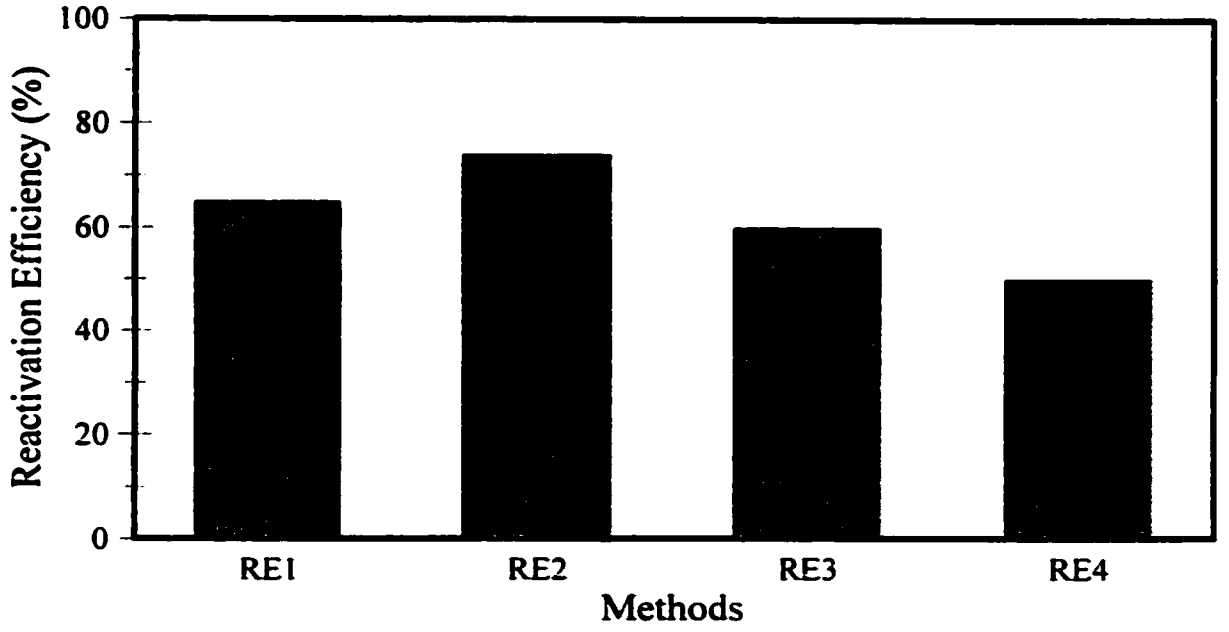

Fig. 6.23 Comparison of methods for the evaluation of reactivation efficiency based on HPLC analysis.

requires less experimental effort, shows the highest reactivation efficiency (74%). As discussed in chapter 3, RE2 is not a representative measure of reactivation, as it does not calculate the ratio of loading and reloading for the same liquid-phase concentration. The RE2 method overestimates the reactivation efficiencies and should be avoided. Method RE4 shows the lowest reactivation efficiency of 50%. This method was developed to model partial or ineffective reactivation and is useful in describing the results of control experiments (Narbaitz and Cen, 1997). This method underestimates the efficiencies of effective reactivation and does not represent the true reactivation efficiencies.

The RE1 and RE3 methods show reactivation efficiencies of 65 and 60%, respectively (Fig. 6.23). This is in agreement with the findings of Narbaitz and Cen (1997). Narbaitz and Cen (1997), during a sensitivity analysis, showed that in many situations the RE1 and RE3 methods yielded similar values.

6.8 Conclusions

- The reactivation efficiency could be increased to a maximum by increasing the current and/or time. The reactivation efficiency increases rapidly with increasing reactivation time in the first few hours followed by a more gradual increase for longer times. Also the effect of current was very marked from 10 to 50 mA and more gradual from 50 to 100 mA. However, the coulombic efficiency for the GAC reactivation was independent of the current/time applied.

- Cathodic reactivation of phenol-loaded F-400 and 2NP-loaded F-400 at pHs of 2 and 12, showed that electrolyte pH controlled the contaminant desorption and consequently the reactivation efficiency.
- A comparison of the percent reactivation of GACs showed that 2NP-loaded F-400 and 2NP-loaded WV-B performed essentially the same for the tested conditions. However, phenol-loaded WV-B showed slightly better performance than phenol-loaded F-400 at higher currents. The observed results were in agreement with fully reversible or partially irreversible adsorption phenomena. Darco GAC showed slightly better performance at lower reactivation times and/or higher currents and lower performance at higher reactivation times and/or currents. It is possible that the surface chemistry of Darco GAC changed over the longer reactivation times and/or higher currents due to its lower conductivity (higher electrical resistance).
- Comparison of the reactivation efficiencies of F-400 loaded with 2NP and phenol at different reactivation currents and times showed similar patterns. However, phenol-loaded F-400 showed higher reactivation efficiencies than 2NP-loaded F-400. This is not consistent with the fully reversible adsorption of 2NP on F-400 and partially reversible phenol adsorption on F-400. (Further investigation of this matter is presented in chapter 7).
- Reactivation of GAC loaded with NOM showed that there was a linear relation between the reactivation efficiency and reactivation time; reactivation increases to 80% as the reactivation time increases to 25 hours.

- Loading and loading time did not significantly affect the reactivation efficiencies of phenol-loaded-F400 and 2NP-loaded-F400.
- The calculated reactivation efficiencies using the TOC and HPLC results were almost the same. However, a reactivation efficiency of less than 100% demonstrates the need for improvements to the electrochemical reactivation process.

CHAPTER 7

RE-EVALUATION OF THE PREVIOUS RESULTS

7.1 Introduction

In the previous chapters there were a number of results that did not seem logical. This chapter outlines these cases, describes potential reasons for the results, tests these hypothesis and finally re-evaluates the principal results in light of these findings.

7.2 Review of Questionable Results

One questionable result presented in section 6.3.2.1 was that the reactivation efficiency of 2NP-loaded F-400 was 20 to 30% lower than that for phenol-loaded F-400 (Figs. 6.12 and 6.13). This was unexpected because 2NP adsorption on F-400 is fully reversible while phenol adsorption is partially irreversible.

Another questionable result was the comparison of the cathodic and anodic reactivation of 2NP-loaded F-400 (Fig. 7.1). Fig. 7.1 shows that the anodic reactivation was slightly more efficient than the cathodic reactivation. This is not in agreement with expectations and earlier results. Based on the high pH of the catholyte (Fig. 5.14) and the higher desorption of the 2NP from GAC at high pHs (Fig. 5.16), one would expect higher cathodic reactivation than anodic reactivation.

Fig. 7.2 also presents another questionable result, the impact of electrolyte mixing on the reactivation efficiency of 2NP-loaded F-400. It shows that electrolyte mixing did not affect

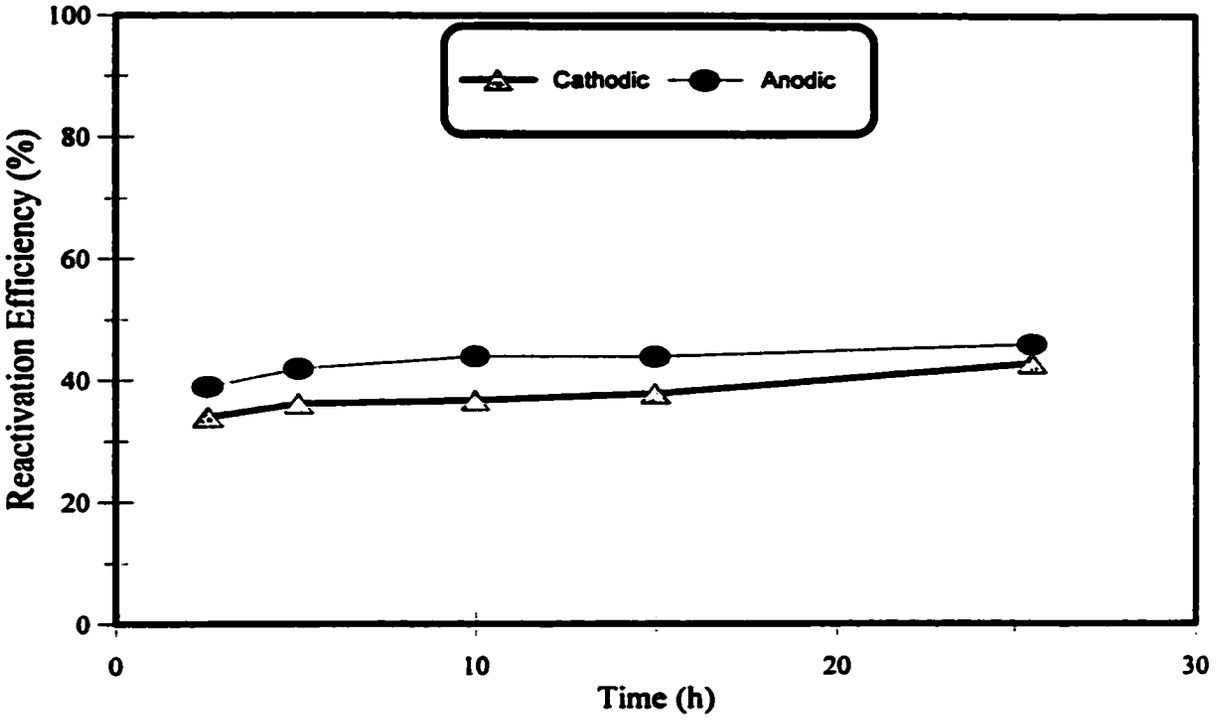

Fig. 7.1 Cathodic versus anodic reactivation of 2NP-loaded F-400 at 50 mA (undivided reactor, unbuffered solutions).

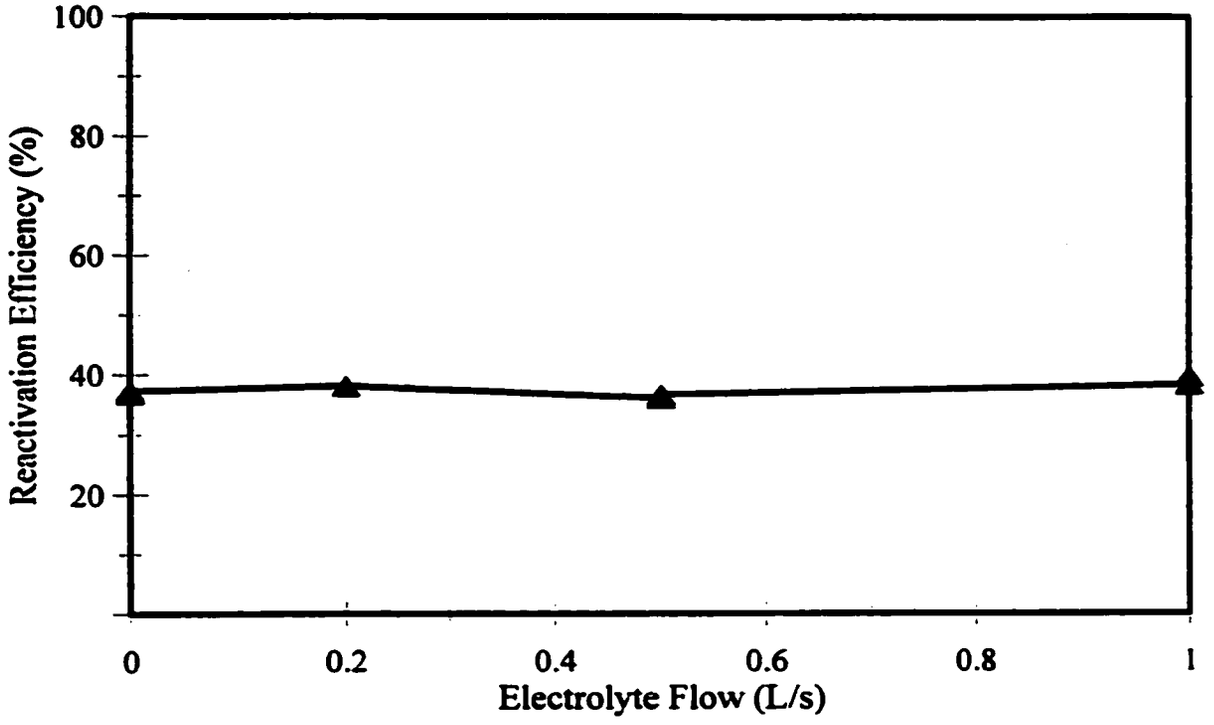

Fig. 7.2 Effect of electrolyte mixing on cathodic reactivation of 2NP-loaded F-400 at 50 mA after 2.5 hours reactivation.

the reactivation efficiency. This is not consistent with the previous findings of the impact of electrolyte mixing on the reactivation efficiency (section 5.4.4). As discussed in section 5.4.5, electrolyte mixing reduced the high pH of the catholyte (pH = 12) to about 3.5 (Fig. 5.14), and hence higher reactivation efficiency was expected when there was no electrolyte mixing.

In addition to these questionable results, it was also observed that in some samples the colour of 2NP reloading solution changed from the initial yellow to orange after the addition of reactivated GAC. Also the colourless phenol solutions became brownish in some cases. The change in colour could be either due to desorption of the by-products from the surface of the reactivated GAC or/and due to variations in pH. 2NP solutions possess different colours at different pHs; they are red at low pHs, yellow in the mid pH range, and orange at high pHs. Phenol solutions are colourless at all pHs. Hence it was decided to monitor the pH of the reloading solutions before and after reloading of the reactivated GAC.

7.3 Hypothesis

It was hypothesized that the questionable results arose from the impact of residual high-pH water within the pores of the electrochemical reactivated GAC on the reloading step. The high pH would account for both the leaching and the reduced adsorption during the reloading. To test this hypothesis a number of reactivation experiments were followed by reloading using buffered and unbuffered solutions.

Table 7.1 presents the changes in colour and pH that occurred during both the loading step and the reloading step. The table shows that there was no colour variation for the loading

solutions but the pHs changed slightly. The magnitudes of the changes of colour of the reloaded samples were proportional to the reactivation current and time. At low current and/or short reactivation time the changes of colour were not noticeable, while at higher current and/or longer reactivation times the colour changes were very noticeable.

As Table 7.1 shows, with larger reactivation times the reloaded phenol solutions became brownish. Knowing that phenol solution was colourless at all the pHs, it can be concluded that desorption of by-products from reactivated GAC to the reloaded solutions was the cause of the colour variation. Since the 2NP solution had different colours at different pHs, the colour variation in 2NP reloaded solutions may have been due to both pH variation and desorption of by-products.

The pH variation in Table 7.1 demonstrates an important point. The pHs of the loading solutions before and after the loading process were less than the pK_as of 2NP (pH = 7.2) and of phenol (pH = 9.9). However, the pHs of the reloading solutions after the reloading process were higher than the pK_as of 2NP and of phenol. This indicates that either the GAC surface became more basic due to the reactivation process (Mehta et al., 1997), and/or the high pH of the liquid within the pores of the GAC (i.e., remaining from the reactivation process) increased the pH of the unbuffered reloading solutions. The high pH (higher than the pK_as of the compounds) of the reloading solution reduces the adsorption capacity (Karimi-Jashni, 1994) of the reloaded GAC and consequently lowers the reactivation efficiency. The differences between the final pH of the reloading solution (i.e., after reloading) and the pK_a were higher for 2NP than those of phenol. This suggests that the effect of pH variation on the 2NP results would be greater than that on the phenol results.

Table 7.1 Observation of loading and reloading solutions for un-buffered solutions.

Compound	GAC	Loading Solution				Reactivation		Reloading Solution			
		Before Loading		After Loading				Before Reloading		After Reloading	
		pH	Colour	pH	Colour	I(mA)	Time(h)	pH	Colour	pH	Colour
2NP	F-400	5	yellow	5.6	yellow	50	1	5	yellow	8	yellow
2NP	F-400	5	yellow	5.4	yellow	50	5	5	yellow	8.5	Yellow-orange
2NP	F-400	5	yellow	5.4	yellow	50	10	5	yellow	8.7	orange
2NP	F-400	5	yellow	5.3	yellow	50	24	5	yellow	8.8	orange
Phenol	F-400	6.4	colourless	5.8	colourless	50	1	6.4	colourless	9.9	colourless
Phenol	F-400	6.4	colourless	5.5	colourless	50	5	6.4	colourless	10.1	Light brown
Phenol	F-400	6.4	colourless	5.2	colourless	50	10	6.4	colourless	10.2	Light brown
Phenol	F-400	6.4	colourless	5.5	colourless	50	24	6.4	colourless	10.4	brownish

This explains the unexpected 2NP results in section 7.2, while those for phenol followed a more logical trend. To verify this conclusion the experiments described in Table 7.2 were repeated with 3% phosphate buffered 2NP and phenol solutions to eliminate the effect of the pH variation.

Table 7.2 shows that pH of the reloading solutions was well below the pK_as of the compounds and there were no colour variations of the reloaded solutions. This demonstrates that desorption of the colour-causing by-products had been prevented by the relatively low pH of the reloaded solutions.

7.4 Re-evaluation of Principal Results

Based on the above findings of the impact of pH upon reloading a number of key experiments were repeated using buffered solutions for reloading. These experiments looked at the impact of cathodic versus anodic reactivation, phenol versus 2NP, electrolyte mixing, current and reactivation time, electrolyte volume, electrolyte concentration, etc.

7.4.1 Cathodic Versus Anodic Reactivation

7.4.1.1 Undivided-Cell Reactor

Figs. 7.3 and 7.4 compare the cathodic reactivation results of the buffered and unbuffered solutions and as well as cathodic versus anodic reactivation. Both figures demonstrate that the buffered solutions resulted in higher reactivation efficiencies. As expected, the difference between the reactivation efficiencies with buffered and unbuffered solutions were higher for 2NP-loaded GAC. Buffering the 2NP solutions resulted in about 60% higher reactivation efficiencies after 10 hours (Fig. 7.3), while buffered phenol solutions resulted in

Table 7.2 Observation of loading and reloading solutions for buffered solutions.

Compound	GAC	Loading Solution				Reactivation		Reloading Solution			
		Before Loading		After Loading				Before Reloading		After Reloading	
		pH	Colour	pH	Colour	I(mA)	Time(h)	pH	Colour	pH	Colour
2NP	F-400	4.5	yellow	4.5	yellow	50	1	4.5	yellow	4.7	yellow
2NP	F-400	4.5	yellow	4.5	yellow	50	5	4.5	yellow	4.7	yellow
2NP	F-400	4.5	yellow	4.5	yellow	50	10	4.5	yellow	4.75	yellow
2NP	F-400	4.5	yellow	4.5	yellow	50	24	4.5	yellow	4.8	yellow
Phenol	F-400	4.5	colourless	4.5	colourless	50	1	4.5	colourless	4.6	colourless
Phenol	F-400	4.5	colourless	4.5	colourless	50	5	4.5	colourless	4.7	colourless
Phenol	F-400	4.5	colourless	4.5	colourless	50	10	4.5	colourless	4.7	colourless
Phenol	F-400	4.5	colourless	4.5	colourless	50	24	4.5	colourless	4.8	colourless

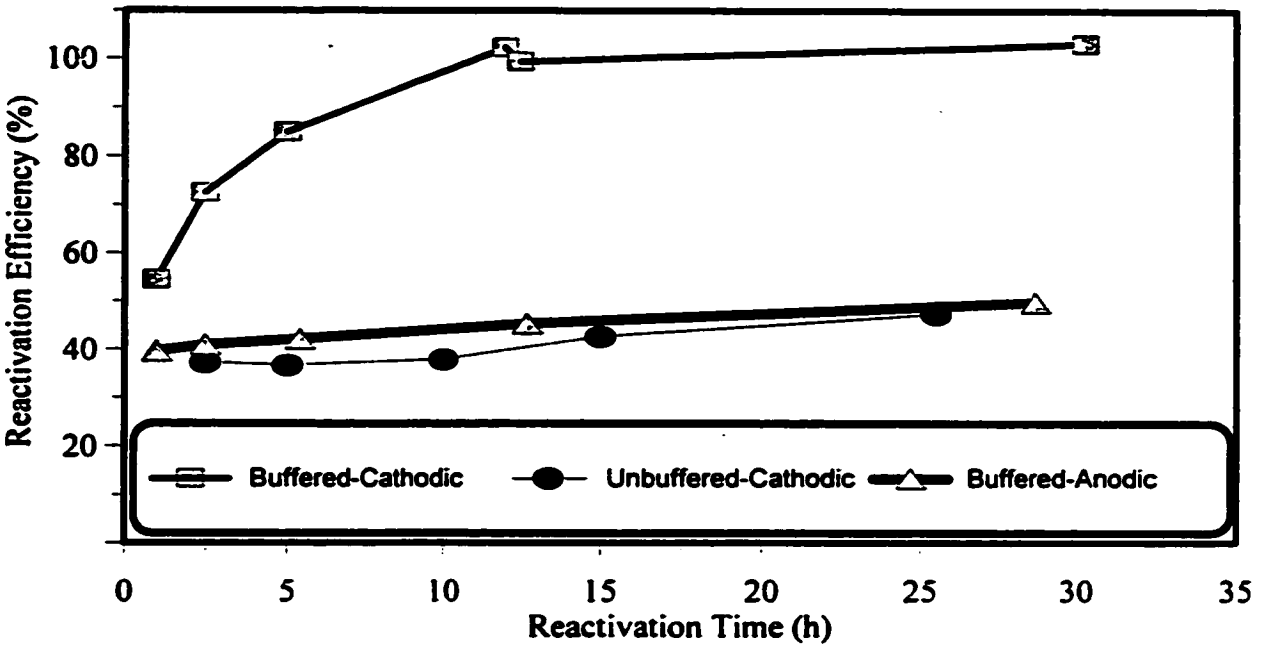

Fig. 7.3 Cathodic versus anodic reactivation of 2NP-loaded F-400 at 50 mA and undivided reactor.

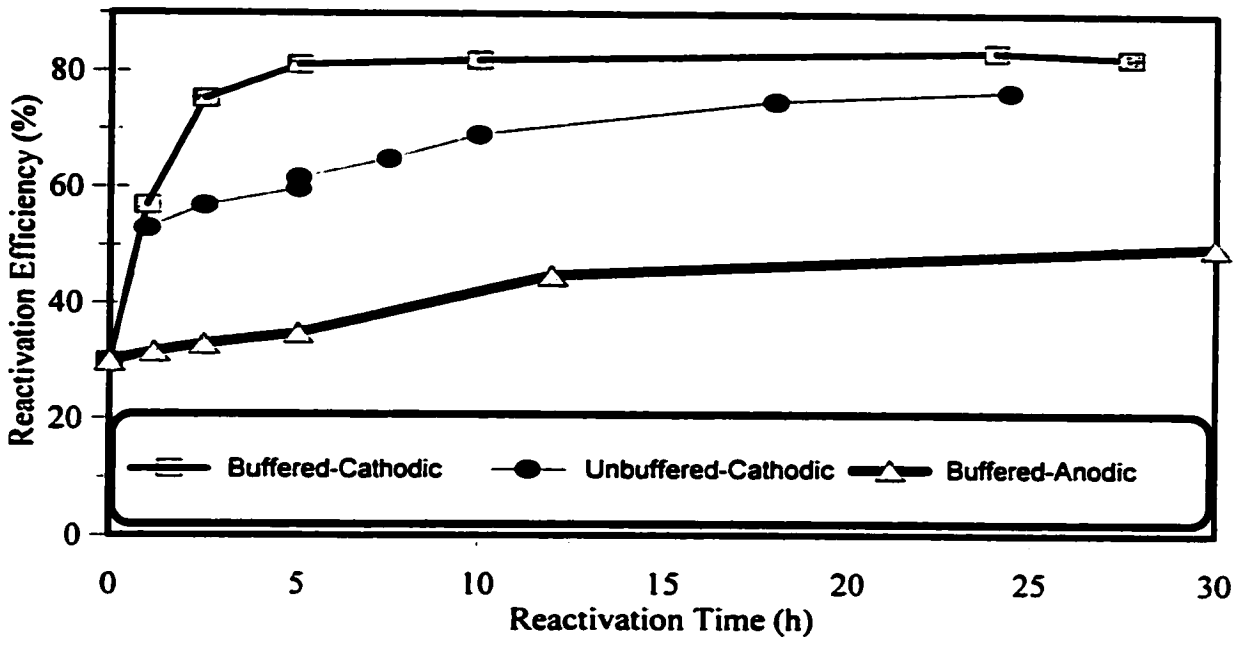

Fig. 7.4 Cathodic versus anodic reactivation of phenol-loaded F-400 at 50 mA and undivided reactor.

about 10% higher reactivation efficiencies than the unbuffered solution (Fig. 7.4). The higher variation in the reactivation of 2NP-loaded GAC was consistent with the higher change in pH during the reloading with the 2NP solution (Table 7.1). This proves that the increase of pH of the unbuffered reloaded solution beyond the pK_a of the compound had reduced the reloading capacity of the GAC and consequently resulted in lower reactivation efficiencies.

Figs. 7.3 and 7.4 also show the impact of cathodic versus anodic reactivation of F-400 loaded with phenol and 2NP, respectively. They show that as the reactivation time increased the reactivation efficiency increased. For a reactivation time of 10 hours the cathodic reactivation efficiency increased to 82% for phenol and to 100% for 2NP. This increase in the cathodic reactivation efficiency was consistent with the increase of pH from 5.5 to 12 (Fig. 5.14) and the higher desorption at pH 12 (Fig. 5.16). The increases in anodic reactivation efficiencies were gradual and they reached 42% for phenol and 45% for 2NP after 10 hours. The lower anodic reactivation efficiencies were consistent with the lower desorption of contaminants (Fig. 5.16) at the low pHs of the anolyte (pH = 2) (Fig. 5.14).

Comparison of the results shows that cathodic reactivation was more efficient than anodic reactivation for both compounds. This discredits the results of Fig. 7.1. The superiority of cathodic over anodic reactivation increased to 30% for phenol and 55% for 2NP as the reactivation time increased to 10 hours. The increase in superiority of cathodic over anodic reactivation was consistent with the variation of pH in the catholyte from 5.5 to 12 (Fig. 5.14). As discussed in chapter 5 this pH variation affects the amount of contaminant

desorption (Fig. 5.16) and thus, the reactivation efficiency (Figs. 7.3 and 7.4). Given the large impact of buffering, most earlier results need to be reassessed.

7.4.1.2 Divided-Cell Reactor

A number of tests were conducted with the divided-cell reactor (Fig 3.4) to answer questions such as: Are there different mechanisms prevalent at the anode and the cathode? Is direct oxidation of the contaminant at the surface of the GAC responsible for the reactivation or is accelerated desorption and anodic contaminant destruction responsible for the reactivation? The cells were separated by cation or anion exchange membranes to investigate their possible effect on the reactivation efficiency.

As mentioned earlier, ion-exchange membranes can be used to stop, selectively, either anions or cations from moving from one cell compartment to the other and to allow electrolysis to be carried out under close pH control. The electrodes were separated by a cation exchange membrane and the pHs of the catholyte and anolyte were measured at the end of each experiment by a pH meter and are shown in Fig. 7.5. Similar to the undivided reactor without mixing, the pHs of the catholyte and anolyte tend to asymptotes at 12 and 2, respectively.

Figs. 7.6 and 7.7 show the cathodic and anodic reactivation of F-400 within the divided cell reactor at 50 mA. From this point on, unless it is otherwise stated, the reloading tests used to calculate the reactivation efficiency were conducted with buffered solutions. As mentioned earlier for consistency reasons, the RE3 method was used to calculate the efficiencies for all the conditions tested and the relatively high reactivation efficiency at time=0 was due to the

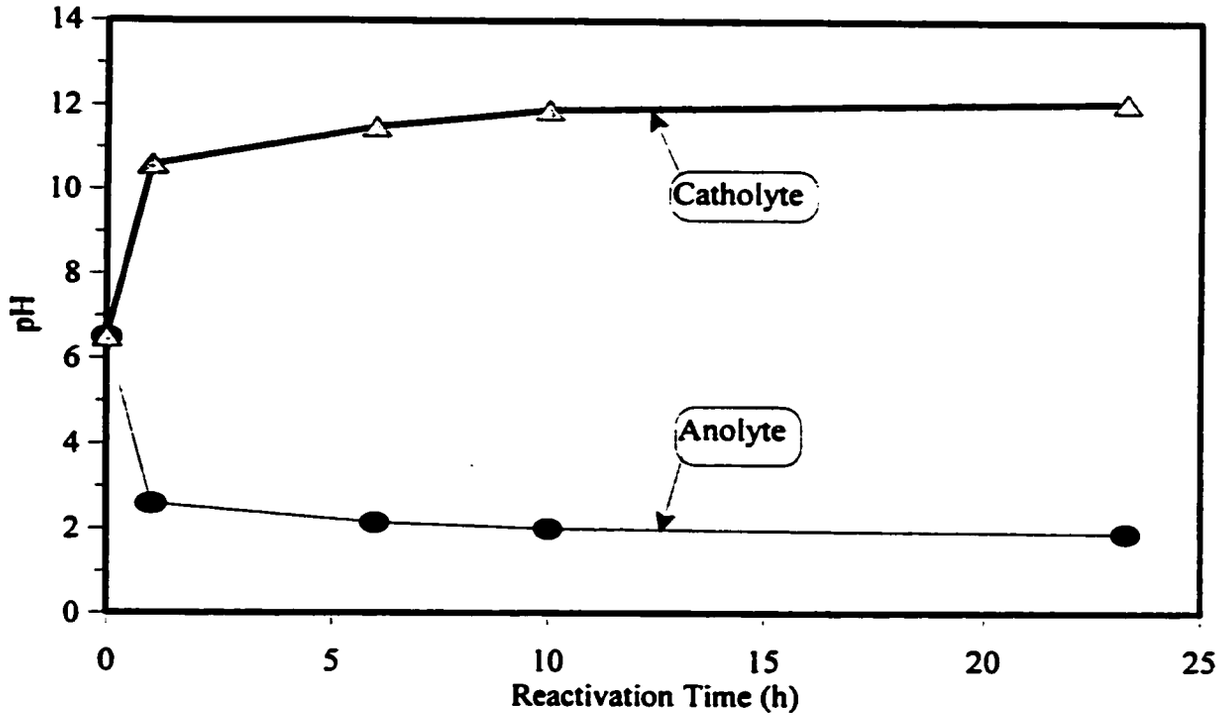

Fig. 7.5 pH variation within the divided-cell reactor during the cathodic reactivation of 2NP-loaded F-400 at 50 mA.

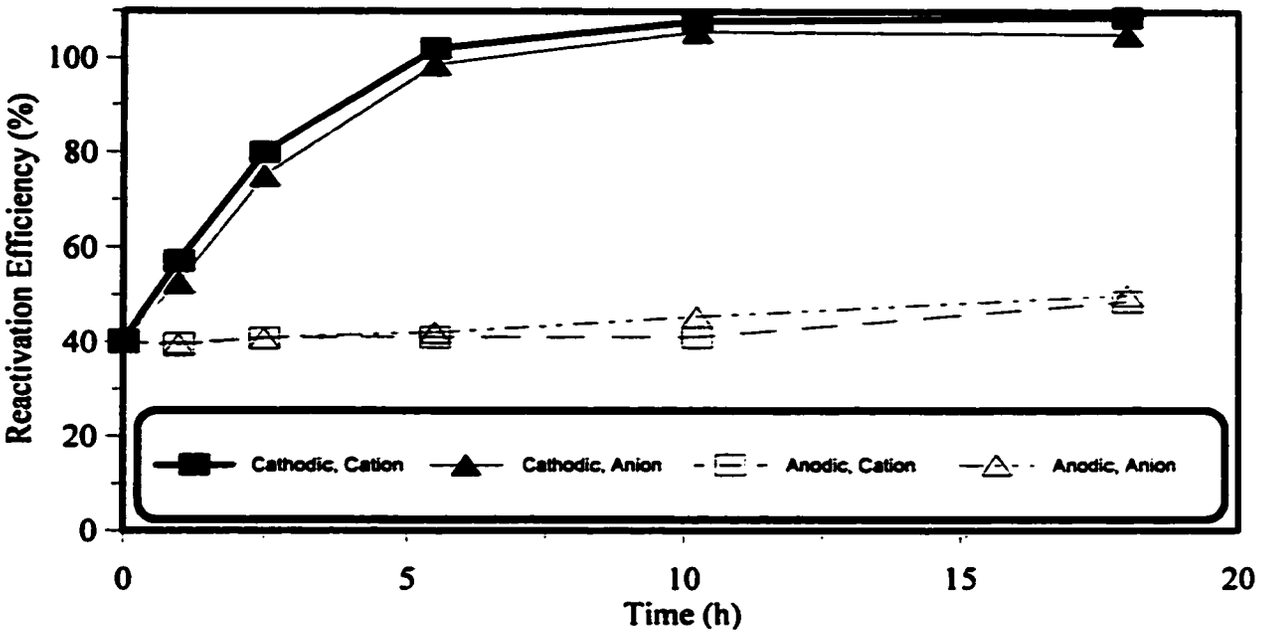

Fig.7.6 Reactivation of 2NP-loaded F-400 in divided-cell reactor at 50 mA (reloading solutions were buffered).

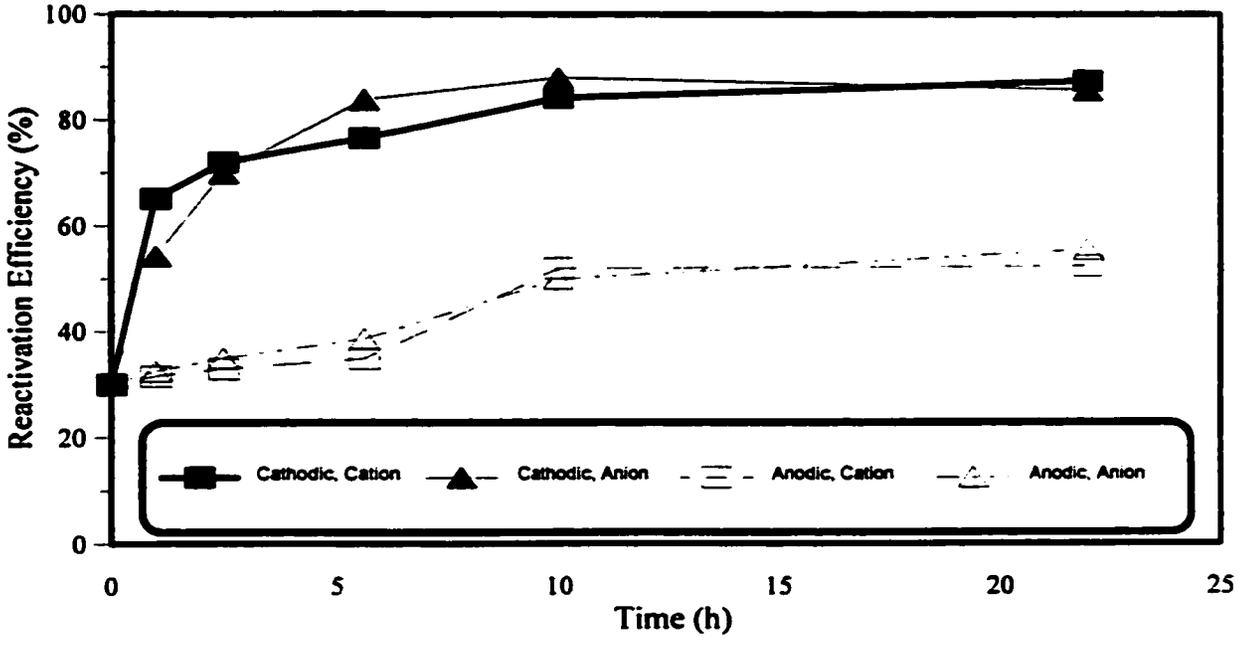

Fig.7.7 Reactivation of phenol-loaded F-400 in divided-cell reactor at 50 mA (reloading solutions were buffered).

RE3 method which overestimates the efficiency at this time. As discussed by Narbaitz and Cen (1997) the RE4 method is the method of choice for the evaluation of control samples (i.e., time = 0 or current = 0) which in these cases would result in reactivation efficiencies of less than 10%.

Fig. 7.6 shows the cathodic and anodic reactivation of 2NP-loaded F-400. This figure shows that reactivation at the cathode was far higher than that at the anode. The cathodic reactivation efficiency reached 100% after about 6 hours, while the anodic reactivation was 40 to 45% for the same time period. A maximum cathodic reactivation of 108% was achieved after 10 hours of reactivation. The higher pH of the catholyte (pH = 12) accelerated the 2NP desorption from the F-400 and resulted in higher reactivation efficiencies.

The reactivation of phenol-loaded F-400 at the cathode and at the anode of the divided-cell reactor at 50 mA is shown in Fig.7.7. Similar to 2NP-loaded GAC, the cathodic reactivation was higher than the anodic reactivation. Cathodic reactivation reached a maximum of 89% after 22 hours while anodic reactivation was about 55% after 22 hours.

Comparison of Figs. 7.6 and 7.7 demonstrates that the anodic reactivation of F-400 loaded with phenol was higher than that of 2NP. This is consistent with the lower phenol adsorption capacity of F-400 at low pHs as compared to neutral pHs (Karimi-Jashni, 1994). Both membranes resulted in almost the same reactivation efficiencies. It was expected that the cation membrane would prevent the diffusion of negative ions such as phenate and hydroxide from the catholyte into the anolyte, which would result in a high pH at the catholyte. The higher pH of the catholyte would then be responsible for the acceleration of

the phenolic desorption from GAC. This was observed. The anion-exchange membrane was expected to allow the diffusion of phenate and hydroxide ions from the catholyte into the anolyte that would lower the pH and reduce the phenolic desorption into the catholyte. Then the lower concentration of phenolics in the catholyte would be responsible for the acceleration of the desorption of phenolics from the GAC. It was expected that the two different mechanisms may affect the reactivation efficiency differently.

pH measurements of the catholyte showed pH = 12 for both sets of experiments. This raised the question: "have the anions diffused through the anion-membrane"? To answer this question the diffusion of phenate through both membranes was measured and is shown in Fig. 7.8. The conditions were set to those in electrochemical reactivation. The cathode compartment was filled with 2NP solution. The initial 2NP concentration at the catholyte was 70 mg/L and its pH was 12. The catholyte was separated from the anolyte with ion exchange membranes. The anode compartment was filled with distilled water. The initial concentration of 2NP in the anolyte was zero and its pH was 2. Fig. 7.8 shows that the cation and anion membranes performed similarly and there was almost no difference between their effects. Similar results were obtained when phenol diffusion was tested. This demonstrates that the chosen anion membrane did not serve its purpose and the diffusion of phenates had been limited perhaps by the pore size of the membrane.

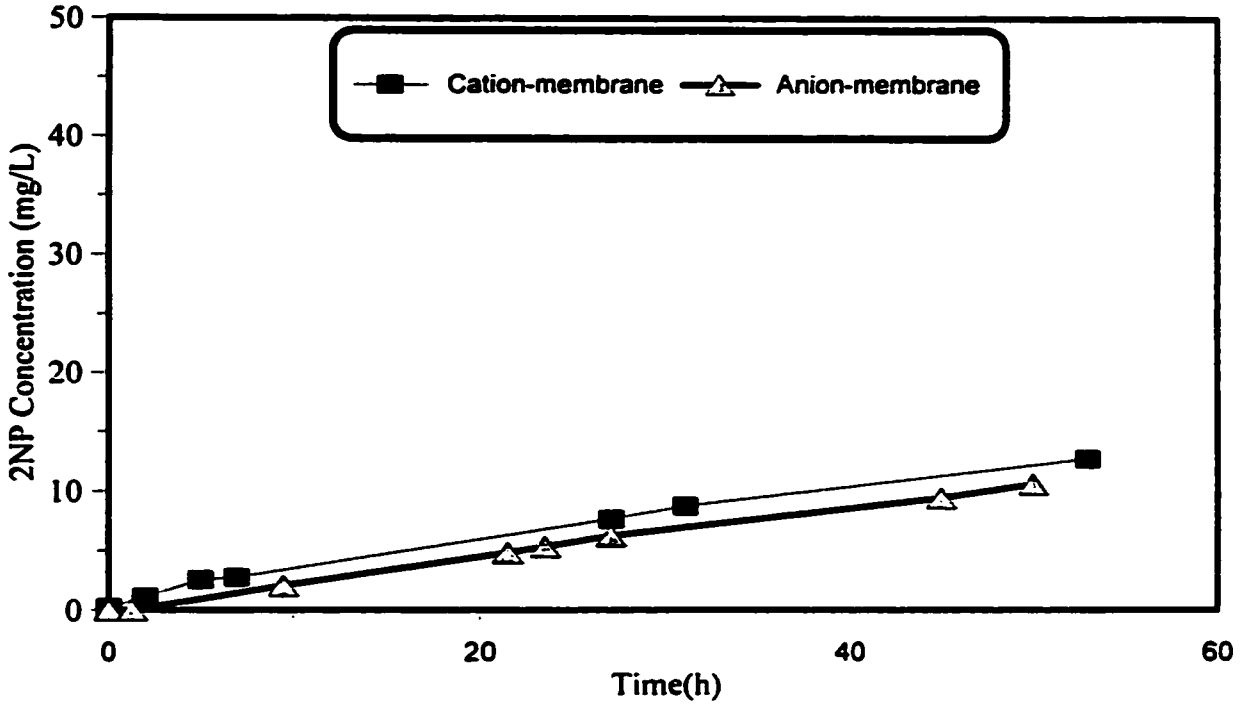

Fig. 7.8 Diffusion of 2NP through membranes at pH 12.

7.4.2 Phenol versus 2NP

The reactivation of F-400 loaded with 2NP and phenol versus time is plotted in Fig. 7.9. This figure shows that 2NP and phenol followed a similar pattern, and increasing the reactivation time increased the reactivation efficiencies. Contrary to Fig. 6.12, the reactivation efficiencies of F-400 loaded with 2NP was up to 20% higher than the reactivation efficiencies of F-400 loaded with phenol. This was consistent with the full reversibility of adsorption of 2NP on F-400 and the partial reversibility of phenol adsorption on F-400. At lower reactivation times both compounds behaved almost the same and their difference appeared at higher reactivation times. This suggests that the reversible portion of the adsorbed phenol is removed from the GAC surface in the early stages of reactivation.

Comparison of the reactivation efficiencies of F-400 loaded with 2NP and phenol after 1 hour of reactivation at different reactivation currents is shown in Fig. 7.10. This figure shows that the results were almost the same and, as expected, higher currents resulted in higher reactivation efficiencies. Similar to Fig. 7.9, Fig. 7.10 shows that in the early stages of reactivation the GAC surface, which adsorbed the partially irreversible phenol, was reactivated and its reactivation was as effective as that adsorbed by fully reversible 2NP.

7.4.3 Impact of Electrolyte Mixing on the Reactivation Efficiency

Fig. 7.11 shows the cathodic reactivation of a monolayer of 2NP-loaded F-400 for different electrolyte flow rates after 2.5 hours of reactivation at 50 mA. Contrary to Fig. 7.2. Fig. 7.11 demonstrates that electrolyte mixing did influence the cathodic reactivation efficiency. The reactivation efficiency decreased with increasing electrolyte flow rates and this was consistent with the previous findings for the phenol solution (Figs. 5.12 and

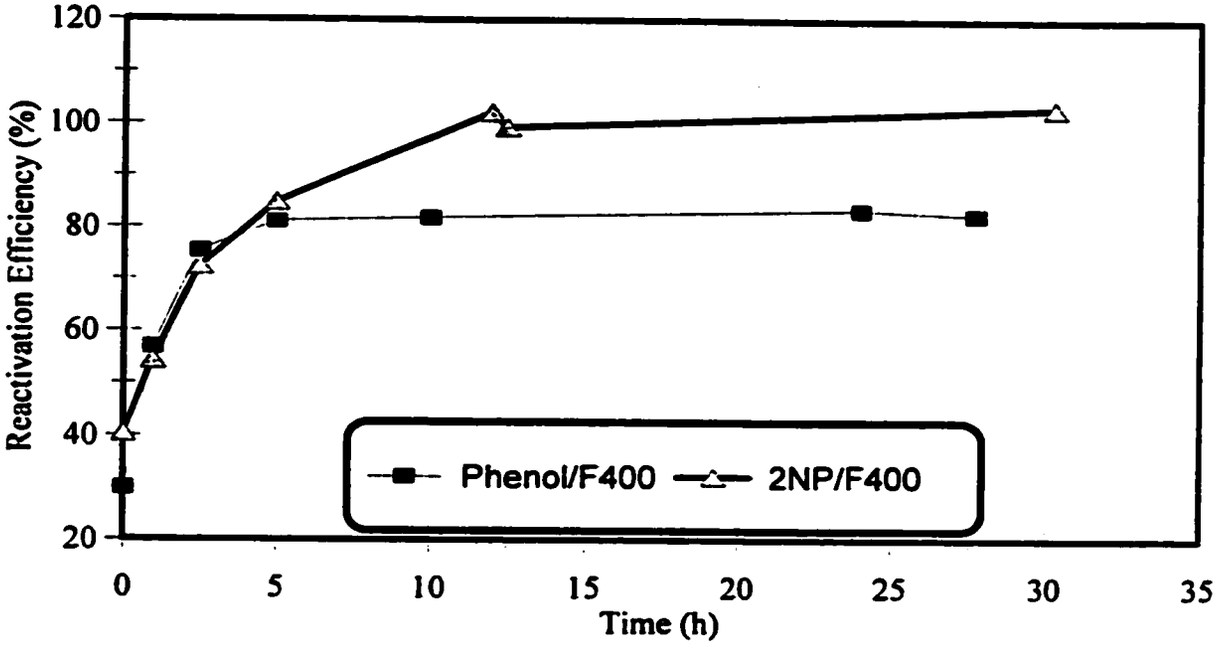

Fig. 7.9 Comparison of cathodic reactivation of 2NP and phenol-loaded F-400 versus time at 50 mA (reloading solutions were buffered).

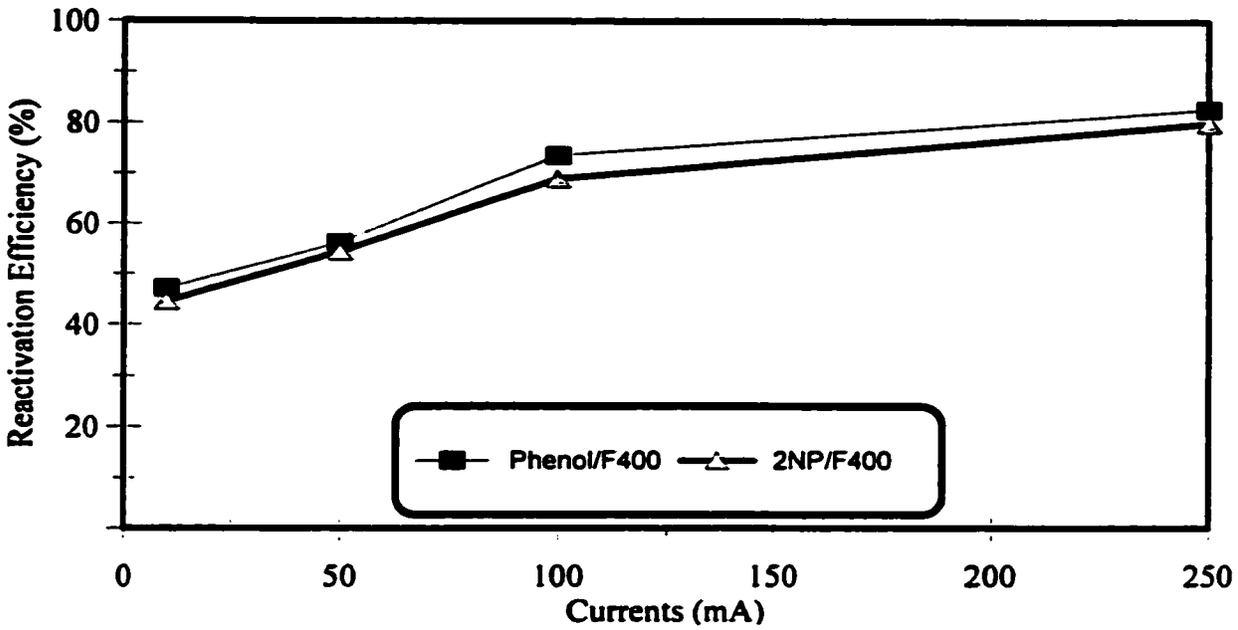

Fig. 7.10 Comparison of cathodic reactivation of 2NP and phenol-loaded F-400 versus current after 1 hour reactivation (reloading solutions were buffered).

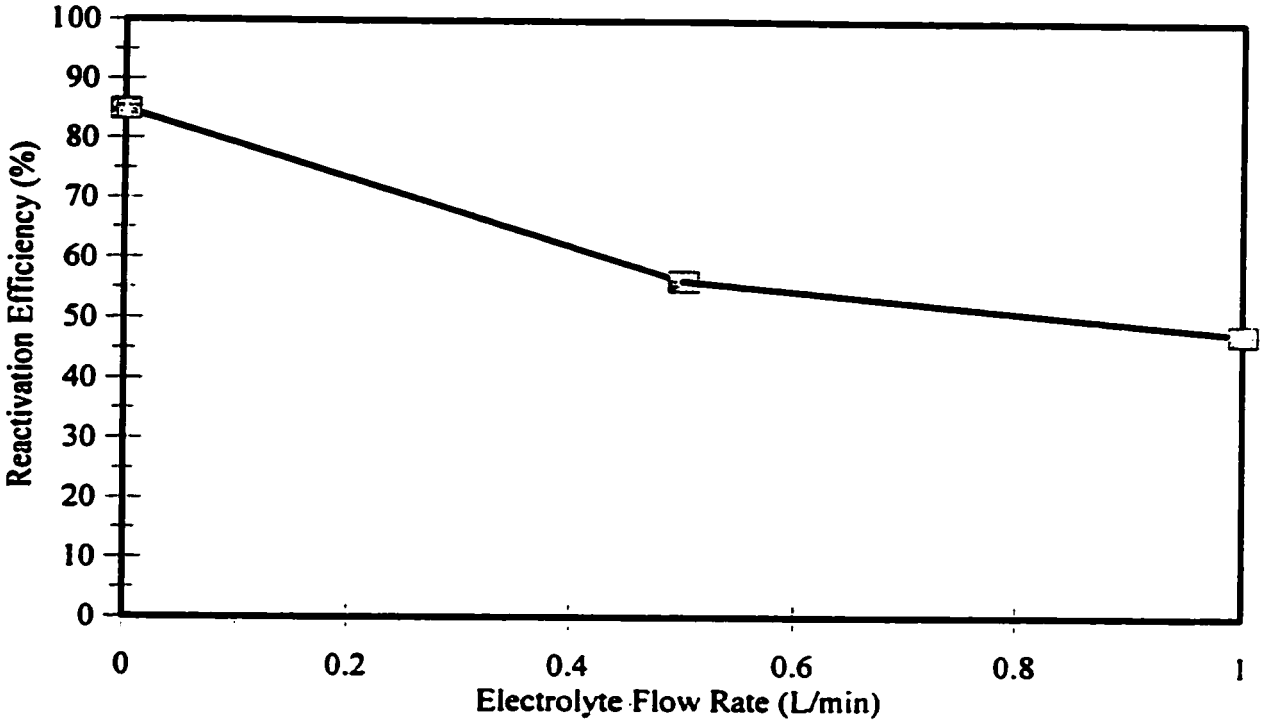

Fig. 7.11 Effect of electrolyte mixing on cathodic reactivation of 2NP-loaded F-400 at 50 mA after 5 hours reactivation (reloading solutions were buffered).

5.17). It was proven in section 5.3 that this phenomenon was caused by the variation of the local pHs at the electrodes. Comparison of Figs. 7.2 and 7.11 shows that buffering of the reloaded 2NP solution did matter, i.e. buffering had eliminated the impact of pH variation of the reloaded solution.

7.4.4 Effect of Current and Time

Experiments on the effect of current and time on the reactivation of GAC were repeated using buffered phenol solutions (pH = 4.5) in the reloading. Fig. 7.12 shows the reactivation efficiencies of phenol-loaded F-400 at various currents and durations. The reactivation efficiency (RE%) could be increased to above 90% by increasing the current and/or time. The effect of current was very marked from 10 to 100 mA but there was no significant difference between 100 and 250 mA. The effect of time shows a similar pattern for the three currents. The RE% increased rapidly with increasing reactivation time in the first 5 hours followed by a more gradual increase for longer times in the cases of 10 and 50 mA. For 100 and 250 mA the reactivation efficiency increased to 92% between 5 and 10 hours of reactivation time, however, for longer reactivation times there was a slight decrease in the reactivation efficiencies. This shows that the surface of the GAC may have been altered at high currents by the longer reactivation times. The maximum 92% reactivation achieved in this study was slightly more than the maximum 88% reported for phenol-loaded GAC with thermal reactivation (Chiang *et al.*, 1997). This shows that electrochemical reactivation can be as effective as thermal reactivation in reactivating phenol-loaded GAC. Considering that thermal reactivation also involves the

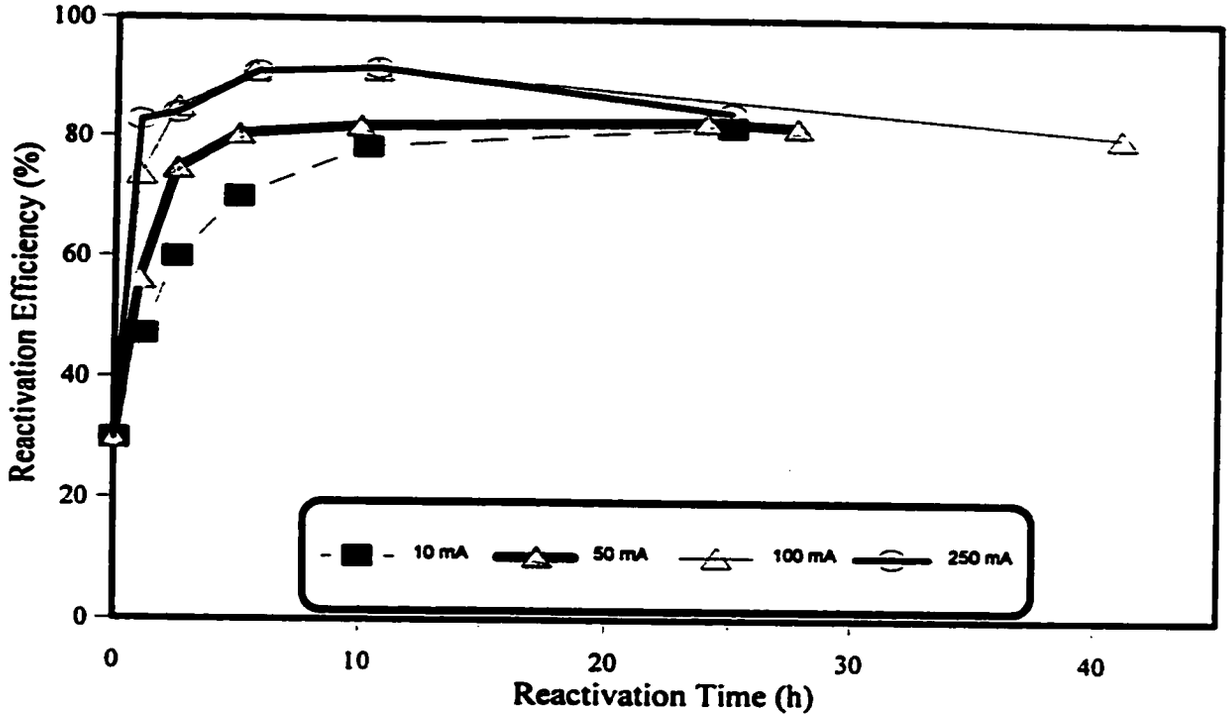

Fig. 7.12 Cathodic reactivation of phenol-loaded F-400 at different currents versus reactivation time (undivided reactor, reloading solutions were buffered).

loss of 5-15% GAC per cycle of reactivation, electrochemical reactivation technology seems to be more promising.

Fig. 7.13 represents the RE% versus the number of coulombs applied. It shows that for the first 500 coulombs, 10 mA produced a higher RE% for the same number of coulombs passed. In addition, all currents resulted in almost the same RE% for the coulombs passed beyond the first 500. However, reactivation at 10 mA (the lowest current tested) yielded only a maximum RE% of 82 after 24 hours (Fig. 7.12). On the other hand, the 10 mA current and up to 15 hours reactivation time could achieve higher coulombic efficiency, that is, with slightly lower energy consumption than other currents. Therefore, the coulombic efficiency for the GAC reactivation was initially dependent on the current/time applied. However, as mentioned earlier a higher current can rapidly oxidize the desorbed contaminant, but it may also alter or reduce the number of adsorption sites.

7.4.5 Effect of Catholyte Volume

One of the mechanisms of electrochemical reactivation of GAC was desorption of the adsorbed contaminant(s). Given that oxidation of the phenolics was not very fast, at the beginning of the experiment there is a temporary accumulation of phenolics in the liquid phase. Increasing the volume of the catholyte in a cathodic reactivation should decrease the phenolic concentration within the catholyte and thus will increase the desorption driving force. To investigate this hypothesis, experiments with different catholyte volumes were conducted. Fig. 7.14 shows the cathodic reactivation efficiency of phenol-loaded F-400 at 50 mA and three different catholyte volumes. This figure indicates that there was no significant difference caused by increasing the catholyte volume. In other words, Fig. 7.14 indicates that

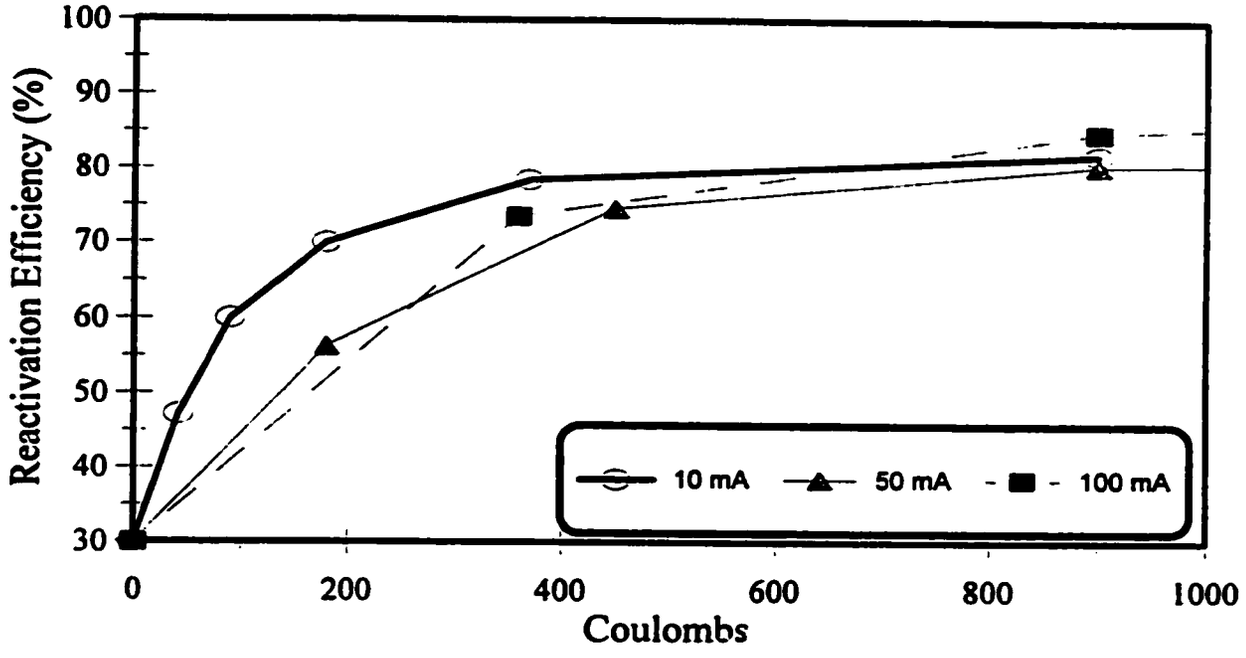

Fig. 7.13 Cathodic reactivation efficiencies of phenol-loaded F-400 at different currents versus charged passed.

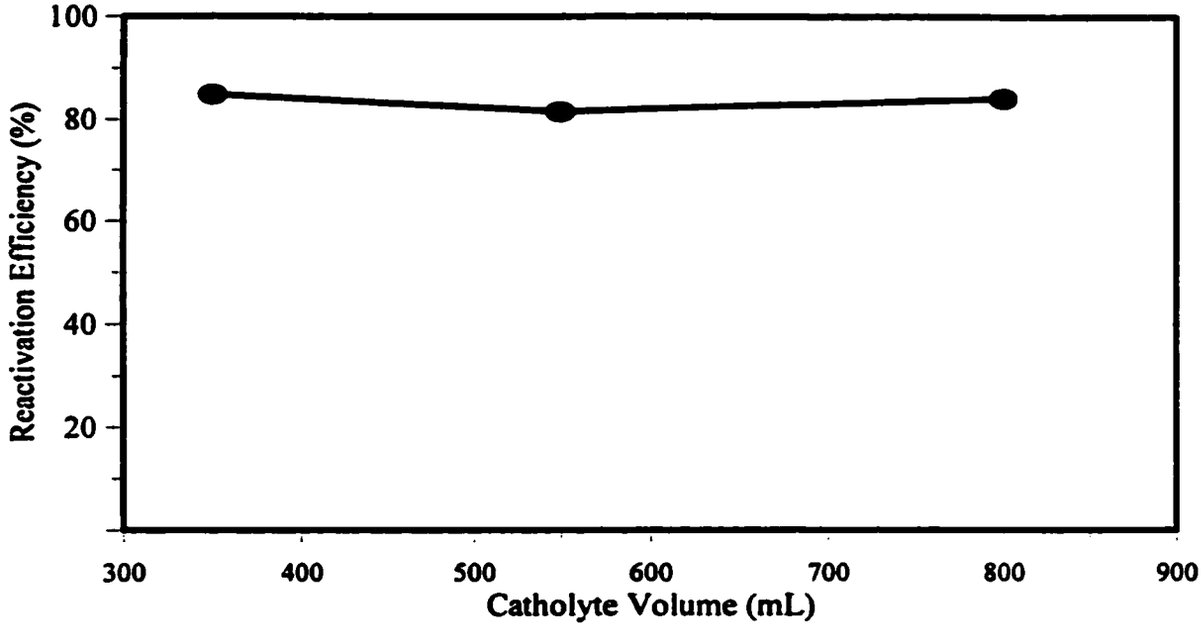

Fig. 7.14 Effect of catholyte volume on cathodic reactivation of phenol-loaded F-400 at 50 mA after 5 hours of reactivation (reloading solutions were buffered).

the desorbed contaminant concentration and/or the by-product concentration of the catholyte does not affect the extent of contaminant desorption, and consequently does not significantly affect the ultimate reactivation efficiency. This shows that the desorption (and consequently the reactivation) is controlled by interior diffusion within the GAC pores rather than by a desorption driving force at the interface.

7.4.6 Effect of NaCl Concentration

The effect of the NaCl concentration on reactivation efficiency was investigated and is shown in Fig. 7.15. The results show that the reactivation increased to 90% when the NaCl concentration increased to 0.5 M (29.25 g/L), but further increases in the NaCl concentration did not improve the reactivation efficiency. However, a further increase in NaCl concentration decreased the 2NP-TOC, non-2NP-TOC, and total-TOC residual concentrations. A possible explanation for these results is that the higher NaCl levels result in the formation of $Cl_2(g)$ which partially dissolves to yield higher levels of HOCl, and OCl^-, which oxidize and/or transform more of the desorbed 2NP. The higher NaCl levels had its disadvantages. The NaCl solution results in the generation of chlorine at the anode. The chlorine reactions with organics may result in production of other toxic compounds such as trihalomethanes (THMs). Hence, one should use a lower NaCl concentration and try to minimize the reactions of chlorine with the organics that may lead to production of other toxic compounds.

7.4.7 Alternative Method to Buffering the Reloaded Solution

From the above experiments it can be concluded that the buffered reloaded solutions resulted in higher reactivation efficiencies than the unbuffered reloaded solutions. This

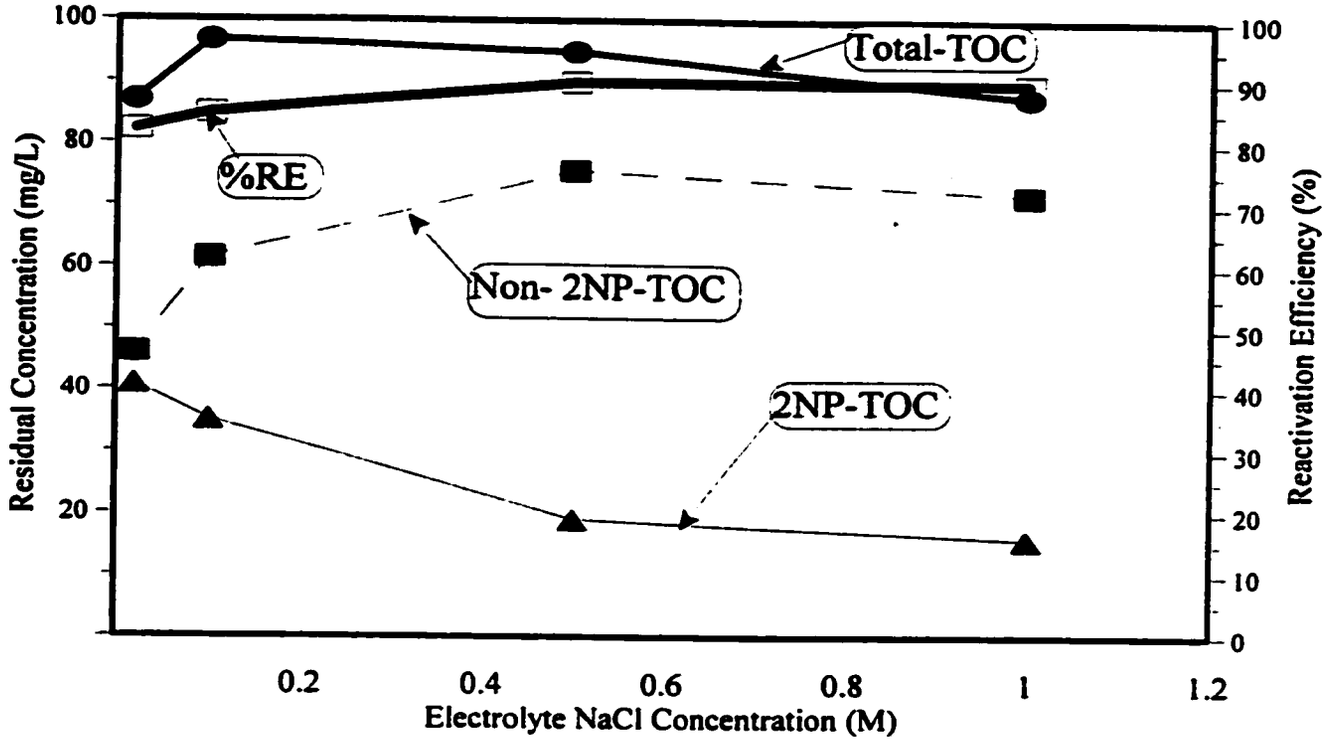

Fig. 7.15 Effect of NaCl concentration on the cathodic reactivation of 2NP-loaded F-400 at 50 mA after 5 hours reactivation (reloading solutions were buffered).

was due to the pH change of the unbuffered reloaded solutions to levels above the pK_as of the compound, while the buffered reloaded solutions limited the pH variation to below the pK_as of the compound. Since buffering of the solution in full-scale applications is not always practical or cost effective, alternative methods need to be investigated. The following alternative methods for the reactivation of 2NP-loaded F-400 at 50 mA for 5 hours were investigated (Fig. 7.16):

A) No treatments were conducted on the reactivated GAC and the reloaded solution was not buffered. The pH of the reloaded solution changed from 5 to 8.5 and the yellow colour of the solution changed to yellow-orange. The reactivation efficiency was about 36%, the lowest among the alternatives investigated.

B) The reactivated GAC particles were soaked in distilled water (DW) for 72 hours and then reloaded with unbuffered solution. The pH of the soaking DW changed from 6.7 to 11.1. The pH of reloaded solution changed from 5 to 7 and the colour of the solution changed slightly from yellow to yellow-orange. The reactivation efficiency was about 57%, about 20% more than the untreated reactivated GAC.

C) No treatments were conducted on the reactivated GAC but the reloaded solution was buffered with 3% phosphate. The pH of the reloaded solution changed slightly from 4.5 to 4.7 and the colour of the solution did not change. The reactivation efficiency was 85%, about 50% more than the untreated reactivated GAC.

D) The reactivated GAC particles were soaked in buffered water, with 3% phosphate (3%-BW), for one hour and then reloaded with unbuffered solution. The pH of the soaking 3%-BW changed from 4.5 to 4.8. The pH of the reloaded solution changed from 5 to 5.85 and the colour of the reloaded solution did not change. The reactivation

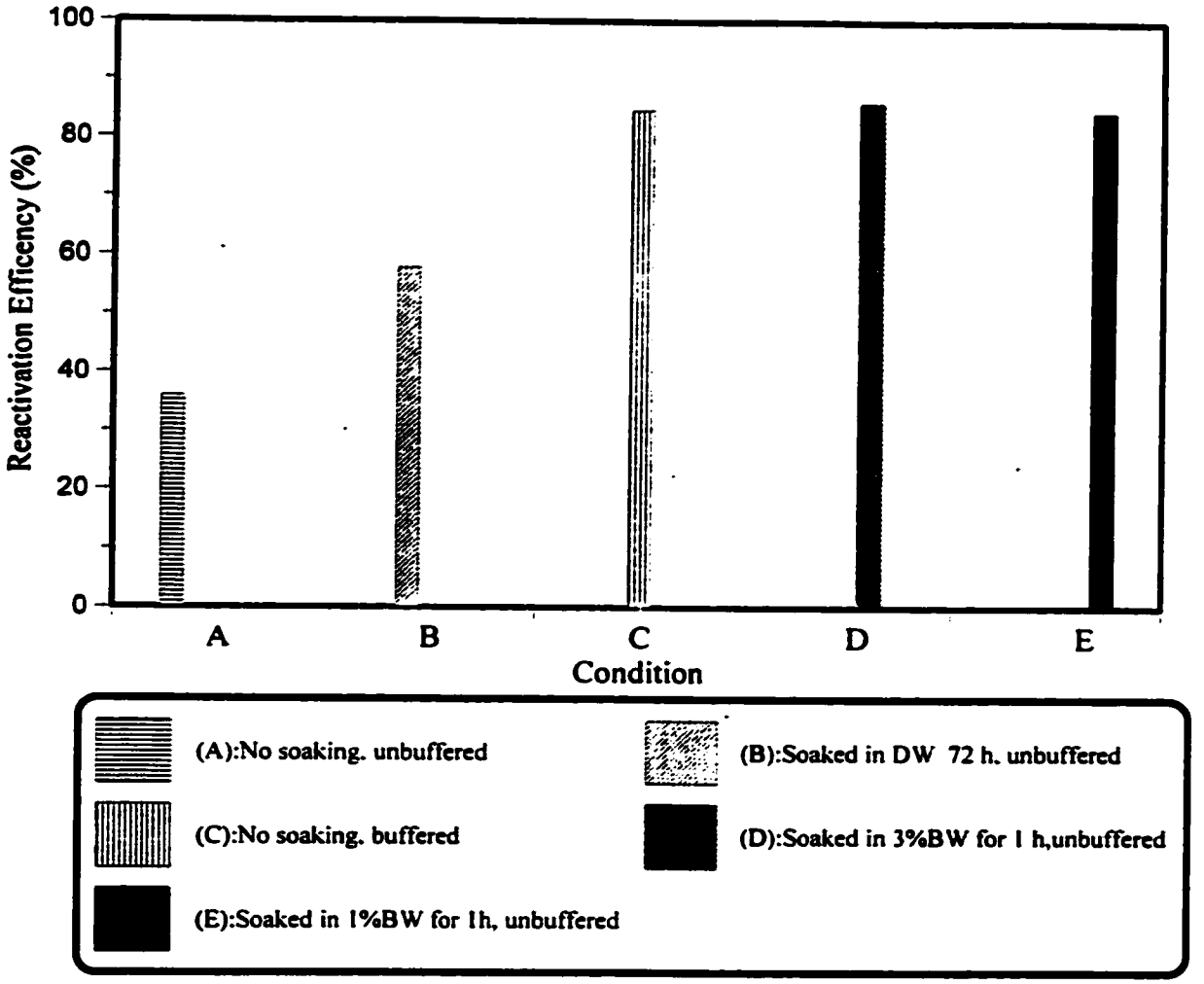

Fig. 7.16 Cathodic reactivation efficiency versus different methods of treatments on the reactivated 2NP-loaded F-400.

efficiency was about 84.5%, almost the same as the GAC reloaded with the buffered solution. Further soaking of the reactivated GAC in the 3% buffered water for 24 and 48 hours did not improve the results.

E) The reactivated GAC particles were soaked in 1% buffered water (1%-BW) for 1 hour and then reloaded with unbuffered solution. The pH of the soaking 1%-BW changed from 4.7 to 5.3. The pH of the reloaded solution changed from 5 to 6 and the colour of the reloaded solution did not change. The reactivation efficiency was about 84%, almost the same as the GAC treated with 3%-BW and the GAC reloaded with buffered solution.

Fig. 7.16 demonstrates that soaking of reactivated GAC in 1% buffered water for as little as 1 hour can result in a reactivation efficiency as high as those obtained by buffering the reloaded solution. This proves that one alternative method to buffering the reloaded solution is the treatment of reactivated GAC before the reloading process by soaking it in buffered water.

7.5 Conclusions

- Some questionable results were described, and the potential reasons were investigated. It was proved that the residual high pH water within the pores of the electrochemically reactivated GAC raised the pH of the reloading solution beyond the pK_a of the contaminants and consequently affected the reloading capacity of GAC and the associated reactivation efficiency. Buffering of the reloaded solution eliminated the impact of pH variation of the reloaded solutions.

- The key experiments that were repeated with buffered reloading solutions resulted in higher reactivation efficiencies than those using unbuffered reloading solutions.
- Comparison of the results showed that cathodic reactivation was more efficient than anodic reactivation. It was also observed that the reactivation of 2NP-loaded GAC was higher than the phenol-loaded GAC. Maximum reactivation of 2NP-loaded F-400 was 108% and that of phenol-loaded F-400 was 90%.
- The electrolyte flowrate decreased the reactivation efficiency of 2NP-loaded F-400 by 30%.
- The tested electrolyte volume did not significantly affect the reactivation efficiencies. Thus it appears that the resulting lower liquid phase concentrations did not seem to have a significant impact on the extent of desorption and reactivation.
- Increases in the NaCl electrolyte concentration to 0.5 M increased the reactivation efficiency but further increases in NaCl concentration did not significantly affect the results. Alternative methods to buffering of the reloading solution were investigated.
- It was shown that soaking the reactivated GAC in buffered water for a period of one hour is a good alternative to buffering the reloading solution.

CHAPTER 8

ELECTROLYTE POST-TREATMENT

8.1 Introduction

Associated with the electrochemical reactivation of GAC is desorption of contaminant from the loaded GAC and the potential for producing by-products from the desorbed organics. These by-products could be different depending on the organics available for reaction in the reactivation reactor. To avoid environmental pollution, the desorbed contaminant and its by-products must be destroyed before the discharge or reuse of the electrolyte. Thus, the contaminated electrolyte must be treated to reach a minimal TOC.

In this chapter the concentration of desorbed contaminants during the electrochemical reactivation of GAC was studied. Also the feasibility of the destruction of phenol and 2NP (without GAC) in the undivided reactor, and in the anolyte and catholyte of the divided-cell reactor was studied. Kinetics of the destruction at both electrodes were measured and the rates of contaminant destruction at the electrodes were determined for possible use in modelling.

8.2 Monitoring of Desorbed Contaminants

8.2.1 Aesthetic Observations and pH measurements

Tables 8.1, 8.2, and 8.3 present the observations during the cathodic reactivation of GAC loaded with phenol, 2NP, and NOM, respectively. A chlorine odour was produced during the experiments. Reactivation caused the electrolyte in both compartments to change colour during the reactivation process. The colour and its intensity were proportional to

Table 8.1 Observations during cathodic reactivation of 1.2 g of F-400 loaded with phenol.

I (mA)	Reactivation Time (h)	NaCl (Mole)	Electrolyte Flow Rate (L/min)	Δv (Volts)	Anolyte		Catholyte		Mixed Electrolyte	
					pH	Color	pH	Color	pH	Color
10	1.2	0.1	0	2.1	3.5	colorless	6	colorless	3.7	colorless
10	10.3	0.1	0	2.8	2.9	very light yellow	10.7	very light brown	3.3	very light yellow
10	25	0.1	0	2.8	2.5	light brownish	11.9	light brown	3.2	light brown
50	2.3	0.1	0	3.3	2.7	light yellow	11.5	colorless	3.2	very light yellow
50	24	0.1	0	3.4	2.6	yellow	11.8	brown	3.7	brown
50	5	0.5	0	3.1	2.4	yellow	12	light brown	3.3	brown
50	5	0.1	0	3	3.1	yellow-brownish with 1 cm white foam on top	10	dark brown	3.8	dark brown
50	5	0.1	0.5	2.8	NA	colorless	NA	colorless	3.5	Colorless
50	5	0.1	1	2.3	NA	colorless	NA	colorless	3.5	Colorless
100	1	0.1	0	3.5	2.6	very light yellow	11.3	very light brown	3.3	very light yellow-brownish
100	5.5	0.1	0	3.6	2.6	yellow-brownish	11.4	brown	3	light brown
100	10.6	0.1	0	3.8	2.6	yellow brownish	11.25	brown	3.6	light brown
100	41	0.1	0	4	2.7	colorless	12.1		5.5	light brown
250	1	0.1	0	4.5	2.6	colorless	11.4	light brown	3.1	light brown
250	5.75	0.1	0	4.6	2.5	light brown	11.75	dark brown	3.1	brown
250	10.75	0.1	0	4.3	2.4	very light white-yellowish with 2.5 cm white foam on top	12	dark brown	3.3	brown
250	25	0.1	0	4.3	6.1	colorless	12.2	colorless	9.6	colorless

Table 8.2 Observations during cathodic reactivation of 1 g of F-400 loaded with 2NP.

I (mA)	Reactivation Time (h)	NaCl (Mole)	Electrolyte Flow Rate (L/min)	Δv (Volts)	Anolyte		Catholyte		Mixed Electrolyte	
					pH	Color	pH	Color	pH	Color
50	0	0.1	0	3	5.6	yellow-greenish	5.6	yellow-greenish	5.6	yellow-greenish
50	0.5	0.1	0	3	3.2	yellow	8	yellow	4.5	yellow-orange
50	2	0.1	0	3	2.8	yellow-orange	11.3	yellow	4.2	yellow-orange
50	3.5	0.1	0	3	2.5	yellow-orange	11.5	yellow	4	orange
50	6.5	0.1	0	3	2.2	yellow-orange	11.8	yellow-greenish	3.9	dark orange
50	10	0.1	0	3	2.1	orange	11.7	yellow-greenish	3.8	dark orange
50	18	0.1	0	3	2	red	11.8	green	3.7	dark red
50	23	0.1	0	3	2	orange	11.8	dark green	3.7	Light red
50	26	0.1	0	3	2	yellow-orange	11.9	dark green	3.7	Light red
50	31	0.1	0	3	2	yellow	11.9	dark green	3.5	yellow
50	44	0.1	0	3	2	yellow-	12	dark green	3.5	yellow
50	53	0.1	0	3	2	colorless	12	green-yellow	3.4	light yellow
50	67	0.1	0	3	2	colorless	12	light yellow	3.4	light yellow
50	79	0.1	0	3	2	colorless	12.1	very light yellow	3.3	very light yellow
50	90	0.1	0	3	2	colorless	12.1	colorless	3.3	colorless

Table 8.3 Observations during cathodic reactivation of 5 g of F-400 loaded with 2NP.

I (mA)	Reactivation Time (h)	NaCl (Mole)	Electrolyte Flow Rate (L/min)	Δv (Volts)	Anolyte		Catholyte		Mixed Electrolyte	
					pH	Color	pH	Color	pH	Color
50	5	0.1	0	3.35	2	colorless	11.4	light yellow	3	slightly turbid
50	10	0.1	0	3.3	1.9	colorless	11.7	yellow with some visible white particulate, some GAC particles turned brown	3.4	slightly turbid, some visible white particulates, some GAC particles turned brown
50	18	0.1	0	3.4	1.95	colorless	11.9	yellow with a few visible white particulates, some GAC particles turned brown	5.3	turbid, some visible white particulates, some GAC particles turned brown
50	25	0.1	0	3.4	1.9	colorless	11.95	yellow with some visible white particulates, some GAC particles turned brown	6.8	turbid, some visible white particulates, some GAC particles turned brown
10	16	0.1	0	2.8	2.4	colorless	8.1	slightly turbid, very small visible white particulates	2.6	slightly turbid, very small visible white particulates
100	5	0.1	0	3.8	2.2	colorless	11.7	yellow with some visible white particulates, some GAC particles turned brown	3.7	turbid, some visible white particulates, some GAC particles turned brown
200	7	0.1	0	4.5	3.3	colorless	12.1	Very light yellow, some visible white particulates	7.1	turbid, some visible white particulates, some GAC particles turned brown

the applied current and time. With longer reactivation times and/or higher currents the colour eventually disappeared. As Table 8.1 shows with a 250 mA current, the electrolyte was colourless after 25 hours. Cathodic reactivation of virgin carbon did not yield a coloured electrolyte. Hence, the colour was presumably due to the by-product compounds (such as, possibly, catechol, p-benzoquinone, hydroquinone, ...) formed during the oxidation of desorbed contaminants (phenol, 2NP, or NOM)..

Cen (1994) observed a similar phenomenon during the electrochemical reactivation of F-400 loaded with phenol. Owen and Barry (1972) also observed a similar phenomenon for a brine solution electrolyte; it became a dark red-brown colour, and slightly opaque. An attempt was made to identify the by-products. Several samples were sent to the GCMS laboratory of the Department of Chemistry of the University of Ottawa for analysis. Unfortunately the analysis could not identify the by-products.

It was observed that the desorbed contaminants and their by-products were adsorbed on the surfaces of the electrodes. Usually a thin layer of brownish material covered the surface of the electrodes. The amount of adsorption of the contaminants and their by-products onto the surfaces of the electrodes was proportional to the applied current and time. At low currents and/or short reactivation times (i.e., current <30 mA, time<5h) the adsorption of the contaminants and their by-products on the surfaces of the electrodes was not noticeable. At moderate currents and/or medium reactivation times (i.e., current of 50 mA and 100 mA, 5<time<15h) the adsorption of materials on the surfaces of both electrodes was visible. At higher currents and/or longer times (i.e., current of 200 mA and higher, time>15h), the adsorption of materials on the anode surface was not visible while

their adsorption on the surface of the cathode was more noticeable. To avoid the possible impact of the adsorbed material on the reactivation efficiency, i.e., fouling, the electrodes were acid washed prior to each experiment.

The variation of pH of the catholyte and anolyte, as well as the pH of the mixed electrolyte, is shown in Tables 8.1, 8.2, and 8.3. The pH and its variation were proportional to the applied current and time. The pH of the catholyte increased to about 12 and that of the anolyte decreased to about 2. The pH of the final mixed electrolyte varied between 3 and 4. In practical application of the electrochemical technology, the pH of the mixed electrolyte would have to be adjusted before discharge or reuse of the electrolyte.

8.2.2 Residual Concentration in the Electrolyte

Fig. 8.1 shows the effect of time and current on the concentration of the residual phenol during cathodic reactivation of phenol-loaded WV-B in an undivided reactor without mixing. The concentrations were measured at the end of each experiment. For all the currents, the phenol concentration increased over time until it reached a peak and then decreased over time. The rising part of the curves shows that the rate of phenol desorption from loaded-GAC was higher than the rate of destruction of phenol, while the falling part of the curve shows that the rate of phenol desorption was lower than the rate of phenol destruction. Fig. 8.1 also shows that the time required to reach the maximum phenol concentration decreased as the current density increased. This was consistent with the fast pH increase of electrolyte at high current (Table 8.1) and the higher oxidizing power of higher current densities.

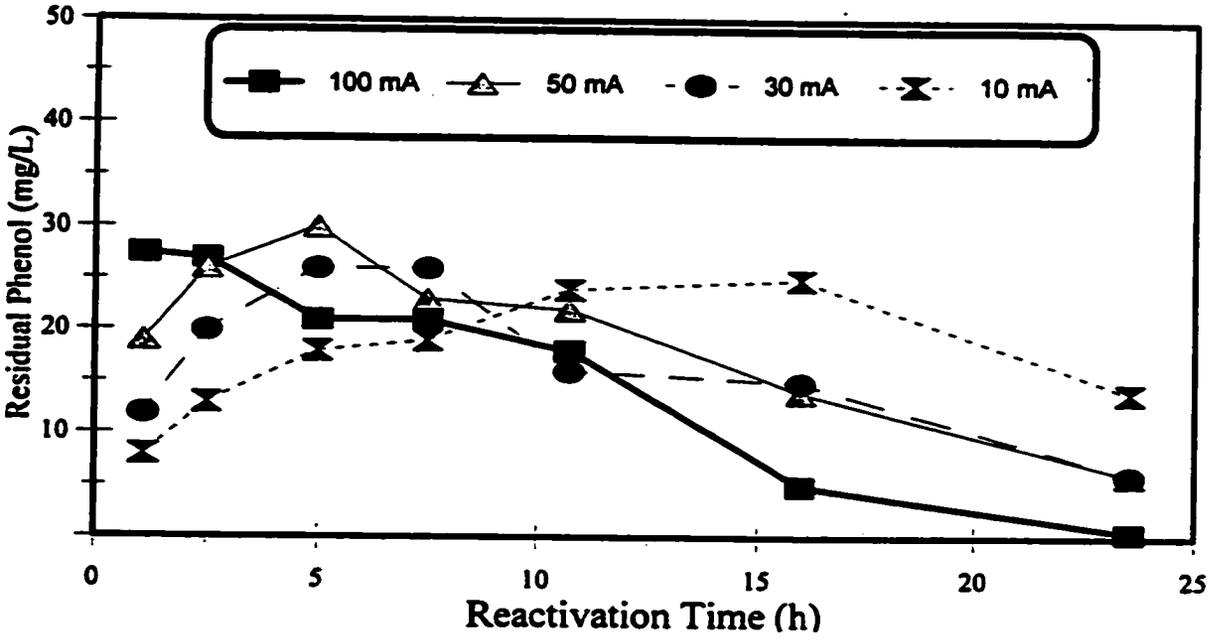

Fig. 8.1 Effect of reactivation time and current on residual phenol during cathodic reactivation of phenol-loaded WV-B (unmixed, undivided reactor).

Fig. 8.2 shows the effect of time and current on the concentration of residuals as total TOC (including phenol) during cathodic reactivation of phenol-loaded WV-B in an undivided reactor without mixing. Similar to phenol, the TOC concentration increased over time until it reached a peak and then decreased over time. However the rate of TOC destruction was much slower than the rate of phenol destruction and the times of the peaks appeared to lag behind those for phenol.

The most effective residual destruction was observed during the 100 mA tests. Fig. 8.3 shows the residual concentration as total-TOC, phenol-TOC, and the non-phenol-TOC versus time. During the cathodic reactivation of phenol-loaded WV-B the concentration of the residual phenol TOC increased from 0 to 20 mg/L in the first hour of the reactivation because the rate of desorption of phenol from GAC was higher than its rate of destruction. After the first hour the concentration of phenol-TOC decreased which shows that the rate of phenol destruction was higher than its rate of desorption. Fig. 8.3 also shows that longer reactivation times reduced the phenol residual in the electrolyte to undetectable levels (<0.1 mg/L) after 24 hours. At this point all the residual phenol had been transformed to by-products and the concentration of non-phenol-TOC equaled the total-TOC concentration. As Fig. 8.3 indicates the rate of complete oxidation of by-products to CO_2 was very slow and a higher current and/or longer times were needed to bring the total TOC concentration to zero.

Results of different current experiments after 7.5 hours of cathodic reactivation of phenol-loaded F-400 within the undivided-cell reactor (not mixed) are presented in Fig. 8.4. Increasing the current to 100 mA enhanced the reactivation efficiencies. Increasing

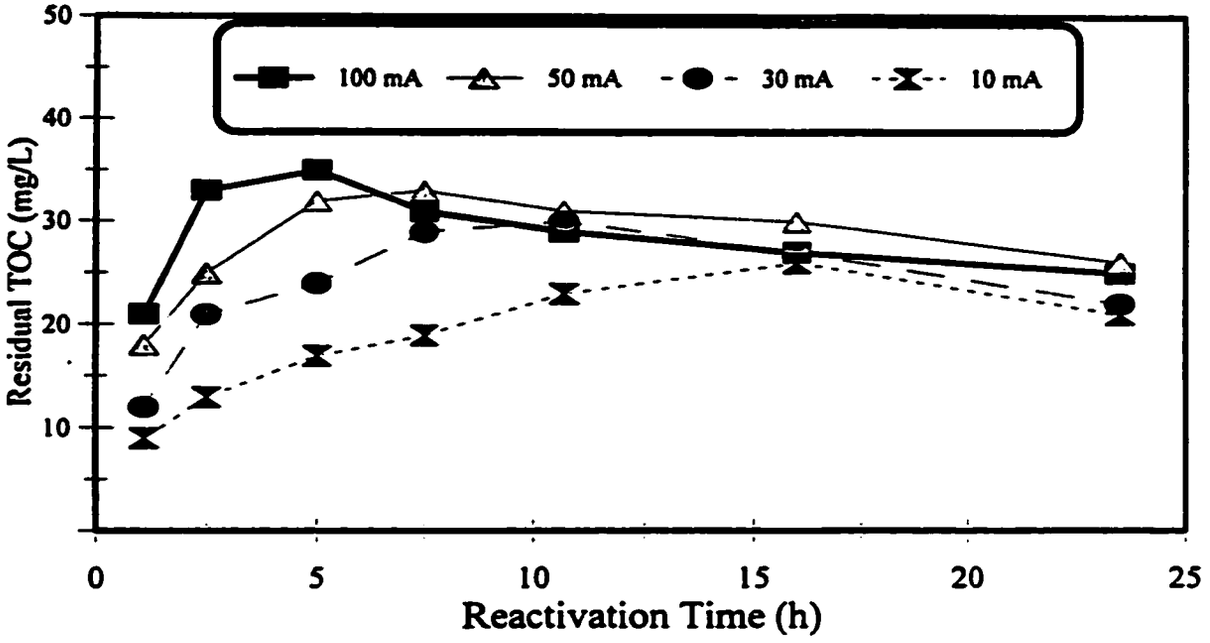

Fig. 8.2 Effect of reactivation time and current on residual TOC during cathodic reactivation of phenol-loaded WV-B (unmixed, undivided reactor).

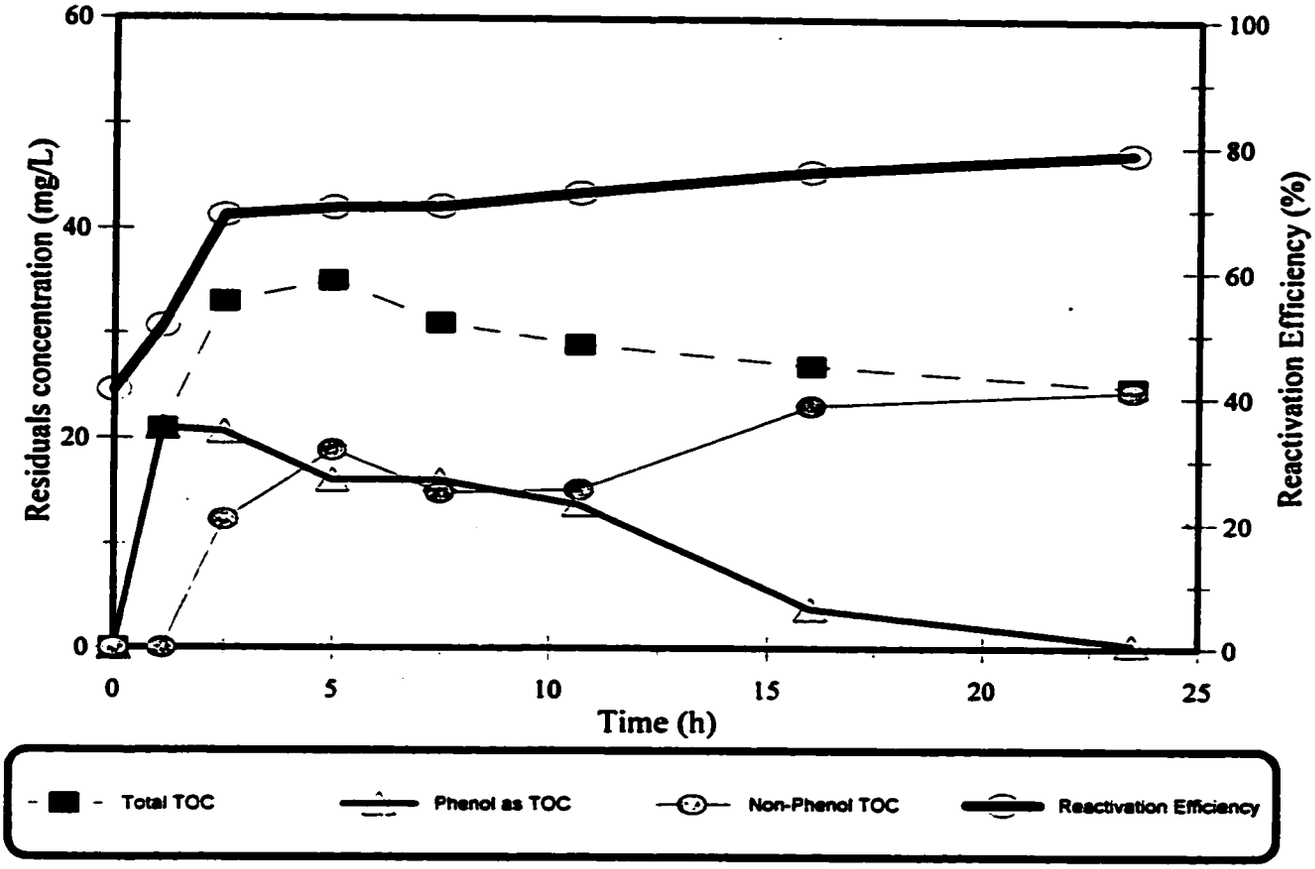

Fig. 8.3 Residuals concentration versus reactivation time during cathodic reactivation of phenol-loaded WV-B at 100 mA (unmixed, undivided reactor).

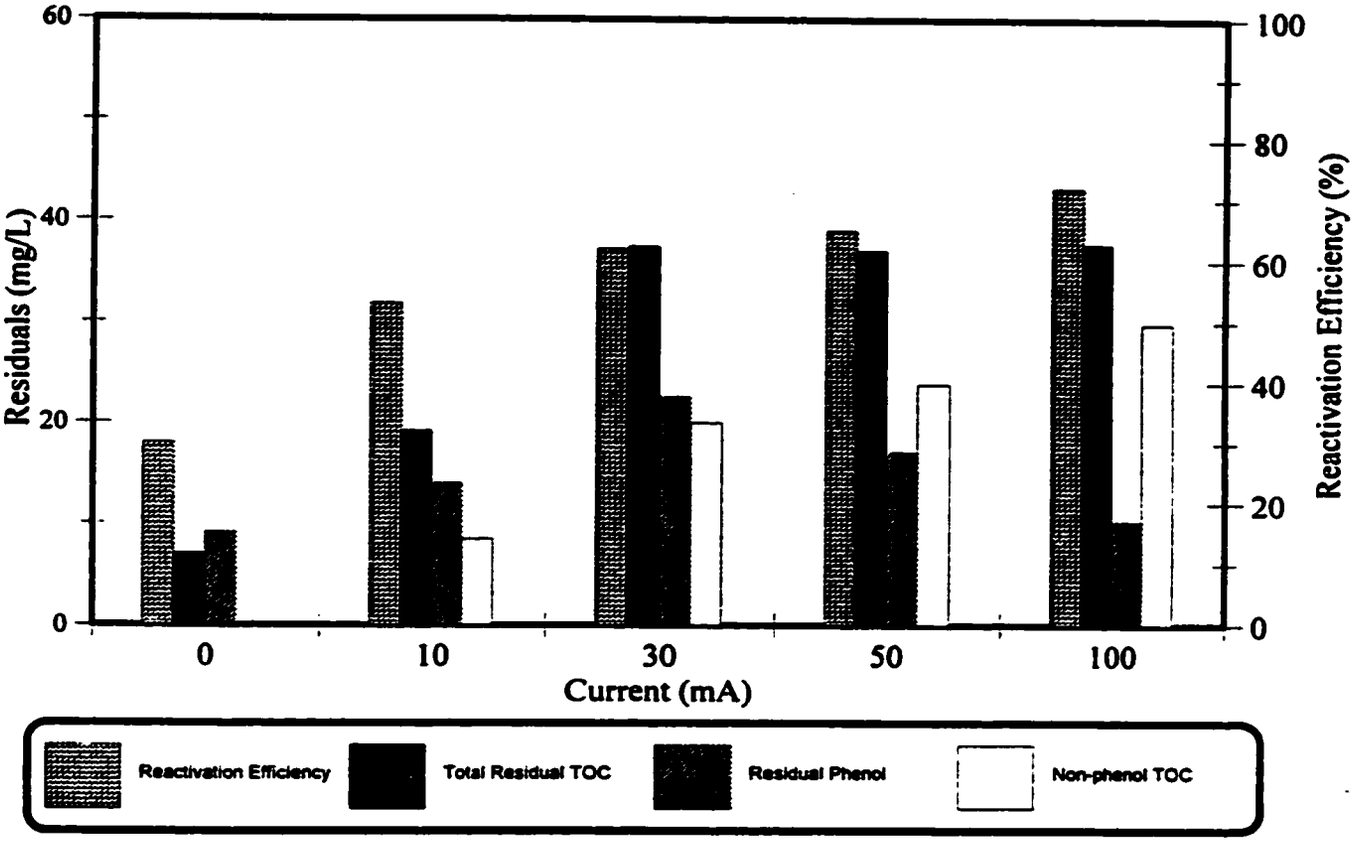

Fig. 8.4 Effect of current on residuals concentration during cathodic reactivation of phenol-loaded F-400 after 7.5 hours of reactivation (unmixed, undivided reactor).

the current to 30 mA increased the residual phenol and total residual TOC. This implies that rate of desorption of phenol from GAC was higher than its rate of destruction. For currents more than 30 mA the concentration of residual phenol decreased but the total TOC concentration did not change. This shows that the rate of phenol destruction was higher than its rate of desorption and the rate of total TOC destruction is almost the same as total TOC production. Thus high currents were more efficient at destroying phenol in the electrolyte than low currents. This is attributable to the high oxidizing power of higher currents. It can be observed from Fig 8.4 that to destroy all of the residual phenol, the current has to be significantly larger or longer reactivation times need to be used. Fig. 8.4 also shows that increasing the currents increased the non-phenol TOC. This shows that the rate of phenol transformation to by-products is more than the rate of by-products destruction. Thus the rate of complete oxidation of by-products to CO_2 was very slow and higher currents and/or longer times were needed to bring the TOC concentrations to zero.

Fig. 8.5 presents analogous results for 2NP-loaded F-400. The 2NP-TOC, non-2NP-TOC and total-TOC curves followed similar patterns to those in Fig. 8.3. The concentration of residual 2NP-TOC increased from 0 to 35 mg/L in the first 5 hours of reactivation because the desorption rate of 2NP from GAC was higher than its rate of destruction. After 5 hours the concentration of 2NP TOC decreased which shows that the rate of 2NP oxidation was higher than its rate of desorption. Fig. 8.5 also shows that longer reactivation times reduced the 2NP residual in the electrolyte to about 15 mg/L after 30 hours. At this point most of the residual 2NP has been transformed to by-products, the concentration of non-2NP-TOC was about 70 mg/L and the total TOC has decreased to

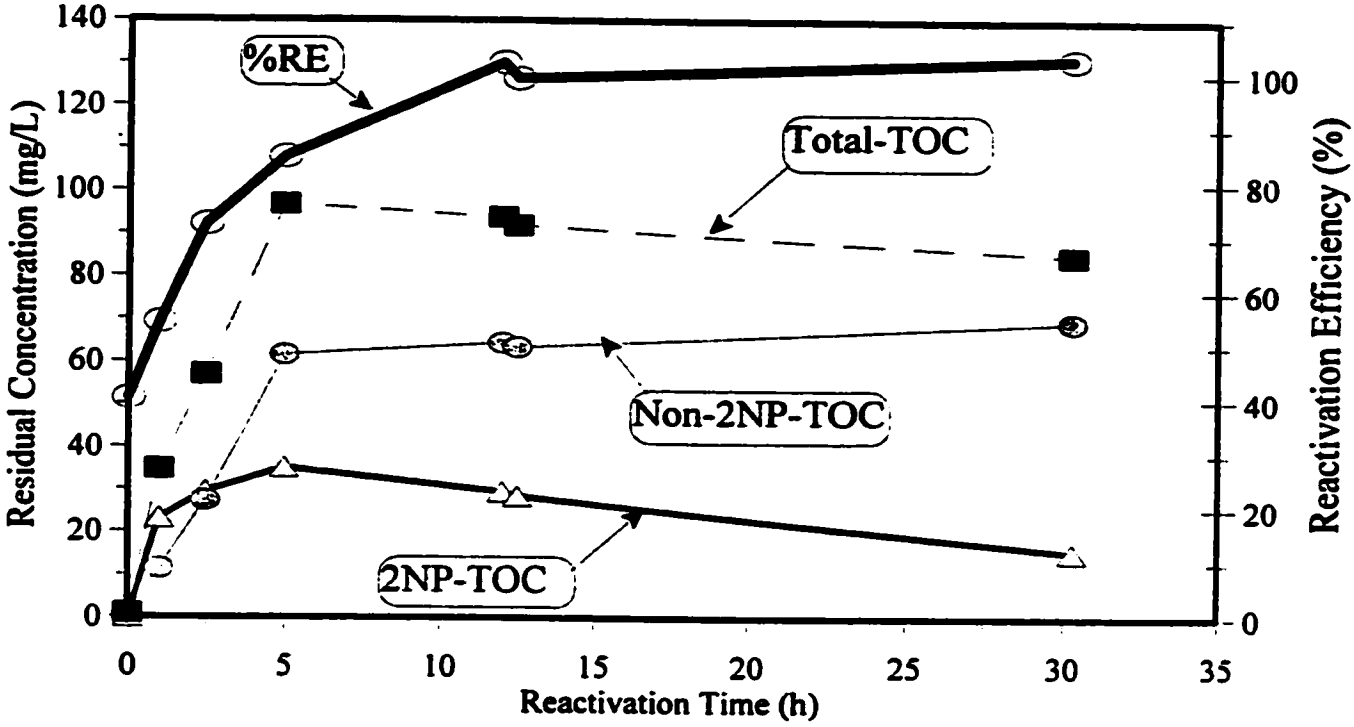

Fig. 8.5 Effect of reactivation time on residuals concentrations during cathodic reactivation of 2NP-loaded F-400 at 50 mA.

85 mg/L. As Fig. 8.5 indicates the rate of oxidation of by-products to CO_2 was very slow and a longer time and/or higher current are needed to convert all the TOC to CO_2.

Fig. 8.6 shows the residuals concentration at different currents after 1 hour of reactivation. Increasing the current to 100 mA increased the residual concentration which means that the rate of 2NP desorption was higher than the rate of its transformation to by-products. At 250 mA the 2NP-TOC concentration decreased to about 17 mg/L, the non-2NP-TOC increased to about 42 mg/L, and the total TOC concentration decreased slightly. This implies that the rate of 2NP destruction/transformation was higher than the rate of its desorption and a higher current and/or longer times are needed to bring the total TOC concentration to zero.

Since high currents and long reactivation times contribute to the destruction of all the residual phenol/2NP and oxidation of by-products, one could possibly take the reactivated GAC out of the reactor, and then increase the current for a certain period to electrochemically oxidize the contaminated electrolyte before discharge or reuse. This hypothesis is investigated in section 8.3.2.

8.2.4 Gas Production

Gas production during the 50 mA cathodic reactivation of 1.1 g of F-400, WV-B, and Darco loaded with phenol was measured and is plotted in Fig. 8.7. Gas generation was highest for WV-B and lowest for F-400 reactivation. Fig. 8.8 shows the gas generation of the different masses of GAC after 5 hours of reactivation at 50 mA. As the GAC mass increased the gas generation decreased. Increasing the mass of GAC results in higher GAC surface area and consequently lowers the current density (current/surface area) at

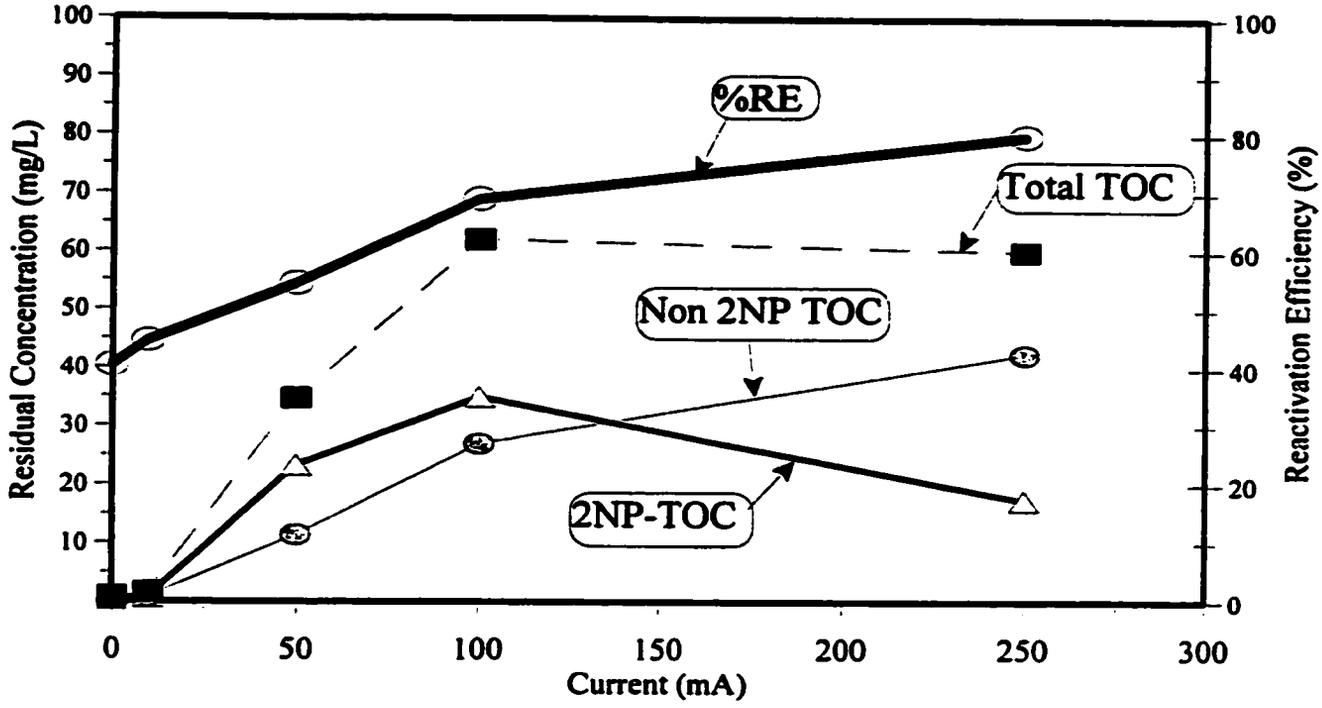

Fig. 8.6 Effect of current on residuals concentration during cathodic reactivation of 2NP-loaded F-400 after 1 hour of reactivation (unmixed, undivided reactor).

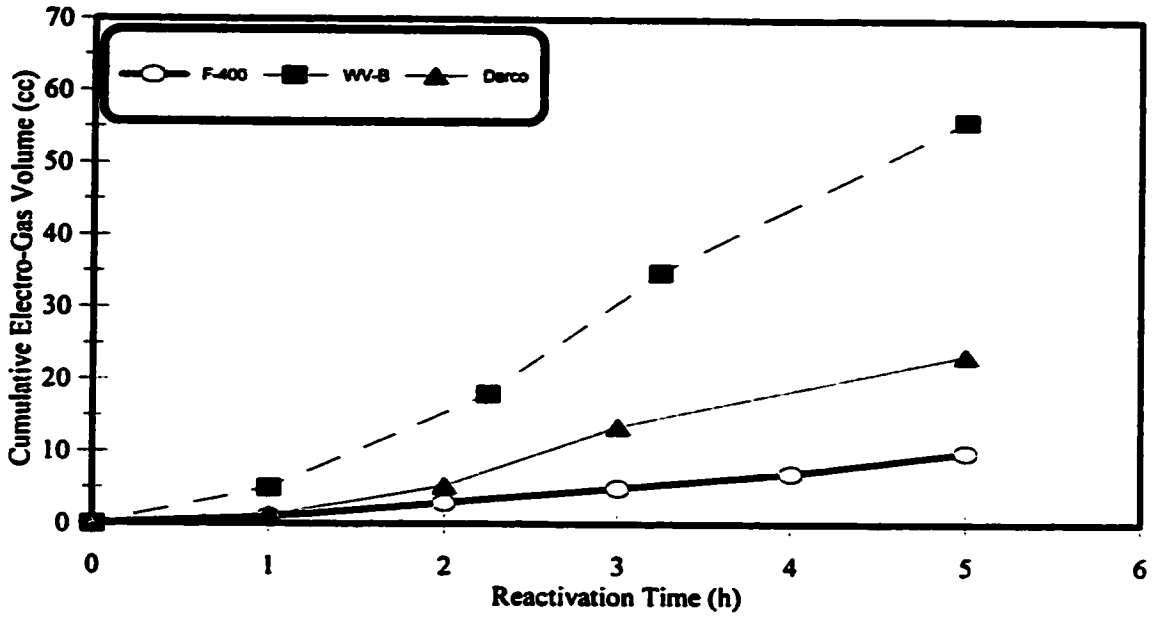

Fig. 8.7 Cumulative electro-gas volume versus reactivation time during cathodic reactivation of 1.1 g of phenol- loaded GACs at 50 mA.

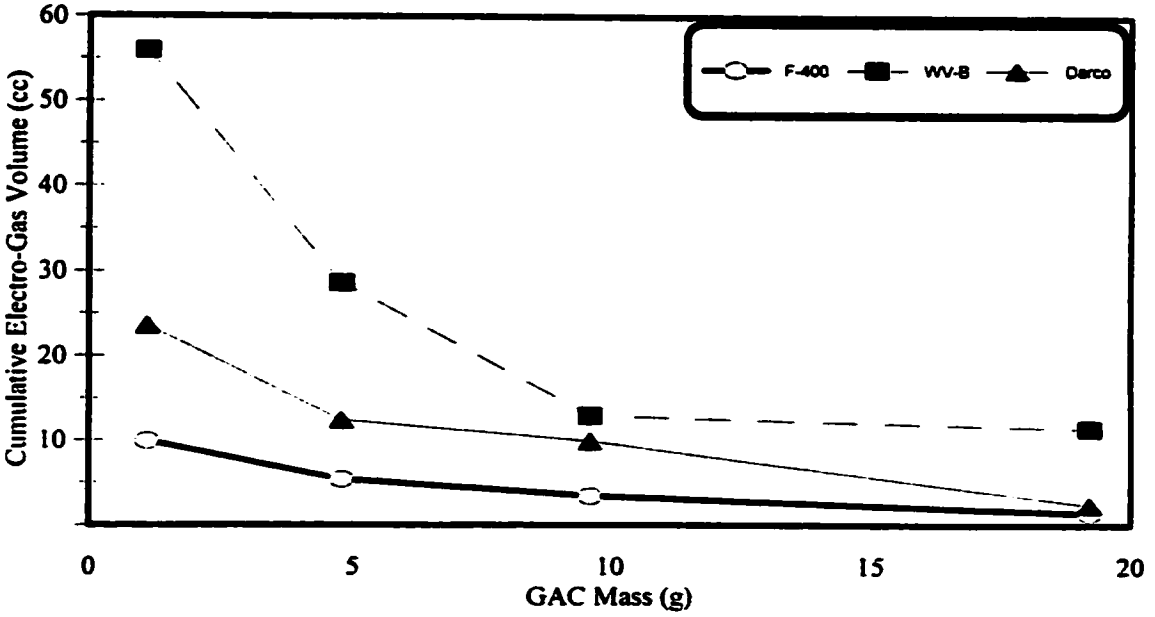

Fig. 8.8 Cumulative electro-gas volume versus GAC mass during cathodic reactivation of phenol-loaded of GACs at 50 mA.

the cathode. Lower current density decreases the side reactions responsible for gas generation.

An attempt was made to analyze the gas generated within the electrochemical reactor. Gas samples were collected from both electrodes after 5 hours of reactivation at 50 mA and were analyzed for CO_2, N_2, and CH_4. Only N_2 was detectable. It is possible that the low current (50 mA), applied in most of the tests within the current study, was the reason for the incomplete phenol oxidation and undetectable CO_2 level.

Although O_2, H_2 and Cl_2 gases were produced because of the side reactions at the electrodes, their concentrations were not measured in this investigation due to time and equipment limitations.

8.3 Feasibility of Contaminant Destruction

The following presents the oxidation of phenol and 2NP without the presence of GAC.

8.3.1 Destruction of Phenol

Fig. 8.9 shows the disappearance of phenol and TOC from a phenol solution (without GAC) in the full reactor (undivided-reactor and electrolyte flow rate of 0.2 L/min) at 50 mA current in a 0.1 M NaCl electrolyte as a function of time. The TOC measurements coupled with phenol analysis provide an indication of the extent of oxidation beyond phenol removal without the need to analyze for the many possible partially oxidized species (products). Fully oxidized carbon would be either expelled from the electrolyte as CO_2 under acidic conditions or be measured as inorganic carbon under alkaline conditions (Smith De Sucre and Watkinson, 1981). Fig. 8.9 shows that the TOC concentration decreased gradually with

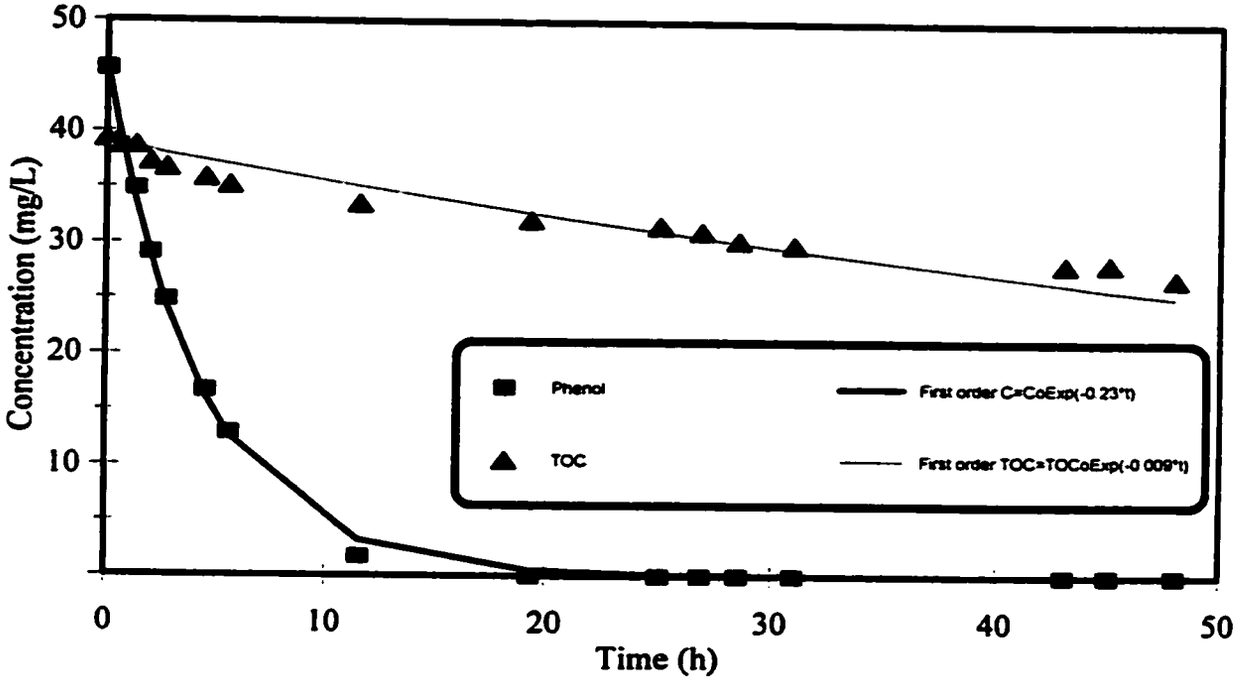

Fig. 8.9 Destruction of phenol in undivided-cells reactor without GAC at 50 mA (electrolyte flow rate = 0.2 L/min).

time but the concentration of phenol decreased at a faster rate. While the phenol concentration was reduced to the detection limit (0.1 mg/L) after 20 to 25 hours, the TOC concentration decreased by only 20%. The fact that TOC was partially eliminated, indicates that phenol was partially oxidized to CO_2.

The experimental data were curve fitted (shown by lines in Fig. 8.9) by a one-parameter model, a first-order reaction rate expression:

$$C = Co\exp(-bt) \qquad (8.1)$$

Other researchers also found that phenol oxidation followed a first-order reaction (Azzam *et al.*, 1999; Murphy, *et al.*, 1992; Smith De Sucre and Watkinson, 1981). The coefficients were determined by a non-linear regression routine in STATGRAPHICS PLUS (Manugistics, Inc., Rockville, Maryland, USA) and are shown in the related graphs. Visually, as well as based on the correlation coefficients and the low standard errors (less than 4%), the fits were very good for the presented data.

The divided-cell reactor was also used to monitor the disappearance of phenol and TOC originating from phenol in each electrode compartment. The two electrodes were separated with a cationic membrane. Fig. 8.10 presents the change in the phenol and TOC concentration in the anolyte as a function of time. Anodic destruction of phenol was relatively fast and the phenol concentration decreased to the detection limit of 0.1 mg/L in about 15 to 20 hours, while the TOC concentration decreased gradually. The slight increase of the phenol concentration in the anolyte observed after 25 hours of operation may have been due to phenol diffusion from the catholyte. The anodic destruction of phenol was well defined by a first-order reaction expression. For example, the solid line

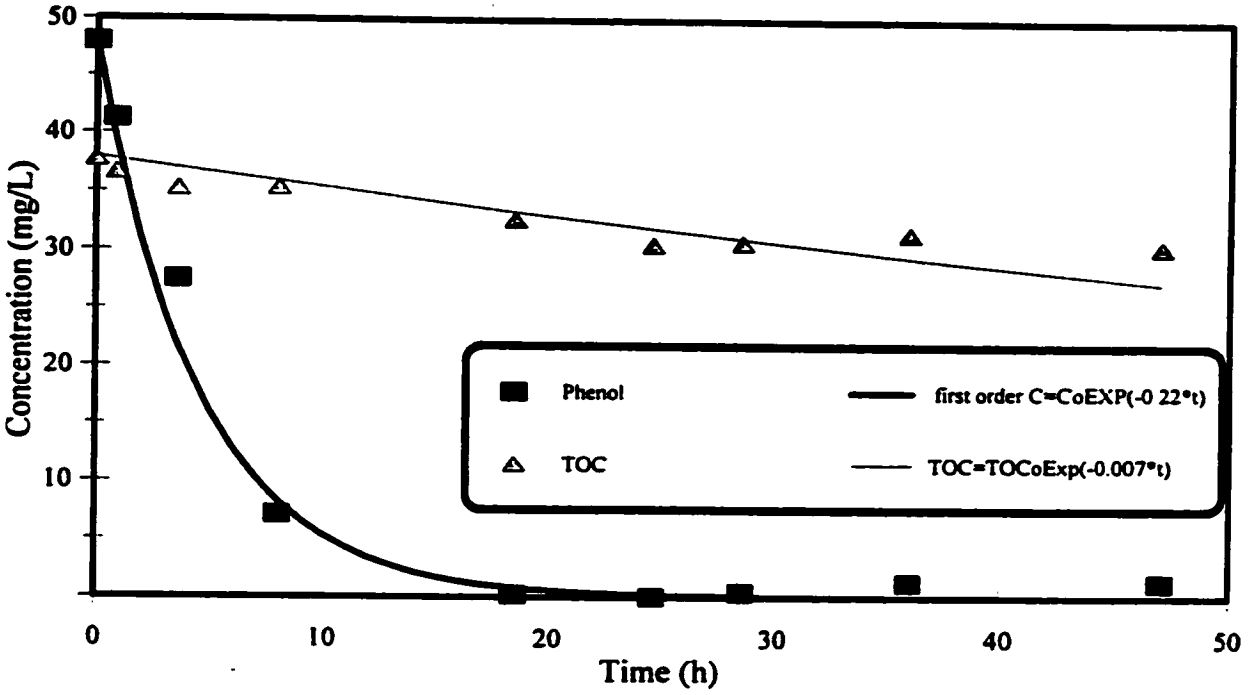

Fig. 8.10 Anodic destruction of phenol in divided-cells reactor without GAC at 50 mA (cation membrane, electrolyte flow rate = 0.2 L/min).

in Fig. 8.10 represents the fitted first-order reaction to the anodic destruction of phenol when the anode was used as the working electrode and the electrolyte flow rate was 0.2 L/min.

The concentration of phenol in the catholyte only changed slightly (Fig. 8.11). The slight decrease in the phenol concentration is due to phenol diffusion through the membrane to the anolyte or the reduction of phenol at the cathode. Although electrochemical destruction of organics can involve either reduction at the cathode or oxidation at the anode, Figs. 8.10 and 8.11 demonstrate that phenol was oxidized at the anode but the phenol reduction at the cathode seems to be minimal.

The effect of current density on the destruction of phenol and TOC originating from the phenol was investigated (Figs. 8.12 and 8.13) using the undivided-reactor. As expected, the mass of phenol oxidized increased with time and the rate of destruction increased with increasing current. Increasing current also decreased the time required to achieve full oxidation. The phenol concentration disappeared in about 1.5, 6, and 19 hours for 500, 250, and 50 mA, respectively. Current changes had a similar effect on TOC oxidation. Fig. 8.13 shows that after 24 hours 75, 50, and 15% of the TOC was eliminated at 500, 250, and 50 mA, respectively. Thus, both figures show that phenol and TOC removal increased with an increase in current. This was attributed to an increase of ionic transport which increases the rate of electrode reactions responsible for the removal process. The aforementioned results agree with previous findings (Awad and Abuzaid, 1999, Comninellis and Nerini, 1995).

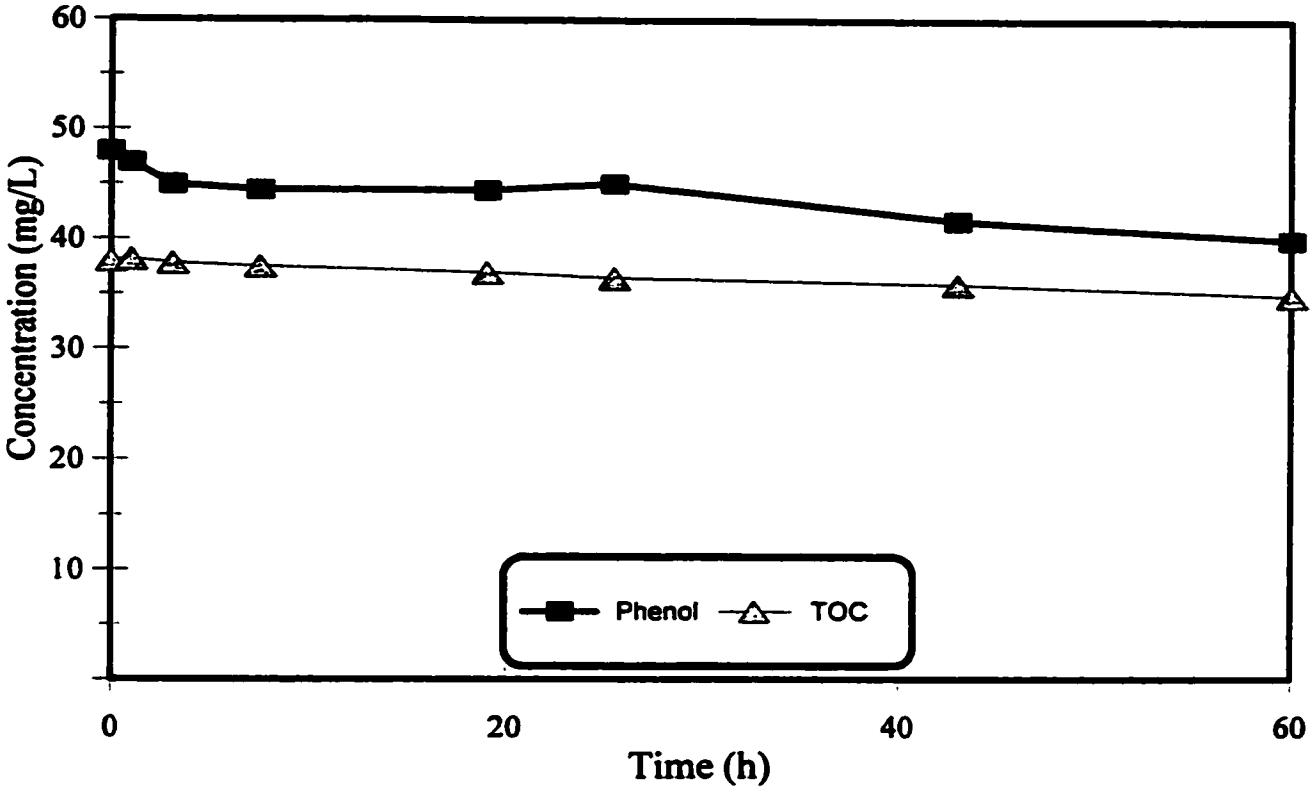

Fig. 8.11 Cathodic destruction of phenol in divided-cells reactor without GAC at 50 mA (cation membrane, electrolyte flow rate = 0.2 L/min).

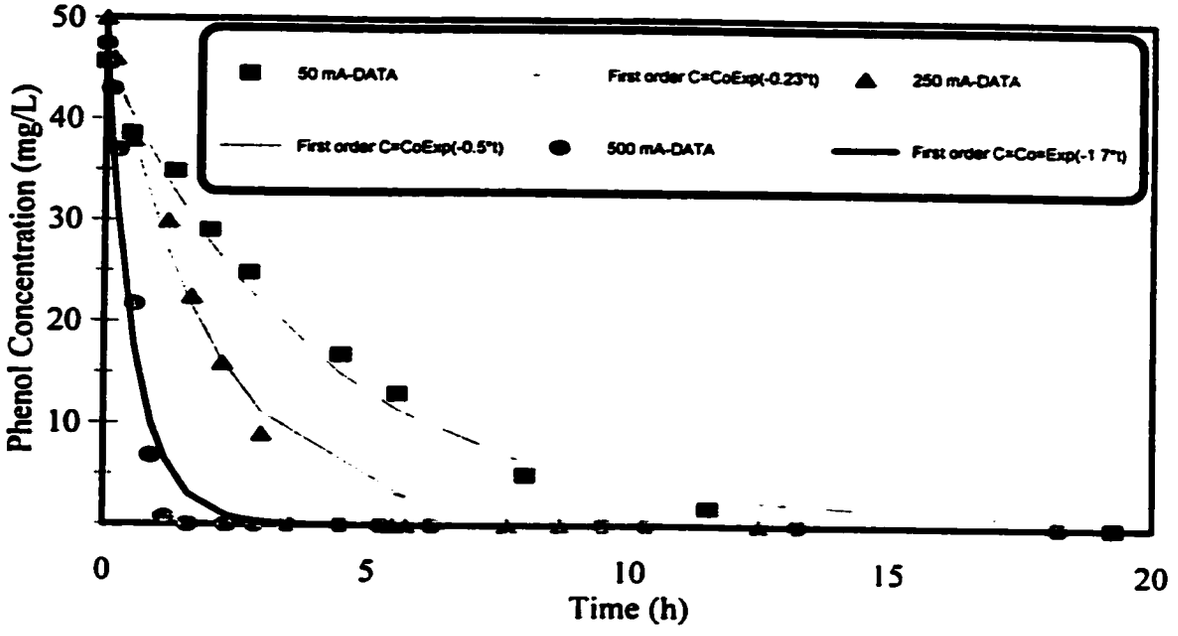

Fig. 8.12 Destruction of phenol in undivided-cells reactor without GAC at different currents (electrolyte flow rate = 0.2 L/min).

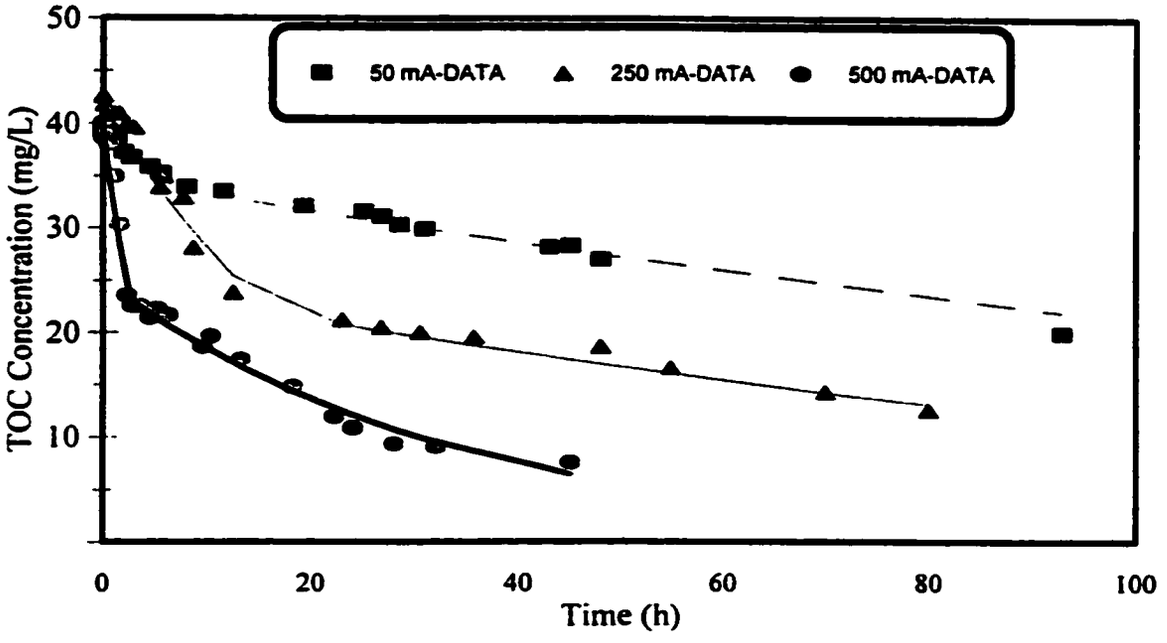

Fig. 8.13 Destruction of TOC (from phenol oxidation) in undivided-cells reactor without GAC at different currents (electrolyte flow rate = 0.2 L/min).

The performance of the undivided-cell reactor (with electrolyte flow of 0.2 L/min) and the anode compartment of the divided-cell reactor under similar conditions is compared in Fig. 8.14. The anolyte of the divided-cell reactor gave similar results to the undivided-cell in terms of phenol and TOC destruction. This is in agreement with results of Figs. 8.10 and 8.11 for the divided-cell reactor in which the phenol destruction occurred mainly at the anode and its reduction at the cathode was minimal.

In Fig. 8.15, the phenol and TOC oxidized are plotted versus charge passed (consumed) for three different current densities. It shows that the removal of the phenol and TOC is a function of the amount of charge passed and is independent of the current densities. The phenol was oxidized fairly rapidly, and virtually no phenol (< 0.1 mg/L) remained after about 5000 coloumbs. However, even after the complete disappearance of phenol, about 70% of the original total organic carbon remained in solution. The complete removal of TOC required a much greater charge. This is in agreement with the results of Smith De Sucre and Watkinson (1981) and Kirk *et al.* (1985). They found that while phenol was readily oxidized on lead dioxide anodes, decreasing the TOC of the wastewater was much more difficult. This is of great concern from a toxicity point of view because the intermediate products, mostly quinones, are more hazardous than phenol; the original contaminant in the wastewater (Anders, 1985). Accordingly, complete oxidation of phenol to CO_2 should be achieved to guarantee environmentally safe discharges.

8.3.2 Destruction of 2NP

Fig. 8.16 shows the destruction of 2NP as a function of time at 50 mA in the undivided-reactor with a 0.1 M NaCl electrolyte recirculation of 0.2 L/min. The initial 2NP

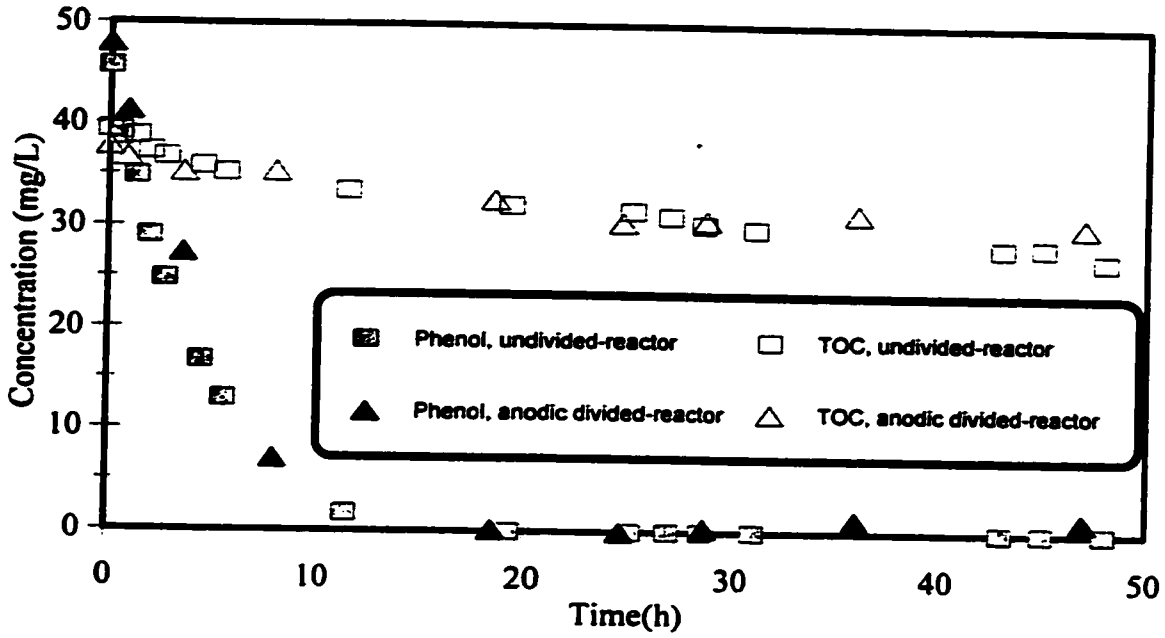

Fig. 8.14 Comparison of destruction of phenol and TOC at 50 mA in divided and undivided-cells reactors (electrolyte flow rate = 0.2 L/min).

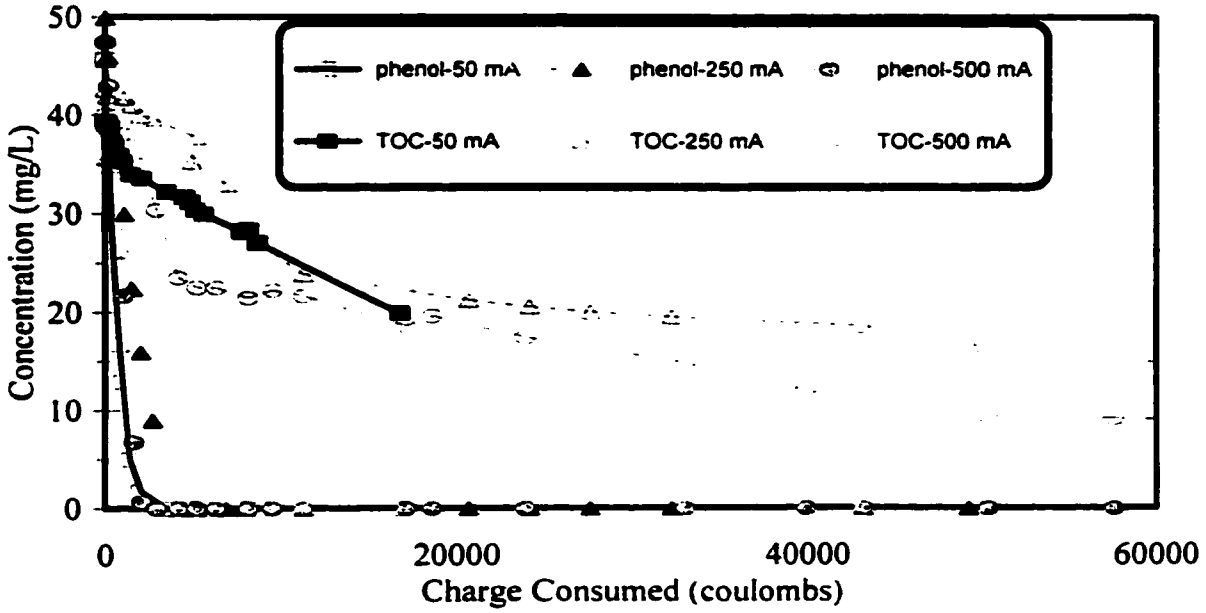

Fig. 8.15 Destruction of phenol and TOC versus applied charge in undivided-cells reactor without GAC at different currents (electrolyte flow rate = 0.2 L/min).

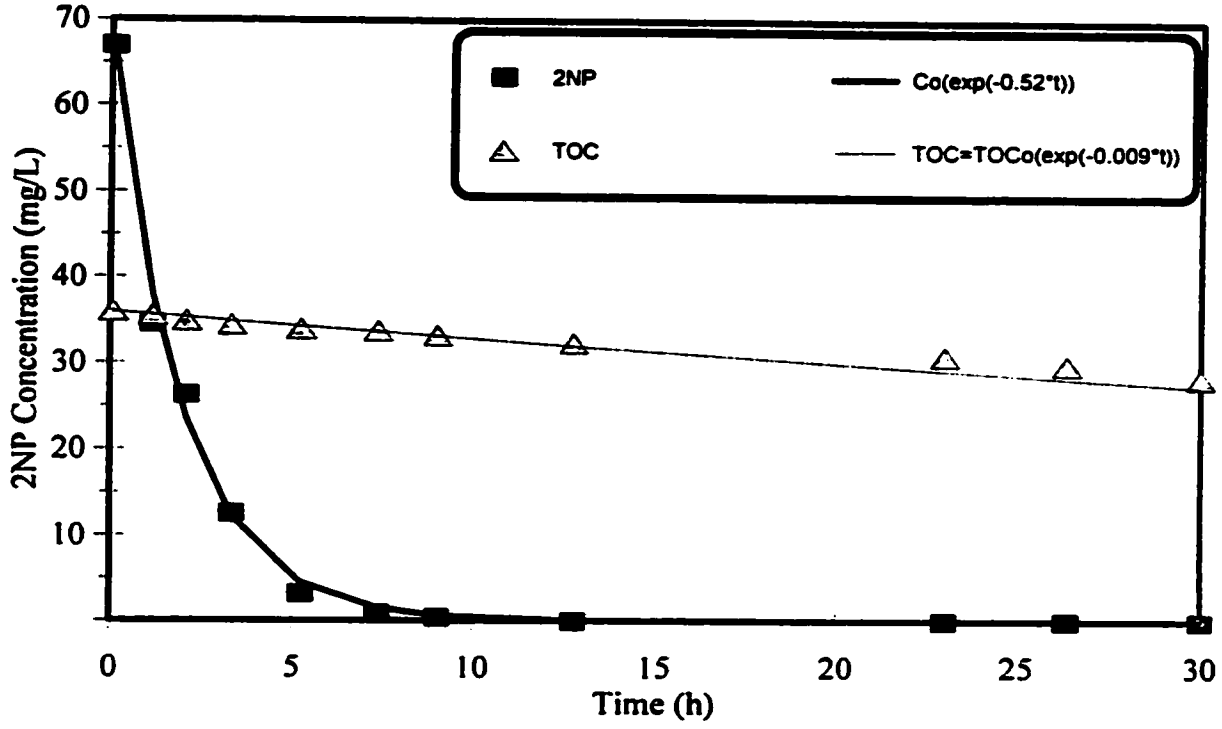

Fig. 8.16 Destruction of 2NP and TOC in undivided-cells reactor without GAC at 50 mA (electrolyte flow rate = 0.2 L/min).

concentration was 68 mg/L. Fig. 8.16 shows that the rate of destruction of 2NP was relatively fast and the 2NP concentration decreased to the detection limit of 0.1 mg/L after about 10 hours. It was also observed that, similar to the phenol experiments, the TOC concentration decreased very slowly with time. The TOC concentration decreased only about 10% after 10 hours, while there was no 2NP left in the solution.

Fig. 8.17 shows that after applying 30 hours of 50 mA, the total-TOC concentration decreased from 35 mg/L to 28 mg/L (20% reduction). Changing the current to 1,000 mA after 30 hours accelerated the by-product oxidation and about 50% of the 30 mg/L of TOC were oxidized in only 5 hours. Finally the TOC concentration reached the zero level after 40 hours of applying 1,000 mA of current. This proves that total oxidation of the by-products was achievable. This also supports the hypothesis that one could possibly take reactivated GAC out of the reactor, then increase the current for a certain period to electrochemically oxidize the contaminated electrolyte before discharge or reuse.

The divided-cell reactor was also used to investigate the destruction of 2NP in each electrode compartment. The two electrodes were separated with a cationic membrane. Fig. 8.18 demonstrates the changes in the concentration of 2NP in the anolyte (volume ~ 650 mL) and catholyte (volume ~625 mL). Anodic destruction of 2NP was rapid and the 2NP concentration decreased to the detection limit (0.1 mg/L) in about 15 hours. Fig. 8.18 shows that the concentration of 2NP in the catholyte decreased with time, but at a slower rate than in the anode compartment. The data were well fitted by a first-order expression (shown as lines in Fig. 8.18) of $C_o\exp(-0.15t)$ and $C_o\exp(-0.25t)$ for the catholyte and anolyte, respectively. The decrease in the catholyte 2NP concentration was likely due to 2NP

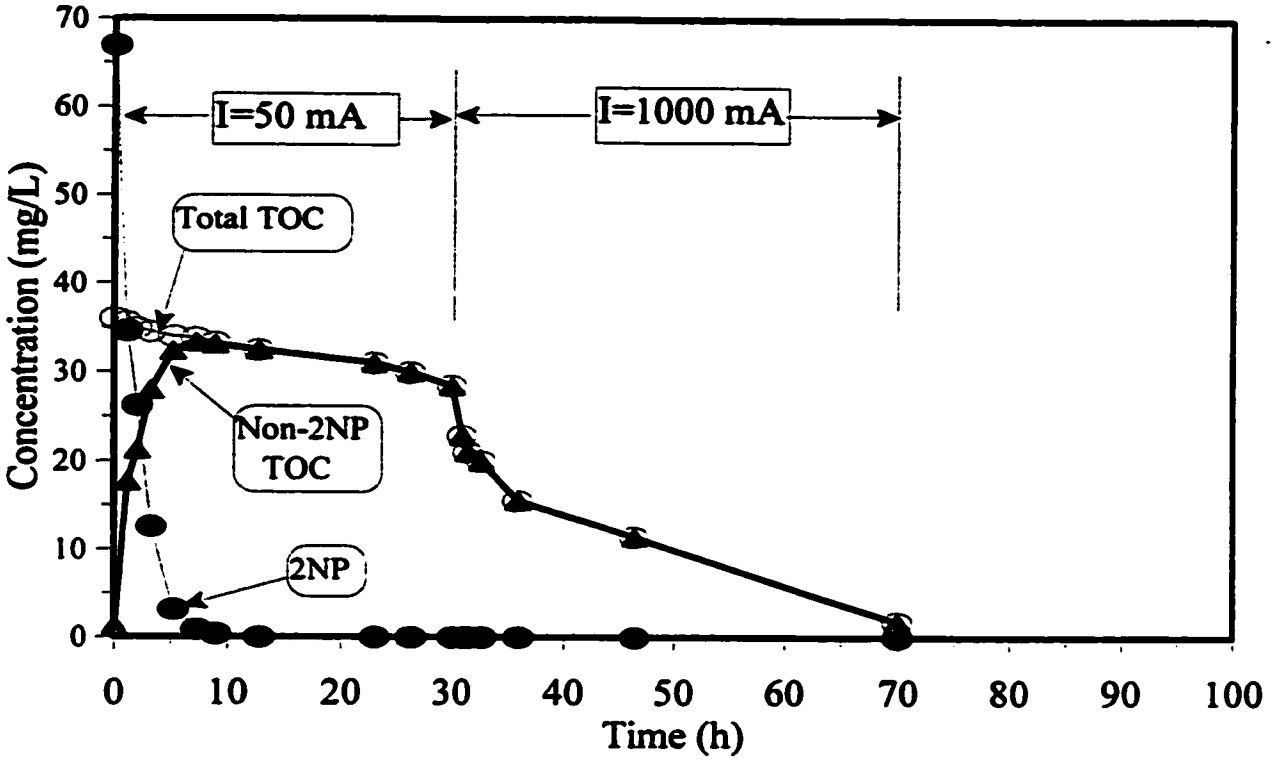

Fig. 8.17 Destruction of 2NP and TOC in undivided-cells reactor without GAC at 50 and 1000 mA (electrolyte flow rate = 0.2 L/min).

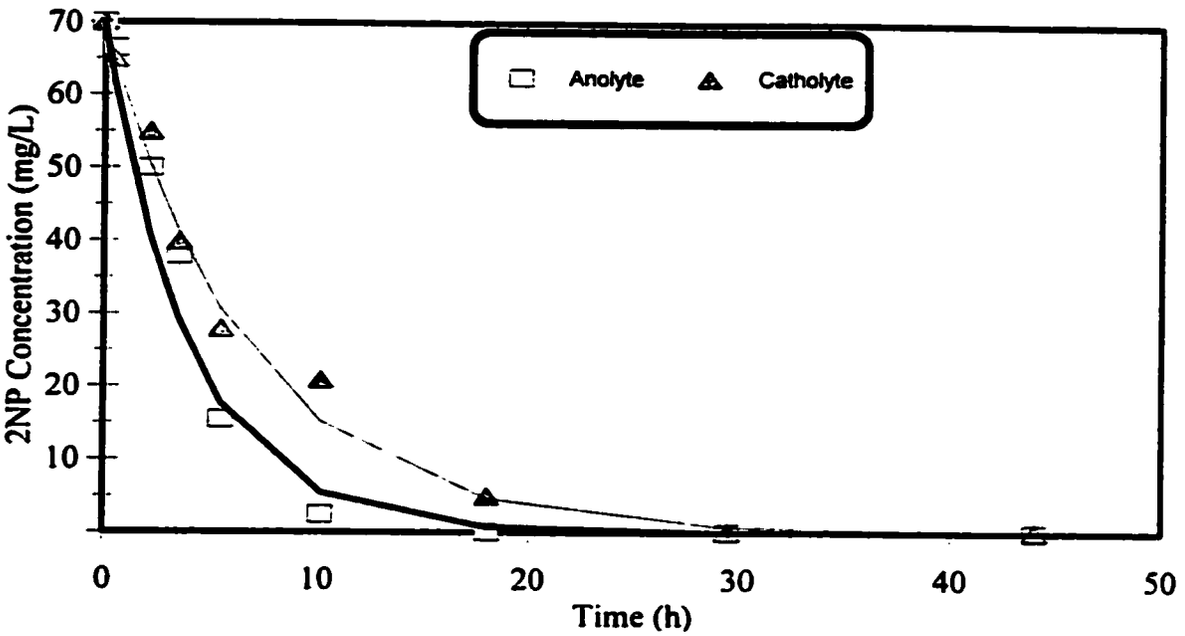

Fig. 8.18 Anodic and cathodic destruction of 2NP in divided-cells reactor without GAC at 50 mA (cation membrane, electrolyte flow rate = 0.2 L/min).

reduction in the catholyte. As mentioned earlier, electrochemical destruction of organics can involve either reduction at the cathode or oxidation at the anode. Figs. 8.17 and 8.18 demonstrate that oxidation of 2NP at the anode and its reduction at the cathode is possible. The observed change in the colour of the catholyte during the experiment also indicated that electrochemical reaction(s) was (were) occurring within the cathode compartment. This is in agreement with the results of Sasaki *et al.* (1983) which showed that reduction of p-nitrophenol and p-chlorophenol was possible and the rate of reduction was much higher than phenol reduction. They found that for p-nitrophenol and p-chlorophenol the reduction occurs mainly at the nitro group. Schmal *et al.* (1986) also showed that the reduction of a chlorinated phenol involved sequential dechlorination of p-chlorophenol at a carbon fibre cathode.

Comparison of the 2NP destruction within the undivided-cells (with electrolyte flow of 0.2 L/min) and the anolyte of the divided reactors under similar conditions is shown in Fig. 8.19. Unlike the phenol results, the undivided-cell reactor performed slightly better than the divided-cell reactor for the destruction of 2NP. The better performance of the undivided-cell reactor may be explained in terms of both 2NP oxidation at the anode and 2NP reduction at the cathode being possible, while in the anolyte of the divided-cells reactor only 2NP oxidation is being presented in the graph. Overall it can be concluded that the undivided cell configuration provided greater 2NP destruction.

8.4 Conclusions

- Desorbed phenol and 2NP react to form a number of reaction by-products that are eventually oxidized to CO_2 and H_2O.

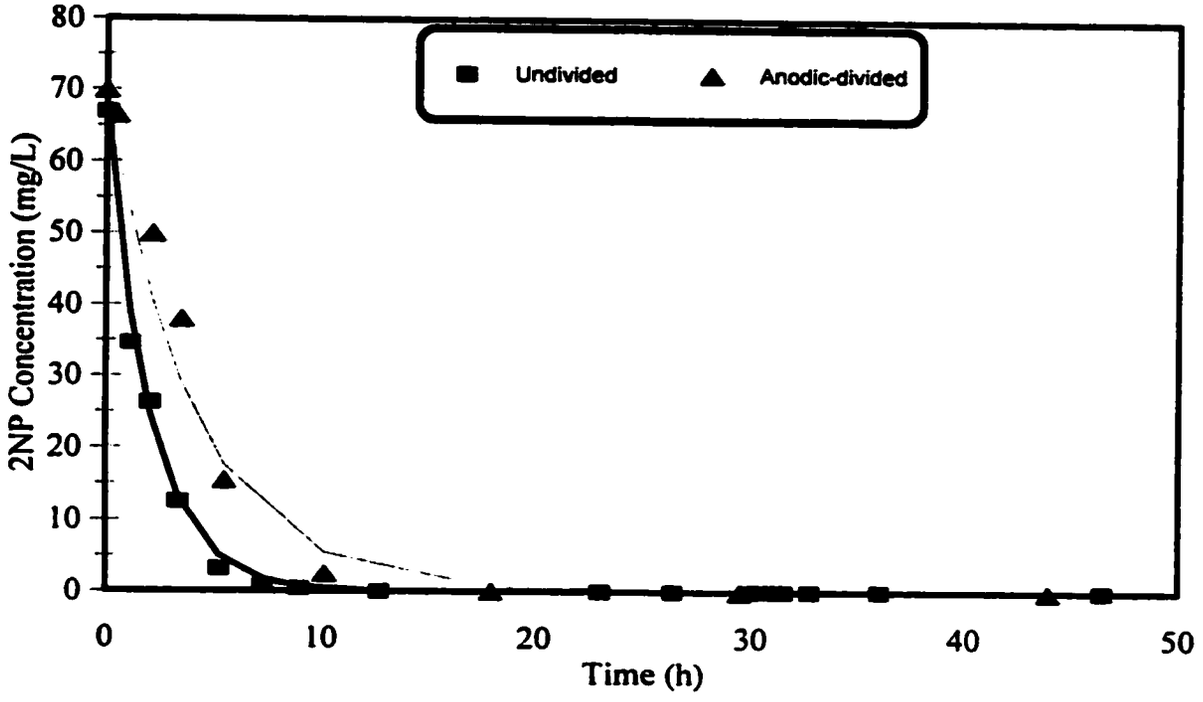

Fig. 8.19 Comparison of destruction of 2NP in divided and undivided-cells reactors at 50 mA (electrolyte flow rate = 0.2 L/min).

- The phenol and 2NP conversion reactions were relatively rapid, and they followed first-order kinetics.
- Destruction of the phenol and 2NP by-products, measured as the non-phenol-TOC and non-2NP-TOC, was very slow.
- The rate of phenol, 2NP, and TOC destruction could be increased by increasing the applied current, but the coulombic efficiency was approximately the same for all the currents.
- It was proved that total oxidation of the by-products is achievable at higher charges. For the total elimination of TOC a proper anode material and an optimized electrochemical reactor design are recommended.
- Phenol and 2NP were oxidized at the anode and 2NP was reduced at the cathode. However, phenol reduction at the cathode was minimal.
- It is recommended that the GAC electrochemical reactivation should be a three step process. First, the GAC is reactivated with a relatively low current to minimize potential alterations of the GAC surface. Second, the GAC is drained and rinsed with a buffered solution. Finally, the electrolyte is treated electrochemically for an extended time at a much higher current (and possibly a different electrode) to reduce the electrolyte's TOC so that it may be reused or discharged.

CHAPTER 9

REACTIVATION MECHANISMS AND MODELLING

9.1 Introduction

To investigate the mechanisms of electrochemical reactivation, the results of selected earlier experiments were analyzed in conjunction with those of some new experiments (desorption studies). First, the extent and kinetics of the contaminant desorption from preloaded GAC in the reactor without current were studied and modelled. Second, the extent and kinetics of contaminant desorption from preloaded GAC in the reactor with current were studied and modelled. Third, the desorption rate constants from the first and second steps along with the destruction rate constant of the contaminant from chapter 8 and the reactivation results with loaded GAC from chapter 7 were used to model the process and predict the extent of reactivation. Two alternative methods were evaluated for the simulation of the reactivation process: the homogeneous solid surface diffusion model (HSSD) and an exponential expression.

9.2 Modelling of the Reactivation Process Using the HSSD model

The HSSD, which is one of most common models in GAC adsorption modelling (Crittenden and Weber, 1978), was evaluated for modelling the reactivation process. The HSSD or surface diffusion model, treats the carbon particle as a solid and assumes that the adsorbate adsorbs at the surface of the particle and migrates along the pore walls to the interior of the particle by surface diffusion (for further details refer to Sontheimer *et al.*, 1988).

The first model evaluated in this study consisted of the HSSD model modified to incorporate two assumed mass transfer mechanisms. The first was enhanced desorption due to polarization (charging of the GAC surface). The second was that the adsorbate would only be oxidized once it desorbed into solution and not directly on the GAC surface. Three sets of experiments (desorption without current, desorption with current, and oxidation of contaminant (without GAC)) were conducted to calibrate the model which was then used to predict the performance of the regeneration process.

As the first step in modelling a modified version of a computer program originally developed by Narbaitz (1985), which solves the HSSD model equations via orthogonal collocation, was used to predict desorption kinetics. Two modifications were made to the program developed by Narbaitz (1985). First, the program was modified for desorption prediction from its original use for adsorption prediction. Second, because the program uses the Freundlich isotherm which is pH dependent, modifications were incorporated to account for the changes of the catholyte pH from 5 to 12.

The pH variation of the catholyte at 50 mA over time was modelled and is shown in Fig. 9.1. Because the values of the Freundlich isotherm are pH dependent (Karimi-Jashni 1994), Freundlich isotherm parameters were modelled to reflect the pH variation over time. The pH dependency of the Freundlich isotherm parameters is illustrated in Figs. 9.2 and 9.3. The modelled pH variations and the pH dependency of the Freundlich isotherm parameters were used in the computer program to predict desorption kinetics. In most cases the program was unable to give a satisfactory prediction of desorption kinetics (Appendix A9) and further

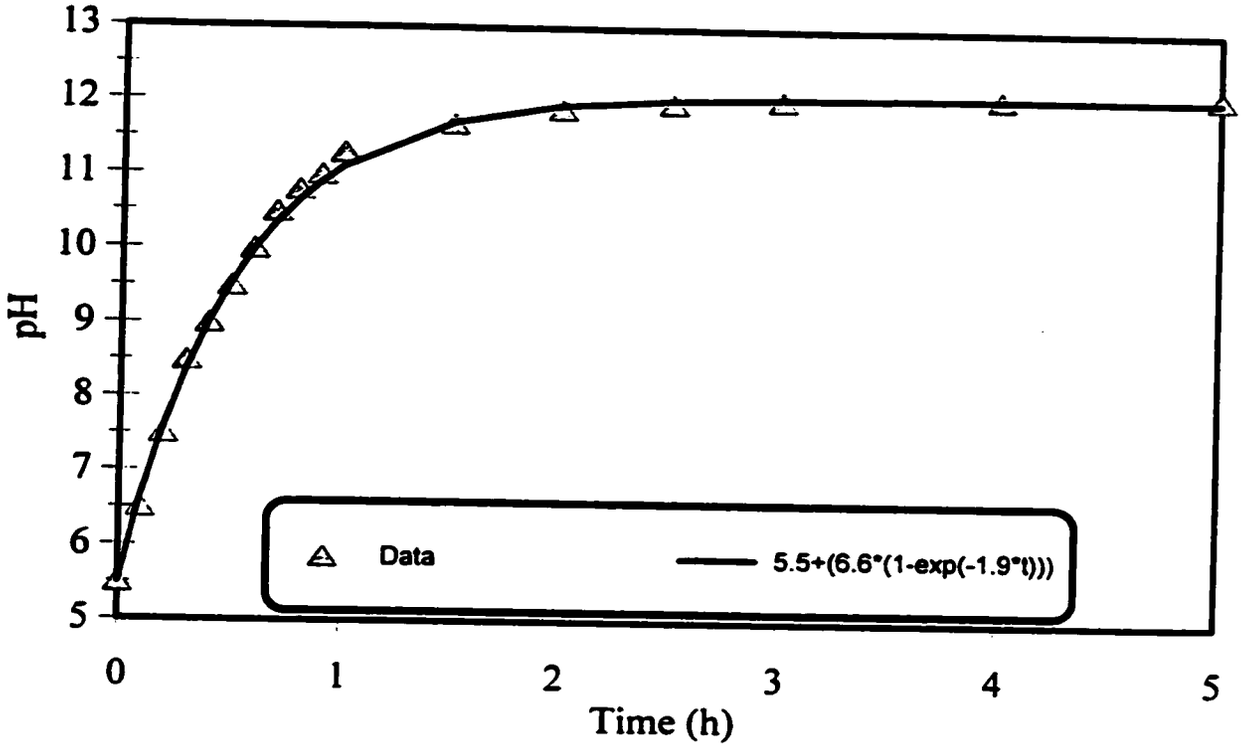

Fig. 9.1 Catholyte pH variation versus cathodic reactivation time at 50 mA.

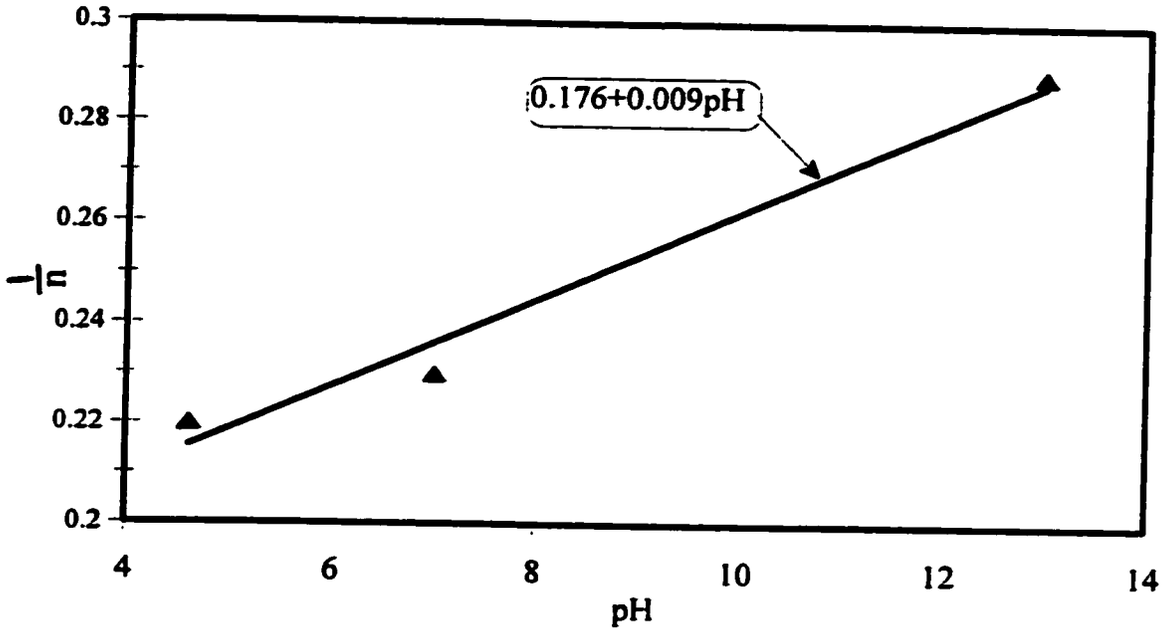

Fig. 9.2 1/n versus pH for 2NP-loaded F-400 isotherm.

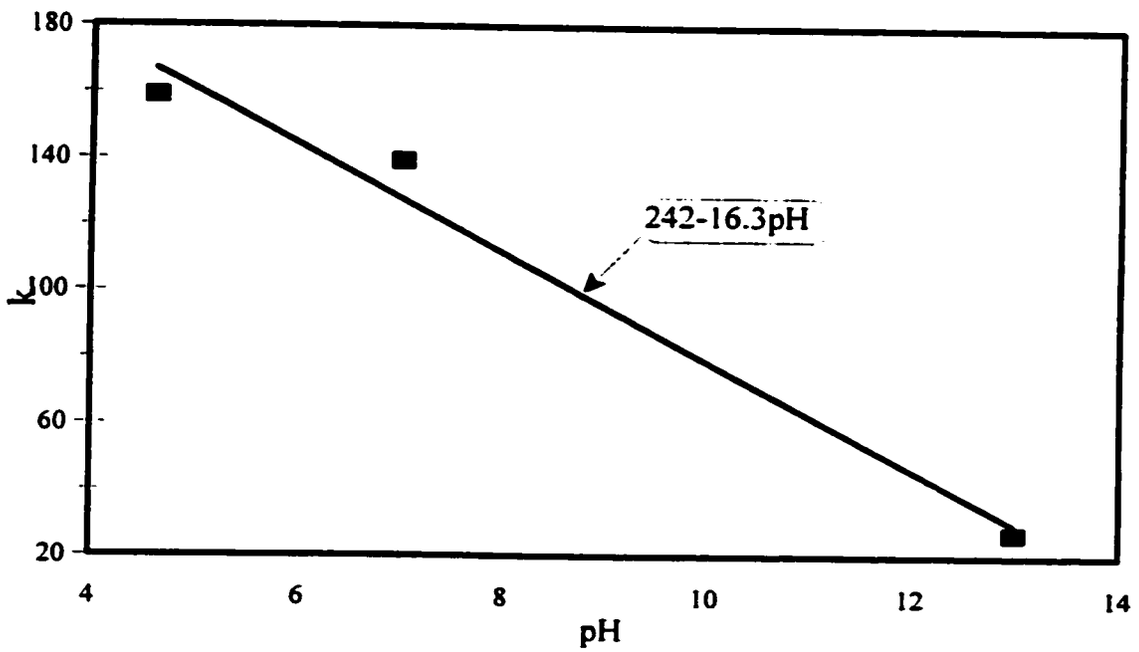

Fig. 9.3 K versus pH for 2NP-loaded F-400 isotherm.

evaluation of the model was not possible. Therefore it was decided to use an alternative method to model the reactivation process.

9.3 Modelling of the Reactivation Process Using an Exponential Expression

9.3.1 Desorption Studies with No Current

The first step in identifying the reactivation mechanisms was a study on the extent and kinetics of the contaminant desorption from preloaded GAC in the reactor without current at pHs of 2 and 12 to determine the impact of pH on contaminant desorption. pHs 2 and 12 were chosen because the tests showed that the pHs of the anolyte and catholyte tend to these pH values, respectively. The GAC used to determine the desorption kinetics at these pHs was preloaded at pH 5. The results of these desorption tests and the regressed curves were plotted in Figs. 9.4 and 9.5. The regressed mathematical expression was in the format of $a^*(1-\exp(-b^*t))$, where t is time in hours and a and b are coefficients. The coefficients were determined by a non-linear regression routine in STATGRAPHICS PLUS (Manugistics, Inc., Rockville, Maryland, USA) and are shown in Table 9.1. Visually as well as based on the low standard errors (generally less than 3%) the model fits the experimental data very well.

Figs. 9.4 and 9.5 also demonstrate the pH dependence of desorption of phenol and 2NP from activated carbon. Given that the pK_as of phenol and 2NP are 9.9 and 7.23, respectively, the maximum extent of desorption occurs for the dissociated form of the molecule (pH = 12) and there was significantly less desorption for pH 2 (pH less than the pK_a). Greater desorption of phenol and 2NP from F-400 at pH 12 is the reason for higher cathodic reactivation efficiencies than anodic reactivation efficiencies observed in previous chapters.

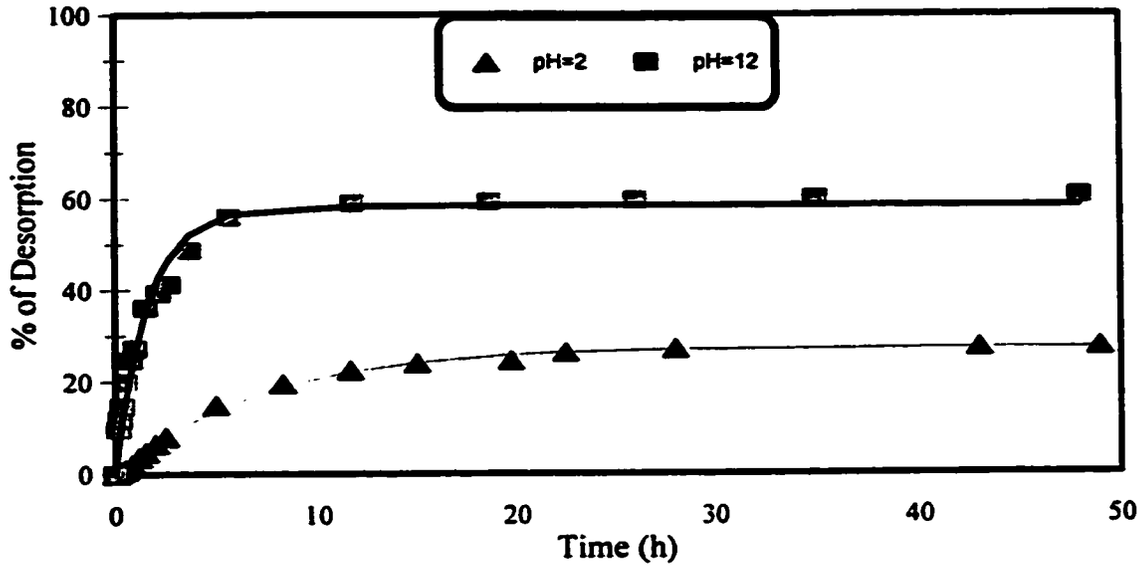

Fig. 9.4 Desorption of 2NP from F-400 at pHs 2 and 12 without current.

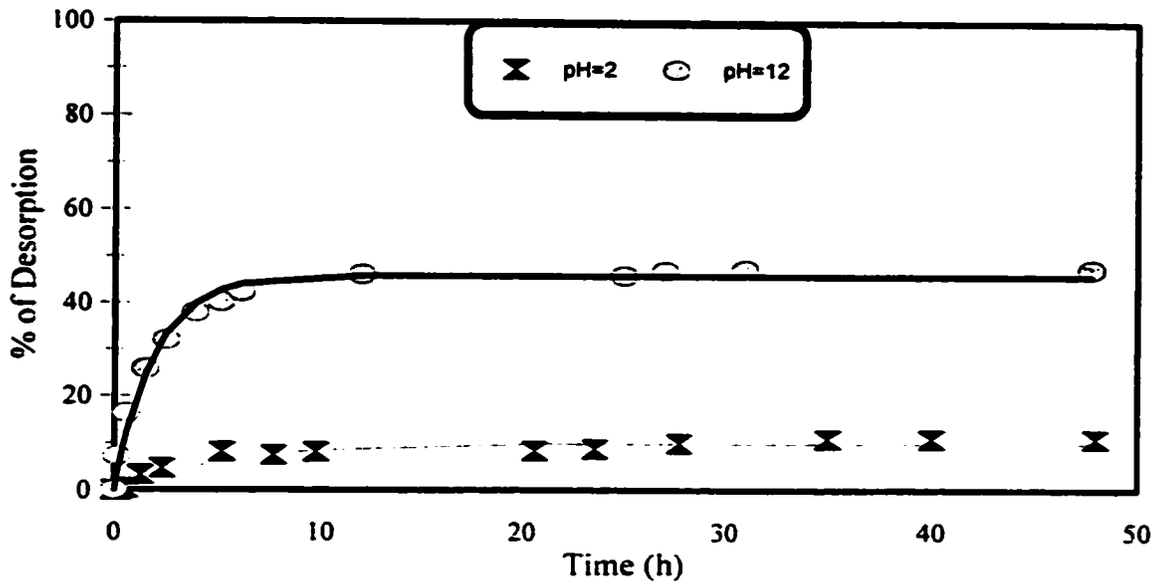

Fig. 9.5 Desorption of phenol from F-400 at pHs 2 and 12 without current.

Table 9.1 Regressed coefficients for the simple desorption model for desorption without current.

	pH	I (mA)	Contaminant	Constant (*a*) (unitless)	Exponent (*b*) (1/h)
Desorption	2	0	2NP	27.36±0.28*	0.143±0.005*
Desorption	12	0	2NP	58.44±1.23	0.610±0.045
Desorption	2	0	phenol	10.06±0.37	0.196±0.030
Desorption	12	0	phenol	45.90±0.92	0.519±0.046

* = standard errors.
Equation: % desorption = $a*(1-e^{-bt})$.

9.3.2 Desorption Studies with Current

The second step studied the extent and kinetics of contaminant desorption from preloaded GAC in the reactor with a 50 mA current at pHs 2 and 12. A cation exchange membrane was installed to separate the two electrodes and create a divided-cell reactor, to prevent the oxidation of the contaminant at the anode. The GAC was placed on top of the cathode which also was the working electrode. Hence these results can be called cathodic desorption. The results are plotted in Figs. 9.6 and 9.7. These figures show that desorption with current followed a similar pattern to that without current (Figs. 9.4 and 9.5). However, they demonstrate that the extent of desorption in the presence of current was higher than the extent of desorption without current. Similar exponential expressions to the ones used for desorption without current were used for curve fitting purposes. The model fit the experimental data well and the regressed coefficients are shown in Table 9.2.

Comparison of 2NP desorption at pH 12 with and without current (Fig. 9.8) demonstrates that the extent of desorption of 2NP from GAC with the applied 50 mA was about 50% greater than that without current. Given that in the case of 2NP there were reducing reactions at the cathode, the actual amount of 2NP desorbed was somewhat higher. A similar result was also obtained for desorption of 2NP at pH 2. Although the results for pH 2 were not really relevant in modelling the cathodic electrochemical reactivation, they show that even at pH 2 the current had a beneficial impact on desorption.

Comparison of phenol desorption at pH 12 with and without current (Fig. 9.9) shows that the extent of desorption of phenol from GAC with the applied 50 mA was about 35% greater than that without current. This demonstrates that electrochemical reactivation of

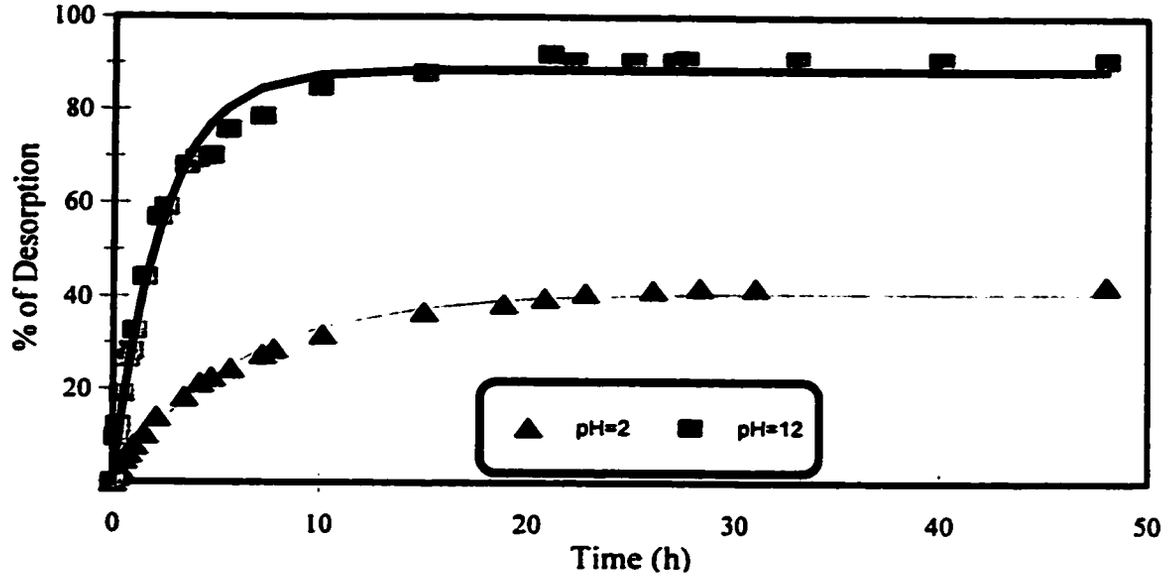

Fig. 9.6 Cathodic desorption of 2NP from F-400 at pHs 2 and 12 at 50 mA within the divided-cell reactor.

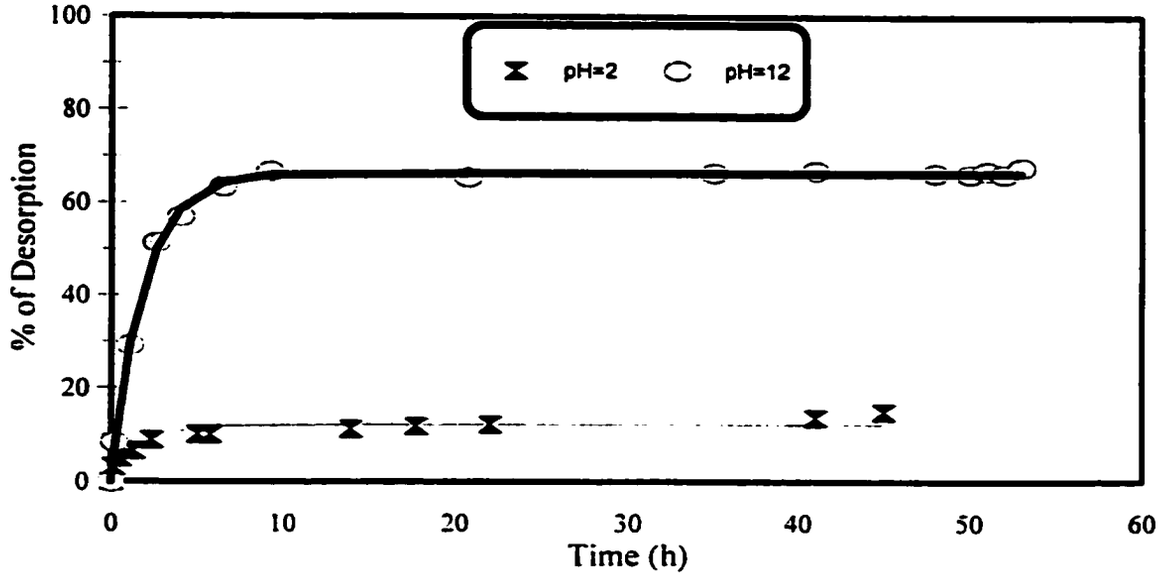

Fig. 9.7 Cathodic desorption of phenol from F-400 at pHs 2 and 12 at 50 mA within the divided-cell reactor.

Table 9.2 Regressed coefficients for the simple desorption model for desorption with current.

	pH	I (mA)	Contaminant	Constant (a_c) (Unitless)	Exponent (b_c) (1/h)
Desorption	2	50	2NP	40.95±0.54*	0.167±0.007*
Desorption	12	50	2NP	88.62±0.97	0.431±0.019
Desorption	2	50	phenol	12.23±0.62	0.649±0.162
Desorption	12	50	phenol	66.48±0.30	0.537±0.015

* = standard errors.
Equation: % desorption = $a_c*(1-e^{-bct})$.

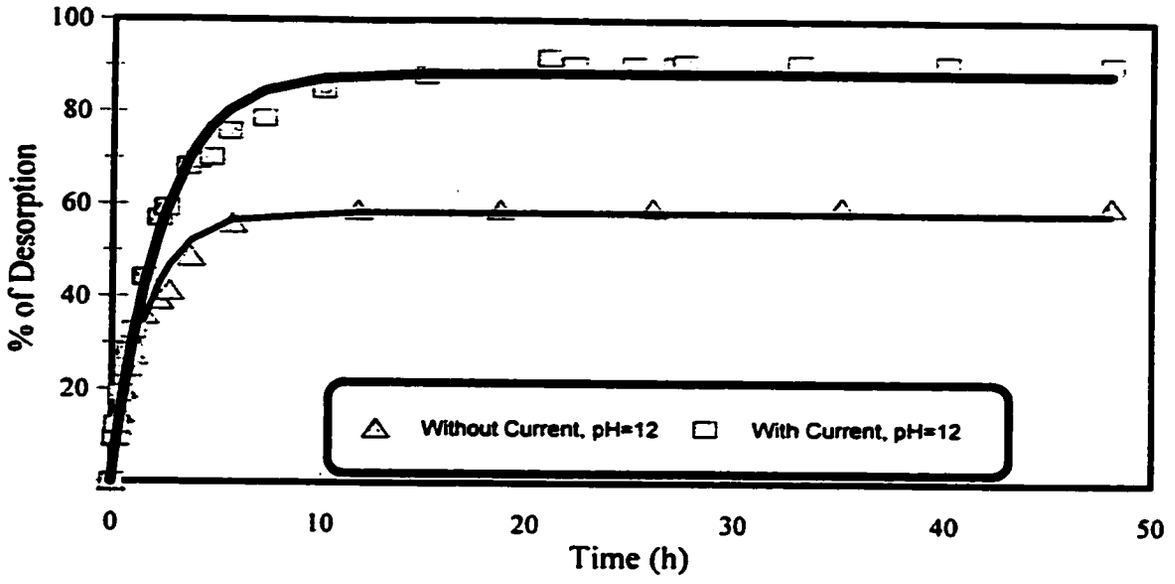

Fig. 9.8 Comparison of 2NP desorption from F-400 at 50 mA and without current.

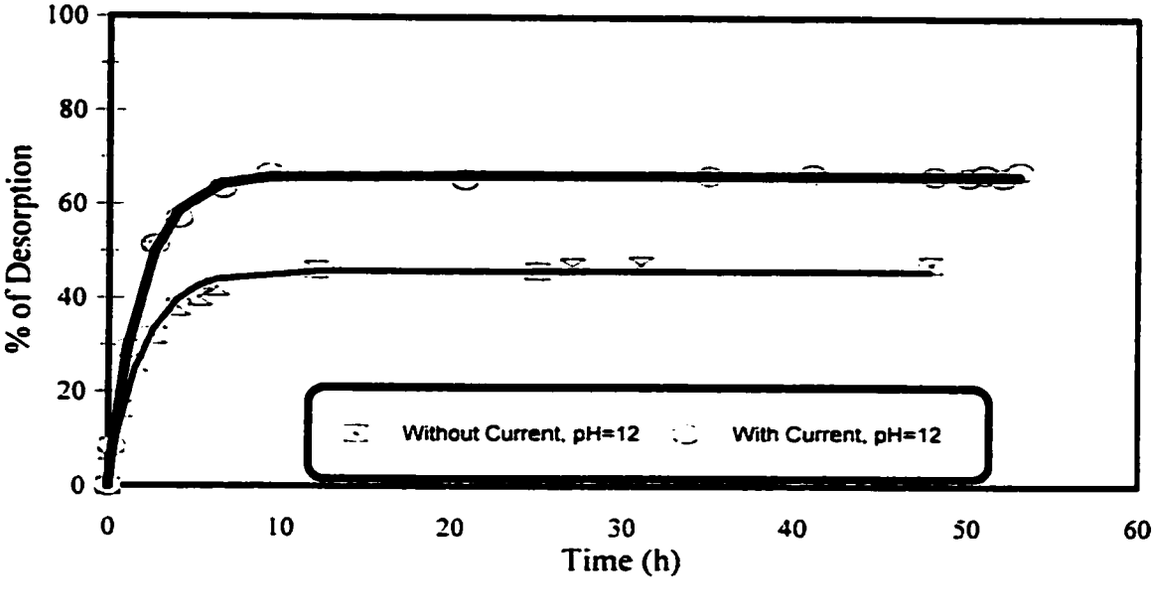

Fig. 9.9 Comparison of phenol desorption from F-400 at 50 mA and without current.

GAC was more efficient than chemical reactivation (i.e., desorption into a high pH solution) of GAC. The greater impact of the electrical current on 2NP desorption over phenol desorption is consistent with the full-reversibility of 2NP from F-400 and the partial irreversibility of phenol from F-400.

The difference between desorption with and without current indicates the impact of GAC surface polarization (charging) due to current on the contaminant desorption. Kastening *et al.* (1985) investigated the electrochemical polarization of powdered activated carbon. A powdered activated carbon suspension in aqueous dilute sulphuric acid exhibited large charge capacities of about 150 F/g. From various considerations Kastening *et al.* (1985) concluded that this charge capacity represents the ordinary double-layer behaviour of the huge pore surface rather than a property of the particle's external surface. After polarization at a charging electrode, the particles maintained the potential forced upon them over long periods (typical rate of discharge = 10^{-7}V/s). The behaviour of the polarization process (charging current) was attributed to the charge transfer mechanism during the collision between a single particle and the charging electrode (Kastening *et al.* (1985)). Replacement of dilute sulphuric acid by dilute potassium hydroxide solutions (pH 13) resulted in the same capacity data. Therefore, the higher desorption with current in Figs. 9.8 and 9.9 are likely caused by polarization (charging) of the GAC surface. The repulsive forces between the charged surface and the adsorbed contaminant(s) may have increased the extent of desorption of contaminant(s) from the GAC.

9.3.3 Extent of Reactivation

Figs. 9.10 and 9.11 show the reactivations of 2NP/phenol-loaded F-400 at 50 mA in the undivided-cell reactor (not mixed). These figures show the total cathodic reactivation, the reactivation due to desorption (desorption with current), and the reactivation due to oxidation. These figures show that the total reactivation efficiency was higher than reactivation predicted via desorption alone and the difference could be due to the destruction of the contaminant and its reaction by-products. As discussed earlier the surface of the GAC is polarized by contact with electrodes and this polarization can lead to electrochemical reactions at the surface of GAC. These reactions may totally oxidize the contaminant (2NP or phenol) to water and CO_2 and eventually more GAC sites reactivate through this process. Also the possible reactions on the surface of GAC may transfer the contaminant (2NP or phenol) to by-products which then may desorb to the bulk solution and reactivate more GAC sites. Desorption of by-products is a function of the concentration of contaminant (2NP or phenol) and their by-products on the surface of the GAC and in the bulk solution. The exponential expressions in Table 9.2 were used to model desorption.

The difference between the reactivation data and the desorption was defined by an exponential expression which is:

$$\text{Reactivation due to oxidation} = (RE_{max} - Des._{max})*(1 - \exp(-b_r*t)) \qquad (9\text{-}1)$$

Where the RE_{max} is the maximum reactivation efficiency for each case (103% for 2NP and 83% for phenol-loaded F-400). $Des._{max}$ is the maximum desorption (with current) for each case (88.6% for 2NP and 66.5% for phenol-loaded F-400), b_r is the coefficient and t is the reactivation time in hours. The reactivation due to oxidation is also shown in Figs. 9.10 and 9.11. The b_r coefficient for 2NP was 0.4 and that of phenol was 1.0.

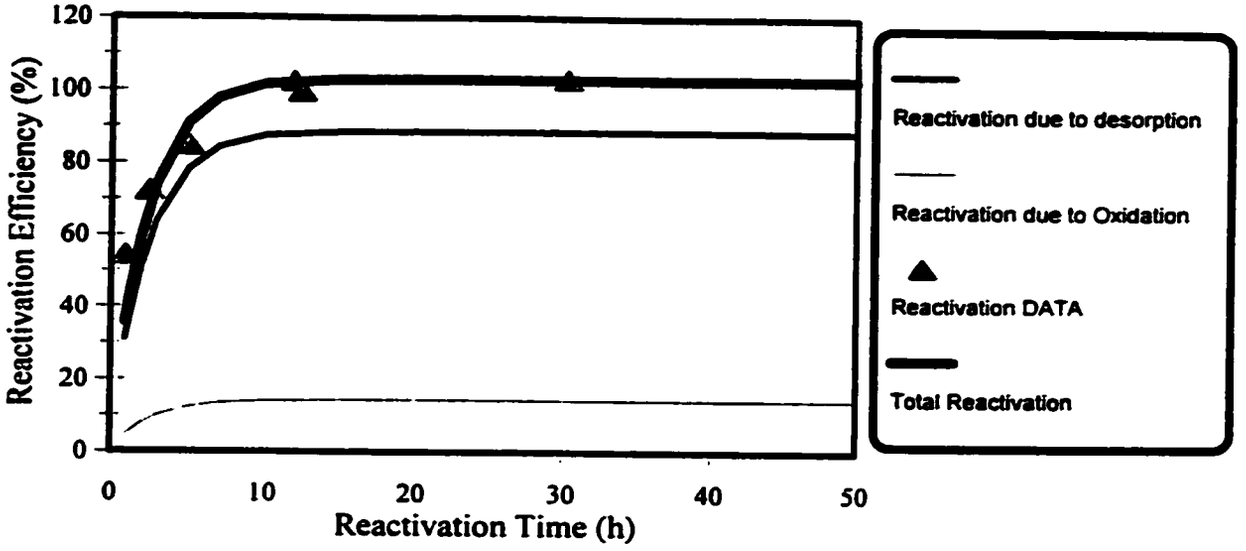

Fig. 9.10 Cathodic reactivation of 2NP-loaded F-400 at 50 mA and undivided-cell reactor.

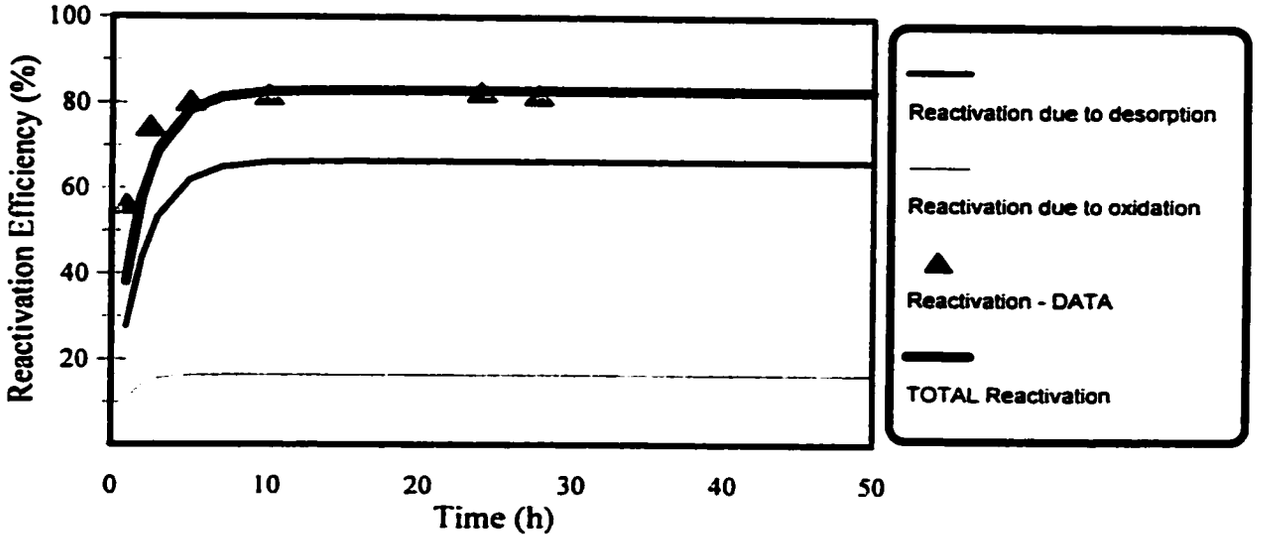

Fig. 9.11 Cathodic reactivation of phenol-loaded F-400 at 50 mA and undivided-cell reactor.

The total reactivation efficiency was calculated as the sum of the reactivation due to desorption (with current) and the reactivation due to oxidation. This summation is shown as a thick line in Figs. 9.10 and 9.11 that is in agreement with the experimental data. From these discussions it can be concluded that the main portion of reactivation was due to desorption. The reactivation due to desorption at high pH (without current) was about 50-60%, the reactivation due to the charging effect (the difference between the desorption with and without current) was about 25-30%, and the reactivation due to oxidation/reduction of the contaminant was about 10-20% of the total reactivation.

Electrochemical reactivation is a complicated process and may include different mechanisms. During the electrochemical reactivation of GAC loaded with a contaminant the following mechanisms may be involved: desorption of contaminant from the GAC surface, destruction of the desorbed contaminant at the liquid phase and/or electrode surface, destruction of the contaminant at the surface of the GAC, adsorption of by-products from the liquid phase by GAC surfaces, transformation of the contaminant to by-products at the surface of GAC, and desorption of by-products from GAC surfaces. These mechanisms occur simultaneously and affect the reactivation efficiency.

Fig. 9.12 represents a schematic of mechanisms involved in the electrochemical reactivation process.

A) Liquid-phase changes include:

1- Contaminant concentration changes: due to desorption of the contaminant, the contaminant concentration increases for some time until it reaches a peak and then decreases, eventually reaching zero. The peak will occur if the rate of contaminant

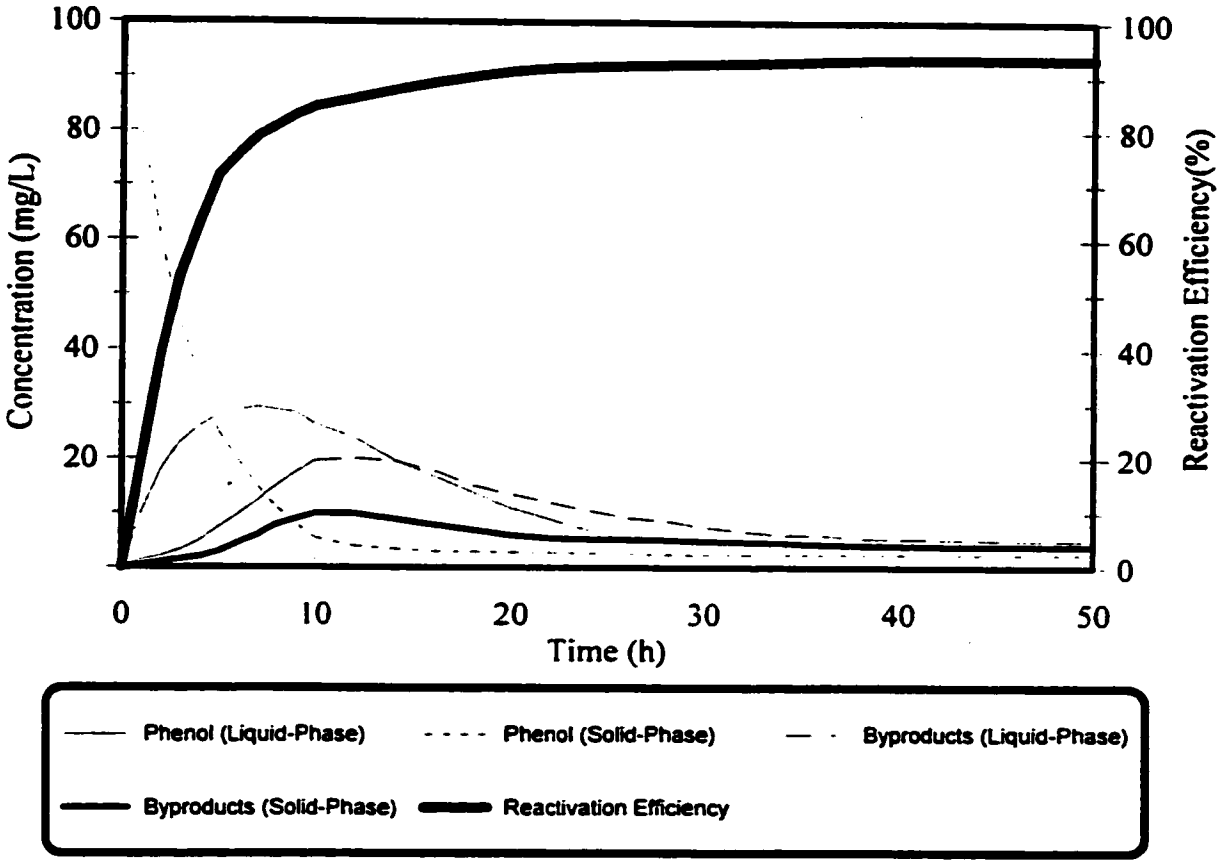

Fig. 9.12 Conceptual model of the solid and liquid phase concentrations during electrochemical reactivation of loaded GAC.

desorption is more than the rate of the contaminant destruction or transformation to by-products.

2- By-products concentration: due to destruction of the contaminant in the liquid-phase or at the surface of electrodes and desorption of by-products from the GAC surface, the by-products concentration increases until it reaches a peak and decreases eventually to zero.

B) Solid-phase changes include: The total solid-phase concentration can be defined as:

$$Q_{total} = Q_{contaminant} + Q_{by\text{-}product} \qquad (9\text{-}2)$$

At the start, $Q_{by\text{-}products} = 0$ and $Q_{total} = Q_{contaminant}$. As time passes $Q_{contaminant}$ decreases due to desorption of the contaminant from the GAC surface to the liquid-phase until it reaches a minimum. As time passes and the contaminant is transformed to by-products either in the liquid-phase or at the GAC surface, the $Q_{by\text{-}products}$ concentration increases due to adsorption of by-products from the liquid-phase or due to transformation of the contaminant to by-products at the GAC surface. As the contaminant and its by-products continue to be destroyed over time, the by-product concentration in the liquid-phase decreases and this causes the desorption of by-products from the surface of the GAC. Hence the solid-phase by-products decrease to a minimum level. Eventually there may be some $Q_{residual}$ due to residual contaminant and its by-products on the GAC surface.

C) Reactivation efficiency changes: the reactivation efficiency increases over time as sites on the GAC surface become available due to desorption of the contaminant, desorption of byproducts, and complete oxidation of the contaminant on the GAC surface. The reactivation efficiency can be defined as:

$$RE\% = 100*(Q_{total} - Q_{residual})/(Q_{total}) \qquad (9\text{-}3)$$

The amount of $Q_{residual}$ depends on the reversibility, current density, and reactivation time. If the $Q_{residual} = 0$ then the reactivation efficiency will be 100%.

9.4 Conclusions

- A model based on a modified version of the HSSD adsorption model was evaluated, however it failed to model desorption experiments well so it was abandoned.
- Exponential expressions described desorption and the reactivation results very well.
- It was found that the main portion of reactivation was due to desorption. The reactivation due to desorption at high pH (without current) was about 50-60%, the reactivation due to current enhanced desorption (the difference between the desorption with and without current) was about 25-30%. and the reactivation due to oxidation/reduction of contaminant is about 10-20% of the total reactivation. A conceptual model of the solid and liquid-phase concentrations during electrochemical reactivation was presented.

CHAPTER 10

SCALE-UP AND COMPARISON OF ELECTROCHEMICAL AND THERMAL REACTIVATION

10.1 Introduction

This chapter presents a discussion on process scale-up and compares the conventional activated carbon reactivation technology (thermal reactivation) with electrochemical reactivation.

10.2 Scale-up

As shown in previous chapters high reactivation efficiencies were achieved for a single layer of GAC but the multi-layer reactivation efficiencies were low. However multi-layer experiments did not use post reactivation buffering, which may improve performance. As direct contact between the GAC particles and the electrode appears to be necessary for high reactivation efficiencies, alternate reactor configurations such as pulse-beds and fluidized-beds, need to be evaluated. Thus, scale-up calculations of electrochemical reactivation at this point are premature.

10.3 Comparison of Electrochemical and Thermal Reactivation.

As there are no full-scale electrochemical GAC reactivation facilities, it is too early to establish capital and maintenance costs of the process. Only two simplified comparisons with thermal reactivation can be made: comparison of efficiency and energy costs.

10.3.1 Comparison of Long-Term Adsorption Efficiency

Although thermal methods result in 90 to 100% reactivation efficiencies for general applications, the maximum first-cycle thermal reactivation efficiency reported for phenol-loaded GAC is 88% (Chiang *et al.*, 1997). The maximum first-cycle electrochemical reactivation efficiencies reported for phenol-loaded and 2NP-loaded GAC in this study are 92 and 108%, respectively. This shows that electrochemical reactivation is as efficient as thermal reactivation and further optimization of the electrochemical operating parameters could result in higher efficiencies for electrochemical reactivation.

Other key elements in this type of comparison are the reactivation efficiency beyond the first cycle (multiple reactivations) and the GAC mass loss. Narbaitz and Cen (1994) showed that the electrochemical reactivation of phenol-loaded F-400 declined 2% per additional cycle of reactivation and there was no GAC loss. Although no reports of multiple cycles of thermal reactivation of phenol-loaded GAC were identified in the literature, a GAC mass loss of 5 to 15% per cycle of reactivation has been reported for thermal reactivation (Adams *et al.*, 1988). The loss of GAC could be due to transport or due to furnace losses. Transport losses are fairly constant at 2-3% and in-furnace losses vary widely and depend on the type of GAC used. The lost GAC needs to be replaced with virgin GAC. Clark and Lykins (1989) have shown that the cost of purchasing replacement GAC can be up to four times greater than the energy cost for thermal reactivation systems.

To compare the efficiency of both process, a simple set of calculations was made using the following assumptions:

1- thermal reactivation results in 5% GAC mass loss.

2- the reactivation efficiency for the first thermal reactivation cycle is 90% and it remains constant for multiple reactivation cycles.

3- electrochemical reactivation results in no GAC mass loss.

4- the reactivation efficiency for the first electrochemical reactivation cycle is 80% (efficiency at 50mA and 5 hours of reactivation for phenol-loaded F-400) and there is a decline of 2% efficiency per cycle for each additional cycle of reactivation.

5- the long term adsorption efficiency is measured as the product of the reactivation efficiency multiplied by the fraction of the GAC mass remaining after the reactivation.

The results of these calculations are presented in Fig. 10.1 and Appendix B17. Fig. 10.1 shows that thermal reactivation initially has higher efficiencies than electrochemical reactivation but the long-term efficiencies reach the same level at the third reactivation cycle. Thereafter the electrochemical alternative is superior.

10.3.2 Energy Costs

The energy costs of the two methods were compared for plants of various sizes. The following assumptions were made:

1- conditions of chosen waste and unit costs

a) the wastewater treated with GAC has a phenol concentration of 300 mg/L.

b) the GAC adsorption characteristics were modeled based on the results of isotherm experiments from Chapter 4 of this study.

c) the cost of electricity was assumed to be $0.06/kw.hr.

d) the cost of natural gas was assumed to be $0.0035/scf.

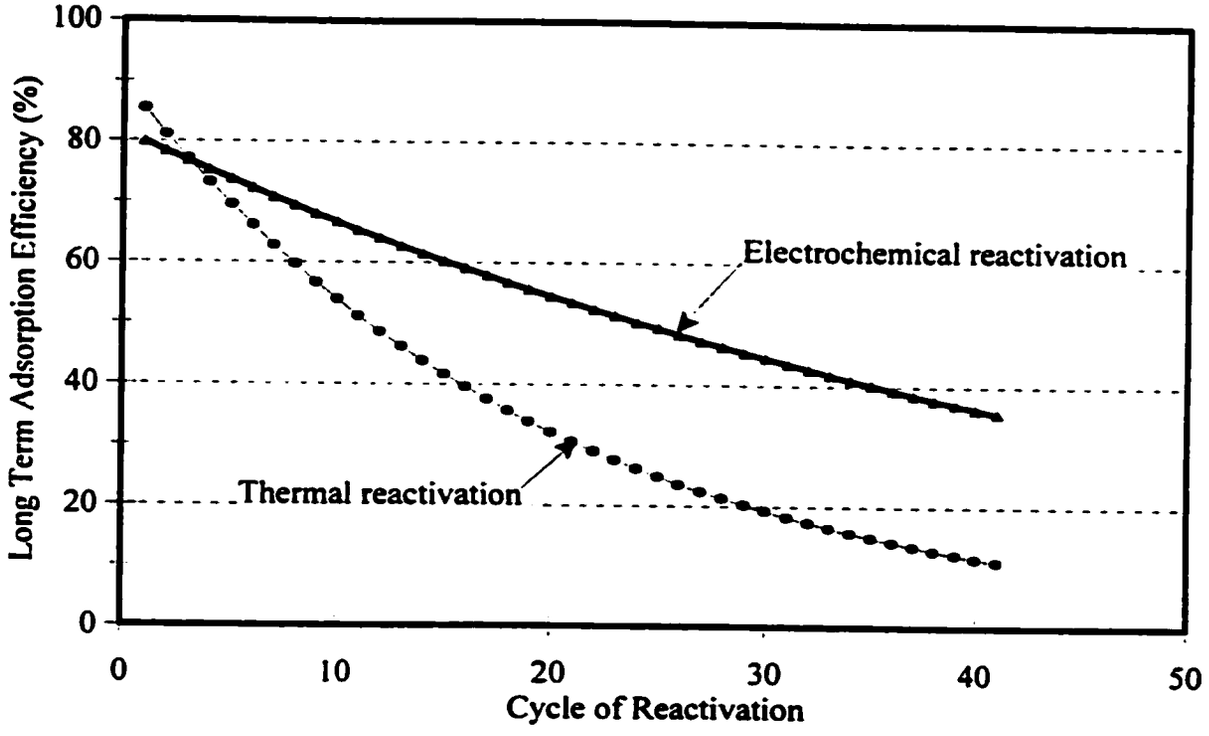

Fig. 10.1 Comparison of long-term adsorption efficiency of thermal and electrochemical reactivation.

e) the price of GAC was assumed to be $1.0/lb.

2- for electrochemical reactivation

a) only electrical inputs were considered.

3- for thermal reactivation

a) the energy costs consist of the electricity costs and the natural gas/fuel costs.

b) The reactivation was conducted in:

a. a multiple hearth furnace with a loading rate of 50 $lb/ft^2/d$.

b. a fluid bed furnace

c. an infrared furnace

c) The costs were calculated based on the data and equations presented in Clark and Lykins (1989), Adams *et al.* (1988), and Koffskey and Lykins (1990) which are presented in Table 10.1.

d) The required natural gas and electricity for the multiple hearth process are calculated from the following equations:

$$\text{Natural gas (scf/year)} = 1.864355 * 10^6 * (\text{hearth area})^{0.34169}$$

$$\text{Electrical energy (kw.hr/year)} = 92{,}617.48 * (\text{hearth area})^{0.339616}$$

The results of the evaluation are presented in Fig. 10.2 and Appendix B18. Fig. 10.2 shows that the electrochemical reactivation has lower energy costs than the fluid bed and infrared thermal reactivation for all sizes of treatment facilities. However electrochemical reactivation has lower energy costs than multiple hearth thermal reactivation for small treatment facilities. For treatment facilities with a wastewater flow rate greater than 3,500 m^3/d the multiple hearth thermal reactivation has lower energy costs.

Table 10.1 Costs of energy consumption for thermal and electrochemical reactivation.

Item	Thermal multiple hearth[1]	Thermal fluid bed[2] ($/kg of GAC)	Thermal Infrared[3] ($/kg of GAC)	Electrochemical[4] ($/kg of GAC)
Natural gas	$0.0035/scft	---	---	---
Electricity	$0.06/kw.hr	0.011	0.13	0.04
Fuel oil	---	0.0492	---	---
Total	0.036 to 0.226 ($/kg of GAC)	0.0602	0.13	0.04

[1] Source: Clark and Lykins (1989) - The total cost is calculated for flowrates of 4,000 to 250 m^3/d, respectively.
[2] Source: Adams *et al.* (1988)
[3] Source: Koffskey and Lykins (1990)
[4] Based on $0.06/kw.hr

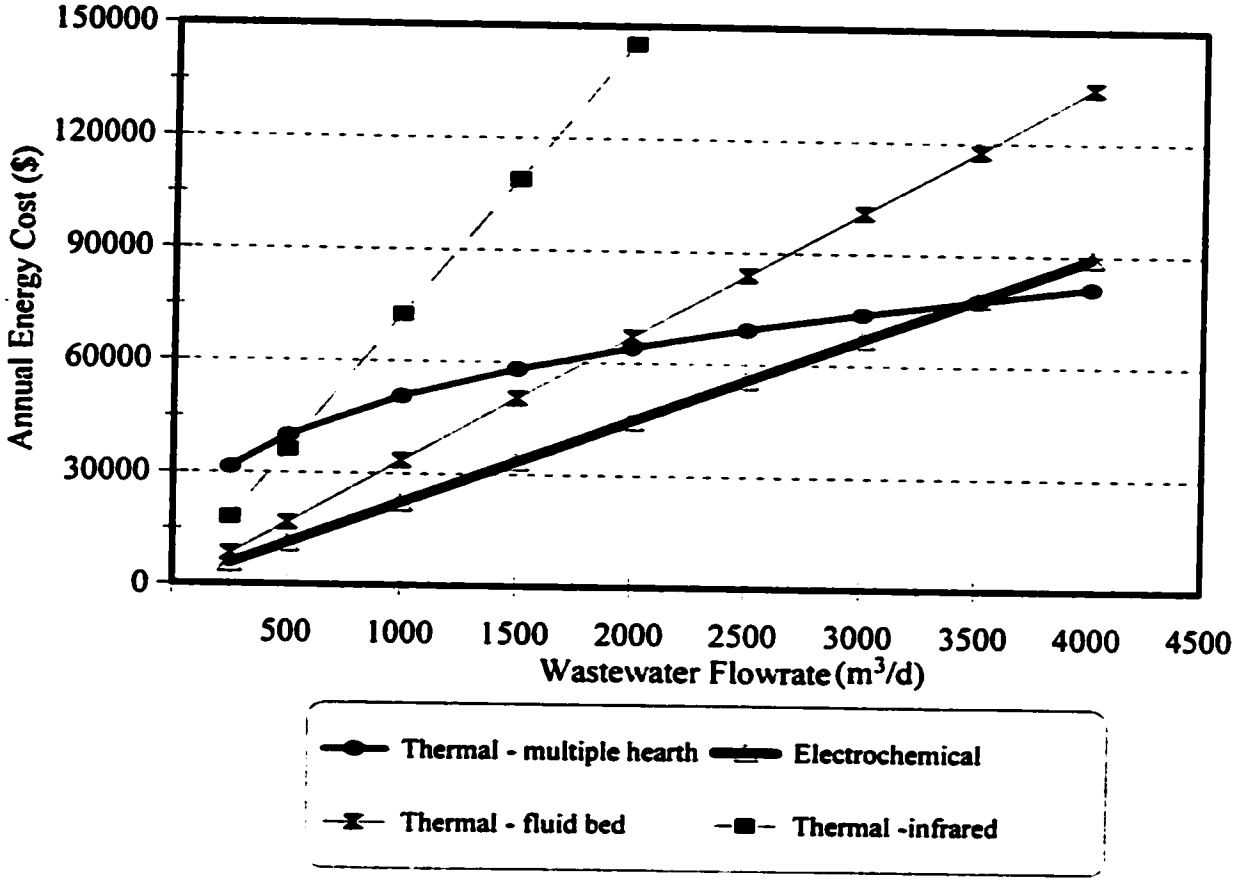

Fig. 10.2 Comparison of energy costs.

Energy costs are an important part of the reactivation operating and maintenance cost. However, according to Clark and Lykins (1989) in water treatment applications it is only about 1/3 of the cost of purchasing replacement GAC to make up for the losses in thermal reactivation. Thus the energy cost for thermal reactivation of GAC used in water treatment applications is not as important as the long-term adsorption efficiency which includes the GAC losses.

Fig. 10.3 compares the cost of energy plus the cost of purchasing new GAC to replace that destroyed in the reactivation. It was assumed that the GAC mass loss for thermal reactivation is 5% and there is no mass loss for electrochemical reactivation. Fig. 10.3 shows that electrochemical reactivation has a lower cost than multiple hearth thermal reactivation for all sizes of treatment facilities. This is due to the high cost of GAC replacement.

10.4 Discussion and Conclusion

The above are three simplistic comparisons. A more realistic comparison would also need to introduce the fact that: a) electrochemical technology would need to reactivate more frequently because of the lower reactivation efficiency; and b) the labor cost for thermal reactivation is more than that for electrochemical reactivation. The GAC replacement costs are expected to be higher than the costs for more frequent electrochemical reactivation. Labor costs for thermal reactivation are more than double that for electrochemical reactivation (Owen and Barry, 1972). Hence by including the GAC replacement and labor costs, the electrochemical reactivation will be more economical even for larger sized treatment plants.

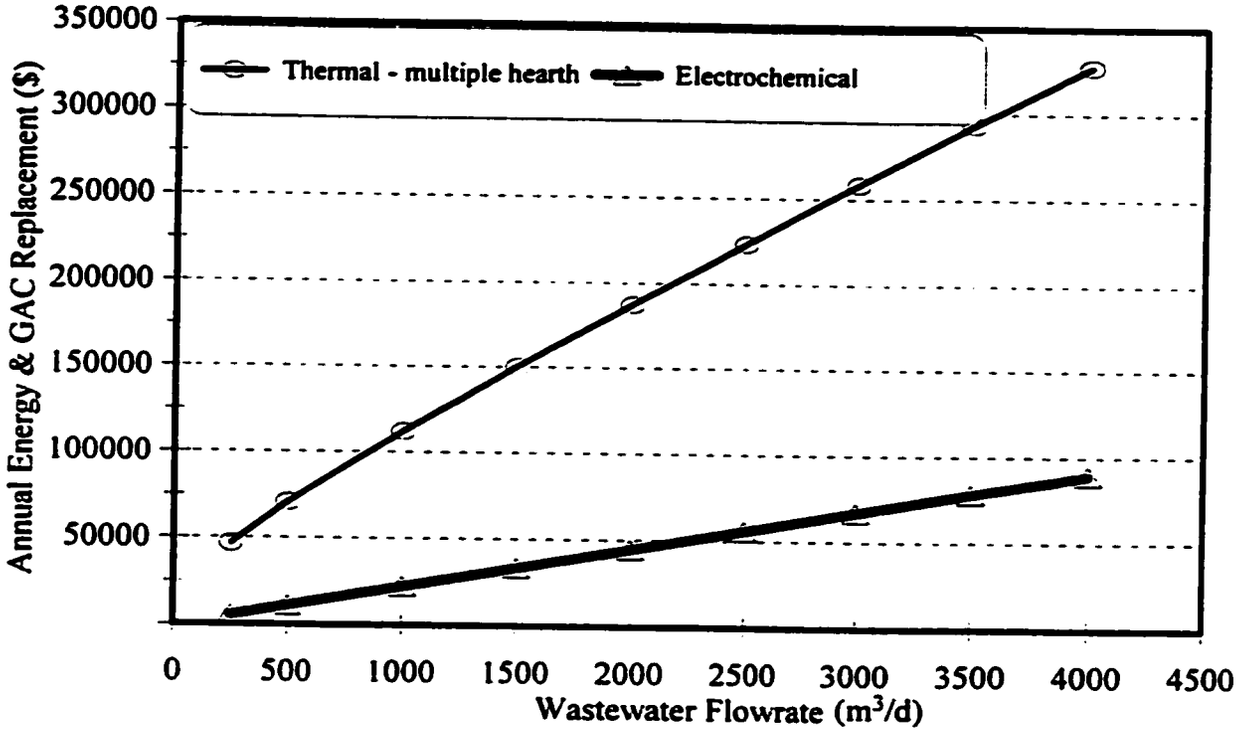

Fig. 10.3 Cost comparison of thermal and electrochemical reactivation (energy cost + GAC replacement cost).

Furthermore these costs comparison are based on the results for unoptimized electrochemical reactivation systems. For example, once the electrochemical reactor is optimized to reactivate multi-layers of GAC with relatively high reactivation efficiency the electrochemical reactivation will be even more economical.

CHAPTER 11

CONCLUSIONS AND RESEARCH RECOMMENDATIONS

11.1 Conclusions

1- Electrochemical reactivation has been shown to be feasible as reactivation efficiencies of up to 108% were reached.

2- Comparison of electrochemical and thermal reactivation showed that electrochemical reactivation has a higher long-term efficiency. Also electrochemical reactivation has less energy and GAC replacement costs and it seems to be more economical.

3- Based on studies conducted with a single layer phenol-loaded or 2NP-loaded F-400 at 50 mA, the main mechanisms responsible for electrochemical reactivation are: high-pH induced desorption at the cathode, desorption due to presence of charge on the GAC surface, and oxidation of phenolics. High-pH induced desorption at the cathode accounts for approximately 50-60% of the total reactivation, the presence of charge on the GAC particles results in an additional 25-30% reactivation, and oxidation/reduction of the phenolics accomplished about 10-20% of the total reactivation.

4- The changes in pH that occur within the electrochemical reactivation reactors are fundamental to electrochemical reactivation. Experiments showed that cathodic reactivation is more efficient than anodic reactivation due to high local pH near/at the cathode. The high pH increased the desorption driving force and resulted in higher desorption and consequently higher reactivation efficiencies.

5- Electrolyte mixing resulted in a decrease in the cathodic reactivation efficiencies, while there was no significant change in the anodic reactivation. Higher degrees of electrolyte mixing decreased the local pH at the cathode and consequently reduced the desorption driving force and therefore reduced the reactivation efficiency. Thus electrolyte mixing is not recommended.

6- Experiments on the reactivation of different numbers of layers of GAC particles showed a significant decrease in the reactivation efficiency with increasing number of layers. It was demonstrated that the decrease in reactivation efficiency was due to a need for direct contact between GAC particles and the electrode and not due to local variations in pH.

7- The reactivation efficiency (RE%) could be increased by increasing the current and/or reactivation time. The RE% increases rapidly with increasing reactivation time in the first few hours followed by a more gradual increase for longer times. Also the effect of current was very marked from 10 to 50 mA and gradual from 50 to 250 mA.

8- It was concluded that electrochemical reactivation of GAC is contaminant dependent. Comparison of the reactivation efficiencies of 2NP-loaded F-400 with phenol-loaded F-400 at different reactivation currents and times showed a similar pattern. However, 2NP-loaded F-400 showed higher reactivation efficiencies (maximum 108%) than phenol-loaded F-400 (maximum 92%). This is consistent with the full reversibility of 2NP from F-400 and partial reversibility of phenol from F-400. Reactivation of GAC loaded with NOM showed that there was a linear relation between the reactivation efficiency and reactivation time; the reactivation efficiency increased to 80% as the reactivation time increased to 25 hours. Given these results and the crucial role of desorption, the efficiency of electrochemical

reactivation of GAC loaded with different adsorbates is expected to be a function of the reversibility of the adsorbate's sorption.

9- A comparison of the reactivation of GACs showed that F-400 and WV-B performed essentially the same for the conditions tested. Darco GAC showed lower performance at higher reactivation times and/or currents. These results were in agreement with GACs conductivities. Darco GAC, which had lower conductivity comparing to F-400 and WV-B, had lower performance at higher reactivation times and/or currents. Thus, if electrochemical reactivation is considered, the selection of the GAC is important. GACs with a resistance in air as high as 13 Ω/4cm bed GAC performed well while the GAC with a resistance in air of 124 Ω/4cm bed GAC did not perform well for long reactivation times or high currents.

10- Residual high pH water within the pores of reactivated GAC particles greatly impacts the adsorption within the reloading step. It was proven that the residual high pH water within the pores of the electrochemically reactivated GAC particles raised the pH of the reloading solution beyond the pK_a of the contaminants and consequently affected the reloading capacity of the GAC and thus the calculated reactivation efficiency. Buffering of the reloaded solutions eliminated the impact of pH variation of the reloaded solutions. Experiments with buffered solutions resulted in higher reactivation efficiencies than unbuffered solutions. It was demonstrated that one alternative method to buffering the reloaded solution is the treatment of reactivated GAC before the reloading process by soaking it in buffered water for one hour.

11- Total destruction of desorbed contaminants and their by-products to CO_2 and H_2O were possible. The phenol and 2NP conversion reactions were relatively rapid and

followed first-order kinetics. Destruction of the phenol and 2NP by-products, measured as the non-phenol-TOC and non-2NP-TOC, was very slow. The rate of phenol, 2NP, and TOC destruction could be increased by increasing the applied current. It was shown that total oxidation of the by-products is only achievable at higher charges.

12- It is recommended that the GAC electrochemical reactivation should be a three step process. First, the GAC is reactivated with a relatively low current to minimize potential alterations of the GAC surface. Second, the GAC is drained and rinsed with a buffered solution. Finally, the electrolyte is treated electrochemically for an extended time at a much higher current (and possibly a different electrode) to reduce the electrolyte's TOC so that it may be reused or discharged.

10.2 Recommendations for Future Research

1- Investigate the effect of current and reactivation time on the activated carbon surface properties (surface area, pore volume, surface chemistry).

2- Study the reactivation of activated carbon loaded with organics whose adsorption and desorption are pH independent.

3- Re-evaluate the multi-layer reactivation of activated carbon by buffering the reloading solutions to eliminate the possible impact of pH variation.

4- Investigate the need for direct contact between the activated carbon particles and electrodes by using a fluidized bed or a pulsed bed reactor.

5- Investigate other electrode materials and their impact on the reactivation efficiencies and contaminant and its by-products destruction.

6- Conduct multi-cycle electrochemical GAC reactivation tests to confirm the GAC mass loss rates and reactivation efficiency.

CHAPTER 12

REFERENCES

Adams, J.Q. and Clark, R.M. (1989) "Cost estimates for GAC treatment systems", *Journal of American Water Works Association*, 81(1), 35-42.

Adams, J.Q.; Clark, R.M.; Lykins, B.W.; DeMarco, J. and Kittredge, D. (1988) "GAC treatment cost experience at two drinking water utilities", *Journal of Environmental Engineering*, 114, 944-961.

Adamson, A.W. (1982) 'Physical Chemistry', Intersience Pub., Wiley, New York, NY.

Anders, M. W. (Ed.) (1985) in 'Bioactivation of Foreign Compounds', Academic Press Inc., NY, NY, 259-281.

Andersen, A. H. (1947) "The pharmacology of activated charcoal. II. Effect of pH on adsorption by charcoal from aqueous solutions". *Acta Pharmacol. Toxicol.*, 3, 199-218.

ASTM D4607-94 (1995) 'Standard test method for determination of iodine number of activated carbon', Annual Book of ASTM Standards, Natic nal Institue of Standards and Technology, U.S. Department of Commerce, Gaithersburg, MD.

Awad, Y.M. and Abuzaid, N.S. (1999) "Electrochemical oxidation of phenol using graphite anodes". *Separation Science and Technology*, 34(4), 699-708.

Azzam, M.O.; Tahboub, Y. and Al-Tarazi, M. (1999) "Effect of counter electrode material on the anodic destruction of 4-Cl phenol solution", *Trsns IChemE.* 77(B), 219-226.

Brauch, H.J. (1984) "Adsorption von naturlichen organischen wasserinhaltsstoffen an aktivkohle" Diss., Univ. Karlsruche, Germany.

Cannon, F.S.; Snoeyink, V.L.; Lee, R.G. and Dagois, G. (1994) "Reaction mechanism of calcium-catalyzed thermal regeneration of spent granular activated carbon", *Carbon*, 32(7), 1285-1301.

Cannon, F.S.; Snoeyink, V.L.; Dagois G. and deWolf, J.R. (1993) "Effect of calcium in field-spent GACs on pore development during regeneration", *Journal of American Water Works Association*, 85(3), 76-89.

Cen, J. (1994) "Electrochemical regeneration of granular activated carbon", M.A.Sc. Thesis, Dept. of Civil Eng., University of Ottawa, Ottawa, ON, Canada.

Chettiar, M. and Watkinson, A. P. (1983) "Anodic oxidation of phenolics found in coal conversion effluents", *The Canadian Journal of Chemical Engineering*, 61, 568-574.

Chiang, P.C.; Chang, E.E. and Wu., J.S. (1997) "Comparison of chemical and thermal regeneration of aromatic compounds on exhausted activated carbon", *Water Science and Technology*, 35(7), 279-285.

Clark, R.M. and Lykins, B.W. Jr. (1989) in 'Granular Activated Carbon; Design, Operation and Cost', Lewis Publisher, Boca Raton, FL.

Comninellis C. and Nerini, A. (1995) "Anodic oxidation of phenol in the presence of NaCl for wastewater treatment", *Journal of Applied Elechtrochemistry*, 25, 23-28.

Comninellis C. and Plattner, E. (1988) "Electrochemical water water treatment", *Chimia*, 42, 250-254.

Cooney, D.O. and Wijaya, J. (1987) "Effect of pH and added salts on the adsorption of ionizable organic species onto activated carbon from aqueous solution", Proc. 2nd Eng. Found. Conf. Fundam. Adsorpt., p.185-194. Liapis, A., I. (ed) Eng. Found.: NY, NY.

Cooney, D.O.; Nagerl, A. and Hines, A.L. (1983) "Solvent regeneration of activated carbon", *Water Research*, 17, 403-410.

Coughlin, R.W. and Ezra, F.S. (1968) "Role of surface acidity in the adsorption of organic pollutants on the surface of carbon", *Environmental Science & Technology*, 2(4), 291-297.

Coughlin, R.W. and Tan, R.N. (1968) "Role of functional groups in adsorption of organic pollutants on carbon", *Chem. Eng. Progress Symp. Series*, Vol. 64(90) 207-214.

Coughlin, R.W.; Ezra, F.S. and Tan, R.N. (1970), "Effects of surface groups on adsorption of pollutants", *Journal of Colloid Interface Science.*, 28, 386.

Crittenden, J.C. and Weber, W.J. (1978) "Model for Design of multicomponent adsorption systems", *Journal of Environmental Division. ASCE*, 104, 1175.

Dabrowski, A.; Mieluch, J.; Sadkaoski, A.;Wild, J. and Zoltowski, P. (1975) "A pilot plant study of electrochemical phenol waste purification", *Przemysl Chemiczny*, 54(11), 653-655.

Davis, J. (1980) in 'Contaminants and Sediments', (R. A. Baker, Ed.), Vol. 2. Ann Arbor Science, Ann Arbor, MI.

Ding, J.; Snoeyink, V.L.; Larson R.A.; Recktenwalt, M. A. and Wedeking C. A. (1987) "Effects of temperature, time, and biomass on wet air regeneration of carbon", *Journal of Water Pollution Control Federation*, 59(3), 139-144.

Dubinin, M.M. (1966) "Porous structure and adsorption properties of active carbons", in 'Chemistry and Physics of Carbon', Vol.2, (Edited by P.L. Walker), Marcel-Dekker Inc.,New York, NY.

Famularo, J.; Muller, J.A. and Pannu, A.S. (1980) "Prediction of carbon column performance from pure-solute data", *Journal of Water Pollution Control Federation*, 52(7), 2019-2032.

Faust, S. D. and Aly, O.M. (1987) in 'Adsorption Processes for Water Treatment', Butterworth Publishers, Stoneham, MA.

Ferro-Garcia, M.A.; Utrera-Hidalgo, E.; Rirera-Utrilla, J. and Moreno-Castilla, C. (1993) "Regeneration of activated carbons exhausted with chlorophenols". *Carbon*, 31(6), 857-863.

Fox, R.D.; Keller, R. T.; Pinamount C. J. and Severson J. L. (1970) "Purification of a waste brine by carbon adsorption with emphasis on wastewater reuse", Proc. 25th Ind. Waste Conf., Purdue Univ., West Lafayette, IN, 322-330.

Gattrell, M. and Kirk, D.W. (1990) "The electrochemical oxidation of aqueous phenol at a glassy carbon electrode", *The Canadian Journal of Chemical Engineering*, 68, 997-1003.

Gomez Serrano, V.; Beltran, F. J. and Duran Segovia, A. (1992) "Adsorption of p-nitrophenol from aqueous solution on activated carbon. Influence of pH and preozonization", *Chemical Engineering Technology*, 15(2), 124-130.

Goto, M.; Hayashi, N. and Goto, S. (1986) "Adsorption and desorption of phenol on anion-exchange resin and activated carbon", *Environmental Science and Technology*, 20, 463-467.

Graham, D.J. (1955) "Characterization of physical adsorption systems. III. The separate effects of pore size and surface acidity upon the adsorbent capacities of activated carbons" *Journal of Physical Chemistry*, 59, 896-900.

Ha, S.R.; Vinitnantharat, S. and Ozaki, H. (2000) "Bioregeneration by mixed microorganisms of granular activated carbon loaded with a mixture of phenols". *Biotechnology Letters.*, 22(13), 1093-1096.

Herzing, D.R.: Snoeyink, V.L. and Wood, N.F. (1977) "Activated carbon adsorption of odorous compound 2-methylisoborneol and geosmin", *Journal of American Water Works Association*, 69(4), 223.

Himmelstein, K. J.; Fox, R. D. and Winter, T. H. (1973) "In-place regeneration of activated carbon", *Chemical Engineering Progress*, 69(11), 65-69.

Hutchinson, D.H. and Robinson, C.W. (1990a) "A microbial regeneration process for granular activated carbon-I. process modelling", *Water Research*, 24, 1209-1215.

Hutchinson, D.H. and Robinson, C.W. (1990b) "A microbial regeneration process for granular activated carbon-II. regeneration studies", *Water Research*, 24, 1217-1223.

Iotov, P.I. and Kalcheva, S.V. (1998) "Mechanistic approach to the oxidation of phenol at a platinum/gold electrode in an acid medium", *Journal of Electroanalytical Chemistry*, 442, 19-26.

Jawaid, M.N.A. and Weber, T.W. (1979) "Effect of mineral salts on adsorption and desorption of activated carbon", *Carbon*, 17, 97-101.

Karimi-Jashni, A. (1994) "Effect of pH on adsorption and desorption equilibria and kinetics of 2-nitrophenol and phenol onto two activated carbon", M.A.Sc. Thesis, Dept. of Civil Eng., University of Ottawa, Ottawa, ON, Canada.

Karimi-Jashni, A. and Narbaitz, R.M. (1997) "Impact of pH on adsorption and desorption kinetics of 2-nitrophenol on activated carbons", *Water Research*, 31(12), 3039-3044.

Karimi-Jashni, A. and Narbaitz, R.M. (1995) "Impact of pH on adsorption and desorption equilibria of phenols on activated carbons", Canadian Society for Civil Engineering, 1995 Annual Conference Proceedings, Volume IV, 105-114.

Kastening, B.; Schiel, W. and Henschel, M. (1985) "Electrochemical polarization of activated carbon and graphite powder suspensions", *Journal of Electroanal. Chem.*, 191, 311-328.

Khabalov, V.V.; Morgun, N.P.; Zhidachevskaya, V.L.; Artem'yanov, A.P. and Glushchenko, V.Yu. (1989) "Electrochemical regeneration of carbon adsorbents with various pore structures", *Khimiya i Tekhnologiya Vody*, 11(7), 597-600.

Khan, K.A.; Suidan, M.T. and Cross. W.H. (1981) "Anaerobic activated carbon filter for the treatment of phenol-bearing wastewater", *Journal of Water Pollution Control Federation*, 53(10), 1519-1532.

Kim, B. R., Chian, E. S. K., Cross, W.H. and Cheng, S-S. (1986) "Adsorption, desorption, and bioregeneration in an anaerobic, granular activated carbon reactor for the removal of phenol", *Journal of Water Pollution Control Federation*, 58(1), 35-40.

Kirk, D.; Sharifian, H. and Floukes, F. (1985) "Anodic oxidation of aniline for waste water treatment", Journal Appl. Electrochem., 15, 285-290.

Knappe, D.R.U.; Snoeyink, V.L.; Dagois, G. and DeWolfe, J.R. (1992) "Effect of calcium on thermal regeneration on GAC", *Journal of American Water Works Association*, 84(8), 73-80.

Koffskey, W.E. and Lykins, B.W. (1990) " GAC adsorption and infrared reactivation: a case study", *Journal of American Water Works Association*, 82(1), 48-56.

Kotz, R.; Stucki, S. and Carcer, B. (1991) "Electrochemical waste water treatment using high overvoltage anodes. Part I: Physical and electrochemical properties of SnO_2 anodes", *Journal of Applied Electrochemistry*, 21, 14-20.

Kudo, A. and Wayner, D. (1990) "Electrochemical degradation of chlorophenols", Canadian Patent Application, No. 2027374.

Kuhl, H.; Jockers, R.; Klein, J. and Juntgen, H. (1986) "Role of surface oxides and pore structure of activated carbon in adsorption from aqueous solutions", Proc. Carbon'86, Baden, BRD, 318-353.

Kuo, J.F.; Stahl J.F.; Chen, C.L. and Bohlier, P.V. (1998) "Dual role of activated carbon process for water reuse"' *Water Environment Research*, 70,(2), 161-170.

Leyva-Ramos, R. (1989) "Effect of temperature and pH on the adsorption of an anionic detergent on activated carbon", *Journal of Chem. Technology and Biotechnology*, 45(3), 231-240.

Lazareva, L.P.; Lisitskaya, I.G.; Gorchakova, N.K. and Khabalov, V.V. (1991) "Investigation of patterns of electrochemical regeneration of carbon sorbents after adsorption of dyes", *Khimiya i Tekhnologiya Vody*, 13(11), 980-983.

Lowry, J. D. and Burkhead, C. E. (1980) "The role of adsorption in biologically extended activated carbon columns", *Journal of Water Pollution Control Federation*, 52(2), 389-398.

Magne, P. and Walker, P. L. Jr. (1986) "Phenol adsorption on activated carbon: Application to the regeneration of activated carbons polluted with phenol", Carbon, 24(2), 101-107.

Martin, R.J. and Ng., W.J. (1984) "Chemical regeneration of exhusted activated carbon-I", *Water Research*, 18, 59-73.

Martin, R.J. and Ng., W.J. (1985) "Chemical regeneration of exhusted activated carbon-II", *Water Research*, 19, 1527-1535.

Mattson, J. S. and Mark, H.B. Jr. (1971) 'Activated Carbon', Marcel Dekker, Inc., NY, NY.

Matsumura, Y.; Yamabe, K. and Takahashi, H., (1985) "The effect of hydrophilic structures of active carbon on the adsorption of benzene and methanol vapors", *Carbon* 23(3), 263-271.

Mehta, P. M. and Flora, J.R.V. (1997) "Effect of electrochemical treatment of granular activated carbon on surface acid groups and the adsorptive capacity for phenol", *Water Research*, 31(12), 2171-2176.

Modell, M.; deFilippi, R. P. and Krukonis, V. (1980) "Regeneration of activated carbon with supercritical carbon dioxide" in Activated Carbon Adsorption of Organics from the Aqueous Phase (Edited by Suffet, I. H. and McGuire M. J.), Vol. 1-Ann Arbor Science, Ann Arbor, MI.

Montgomery, H. and Welkom, L.M. (1990) Groundwater Chemicals Desk Reference, Lewis Publishers, inc., Chelsea, MI.

Mortimer, C. E. (1979) Chemistry a Conceptual Approach, Fourth edition. D. Van Nostrand Company, NY, NY.

Muller, G.; Radke, C.J. and Prausnitz, J.M. (1980) "Adsorption of weak organic electrolytes from aqueous solution on activated carbon", *Journal of Physical Chemistry*, 84(4), 369-376.

Mundale, V.D.; Joglekar, H.S.; Kalam, A. and Joshi, J.B. (1991) "Regeneration of spent activated carbon by wet air oxidation" *The Canadian Journal of Chemical Engineering*, 69, 1149-1159.

Murphy, O.J.; Hitchens, D.G.; Kaba, M. and Verostko, C.E. (1992) "Direct electrochemical oxidation of organic for wastewater treatment", *Water Research*, 26, 443-451.

Narbaitz, R.M. (1985) "Modeling the competitive of 1,1,2-trichloroethane with naturally occuring background organics onto activated carbon", Ph.D. Thesis, Dept. of Chemical Engineering, McMaster University, ON, Canada.

Narbaitz, R.M. and Benedek, A. (1994) "Adsorption of 1,1,2--Trichloroethane from River Water", *Journal of Environmental Engineering, ASCE*, 120(6), 1400-1415.

Narbaitz, R.M. and Cen, J-Q. (1997) "Alternative methods for determining the percent regeneration of activated carbon", *Water Research*, 31(10), 2532-2542.

Narbaitz, R.M. and Cen, J-Q. (1994) "Electrochemical regeneration of activated carbon" *Water Research*, 28(8), 1771-1778.

Newcombe, G. and Drikas, M. (1993) "Chemical regeneration of granular activated carbon from an operating water treatment plant", *Water Research*, 27, 161-165.

Ning, Z. (1997) 'Modeling of Simultaneous removal of easily degradable substrates and chlorinated phenols in UASB reactors', Ph.D. Thesis, Dept. of Civil Eng., University of Ottawa, Ottawa, ON, Canada.

Oda, H.; Sugawara, T.; Kikuchi, K.L. and Konno, H. (1981) "Adsorption of benzoic acid and phenol from aqueous solution by activated carbons: Effect of surface acidity", *Carbon* 19(4), 243-248.

Oxenford, J.L. and Lykins, B.W. Jr. (1991) "Conference summary: Practical aspects of the design and use of GAC", *Journal of American Water Works Association*, 83(1), 58-64.

Owen, P.H. and Barry, J.P. (1972) "Electrochemical carbon regeneration", EPA 670/2-75028. U.S. EPA, Washington, D.C., PB 239 156, p43.

Peel, R.G. (1980) "The roles of slow adsorption and biological activity in activated carbon modelling", Ph.D. Thesis, Dept. of Chemical Engineering, McMaster University. Hamilton, ON, Canada.

Peel, R.G. and Benedek, A. (1980-a) "Equilibrium attainment in activated carbon isotherm studies", *Environmental Science & Technology*, 14, 66.

Peel, R.G. and Benedek, A. (1980-b) "Dual rate kinetic model of fixed bed adsorber". *Journal of Environmental. Engineering Div., ASCE*, 106(4), 797-813.

Picht, R.D.; Dillman, T.R.; Burke, D.J. and deFilippi, R.P. (1982) "Regeneration of adsorbents by a supercritical fluid", *The American Institute of Chemical Engineers Symposium Series*, 78(219), 136-149.

Pirbazari, M. and Weber,W.J. (1981-a) "Adsorption of polychlorinated biphenyls from water by activated carbon", in Chemistry in Water Reuse, Vol.2, Cooper, W.J., (ed).; Ann Arbor Science Publishers: Ann Arbor, MI.

Pirbazari, M. and Weber,W.J. (1981-b) "Adsorption of benzene from water by activated carbon", in Chemistry Water Reuse, Vol.2, Cooper, W.J., (ed).; Ann Arbor Science Publishers, Ann Arbor, MI.

Prober, R.; Pyeha, J. J. and Kidon, W. E. (1975) "Interaction of activated carbon with dissolved oxygen", *AICHE J.*, 21(6), 1200-1204.

Randtke, S. J. and Jepsen, C. P. (1982) "Effect of salts on activated carbon adsorption of fulvic acids", *Journal of American Water Works Association*, 74(2), 84.

Razzaghi, M. (1976) "The competitive adsorption of carbohydrates, proteins, and lignosulfonates on activated carbon". M.Eng. Thesis, Dept. of Chemical Engineering, McMaster University, Hamilton, Ontario, Canada.

Rinkus, K.; Reed, B.E. and Lin, W. (1997) "NaOH regeneration of Pb and phenol-laden activated carbon. 1. Bath study results", *Separation Science and Technology*, 32(14), 2367-2384.

Sasaki, K.; Kunai, A.; Harada, J. and Nakabori, S. (1983) "Electrolytic hydrogenation of phenols in aqueous acid solutions", *Electrochimica Acta*, 28(5), 671-674.

Schmal, D.; van Erkel, J. and van Duin, P.J. (1986) "Electrochemical reduction of halogenated compounds in process wastewater", The Institution of Chemical Engineers Symposium Series, no 98 (Electrochemical Engineering), 281-291.

Schuliger, W.G. and MacCrum, J.M. (1974) "Granular activated carbon reactivation system design and operating conditions", *AIChE symposium Series, Water-1974. I. Industrial waste treatment.* 70(144), 352-359.

Schuliger, W.G.; Riley, G.N. and Wagner, N.J. (1987) "Thermal reactivation of granular activated carbon: a proven technology". *Proceeding of 1987 AWWA Ann. Conf., Sunday Seminar: Treatment problems for the control of synthetic organic chemicals. Kansas City, MO.* 96-133.

Schultz, J.R. (1982) "PACT Process Mechanism", Ph.D. Thesis, Clemson University, Clemson, SC, USA.

Scott, K. (1995) Electrochemical Process for Clean Technology, Hartnolls Ltd., Bodmin, Cornwall, UK.

Sebastiani, E.G.; Snoeyink, V.L. and Angelotti, R.W. (1994) "Thermal regeneration of spent and acid-washed GAC from the Upper Occoquan Sewage Authority'. *Water Environment Research*, 66(3), 199-205.

Seidel, A. and Radeke, K. H. (1990) "Effect of pH on adsorption equilibria for dissolved weak organic electrolytes on activated carbon", *Acta Hydrochem. Hydrobiol.*, 18(6), 691-699.

Semmens, M. J.; Norgaard, G. E.; Hohenstein, G. and Staples, A. B. (1986) "Influence of pH on the removal of organics by granular activated carbon", *Journal of American Water Works Association*, 78(5), 89-93.

Sharifian, H. and Kirk, D.W. (1986) "Electrochemical oxidation of phenol", *Electrochemical Science and Technology*, 133(5), 921-924.

Sigurdson, S.P. and Robinson, C. W. (1978) "Substrate-inhibited microbiological regeneration of granular activated carbon", *The Canadian Journal of Chemical Engineering*, 56, 330-339.

Singer, P.C. and Yen, C. (1980) "Adsorption of alkyl phenols by activated carbon", Chapter 8 in Activated Carbon Adsorption of Organics from the Aqueous Phase, Volume 1, I.H Suffet and M.J., McGuire(ed.), Ann Arbor Science, Ann Arbor, MI.

Slavinskii, A.S.; Velikaya, L.P.; Karimova, A.M. and Baturin, A.P. (1984) "Electrochemical regeneration of activated carbon saturated with p-nitrotoluene", *Khimiya i Tekhnologiya Vody*, 6(6), 509-511.

Smith de Sucre, V. and Watkinson, A.P. (1981) "Anodic oxidation of phenol for wastewater treatment", *The Canadian Journal of Chemical Engineering*, 59, 52-59.

Snoeyink, V.L. (1968) "Adsorption of strong acids, phenol and 4-Nitrophenol from aqueous solution", Ph.D. Thesis, Dept. of Civil Eng., University of Michigan, Ann Arbor, MI.

Snoeyink, V.L. (1990) "Adsorption of organic compounds", Chapter 13 in AWWA Water Quality and Treatment, McGraw-Hill Inc., New York, NY, 781-875.

Snoeyink, V.L.; La, H.T.; Johnson, J.H. and Young, J.F. (1974) "Active carbon dechlorination and the adsorption of organic compounds", In A. Rubin (ed.) Chemistry of Water Supply, Treatment and Distribution, Ann Arbor Science, Ann Arbor, MI.

Snoeyink, V.L.; Weber, W.J. Jr. and Mark, H.B. (1969) "Sorption of phenol and nitrophenol by activated carbon". *Environmental Science & Technology*, 3, 918.

Sontheimer, H.; Crittenden, J. C. and Summers, R. S. (1988) Activated Carbon for Water Treatment, 2th ed., Druckerei G.Braun Gmbh, Karlsruhe, FRG.

Speitel, G.E. Jr. and DiGiano, F.A. (1987) "Bioregeneration of GAC used to treat micropollutants", *Journal American Water Works Association*, 79(1), 64-73.

Srivastava S. K. and Tyagi R. (1995) "Organic desorption and chemical regeneration of spent carbon developed from fertilizer waste slurry", *Journal of Enivironmental Engineering. (ASCE)*, 121, 186-193.

STM 5310B (1992) 'Total organic carbon: combustion-infrared method', Standard Methods For The Examination of Water and Wastewater, EPS Group, Inc., Hanover, Maryland.

Suidan, M.T.; Cross W.H.; Fong, M. and Calvert, J.W. (1981) "Anaerobic carbon filter for degradation of phenols", *Journal of the Environmental Engineering Division, ASCE*, 107, EE3, 563-579.

Summers, R.S. (1986) "Activated carbon adsorption of humic substances: Effect of molecular size and heterodispersity, Ph.D. Thesis, Dept. of Civil Engineering, Stanford University, Stanford, CA.

Summers, R. S. and Roberts, P.V. (1988-a) "Activated carbon adsorption of humic substances. I. Heterodisperse mixtures and desorption", *Journal of Colloid Interface Science.*, 122(2), 367-381.

Summers, R. S. and Roberts, P.V. (1988-b) "Activated carbon adsorption of humic substances. II. Size exclusion and electrostatic interaction", *Journal of Colloid Interface Science*, 122(2), 382-397.

Sveshnikova, D.A.; Ramazanov, A. K.; Aliev, Z.M., Shakhnazarov, T.A.; Kamalutdinova, I.A. and Babaev, M.-S. (1987) "Electrochemical regeneration of activated carbon", *Khimiya i Tekhnologiya Vody*, 9(5), 466-467.

Suzuki, Y. and Takeuchi, Y. (1986) "Effect of pH on adsorption equilibria for a few systems of aqueous dissolved single or binary organic weak electrolytes and activated carbon", *Journal of Chemical Engineering of Japan*, 19(4), 307-311.

Taher, N.B. and Savall, A. (1999) "Electrochemical degradation of phenol in aqueous solution on bismuth doped lead dioxide: a comparison of the activities of various electrode formulations", *Journal of Applied Electrochemistry*, 29, 277-283.

Tan, C-S. and Liou, D-C. (1989) "Regeneration of activated carbon loaded with toluene by supercritical carbon dioxide", *Separation Science and Technology*, 24(1&2), 111-127.

Uranowski, L.J.; Tessmer, C.H. and Vidic, R.D. (1998) "The effect of surface metal oxides on activated carbon adsorption of phenolics", *Water Research*, 32(6), 1841-1851.

U.S. Environmental Protection Agency (1973) "Process design manual for carbon adsorption", EPA 625/1-71-002a. USEPA Technology Transfer, Cincinnati, OH.

Van der Loop, S.L.; Suidan, M.T.; Berchtold, S.R.; Moteleb, M.A. and Maloney, S.W. (1997) "Effects of molecular oxygen on GAC adsorption of energetics", *Water Science and Technology*, 35(7), 197-204.

Van Vliet, B.M. and Venter, L. (1984) "Infrared thermal regeneration of spend carbon from water reclamation", *Water Science and Technology*, 17, 1029-1042.

Vidic, R.D.; Suidan; M.T., Traegner,U.K. and Nakhla, G.F. (1990) "Adsorption isotherms: illusive capacity and role of oxygen", *Water Research*, 24(10), 1187-1195.

Vidic, R.D.; Suidan, M.T.; Sorial, G.A. and Brenner, R.C. (1993) "Molecular oxygen and the adsorption of phenols-effect of functional groups", *Water Environment Research*, 65, 156-161.

Waer, M.A. and Snoeyink, V.L. (1994) "Effects of oxidant on thermal regeneration of granular activated carbon", *Journal of Environmental Engineering*, 120(1), 190-201.

Waer, M.A.; Snoeyink, V.L. and Mallon, K.L. (1992) "Carbon regeneration dependence on time and temperature", *Journal of American Water Works Association*, 84(3), 82-91.

Wallis, D.A. and Bolton, E.E. (1982) "Biological regeneration of activated carbon", *AIChE Symposium Series*, 78, 64-70.

Ward, T.M. and Getzen, F.W. (1970) "Influence of pH on the adsorption of aromatic acids on activated carbon", *Environmental Science & Technology*, 4(1), 64-67.

Weber, W.J. Jr. (1972) Physicochemical Processes for Water Quality Control. John Wiley and Sons, Inc., NY, NY.

Weber, W. J. and Morris, J. C. (1963) "Kinetics of adsorption on carbon from solution", *Journal of the San. Eng. Div., ASCE* April 1963, 31-35.

Wedler, G. (1976) Chemisorption: An Experiment Approach., Butterworths publishers Inc., Boston, MA, 22-32.

Wills, G.B. (1971) "Electrochemical activation and regeneration of carbon surface for tertiary water treatment". United States Department of the Interior, Office of Water Resources Research. PB-202 628. P9.

Yenkie, M.K.N. and Natarajan, G. S. (1993) "Determination of specific surface area of granular activated carbon by aqueous phase adsorption of phenol and from pore size distribution measurements", *Separation Science and Technology*, 28(5), 1177-1190.

Ying, W. (1978) "Investigation and modeling of bio-physicochemical processes in activated carbon columns", Ph.D. Thesis, University of Michigan, Ann Arbor, MI.

Young, D.M. and Crowell, A.D. (1962) Physical Adsorption of Gases, Butterworths. London, UK.

Yonge, D. R.; Keinath, T. M.; Pozananska, K. and Jiang, Z. P. (1985) "Single-solute irreversible adsorption on granular activated carbon", *Environmental Science & Technology* 19(8), 690-694.

Youssef, A.M.; Ghazy, T.M. and El-Nabarawy, T. (1982) "Moisture sorption by modified-activated carbons", *Carbon*, 20(2), 113-116.

Zogorski, J.S. and Faust, S.D. (1978) "Equilibria of adsorption of phenols by granular activated carbon", Chapter 9 in Chemistry of Wastewater Technology. A.J.Rubin, ed. Ann Arbor Science Publishers, Ann Arbor, MI, p.143.

Zogorski, J.S. and Faust, S.D. (1976-a) "The effect of phosphate buffer on the adsorption of 2.4-dichlorophenol and 2,4-dinitriphenol", *Journal of Environmental Science Health*, All(8&9),501-515.

Zogorski, J.S. and Faust, S.D. (1976-b) "The kinetics of adsorption of phenols by granular activated carbon", *Journal of Colloid Interface Science*, 55(2), 329-341.

Zogorski, J. S. (1975) "The adsorption of phenols onto granular activated carbon from aqueous solution", Ph.D. Thesis, Dept. of Environmental Sciences, Rutgers University, New Brunswick, NJ.

Appendix A1

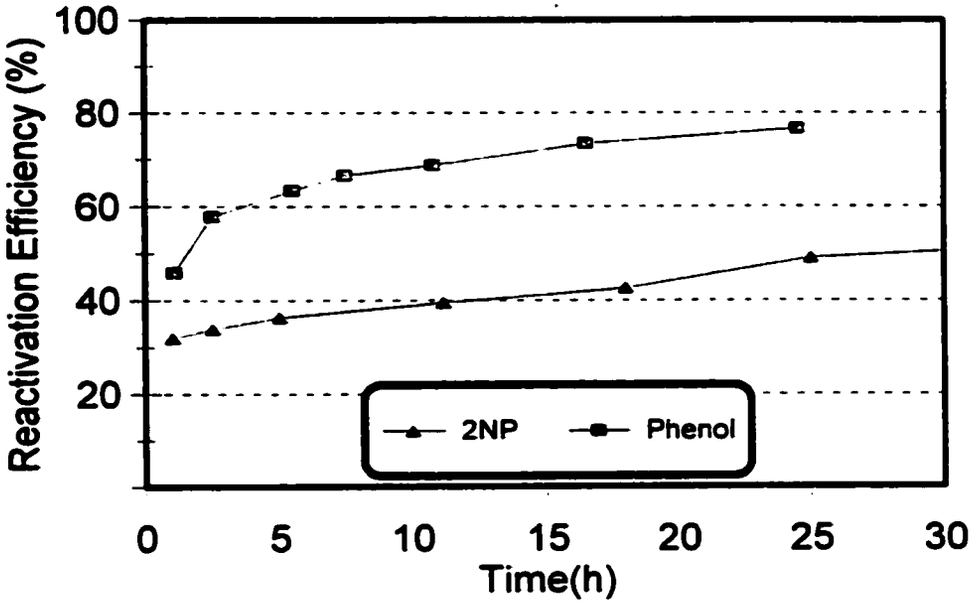

Comparison of reactivation of WV-B loaded with 2NP and phenol at 50 mA.

Appendix A2

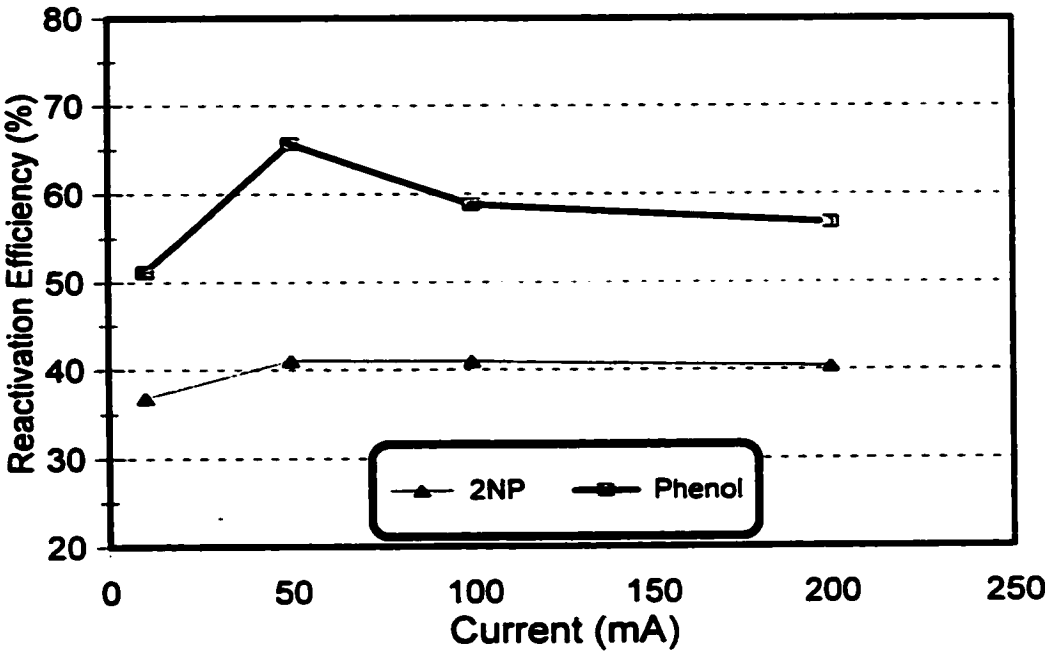

Comparison of reactivation of Darco loaded with 2NP and phenol after 5 hours of reactivation.

Appendix A3

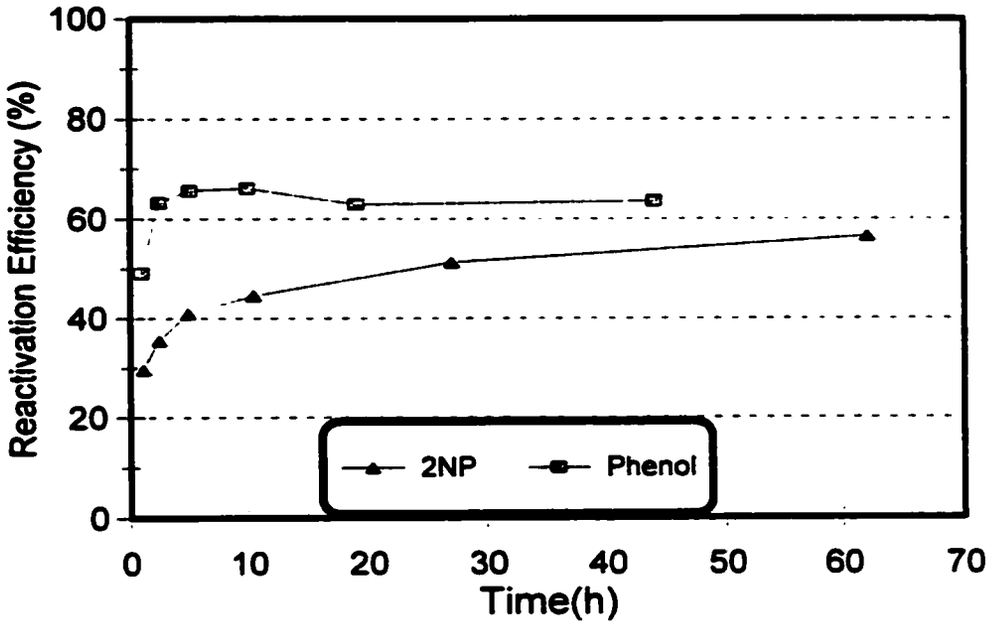

Comparison of reactivation of Darco loaded with 2NP and phenol at 50 mA.

Appendix A4

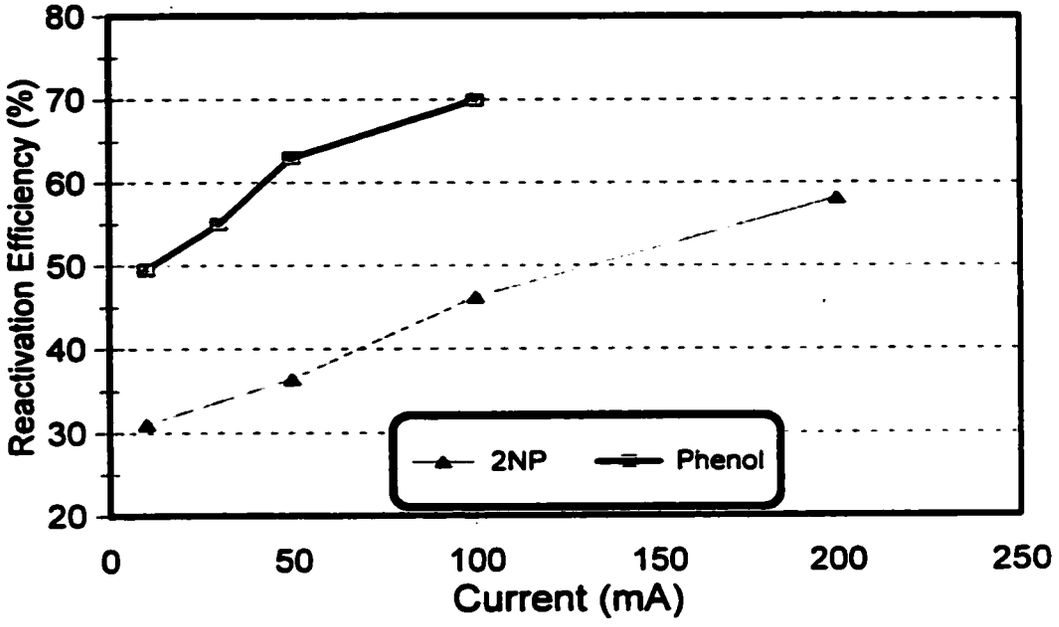

Comparison of reactivation of WV-B loaded with 2NP and phenol after 5 hours of reactivation.

Appendix A5

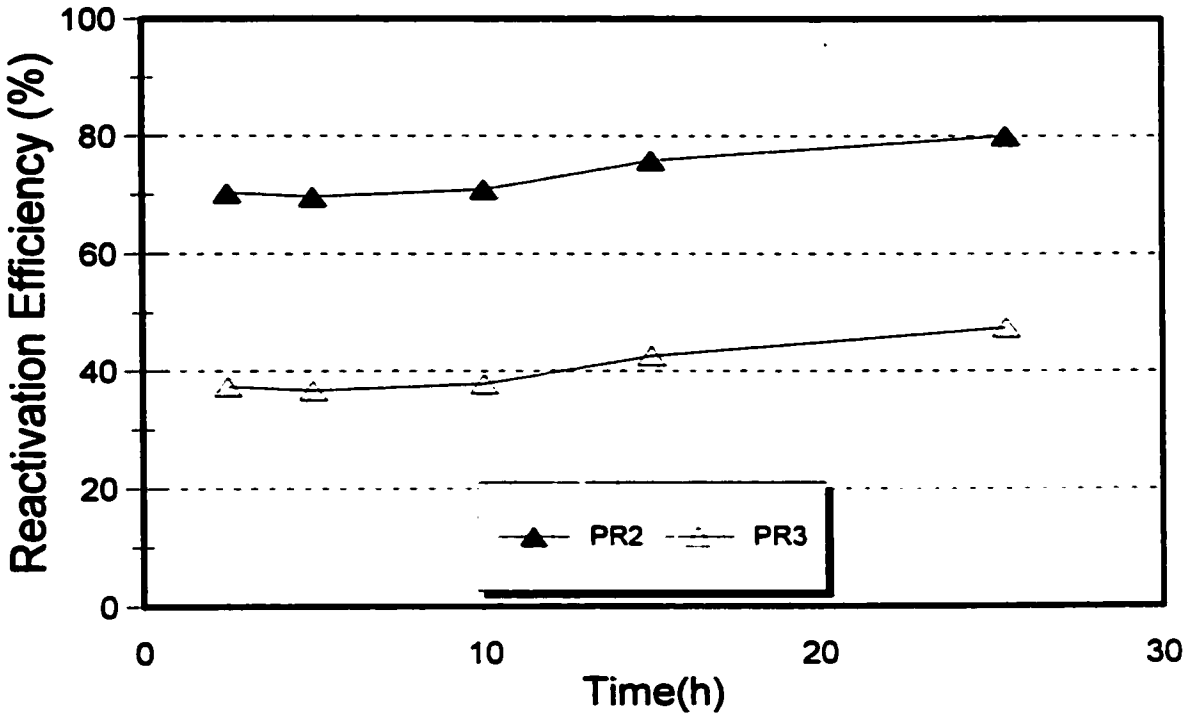

Comparison of RE2 and RE3 methods (cathodic, 2NP, F-400, 50 mA).

Appendix A6

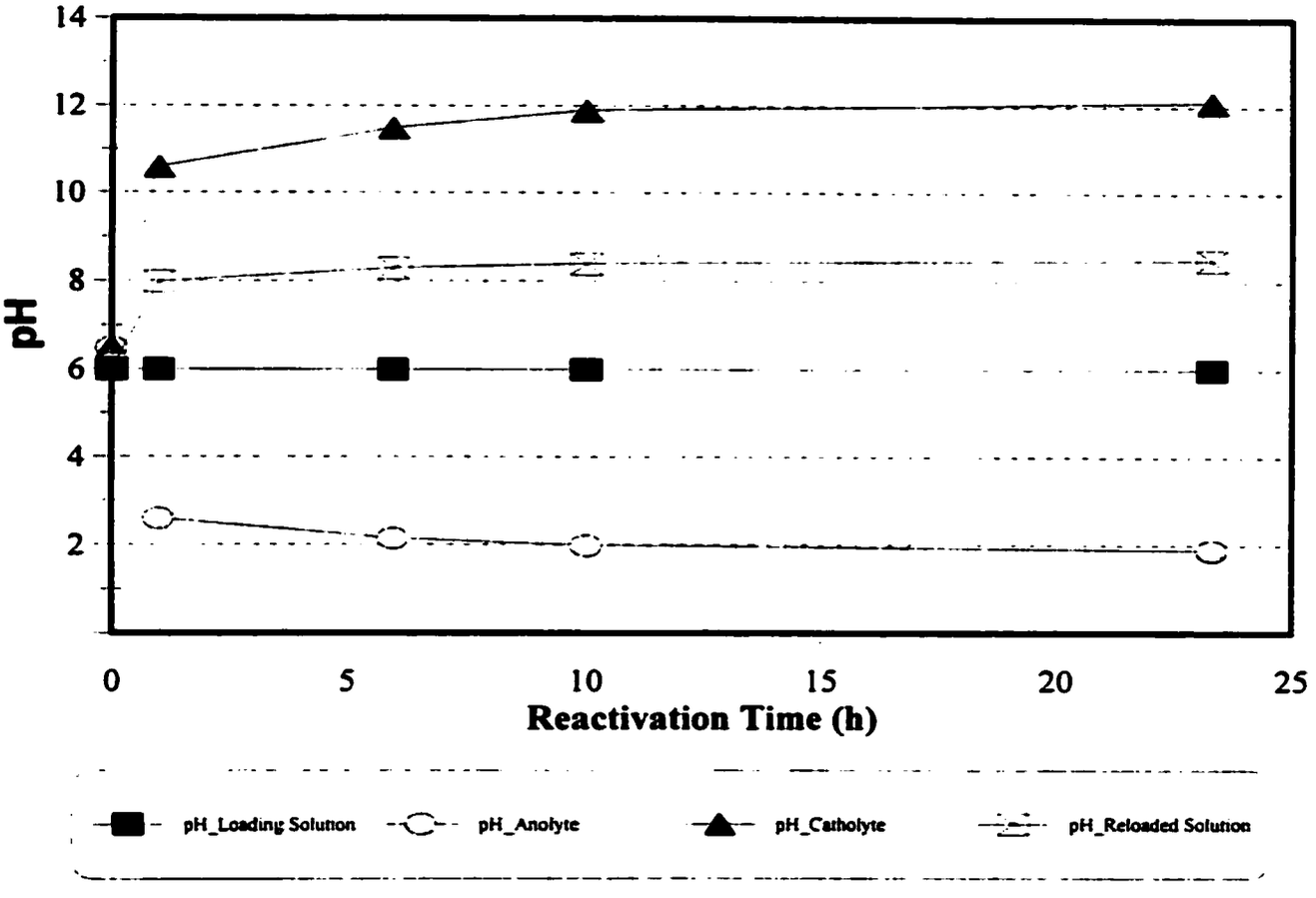

pH variation within the electrolyte, loading, and reloading solutions (catholic, 2NP, F-400, divided-cell).

Appendix A7

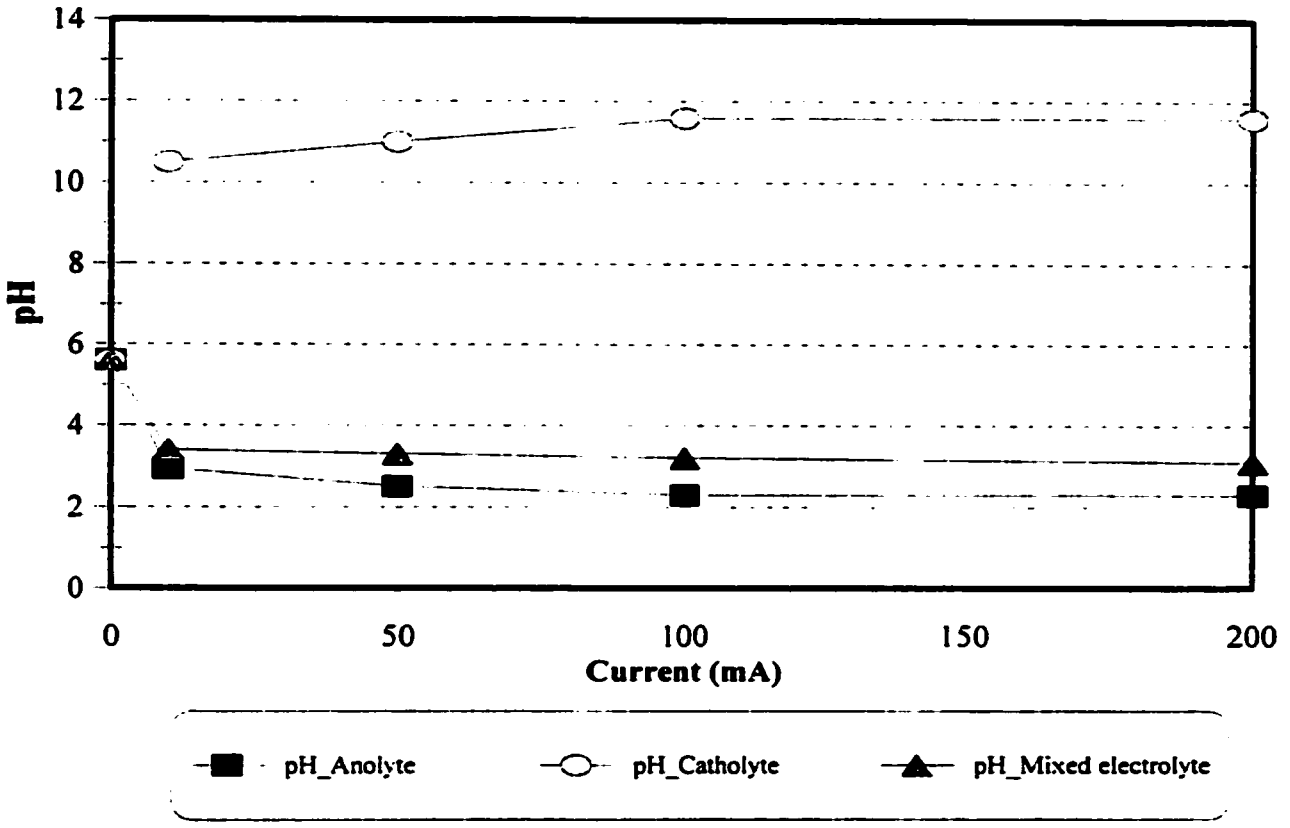

pH variation within the reactor compartments (catholic, 2NP, F-400, undivided-cell).

Appendix A8

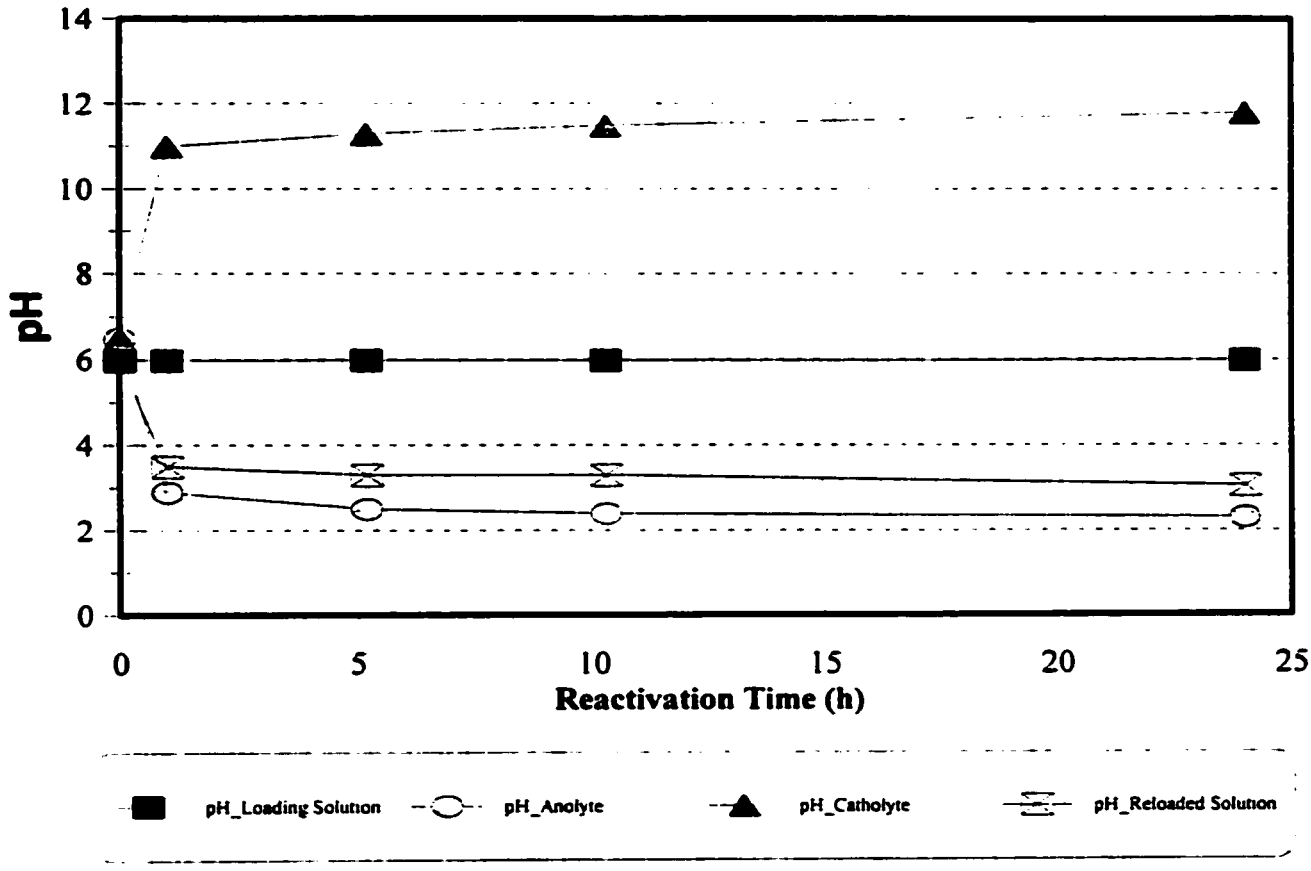

pH variation within the electrolyte, loading, and reloading solutions (anodic, 2NP, F-400, divided-cell).

Appendix A9

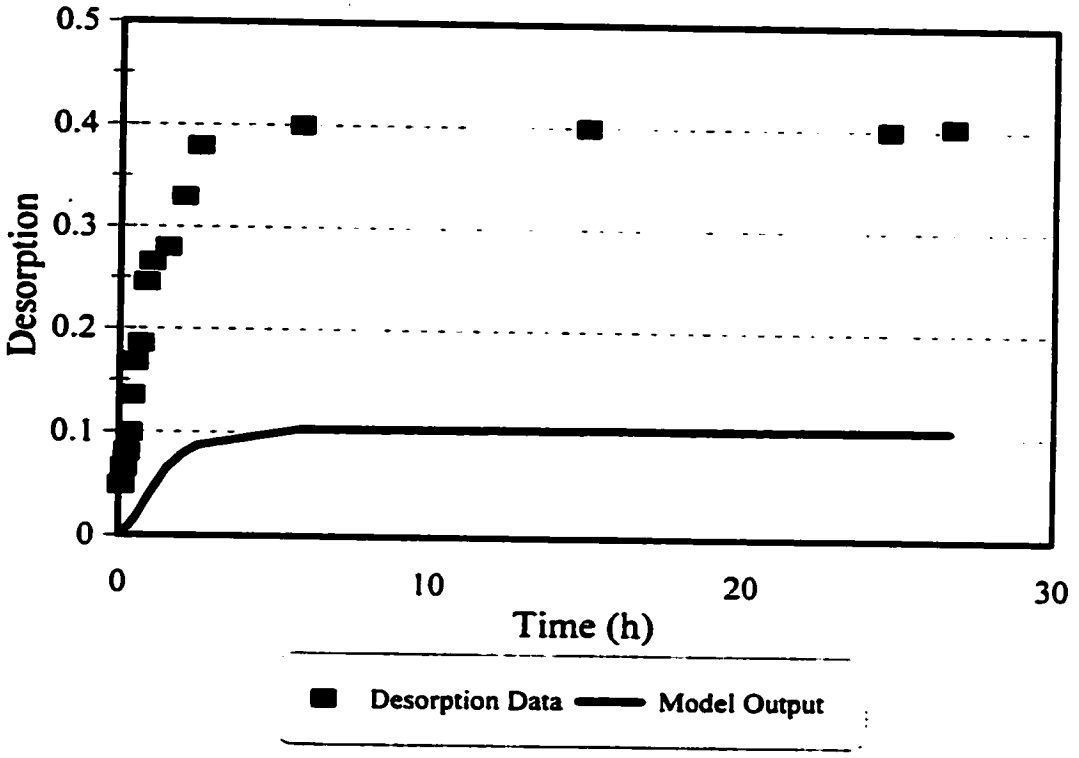

Desorption modeling by the modified HSSD model (phenol. F-400. no current).

Appendix B1

Adsorption Kinetics
Co=300 mg/L **Phenol/F400**

Time(h)	Time(d)	Ce(mg/L)	reduced Concentration
0	0.00	300	1.000
0.3	0.01	190	0.633
0.6	0.03	150	0.500
1.5	0.06	105	0.350
2	0.08	98	0.327
3	0.13	80	0.267
4	0.17	75	0.250
5	0.21	73	0.243
6	0.25	73	0.243
7	0.29	67	0.223
8	0.33	67	0.223
9	0.38	65	0.217
10	0.42	66	0.220
12	0.5	65	0.217
18	0.75	62	0.207
24	1	60	0.200
36	1.5	55	0.183
48	2	53	0.177
	3	51	0.170
	4	51	0.170
	5	51	0.170
	6	50	0.167
	7	51	0.170
	8	50	0.167
	9	50	0.167
	10	50	0.167
	11	49	0.163
	12	48	0.160
	13	50	0.167
	14	49	0.163

Phenol/WV-B

Time(d)	Ce(mg/L)	reduced Concentration
0	300	1
0.0125	225	0.75
0.025	180	0.6
0.05	165	0.55
0.1	141	0.47
0.25	135	0.45
1	129	0.43
2	126	0.42
2.5	124.5	0.415
3	123	0.41
5	120	0.4
6	120	0.4
7	117	0.39
9	114	0.38
11	114	0.38
13	114	0.38
14	114	0.38

Phenol Isotherms
Co=300 mg/L
Feb, 23, 2000

Phenol/WV-B Isotherm (not buffered)

#	Volume(ml	GAC(g)	Ce(mg/L)	qe(mg/g)
11	478	0.207	244	129.31
12	534.6	0.4	206.7	124.70
17	535.8	0.604	174.6	111.24
18	519	0.825	149	94.99
20	472	1.015	113.3	86.82
21	477.5	1.203	93.4	82.00
22	478	1.204	93	82.18
23	474	1.514	73.2	71.01

NoV. 18, 99
Phenol/Darco Isotherm

#	GAC(g)	Vol	Ce(mg/l)	qe(mg/g)
2	0.23	475	236	132.17
3	0.42	528	200	125.71
4	0.62	477	150.8	114.79
5	0.807	519	120.1	115.70
6	1.017	477	79.8	103.28
7	1.21	477	70.3	90.55
9	1.205	501	70.1	95.58
10	1.49	535	49.6	89.91

Phenol/F-400 Isotherm

#	GAC(g)	Volume(mL)	Ce(mg/l)	qe(mg/g)
102	0.203	480.23	223.3	181.45
103	0.403	476.05	164.5	160.06
104	0.404	480.36	165.9	159.45
105	0.6015	493.73	117.5	149.80
106	0.8015	535.31	97.9	134.98
107	1	481.25	57.5	116.70
108	1.2	475.66	36.6	104.41
109	1.2	476.6	36.6	104.61
110	1.2	470.12	32.6	104.76

Appendix B2

Adsorprtion Kinetics (2-nitrophenol on Granular Activated carbons)

Time (h)	Darco Ce(mg/L)	Darco Reduced	Time (h)	F-400 Ce(mg/L)	F-400 Reduced	Time(h)	WV-B Ce(mg/L)	WV-B Reduced
0	500	1	0	500	1	0	500	1
0.08	267	0.534	0.5	235	0.47	0.5	195	0.39
0.16	256	0.512	1	145	0.29	1	135	0.27
0.32	218	0.436	2	55	0.11	2	85	0.17
0.75	176.7	0.3534	3	30	0.06	3.1	47	0.094
1	155.6	0.3112	4	25	0.05	4.15	43	0.086
2	113.96	0.22792	4.5	16	0.032	6	42	0.084
4	86	0.172	6.8	13	0.026	8	41	0.082
7.5	40	0.08	8	11	0.022	12	41	0.082
11	11	0.022	10	10	0.02	16.15	41	0.082
16	7	0.014	12	9	0.018	18	40	0.08
22	4.5	0.01	15	8	0.016	21	40	0.08
23.5	2.2	0.01	18	7	0.014	23.5	40	0.08
48	2	0.01	25.5	7	0.014	30	40	0.08
78	0.02	0.01	28.7	7	0.014	36.75	40	0.08
168	0	0.01	36	7	0.014	44.75	39	0.078
336	0	0.01	48	7	0.014	50	38	0.076

2NP, Isotherms
initial Co= 500 mg/L

2NP/F400 not buffered at 20 Dec, 99

#	Volume(ml)	GAC(g)	Ce(HPLC) (mg/L)	qe(mg/g)
123	502	0.21	303	470.92
124	471	0.403	130.7	431.61
125	481	0.6	35	372.78
126	469	0.808	29.1	273.33
127	497.6	1.002	15.2	240.75
129	480	1.202	7.7	196.59

2NP/F400 buffered at pH=5 with %3 solution Jan, 2000

#	Volume(ml)	GAC(g)	Ce(HPLC)(mg/L)	qe(mg/g)
40	477	0.21	280	499.71
41	477.5	0.408	128	435.37
42	472	0.63	53.2	334.75
43	471	0.813	27	274.03
32	478	1	12.1	233.22
33	475.5	1	12.1	232.00
218	470	1	14	228.42
44	477	1.108	9.7	211.08

2NP/Darco not buffered at NOV, 99

#	Volume(ml)	GAC(g)	Ce(HPLC)(mg/L)	qe(mg/g)
209	528	0.228	348	352.00
210	527	0.401	232.6	351.42
211	524	0.625	159	285.89
212	525	0.812	86.2	267.54
213	525	1.002	53.2	234.10
214	524	1.005	55.4	231.81
215	524	1.213	23.1	206.01
216	527	1.512	8.6	171.28

Appendix B3

Impact of flow on the reactivation of GACs loaded with phenol

FLOW(L/min)	RE time (h)	Anodic Downflow, GAC between meshes-F400	Cathodic DownFlow, GAC on lower Mesh-F-400	Cathodic DownFlow, GAC on upper Mesh - F400	Cathodic UpFlow, GAC on Lower Mesh - F400
0	2.5	46.8	61.7	58	61.7
0	2.5	42.5	66.8	61	66.8
0.1	2.5	48.1			63
0.1	2.5		60		60.5
0.2	2.5	42.5	49.4	54.5	48.6
0.2	2.5	47.3			47.3
0.5	2.5	44.2	45.3	47.6	50.8
0.5	2.5			49.3	
1	2.5	43.9	44	44.2	43
1	2.5	44.2			

For F-400

RE time (h)	Flow = 0	Flow=0.2 L/min	Flow = 0.5 L/min
1	54	42	40
2.5	62	48	45
5	64	52	48
7.5	66	53.5	50
10	69	55	53

For WV-B

FLOW(L/min)	RE time (h)	RE (%)
0	2.5	59
0	2.5	
0.1	2.5	51.2
0.1	2.5	
0.2	2.5	50.9
0.2	2.5	
0.5	2.5	46.4
0.5	2.5	
1	2.5	46.2

Appendix B4

Impact of time and current on the reactivation of F-400 loaded with phenol.

Time(h)	100 mA	50 mA	30 mA	10 mA	#Coulombs
0	35				0
1	51.1				360
2.5	60				900
5	65				1800
7.5	71.7				2700
10	73.2				3600
18.5	75.8				6660
0		35			0
1		53			180
2.5		57			450
5		59.9			900
5		61.7			900
7.5		65			1350
10		69.2			1800
11		74			1980
18		75			3240
24.4		76.7			4392
0			35		0
1.15			48		124.2
2.5			53		270
5			54.4		540
7.5			61.1		810
10			60.9		1080
16.8			63		1814.4
24.5			65		2646
0				35	0
1				40.3	36
2.5				50.6	90
5				50.6	180
7.5				52.3	270
10				53.7	360
16.5				57	594
24.8				59.9	892.8
37.8				76	1360.8

Appendix B5

Imapct of Reactivation Time and Current on the Reactivation of WV-B loaded with Phenol.

Time(h)	100 mA	50 mA	30 mA	10 mA	#Coulombs
0	41				0
1.1	51.2				396
2.5	65				900
5	70				1800
7.5	70.3				2700
10.7	72.4				3852
16	76				5760
23.5	78.9				8460
0		41			0
1.1		46			198
2.5		57.9			450
5.5		63.4			990
7.5		66.7			1350
10.8		68.9			1944
16.5		73.5			2970
24.5		76.7			4410
0			41		0
1.1			41.6		118.8
2.5			50.4		270
5			55.4		540
7.5			61.6		810
11.9			60.9		1285.2
16.1			64.8		1738.8
25.1			65.8		2710.8
0				41	0
1.1				39.6	39.6
2.5				43.3	90
5				49.6	180
7.5				47.6	270
10.7				55	385.2
16.3				56.5	586.8
29				62.3	1044

Appendix B6

Reactivation of 2NP-loaded F-400, Buffered solutions

Effect of Catholyte Volume

Volume(ml)	GAC(g)	I (mA)	Time (h)	NaCl(M)	Flow(L/min)	Ce(L)	Ce(RL)	Ce (RE)	TOC(L)	TOC(RL	TOC(RE	RE3%
475	1	50	5	0.1	0	20.2	22.3	68	9.1	12.7	96.8	84.96
475	1	50	5	0.1	0	14.8	25.3	72	8	16.1	78.7	81.60
520	1	50	5	0.1	0	19.6	30.3	82.88	11.7	19	92.9	84.19

Effect of NaCl Concentration

Volume(ml)	GAC(g)	I (mA)	Time (h)	NaCl(M)	Flow(L/min)	Ce(L)	Ce(RL)	Ce (RE)	TOC(L)	TOC(RL	TOC(RE	RE3%
518	1	50	5	0.02	0	18.8	32.1	79	10	19.9	87	82.25
475	1	50	5	0.1	0	20.2	22.3	68	9.1	12.7	96.8	84.96
475	1	50	5	0.5	0		18.5	37			95	90.07
475	1	50	5	1	0	16.6	18.6	30.8	7.8	21.1	87.8	89.92
471	1	50	5.3	0.5		16.9	14.5	35	9.2	10.2	93.6	96.17

Anodic regeneration of 2NP-F400 in Full-Reactor- I= 50 (mA)

Volume(ml)	GAC(g)		Time(h)	NaCl	Flow	Ce(L)	Ce(RL)	Ce (RE)	TOC(L)	TOC(RL	TOC(RE	RE3%
		50	0	0.1								40.00
475	1	50	1	0.1	0	1.2	140.6					41.00
		50	2.5	0.1								42.00
475	1	50	5	0.1	0	0.95	116.3					43.69
		50		0.1								44.00
475	1	50	10.5	0.1	0	1	117					43.54
475	1	50	24	0.1	0	1.2	102.5					46.83

Anodic Regeneration of 2NP-F400 at divided cell reactor, using cation Raipor membrane

Volume (ml)	GAC(g)	Curren	Time (h)	NaCl	Flow	Ce(L)	Ce(RL)	Ce (RE)	TOC(L)	TOC(RL	TOC(RE	RE3%
475		50	0	0.1			135					39.92
475	1	50	1	0.1	0	1.1	135.4				5	39.85
475		50	2.5	0.1			129					41.08
475	1	50	5.2	0.1	0	1	128.2				20.7	41.24
475	1	50	10.4	0.1	0	0.8	128.4				5.3	41.20
475	1	50	24	0.1	0	1.1	95.1				2.6	48.68

Anodic Regeneration of 2NP-F400 at divided cell reactor, using Anion Raipor membrane

Volume (ml)	GAC(g)	Curren	Time (h)			Ce(L)	Ce(RL)	Ce (RE)	TOC(L)	TOC(RL	TOC(RE	RE3%
475		50	0	0.1			135					39.92
472.3	1	50	1	0.1	0	2	135.4			62	0	39.62
475		50	2.5	0.1			130					40.88
478.3	1	50	5.4	0.1	0	2.5	124.8			57	0.2	42.21
477.5	1	50	12.7	0.1	0	1.8	109.3			51	0.4	45.48
474.17	1	50	28.7	0.1	0	1.9	89.8			54	0.05	50.00

Appendix B7

Reactivation of 2NP-loaded F-400, Buffered solutions

Effect of Electrolyte flow (undivided reactor)

Volume(ml)	GAC(g)	I (mA)	Time (h)	NaCl(M)	Flow(L/min)	Ce(L)	Ce(RL)	Ce (RE)	TOC(L)	TOC(RL	RE3%
475	1	50	5	0.1	0	20.2	22.3	68	9.1	12.7	84.96
477.26	1	50	5	0.1	0.5	13.5	70.2	26	8.5	36.8	56.35
475	1	50	5.6	0.1	1	15.6	98.9	14.6	7.8	40.8	47.72

Divided cell, Cation membrane, cathodic

Volume(ml)	GAC(g)	I (mA)	Time (h)	NaCl(M)	Flow(L/min)	Ce(L)	Ce(RL)	Ce (RE)	TOC(L)	TOC(RL	RE3%
475	1	0	0	0.1	0	16.7	132.2		8.7		40.46
535.2	1	50	1	0.1	0	19.6	87.3		11.7		57.21
475		50	2.5				27				79.89
533.2	1	50	5.5	0.1	0	19	17.9		11		102.14
475.2	1	50	10.25	0.1	0	11.9	31.7		7.7		108.00
535.7	1	50	18	0.1	0	18	14.7		10.1		108.94

Divided cell, Anion membrane, cathodic

Volume(ml)	GAC(g)	I (mA)	Time (h)	NaCl(M)	Flow(L/min)	Ce(L)	Ce(RL)	Ce (RE)	TOC(L)	TOC(RL	RE3%
475	1	0	0	0.1	0	16.7	132.2		8	57	40.46
475	1	50	1	0.1	0	12.4	81		7.7	48	52.61
475			2.5				32				75.50
473	1	50	5	0.1	0	13.1	13.5		6.5	8.1	98.67
530	1	50	10	0.1	0	14.8	15.7		10.8	10.8	105.66
475	1	50	19	0.1	0	14.3	11		7.3	6.7	105.26

Impact of Current (undivided-unmixed)

Volume(ml)	GAC(g)	I (mA)	Time (h)	NaCl(M)	Flow(L/min)	Ce(L)	Ce(RL)	Ce (RE)	TOC(L)	TOC(RL	RE3%
475	1	0	0	0.1	0	16.7	132.2	1	8	57	40.46
473.1	1	10	1	0.1	0	12.8	111.1	1.5	8.7	56.4	44.65
475	1	50	1	0.1	0	16	75	45	7.6	33.4	54.48
475	1	100	1	0.1	0	16.2	41.5	67.7	7.6	17.9	68.96
475	1	250	1	0.1	0	14.1	32	34	8.4	21	80.00

Appendix B8

Reactivation of F-400 loaded with phenol. Buffered reloading Solutions, divided-Cell Reactor

Divided Cell Reactor-Chatodic-Cation Membrane(phenol/F400)

Volume(ml)	GAC(g)	I (mA)	'Time (h)	NaCl(M)	Flow(L/min)	Ce-RL(mg/L)	RE3 (%)
475	1.2	50	0	0.1	0	175	29.48
485	1.2	50	1	0.1	0	84	65.23
475	1.2	50	2.5	0.1	0	70	71.96
542	1.2	50	5.6	0.1	0	78	76.65
542	1.2	50	10	0.1	0	67	84.31
489	1.2	50	22	0.1	0	52.2	87.38

Divided Cell Reactor-Chatodic-Anion Membrane(Phenol/F400)

Volume(ml)	GAC(g)	I (mA)	'Time (h)	NaCl(M)	Flow(L/min)	Ce-RL(mg/L)	RE3 (%)
475	1.2		0	0.1	0	175	29.48
542	1.2	50	1.15	0.1	0	120	54.41
475	1.2	50	2.5	0.1	0	73	70.11
542	1.2	50	5	0.1	0	67.5	83.94
526	1.2	50	11.25	0.1	0	59	88.02
480	1.2	50	22.5	0.1	0	52.2	85.77

Anodic Regeneration of phenol-F400 at divided cell reactor, using cation Raipor membrane

Volume(ml)	GAC(g)	I (mA)	'Time (h)	NaCl(M)	Flow(L/min)	Ce-RL(mg/L)	RE3 (%)
475	1.2	50	0	0.1	0	175	29.48
519.3	1.2	50	1.2	0.1	0	176.8	31.66
475	1.2	50	2.5	0.1	0	164	32.72
528	1.2	50	5	0.1	0	168.4	34.91
518.9	1.2	50	12	0.1	0	120	52.09
474.6	1.2	50	30	0.1	0	108	52.50

Anodic Regeneration of Phenol-F400 at divided cell reactor, using Anion Raipor membrane

Volume (ml	GAC-F4(	Current (	'Time (h)	NaCl	Flow	Ce-RL(mg/L)	RE3 (%)
475	1.2	50	0	0.1	0	175	29.48
477.3	1.2	50	1.1	0.1	0	165	32.57
475	1.2	50	2.5	0.1	0	157	34.87
477.9	1.2	50	5.3	0.1	0	145.7	38.74
475.6	1.2	50	12	0.1	0	114.3	50.00
473.1	1.2	50	23.3	0.1	0	100.5	55.60

Appendix B9

Reactivation of F-400 loaded with phenol. Buffered reloading Solutions, Undivided-Cell Reactor

Volume(ml)	GAC(g)	I (mA)	Time (h)	NaCl(M)	Flow(L/min)	Ce-RL(mg/L)	RE3 (%)
475	1.2	10	0			174.83	29.53
480	1.2	10	1.15	0.1	0	122.56	47.19
475	1.2	10	2.5	0.1	0	91.58	60.02
475	1.2	10	5	0.1	0	82.33	64.78
476	1.2	10	10.3	0.1	0	61.42	77.88
517	1.2	10	25	0.1	0	73.54	75.95
475	1.2	50	0	0.1	0	174.83	29.53
535.3	1.2	50	1	0.1	0	114.24	56.31
546	1.2	50	2.5	0.1	0	81.96	74.69
538.6	1.2	50	5	0.1	0	71.60	80.47
474.6	1.2	50	10	0.1	0	58.28	79.96
546	1.2	50	24	0.1	0	69.84	82.83
474.6	1.2	50	27.7	0.1	0	55.50	82.11
475	1.2	100	0	0.1	0	174.83	29.53
467	1.2	100	1	0.1	0	65.68	73.51
475	1.2	100	2.5	0.1	0	174.83	29.53
494	1.2	100	5.6	0.1	0	48.93	91.24
480	1.2	100	10.7	0.1	0	58.28	80.87
530	1.2	100	41	0.1	0	69.65	80.54
475	1.2	250	0	0.1	0	174.83	29.53
476	1.2	250	1	0.1	0	54.85	82.87
475	1.2	250	2.5	0.1	0	53.19	84.05
535	1.2	250	5.75	0.1	0	64.75	84.92
481	1.2	250	10.75	0.1	0	45.70	91.90
537	1.2	250	25	0.1	0	65.86	84.39

Appendix B10

Destruction of phenol in divided-cell reactor.

Anodic destruction of phenol in divided-Cell

Time(h)	I(mA)	Phenol (mg/L)	TOC (mg/L)
0	50	48	37.8
0.9	50	41.3	36.7
3.6	50	27.5	35.3
8	50	7.1	35.4
18.5	50	0.23	32.7
24.6	50	0.01	30.6
28.6	50	0.45	30.8
36	50	1.3	31.6
47	50	1.3	30.5

Cathodic destruction of phenol in divided-Cell

Time(h)	I(mA)	Phenol (mg/L)	TOC (mg/L)
0	50	48	38
1.05	50	47	38.2
3.13	50	45	37.8
7.5	50	44.5	37.5
19	50	44.5	37
25.5	50	45.1	36
43	50	41.8	35
61	50	40.1	35

Appendix B11

Anodic destruction of phenol in undivided-cell reactor

Time (min)	Time(h)	I (mA)	Phenol (mg/L)	TOC (mg/L)
0	0.00	50	45.7	39.4
30	0.50	50	38.6	39.2
80	1.33	50	34.9	38.8
120	2.00	50	29.1	37.3
165	2.75	50	24.9	36.8
270	4.50	50	16.8	35.9
335	5.58	50	13	35.3
480	8.00	50	5	34
690	11.50	50	1.8	33.6
1157	19.28	50	0	32.2
1500	25.00	50	0	31.7
1610	26.83	50	0	31.2
1710	28.50	50	0	30.4
1860	31.00	50	0	30
2580	43.00	50	0	28.3
2700	45.00	50	0	28.4
2880	48.00	50	0	27.1
5580	93.00	50	0	20
0	0.00	250	50	42.7
10	0.17	250	46	41.9
32	0.53	250	38	41.3
73	1.22	250	30	41
100	1.67	250	22.5	41
135	2.25	250	16	40
180	3.00	250	9	39.7
345	5.75	250	0	35
330	5.50	250	0	34
460	7.67	250	0	33
520	8.67	250	0	28.2
750	12.50	250	0	23.9
1380	23.00	250	0	21.3
1605	26.75	250	0	20.6
1830	30.50	250	0	20.1
2140	35.67	250	0	19.6
2880	48.00	250	0	18.7
3285	54.75	250	0	16.7
4200	70.00	250	0	14.4
4800	80.00	250	0	12.7
0	0.00	500	47.5	40.1
7	0.12	500	43	38.7
15	0.25	500	37	39.1
35	0.58	500	21.7	38.1
55	0.92	500	6.8	38.1
70	1.17	500	0.7	35
97	1.62	500	0	30.4
140	2.33	500	0	23.6
173	2.88	500	0	22.6
210	3.50	500	0	22.6
270	4.50	500	0	21.5
315	5.25	500	0	22.3
375	6.25	500	0	21.7
570	9.50	500	0	18.7
620	10.33	500	0	19.7
795	13.25	500	0	17.5
1095	18.25	500	0	14.9
1330	22.17	500	0	12
1440	24.00	500	0	10.94
1680	28.00	500	0	9.4
1920	32.00	500	0	9.2

Appendix B12

Destruction of 2NP

Destruction of 2NP in undivided-cell reactor

Time (min)	Time(h)	I (mA)	2NP (mg/L)	TOC (mg/L)
5	0.08	50	67	36
70	1.17	50	34.6	35.6
125	2.08	50	26.3	34.9
200	3.33	50	12.6	34.5
315	5.25	50	3.2	34
440	7.33	50	0.9	33.8
540	9.00	50	0.4	33.3
765	12.75	50	0	32.5
1380	23.00	50	0	31
1580	26.33	50	0	30
1800	30.00	50	0	28.5

Destruction of 2NP in divided-cell reactor

Time (min)	Time(h)	I (mA)	Anolyte (2NP mg/L)	Catholyte (2NP mg/L)
0	0.00	50	70	
30	0.50	50	66.5	
130	2.17	50	50	
210	3.50	50	38	
330	5.50	50	15.5	
610	10.17	50	2.5	
1080	18.00	50	0.1	
1770	29.50	50	0	
2640	44.00	50	0	
3180	53.00	50	0	
4020	67.00	50	0	
4740	79.00	50	0	
5580	93.00	50	0	
0	0.00	50		70
30	0.50	50		65
130	2.17	50		55
210	3.50	50		40
330	5.50	50		28
610	10.17	50		21
1080	18.00	50		5
1770	29.50	50		0.2
2640	44.00	50		0.2
3180	53.00	50		0.04
4020	67.00	50		0
4740	79.00	50		0
5580	93.00	50		0

Appendix B13

Desorption of phenol from F-400 at pH =12

Time(h)	I (mA)	Loading (mg TOC/L)	TOC(mg/L)	%desorption	45.9*(1-exp(-0.519*t))
0	0	95.38	0	0.00	0.00
0.15	0	95.38	10.3	7.29	3.44
0.6	0	95.38	23.2	16.42	12.28
1.5	0	95.38	36.7	25.97	24.83
2.5	0	95.38	45.3	32.06	33.36
3.9	0	95.38	53.7	38.00	39.84
5.15	0	95.38	56.8	40.20	42.73
6.15	0	95.38	59.8	42.32	44.02
12	0	95.38	65.3	46.21	45.81
25	0	95.38	65	46.00	45.90
27	0	95.38	60.7	42.96	45.90
31	0	95.38	67	47.42	45.90
47.8	0	95.38	67.3	47.63	45.90

Time(h)	I (mA)	Loading (mg TOC/L)	TOC(mg/L)	%desorption	66.481*(1-exp(-0.537*t)
0	50	95.285	0	0.00	0.00
0.2	50	95.285	12.1	8.57	6.77
1.1	50	95.285	41.2	29.19	29.65
2.6	50	95.285	72.6	51.43	50.02
4	50	95.285	80.5	57.03	58.72
6.5	50	95.285	89.6	63.47	64.45
9.25	50	95.285	94.4	66.87	66.02
20.75	50	95.285	92.6	65.60	66.48
35	50	95.285	93.9	66.52	66.48
41	50	95.285	94.6	67.01	66.48
48	50	95.285	94.1	66.66	66.48
54	50	95.285	93.6	66.31	66.48
73	50	95.285	94.6	67.01	66.48
91	50	95.285	93.6	66.31	66.48
110	50	95.285	95.6	67.72	66.48

Appendix B14

Desotption of Phenol From F-400 at pH =2

Time(h)	I (mA)	Loading (mg TOC/L)	TOC(mg/L)	%desorption	10.062*(1-exp(-0.196*t)
0	0	98.4	0	0.00	0.00
0.2	0	98.4	0	0.00	0.39
0.5	0	98.4	0.6	0.41	0.94
1.25	0	98.4	4.8	3.29	2.19
2.3	0	98.4	6.8	4.67	3.65
5.2	0	98.4	12	8.23	6.43
7.75	0	98.4	11	7.55	7.86
9.8	0	98.4	11.9	8.17	8.59
20.6	0	98.4	12.2	8.37	9.88
23.6	0	98.4	12.8	8.78	9.96
27.7	0	98.4	14.6	10.02	10.02
35	0	98.4	15.5	10.64	10.05
40	0	98.4	16	10.98	10.06
48	0	98.4	16.1	11.05	10.06

Time(h)	I (mA)	Loading (mg TOC/L)	TOC(mg/L)	%desorption	12.226*(1-exp(-0.649*t)
0	50	99.0	0	0.00	0.00
0.15	50	99.0	4.8	3.27	1.13
0.5	50	99.0	7.5	5.11	3.39
1.3	50	99.0	9.9	6.75	6.97
2.3	50	99.0	13.2	9.00	9.48
5	50	99.0	15	10.23	11.75
5.75	50	99.0	14.8	10.09	11.93
14	50	99.0	16.6	11.32	12.22
17.75	50	99.0	17.6	12.00	12.22
22	50	99.0	18	12.27	12.22
41	50	99.0	20	13.64	12.22
45	50	99.0	22	15.00	12.22

Appendix B15

Desorption of 2NP from F-400 at pH =12

Time (mir	Time(h)	I (mA)	Loading (mg	TOC(mg/L)	%desor	58.443*(1-exp(-0.61*t))
	0	0	110.01	0	0.00	0.00
11	0.1833	0	110.01	15.9	9.76	6.18
16	0.2667	0	110.01	19.6	12.03	8.77
22	0.3667	0	110.01	24.1	14.79	11.71
30	0.5	0	110.01	32.6	20.00	15.36
45	0.75	0	110.01	40.3	24.73	21.46
60	1	0	110.01	48.1	29.51	26.69
90	1.5	0	110.01	59	36.20	35.04
130	2.1667	0	110.01	64.1	39.33	42.86
160	2.6667	0	110.01	67.4	41.36	46.95
220	3.6667	0	110.01	79 5	48.78	52.20
340	5.6667	0	110.01	91.3	56.02	56.60
705	11.75	0	110.01	96.2	59.03	58.40
1120	18.667	0	110.01	96.5	59.21	58.44
1560	26	0	110.01	97.1	59.58	58.44
	35	0	110.01	98	60.13	58.44
	48	0	110.01	98.5	60.44	58.44

Time (mir	Time(h)	I (mA)	Loading (mg	TOC(mg/L)	%desor	88.62*(1-exp(-0.432*t))
0	0	50	108.0625	0	0.00	0.00
11	0.1833	50	108.0625	15.35	9.59	6.75
15	0.25	50	108.0625	19.54	12.21	9.07
25	0.4167	50	108.0625	30.52	19.06	14.60
40	0.6667	50	108.0625	42.52	26.56	22.18
50	0.8333	50	108.0625	45.11	28.18	26.79
60	1	50	108.0625	52.37	32.71	31.09
90	1.5	50	108.0625	70.79	44.22	42.26
130	2.1667	50	108.0625	91.3	57.03	53.86
150	2.5	50	108.0625	94.8	59.22	58.53
210	3.5	50	108.0625	109.1	68.15	69.08
240	4	50	108.0625	111.3	69.52	72.88
280	4.6667	50	108.0625	112.4	70.21	76.82
330	5.5	50	108.0625	121.4	75.83	80.39
430	7.1667	50	108.0625	125.9	78.64	84.61
600	10	50	108.0625	135.9	84.89	87.44
900	15	50	108.0625	140.9	88.01	88.48
1260	21	50	108.0625	147.3	92.01	88.61
1330	22.167	50	108.0625	144.9	90.51	88.61
1500	25	50	108.0625	144.9	90.51	88.62
1620	27	50	108.0625	144.9	90.51	88.62
1650	27.5	50	108.0625	145.7	91.01	88.62
	33	50	108.0625	15.8	9.87	88.62
	40	50	108.0625	15.9	91.13	88.62

Appendix B16

Desorption of 2NP from F-400 at pH =2

Time (mir	Time(h)	I (mA)		Loading (mg	TOC(mg/L)	Desorption (%)	27.36*(1-exp(-0.1434*t))
0	0.00		0	116.4	0	0.00	0.00
5	0.08		0	116.4	0.31	0.18	0.33
10	0.17		0	116.4	0.75	0.43	0.65
20	0.33		0	116.4	1.2	0.70	1.28
30	0.50		0	116.4	1.9	1.10	1.89
50	0.83		0	116.4	3.7	2.15	3.08
70	1.17		0	116.4	6.4	3.71	4.21
90	1.50		0	116.4	8.4	4.87	5.30
120	2.00		0	116.4	11.4	6.61	6.82
150	2.50		0	116.4	14.1	8.18	8.24
300	5.00		0	116.4	25.9	15.02	14.00
500	8.33		0	116.4	33.7	19.54	19.08
700	11.67		0	116.4	38.9	22.56	22.22
900	15.00		0	116.4	41.4	24.01	24.18
1185	19.75		0	116.4	42.4	24.59	25.75
1350	22.50		0	116.4	45.3	26.27	26.27
1680	28.00		0	116.4	46.8	27.14	26.87
2580	43.00		0	116.4	47.3	27.43	27.30
2970	49.00		0	116.4	47.7	27.66	27.34

Time (mir	Time(h)	I (mA)		Loading (mg	TOC(mg/L)	Desorption (%)	40.95*(1-exp(-0.167*t))
0	0.00		50	110.2	0	0.00	0.00
10	0.17		50	110.2	2	1.23	1.12
20	0.33		50	110.2	4	2.45	2.22
30	0.50		50	110.2	8	4.90	3.28
45	0.75		50	110.2	10	6.13	4.82
60	1.00		50	110.2	13	7.96	6.30
90	1.50		50	110.2	17	10.41	9.07
125	2.08		50	110.2	23	14.09	12.03
205	3.42		50	110.2	30	18.38	17.81
250	4.17		50	110.2	35	21.44	20.53
285	4.75		50	110.2	37	22.66	22.43
340	5.67		50	110.2	40	24.50	25.05
435	7.25		50	110.2	45	27.56	28.75
465	7.75		50	110.2	47	28.79	29.73
610	10.17		50	110.2	52	31.85	33.45
900	15.00		50	110.2	60	36.75	37.61
1130	18.83		50	110.2	63	38.59	39.19
1250	20.83		50	110.2	65	39.81	39.69
	22.75		50	110.2	67	41.04	40.03
	26.00		50	110.2	68	41.65	40.42
	28.25		50	110.2	69	42.26	40.58
	31.00		50	110.2	69	42.26	40.72
	48.00		50	110.2	70	42.88	40.94

Appendix B17

Thermal and electrochemical Long term adsorption efficiency

cycle #	Thermal efficiency(%)	Thermal GAC mass	Thermal long term efficiency (%)	Electrochemical efficiency(%)	Electrochemical GAC mass	Electrochemical long term efficiency (%)
0		1.00			1.00	
1	90	0.95	85.50	80.00	1.00	80.00
2	90	0.90	81.22	78.40	1.00	78.40
3	90	0.86	77.16	76.83	1.00	76.83
4	90	0.81	73.31	75.30	1.00	75.30
5	90	0.77	69.64	73.79	1.00	73.79
6	90	0.74	66.16	72.31	1.00	72.31
7	90	0.70	62.85	70.87	1.00	70.87
8	90	0.66	59.71	69.45	1.00	69.45
9	90	0.63	56.72	68.06	1.00	68.06
10	90	0.60	53.89	66.70	1.00	66.70
11	90	0.57	51.19	65.37	1.00	65.37
12	90	0.54	48.63	64.06	1.00	64.06
13	90	0.51	46.20	62.78	1.00	62.78
14	90	0.49	43.89	61.52	1.00	61.52
15	90	0.46	41.70	60.29	1.00	60.29
16	90	0.44	39.61	59.09	1.00	59.09
17	90	0.42	37.63	57.90	1.00	57.90
18	90	0.40	35.75	56.75	1.00	56.75
19	90	0.38	33.96	55.61	1.00	55.61
20	90	0.36	32.26	54.50	1.00	54.50
21	90	0.34	30.65	53.41	1.00	53.41
22	90	0.32	29.12	52.34	1.00	52.34
23	90	0.31	27.66	51.29	1.00	51.29
24	90	0.29	26.28	50.27	1.00	50.27
25	90	0.28	24.97	49.26	1.00	49.26
26	90	0.26	23.72	48.28	1.00	48.28
27	90	0.25	22.53	47.31	1.00	47.31
28	90	0.24	21.40	46.37	1.00	46.37
29	90	0.23	20.33	45.44	1.00	45.44
30	90	0.21	19.32	44.53	1.00	44.53
31	90	0.20	18.35	43.64	1.00	43.64
32	90	0.19	17.43	42.77	1.00	42.77
33	90	0.18	16.56	41.91	1.00	41.91
34	90	0.17	15.73	41.07	1.00	41.07
35	90	0.17	14.95	40.25	1.00	40.25
36	90	0.16	14.20	39.45	1.00	39.45
37	90	0.15	13.49	38.66	1.00	38.66
38	90	0.14	12.82	37.88	1.00	37.88
39	90	0.14	12.17	37.13	1.00	37.13
40	90	0.13	11.57	36.38	1.00	36.38
41	90	0.12	10.99	35.66	1.00	35.66
42	90	0.12	10.44	34.94	1.00	34.94
43	90	0.11	9.92	34.24	1.00	34.24
44	90	0.10	9.42	33.56	1.00	33.56
45	90	0.10	8.95	32.89	1.00	32.89
46	90	0.09	8.50	32.23	1.00	32.23
47	90	0.09	8.08	31.59	1.00	31.59
48	90	0.09	7.67	30.95	1.00	30.95
49	90	0.08	7.29	30.33	1.00	30.33
50	90	0.08	6.93	29.73	1.00	29.73

Appendix B18

Enery cost comparison of thermal and electrochemical reactivation

compound:	Phenol						
Concentration (mg/L):	300						
k	34.2						
1/n	0.306						
Qo (mg/g of GAC)	195.9						
Flowrate (m^3/d)	250	500	1000	1500	2000	2500	3000
Flowrate (ft^3/d)							
carbon usage rate (g/d)	382848.39	765696.78	1531393.57	2297090.35	3062787.14	3828483.92	4594180.70
carbon usage rate (kg/d)	382.85	765.70	1531.39	2297.09	3062.79	3828.48	4594.18
carbon usage rate (lb/d)	844.03	1688.06	3376.11	5064.17	6752.22	8440.28	10128.33
Hearth loading rate(lb/ft^2/d)	50	50	50	50	50	50	50
hearth area (ft^2)	16.88	33.76	67.52	101.28	135.04	168.81	202.57
Electrical energy (kw.hr/year)	241842.76	306032.61	387259.70	444432.40	490046.06	528626.70	562393.53
Natural gas (10^6 scf/year)	4.90	6.21	7.86	9.03	9.97	10.75	11.45
Cost of electricity ($/kw.hr)	0.0600	0.0600	0.0600	0.0600	0.0600	0.0600	0.0600
Cost of natural gas ($/scft)	0.0035	0.0035	0.0035	0.0035	0.0035	0.0035	0.0035
Annual electricity cost ($)	14510.57	18361.96	23235.58	26665.94	29402.76	31717.60	33743.61
Annual natural gas cost ($)	17138.88	21719.08	27523.29	31613.23	34878.61	37641.97	40061.56
Total annual energy cost ($)	31649.44	40081.03	50758.87	58279.18	64281.38	69359.58	73805.17
GAC cost ($/lb)	1.00	1.00	1.00	1.00	1.00	1.00	1.00
Annual GAC cost ($) 5% lost	15403.50	30807.01	61614.01	92421.02	123228.02	154035.03	184842.04
TOTAL cost (Energy + GAC lost)	47052.95	70888.04	112372.88	150700.19	187509.40	223394.61	258647.21
Annual energy cost/kg	0.23	0.14	0.09	0.07	0.06	0.05	0.04
Electrochemical cost($/kg)	0.04	0.04	0.04	0.04	0.04	0.04	0.04
Electrochemical annual cost($)	5589.59	11179.17	22358.35	33537.52	44716.69	55895.87	67075.04
Thermal Fluid bed ($/kg)	0.0602	0.0602	0.0602	0.0602	0.0602	0.0602	0.0602
Thermal Fluid bed annual cost($/kg)	8412.33	16824.66	33649.31	50473.97	67298.62	84123.28	100947.93
Thermal infrared ($/kg)	0.1300	0.1300	0.1300	0.1300	0.1300	0.1300	0.1300
Thermal infrared annual cost($/kg)	18166.16	36332.31	72664.62	108996.94	145329.25	181661.56	217993.87